REAL-TIME DIGITAL MODELS FOR POWER PLANTS

By

JOHN A. TSIGANIS, Dip.El.Eng., M.Sc.

A Thesis submitted for the Degree of
Doctor of Philosophy
in the University of London

Department of Electrical Engineering,
Imperial College of Science and Technology,

ABSTRACT

Models for the boiler dynamics of a conventional and a nuclear plant and the hydraulic dynamics of a hydro plant were developed. They constitute the digital part of a Hybrid Power Systems Simulator, built in the Power System section at Imperial College. They were designed to run in real-time. This requirement imposes restrictions on the processor time and core usage. For this reason, the models were kept relatively simple and include only the main variables of each process.

It was found necessary to keep the models non-linear. This makes their response credible over a large part of their operating range. A linearised version would restrict their use near to an operating point. The conversion of the continuous equations to difference equations was made using the direct substitutional method of digital simulation. This method is based on the Z-transform theory.

Two versions of the conventional plant model were developed; one operating on the constant-pressure principle, the other on the variable-pressure operating mode. The fundamental difference lies in the overall control of the unit's output, with little difference in the equations describing the process. A High Temperature Gas-Cooled reactor was assumed to drive the nuclear plant.

The digital simulation can be started at will by the simulator user, in an interactive mode. Appropriate initialization programs were developed for each type of model. They acquire the necessary information from the user and the analog part of the simulator, so as to start each unit without upsetting the rest of the system.

The work of the development of these models is described in this thesis and the problems associated with it. The responses of the models to typical disturbances are presented. They were taken both off-line and in real-time operation, to assess the usefulness of this kind of simulation in the context of the simulator performance.

ACKNOWLEDGEMENTS

This work has been carried out under the supervision of Dr. M.J. Short, B.Sc., D.I.C., C.Eng., M.I.E.E., whom I should like to thank for his guidance and encouragement.

I would also like to thank Dr. B.J. Cory, D.Sc., A.C.G.I., C.Eng., F.I.E.E., M.I.E.E.E. for his interest in this work and his valuable suggestions.

Many thanks are due to my colleagues in the Power System Section for their assistance, especially Drs. Giles and Mogridge, Mr. Horne and Mr. Sulley of the Electrical Engineering Department staff.

Finally, I would like to express my deep gratitude to my parents, whose financial assistance made this work possible.

CONTENTS

NOMENCLATURE

Economiser

ρ_{EO}	=	water density at the economiser output	(lb/ft^3)
W_{EO}	=	water flow rate at the economiser output	(lb/s)
h_{EO}	=	enthalpy of the water at the economiser output	(Btu/lb)
T_{EO}	=	water temperature at the economiser output	(^oF)
W_{EI}	=	water flow rate at the economiser input	(lb/s)
h_{EI}	=	water enthalpy at the economiser input	(Btu/lb)
V_E	=	economiser volume	(ft^3)
M_E	=	mass of the economiser metal tubes	(lb)
T_{EM}	=	temperature of the economiser metal tubes	(^oF)
Q_E	=	heat flow rate from metal to the water	(Btu/s)
Q_{GE}	=	heat flow rate from gas to the tube metal	(Btu/s)
C_E	=	specific heat of the economiser metal	(Btu/lb, ^oF)
k_E	=	heat transfer coefficient	
T_{GE}	=	temperature of the flue gas leaving the economiser	(^oF)
C_{GE}	=	specific heat of the flow gas leaving the economiser	(Btu/lb, ^oF)
k_{E1}	=	heat transfer coefficient	

Downcomers

W_D	=	water flowrate in the downcomers (forced circulation)	(lb/s)
h_D	=	water enthalpy in the downcomers (forced circulation)	(Btu/lb)
W_{DI}	=	water flow rate at the downcomer input (natural circulation)	(lb/s)
W_{DO}	=	water flow rate at the downcomer output (natural circulation)	(lb/s)
L_D	=	length of downcomer circuit	(ft)
d_D	=	diameter of downcomer tubes	(ft)
A_D	=	total flow area of downcomer tubes	(ft^2)
V_D	=	downcomer storage volume	(ft^3)
h_{DO}	=	enthalpy of water at the downcomer output	(Btu/lb)
ρ_{DO}	=	density of water at the downcomer output	(lb/ft^3)
P_{DO}	=	pressure at the downcomer output	(psi)
P_{DR}	=	pressure in the drum	(psi)
f_D	=	friction coefficient of the flow in the downcomers	
g	=	acceleration of gravity	(ft/s^2)

Risers

h_m	=	enthalpy of the water/steam mixture in the risers (forced circulation)	(Btu/lb)
x	=	steam quality	
Q_W	=	heat rate input from metal tube to the boiling water	(Btu/s)
L_R	=	frictional tube length of risers (natural circulation)	(ft)
d_R	=	diameter of riser tubes	(ft)
A_R	=	total flow area of risers	(ft^2)
V_R	=	riser storage volume	(ft^3)
h_{RO}	=	enthalpy of the water/steam mixture at the riser output	(Btu/lb)
ρ_{RO}	=	density of the water/steam mixture at the riser output	(lb/ft^3)
W_{RO}	=	mixture flow rate at the riser outlet	(lb/s)
T_{RM}	=	temperature of the riser metal tube	(^oF)
T_{RO}	=	temperature of the mixture at the riser outlet	(^oF)
h_{SV}	=	enthalpy of the saturated vapour	(Btu/lb)
ρ_{SV}	=	density of the saturated vapour	(lb/ft^3)
M_W	=	metal mass of the risers	(lb)
C_W	=	specific heat of the riser metal	(Btu/lb $,^oF$)
Q_{GW}	=	heat rate input from the gas to the riser tubes	(Btu/s)
k_{RW}	=	heat transfer coefficient	
k_{RS}	=	heat transfer coefficient	

Drum

ρ_{DW}	=	density of the water in the drum	(lb/ft^3)
h_{DW}	=	enthalpy of the water in the drum	(Btu/lb)
W_{SD}	=	steam flow rate out of the drum	(lb/s)
h_{SD}	=	enthalpy of the steam in the drum	(Btu/lb)
ρ_{SD}	=	density of the steam in the drum	(lb/ft^3)
P_{SD}	=	steam pressure in the drum	(psi)
V_{DR}	=	total volume of the drum	(ft^3)
V_{DW}	=	volume of the drum occupied by water	(ft^3)
C_D	=	drum time constant	(s)
T_{SD}	=	steam temperature in the drum	(^oF)

<u>Radiant Superheater</u> (RSH)

P_{RSHO}	=	steam pressure at the RSH output	(psi)
W_{RSHO}	=	steam flow rate at the RSH output	(lb/s)
ρ_{RSHO}	=	steam density at the RSH output	(lb/ft^3)
h_{RSHO}	=	steam enthalpy at the RSH output	(Btu/lb)
T_{RSHO}	=	steam temperature at the RSH output	(^oF)
f_{RSH}	=	friction coefficient of the flow in the RSH	
V_{RSH}	=	RSH storage volume	(ft^3)
Q_{RSH}	=	heat transfer rate by convection from metal to steam	(Btu/s)
Q_{GRSH}	=	heat transfer rate by radiation from gas to the metal tube	(Btu/s)
T_{RSHM}	=	temperature of the metal tubes	(^oF)
M_{RSH}	=	mass of the RSH metal tubes	(lb)
C_{RSH}	=	specific heat of the RSH metal	(Btu/lb ^oF)
k_{RSH}	=	heat transfer coefficient	
k_{RSH1}	=	heat transfer coefficient	

<u>Primary Superheater</u> (SH)

P_{SO}	=	steam pressure at the SH output	(psi)
W_{SO}	=	steam flow rate at the SH output	(lb/s)
ρ_{SO}	=	steam density at the SH output	(lb/ft^3)
h_{SO}	=	steam enthalpy at the SH output	(Btu/lb)
T_{SO}	=	steam temperature at the SH output	(^oF)
f_{SH}	=	friction coefficient of the flow in the SH	
V_{SH}	=	SH storage volume	(ft^3)
Q_{SH}	=	heat transfer rate by convection from metal to steam	(Btu/s)
Q_{GSH}	=	heat transfer rate by convection from gas to metal	(Btu/s)
T_{SHM}	=	temperature of the SH metal tubes	(^oF)
M_{SH}	=	mass of the SH metal tubes	(lb)
C_{SH}	=	specific heat of the SH metal	(Btu/lb ^oF)
T_{GSH}	=	temperature of the flue gas leaving the SH	(^oF)
C_{GSH}	=	specific heat of the flow gas leaving the SH	(Btu/lb ^oF)
k_{SH}	=	heat transfer coefficient	
k_{SH1}	=	heat transfer coefficient	

Secondary Superheater (SSH)

P_T	=	steam pressure at the SSH output (or at the throttle valve)	(psi)
P_{SSI}	=	steam pressure at the SSH output	(psi)
W_{SSI}	=	steam flow rate at the SSH input	(lb/s)
W_T	=	steam flow rate at the SSH output (or at the throttle valve)	(lb/s)
ρ_{SS}	=	average steam density in the SSH	(lb/ft^3)
ρ_{SSI}	=	average steam density at the SSH input	(lb/ft^3)
h_{SS}	=	average steam enthalpy in the SSH	(Btu/lb)
h_{SSI}	=	steam enthalpy at the SSH input	(Btu/lb)
h_{SSO}	=	steam enthalpy at the SSH output	(Btu/lb)
T_{SSO}	=	steam temperature at the SSH output	(^oF)
f_{SS}	=	friction coefficient of the flow in the SSH	
$\bar{T}_{SS}$	=	average steam temperature in the SSH	(^oF)
Q_{SS}	=	heat transfer rate from gas to steam	(Btu/s)
M_{SS}	=	"effective mass" of the SSH	(lb)
V_{SS}	=	SSH storage volume	(ft^3)
M_{MSS}	=	metal mass of the SSH	(lb)
T_{SSM}	=	metal temperature of the SSH tubes	(^oF)
$\bar{C}_{SS}$	=	average specific heat of the steam in the SSH	(Btu/lb ^oF)
C_{MSS}	=	specific heat of the SSH metal	(Btu/lb ^oF)
W_{SHS}	=	spray attemperator flow rate	(lb/s)
T_{GSS}	=	temperature of flue gas leaving the SSH section	(^oF)
C_{GSS}	=	specific heat of flue gas leaving the SSH section	(Btu/lb ^oF)
k_{RSS}	=	heat transfer coefficient	

Reheater (RH)

P_{TO}	=	pressure at the HP turbine output	(psi)
P_{RO}	=	pressure at the RH output	(psi)
W_{RI}	=	steam flow rate at the RH input	(lb/s)
W_{RO}	=	steam flow rate at the RH output	(lb/s)
W_{TO}	=	steam flow rate at the HP turbine output	(lb/s)
ρ_{RO}	=	steam density at the RH output	(lb/s)
h_{RO}	=	steam enthalpy at the RH output	(Btu/lb)
T_{RO}	=	steam temperature at the RH output	(^oF)
h_{TO}	=	steam enthalpy at the HP turbine output	(Btu/lb)

f_R	=	friction coefficient of the flow in the RH	
V_R	=	RH volume	(ft^3)
Q_{RH}	=	heat transfer rate by convection from metal to steam	(Btu/s)
Q_{GRH}	=	heat transfer rate by convection from gas to metal	(Btu/s)
T_{RHM}	=	RH metal temperature	(^oF)
M_{RH}	=	RH metal mass	(lb)
C_{RH}	=	specific heat of the RH metal	(Btu/lb ,^oF)
k_R	=	heat transfer coefficient	
T_{GRH}	=	temperature of flue gas leaving the RH section	(^oF)
C_{GRH}	=	specific heat of flue gas leaving the RH section	(Btu/lb ,^oF)
k_{RH}	=	heat transfer coefficient	

Air-Fuel Section

W_{FD}	=	fuel flow rate into the pulveriser	(lb/s)
L_F	=	feeder stroke (control signal)	
M_{CR}	=	mass of fuel in the pulveriser	(lb)
W_{OUT}	=	fuel flow rate out of the pulveriser	(lb/s)
W_{FI}	=	fuel input into the burners	(lb/sec)
A	=	power in forced draught fan	
W_A	=	air flow rate input into the burners	(lb/s)
T_p	=	fuel pipe time constant	(s)
T_{AA}	=	forced-draught fan and/or damper time constant	(s)

Combustion-Furnace

W_{GF}	=	total gas flow rate	(lb/s)
T_G	=	temperature of the gas in the furnace	(^oF)
W_{ash}	=	percentage of the fuel lost as ash	(lb/s)
T_A	=	temperature of the air coming into the burners	(^oF)
F	=	heating value of the used fuel	(Btu/lb)
n	=	burner combustion efficiency	
C_{GF}	=	specific heat of gas in the furnace	(Btu/lb ,^oF)
T_{out}	=	temperature of gas leaving the furnace	(^oF)

Hydro-Plant

L_2	=	tunnel length	(ft)
A_2	=	tunnel cross-section area	(ft^2)
V_2	=	tunnel water velocity	(ft/s)

Q_2	=	tunnel volumetric water flow	(ft^3/s)
A_S	=	surge tank cross section area	(ft^2)
V_S	=	water velocity in surge tank	(ft/s)
Q_S	=	surge tank volumetric water flow	(ft^3/s)
L_1	=	penstock length	(ft)
A_1	=	penstock cross section area	(ft^2)
V_1	=	water velocity at the turbine entrance	(ft/s)
Q_1	=	penstock volumetric water flow	(ft^3/s)
H_T	=	pressure head at the turbine entrance	(ft)
V_{S1}	=	water velocity at the beginning of the penstock	(ft/s)
H_{S1}	=	pressure head at the base of the surge tank or the beginning of the penstock	(ft)
V_{S2}	=	water velocity at the tunnel intake	(ft/s)
H_S	=	water head in the surge tank	(ft)
H_{SS}	=	head available at the surge tank at S.S.	(ft)
H_R	=	head at the forebay	(ft)
P_{TI}	=	mechanical power at the turbine	(MW)
G	=	valve (gate) position - normalized	
R	=	valve acceleration - normalized	
D_N	=	frequency error (f_{ref}-f), in p.u.	
σ	=	permanent droop	
δ	=	transient drop	

Variable-Pressure Boiler Model

PED	=	electrical output demand	expressed in p.u.
ATREF	=	valve-opening set-point	expressed in p.u.
PTDES	=	pressure set-point	expressed in p.u.
WTI	=	desired steam flow	expressed in p.u.
DF	=	nominal regulation	expressed in p.u.
TWT TAT TFR	=	time constants as shown in Fig. 5.2	
ADPE	=	additional changes in demand	

Note

It must be noted that, in the Figures, the variables are printed in a linear fashion to correspond to the computer output; for example:

$A_T \longrightarrow$ AT

and $W_{SD} \longrightarrow$ WSD.

UNIT CONVERSION TABLE

Variable		S.I.	Conversion factor
Density	lb/ft^3	Kg/m^3	1 (lb/ft^3) = 16.016949 (Kg/m^3)
Flow Rate	lb/sec	Kg/s	1 (lb/sec) = 0.453592 (Kg/s)
Enthalpy	Btu/lb	Kcal/Kg	1 (Btu/lb) = 0.555556 (Kcal/Kg)
Temperature	^oF	^oC	$T_F = (9/5).T_C + 32$
Volume	ft^3	m^3	1 (ft^3) = 0.02832 (m^3)
Mass	lb	Kg	1 (lb) = 0.453592 (Kg)
Heat Flow Rate	Btu/sec	KJ/s	1 (Btu/sec) = 1.054852 (KJ/s)
Specific heat	Btu/lb, ^oF	Kcal/Kg, grad	1 (Btu/lb, ^oF) = 0.308642 (Kcal/Kg,grad)
Length	ft	m	1 (ft) = 0.3048 (m)
Area	ft^2	m^2	1 (ft^2) = 0.0929 (m^2)
Pressure	psi	Newton/m^2 or Bar	1 (psi) = 0.069 x 10^5 (N/m^2) = 0.069 (Bar)
Acceleration	ft/sec^2	m/s^2	1 (ft/sec^2) = 0.3048 (m/s^2)
Velocity	ft/sec	m/s	1 (ft/sec) = 0.3048 (m/s)

LIST OF TABLES

CHAPTER ONE

INTRODUCTION

1.1 OVERVIEW OF THE POWER GENERATION PROBLEM

The use of steam to drive a turbine for production of electricity is established worldwide. Thus a great deal of effort was put into the research and the development of every component of the power plant, from their original design. As a result, there has been a dramatic increase in the capacity of the turbines, boilers and generating units from a few hundred kilowatts up to 660 MW. The advances in the technology in fields such as metallurgy, welding, cooling etc. made possible the use of cycles with high pressures and temperatures. At the same time, the size of the units was increased and the trend is towards units rating above 1000 MW.

Equally well established is the use of hydro plants, in places where the terrain favours such schemes. The potential and the kinetic energy of the water were used for the production of work for hundreds of years. But again, it was during this century that it was made possible to extract this energy with greater efficiency with hydro-units producing electricity. The high capital cost of their construction is greatly offset by the cheap energy produced. Their flexibility is valuable in the operation of the power system of which the power plant is a part. Inevitably the size of the hydro generators is increasing, with units of 600 MW already installed (as in Grand Coulee power complex in the U.S.A.) and others of greater capacity being planned.

The nuclear energy came in the scene increasingly during the last 20 years. Reactors of various kinds came into operation around the world, supplying base loads. The U.K. was one of the countries which adopted the new technology very early and has been among the leaders since. Its first nuclear program with the series of Magnox reactors has come to an end successfully. The Advanced Gas-Cooled reactor was adopted for the second nuclear program. Also, the Steam-Generating Heavy Water Reactor system (SGHWR) is under development.

The escalation of the fossil fuel prices during the last four years brought a completely new situation in short- and long-term planning in the power industry. Countries reluctant to embark upon large scale nuclear programs were led to the decision to build more nuclear stations. More effort was directed towards exploiting the water resources by building more hydro stations. Of course, the problem is not the same in every country. Countries like Norway and Brazil have the benefit of cheap electricity from their hydro plants. In England the alternative is nuclear stations and coal-fired plants as long as the production of coal remains competitive. All these alternatives have to be given careful consideration, since the economic incentive to do so is large.

Coming down to the operational aspect of the power system, it is clear that the kind of plants involved determines operational and control policies. Many questions have to be asked and options to be studied. Which units will be run base-loaded? How will the peak load be met? Will it be by a pumped-storage, a normal hydro-station or gas turbines? If plants are operated at variable pressure, will they be used or are they base-loaded because of their large capacity? Emphasis must be given to different points and details in each case.

At the local level the control and management problems are increasing with the size and the complexity of both the plant and the process. An improvement in the burning efficiency of the boiler by 1-2% results in substantial savings with today's prices. Therefore the incentive to study also the details of the process exists. In the last 10-15 years the controllers in the power plants were developed substantially. The analog PID controller still reigns supreme, but the all-digital control loops are beginning to be applied with increased confidence.

The digital computer presents the planner, the designer and the researcher with a powerful tool. The need to rethink the overall operational strategies and the need to improve the efficiency and the safety of the local plant, dictate that this tool must be used to its maximum advantage. Therefore techniques and methods must be further developed towards this goal.

1.2 THE ROLE OF SIMULATION

Simulation in various forms is used in almost every field of human activity. Its use in the field of power engineering is dictated by the nature of the processes involved and its applications cover a wide spectrum.

As was mentioned in the previous section, there is a variety of power plants with different economic and operational constraints. The planner of a new power system or of an extension to an existing one, must study all the possibilities and evaluate the alternative solutions beforehand. A model or a representation has to be devised which will give him a view of the system's behaviour so that its performance can be judged speedily. So simulation is an important element in planning, because it helps to eliminate unfavourable solutions which would prove very costly to implement.

From the operational standpoint, the control engineer of an area and the operator in the plant, need to be advised and quickly understand the implications of their actions. A model of their respective process will provide them with information cheaply and without delay.

For an engineer who will be given the responsibility of supervising and running a big plant, it is very important that he should have a fundamental understanding of the job. No better place to acquire this experience at low cost and without risk exists,than a simulator giving roughly the same response of the real system. So training of engineers is another field in which simulation plays a key role.

There are several levels of simulation. For the study of the behaviour of a whole area, only the gross behaviour of a power plant is needed. For the design of a control loop, the detailed representation must be made of the part of the process involved. Simulation of parts of the power system has been a practice for many years, starting with the network analyser, the analog computer and finally the digital computer. Analog simulation might mean analog computer, micromachines, electronic circuits or even entire old small power stations. Analog and digital techniques have their advantages and disadvantages and must be applied accordingly. It can be said therefore that the simulation plays a fundamental role in the design, operation and control in the power industry.

1.3 SIMULATOR HARDWARE

The simulator built at Imperial College aims at the study of a small power system inside the 1 second to 20 minutes time span[1]. It is designed to accommodate:

- 6 generating units,
- 10 transmission lines,
- 4 transformers,
- 16 circuit breakers,
- 5 load units.

All these sections were simulated in analog form using electronic circuits. The reason for this was that, to simulate digitally fast dynamics, a very small integration step is required by the numerical methods. Otherwise the model gives an unstable response. But small integration step means a lot of computation time. Therefore such technique would not be suitable for a real-time application, for which the simulation was intended. The whole arrangement is connected via a specially designed interface to a D.E.C. PDP-15 computer.

The construction of the generating units follows two principles, resulting in two different designs. The first was an EMF behind a synchronous reactance[2]. In this, the magnitude of the EMF is determined by an AVR and the frequency is determined by the speed governor. In the second, the synchronous machine is represented according to the two-axis principle using Park's equations. This was developed by Giles[3]. A Voltage-Controlled Oscillator (VCO) is at the heart of both designs. Its sinusoidal output is fed into the machine representation. The prime mover dynamics are included. Their input signal is the steam flow. Their output is the mechanical power, which is fed into the main integrator to solve the equation of motion. The first design was used to test the models developed in this thesis. The block diagram of this generating unit is shown in Fig. 2.2a.

For the transmission lines a lumped π representation was used. They were made to represent single circuit 132 KV lines[3]. Voltage and current transducers are provided at the end of each line. Their outputs are taken to a measurement panel, to provide the voltage and power flows of each line. The same technique is used for voltage and current measurements of the four tap-change transformers.

The circuit breakers are represented by electromechanical switches. They can be operated either manually or by the digital computer, by which their current status is continually monitored.

The load units were built as sinks of in-phase current and sinks or generators of quadrature (with the terminal voltage) current. The reference values of the two currents are set by two d.c. control signals. They can be operated manually or by the digital computer. Their voltage and frequency characteristics are specified for small variations of those two quantities. The loads were designed to represent bulk supply points within the power system.

The interface consists of a control unit which switches the measurement and control voltages to and from the PDP-15 interface (i.e. the ADC's, DAC's and the digital I/O unit). It contains also timing facilities and some analog circuitry, for the conversion of raw model data into derived quantities of standard voltage levels. There are 96 analog inputs to the computer, multiplexed to 6 channels, fed into the A/D converters. 64 analog outputs coming out of the D/A converter are demultiplexed from 4 channels. Of them, 24 are stored in zero order holds.

There are 64 bits of digital input/output information. They are contained in groups of 16 in four 18-bit words of the PDP-15. They are multiplexed to the digital I/O unit. A status discrepancy bit in the first of those words is set when the status of any of the digital inputs changes.

The model-computer arrangement described up to this point is shown in Fig. 1.1. The interface can be operated manually and also by the digital computer.

The PDP-15 computer has 24k of memory and 250k of mass storage on two fixed head disks. Their access time is 20 ms. The word length is 18 bits and the core cycle time 0.8 microseconds.

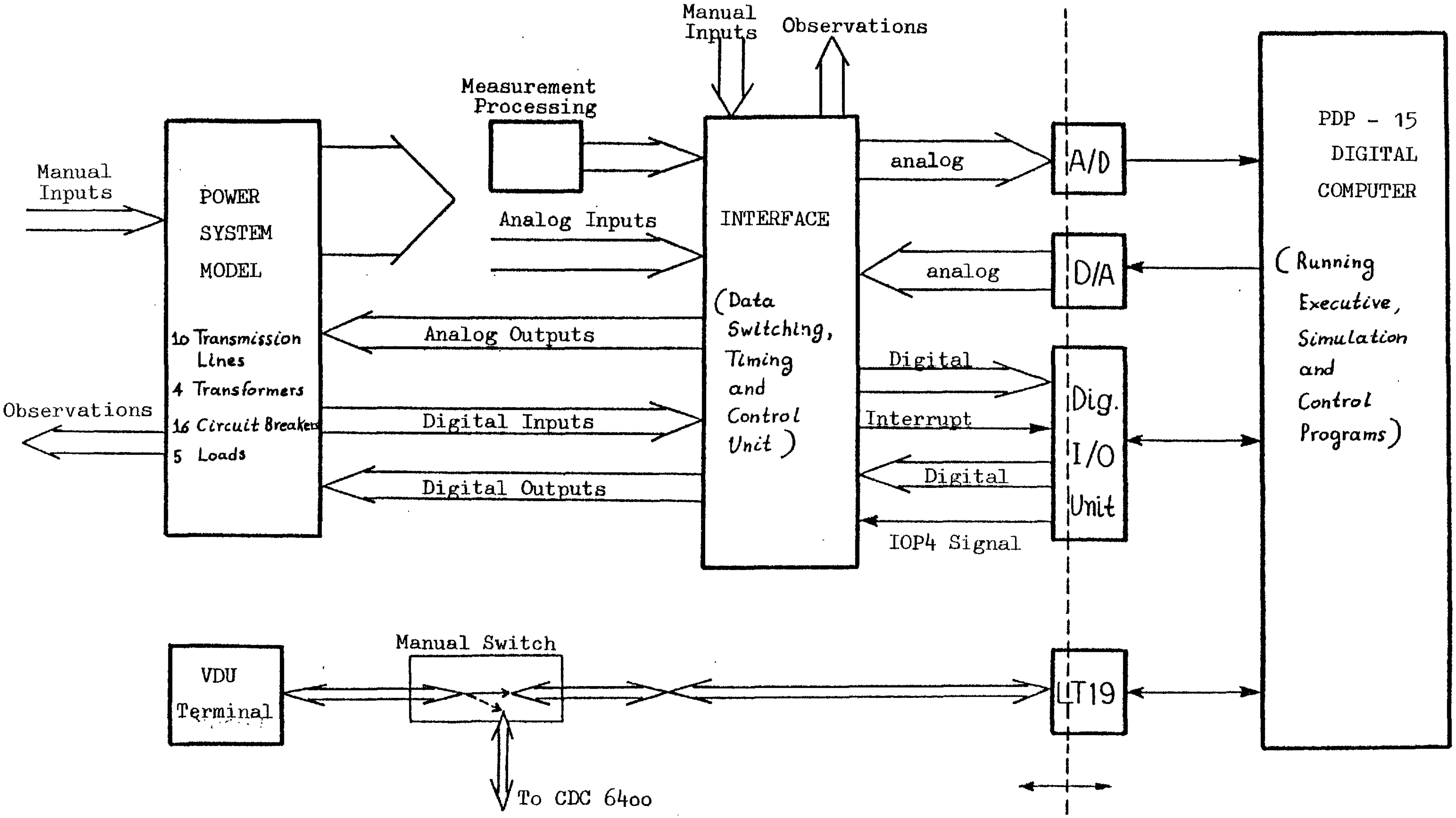

Fig. 1.1 Data flow in the computer simulator system.

The peripherals include a twin Dectape unit, a serial printer and a console teletype (KSR-35), which provides the main means of communication between the operator and the machine. A Tektronix 4010 VDU is connected in parallel with this teletype. In addition, a Hazeltine 2000 character display unit is connected via the LT19 peripheral interface of the computer. This unit is situated by the simulator on level 8 of the building, while the computer and its other peripherals are three floors below, on level 5.

Finally, a 10 bit accuracy is used by the A/D converter which has a variable accuracy from 6-12 bits. The conversion time is 18 μs and the accuracy 0.1%. The D/A converter used also 10-bit accuracy. The details of the various computer sections can be found in the DEC manuals.

1.4 THE SOFTWARE

There are three operating systems that can be used on the computer. The main system is the DOS-15 (Disk Operating System). The Advanced Monitor System is similar to DOS-15, with the difference that it provides the facilities of task building (more details in Section 2.6.1). Facilities for compiling, assembling, editing etc. are included in both these systems. They are provided by the computer manufacturer together with other standard software.

None of the above systems is suitable for real-time operation. This gap is filled by the RSX Phase 1 Real-Time System. It has the facilities of scheduling, I/O supervision, resource allocation and operator communication. But no editing, compiling or assembling can be done. These facilities are provided by the DOS-15 and the Advanced Monitor.

The basic data acquisition software was developed by Mogridge[4]. It provides the means of communication between the analog and the digital parts of the simulator, with:

- an analog input program (ANIN2) - executed every 100 ms,
- an analog output program (ANOUT) - executed every 400 ms,
- a digital input program (DIGIN) - executed every 200 ms.

and relevant start and stop programs. Mogridge has also written the basic logging and monitoring programs.

Further development of software was done for analysis, control and simulation. The part related to the digital simulation of power plants is described in this thesis.

1.5 THE WORK IN THE THESIS

As was mentioned in Section 1.1, the primary function of the simulator is to represent the behaviour of a power system several minutes after the occurrence of a disturbance. But long-term phenomena are determined (apart from the responses of the loads and the transmission equipment) by the prime-mover storage times. Therefore the simulator would not be complete without the inclusion of the plant dynamics.

It was decided that the model of the boiler would be implemented digitally. The long time constants involved in this process make its analog representation no simple matter, with problems of drift in the electronic circuits. In Chapter 2 the development of this model is described. Boiler models of various degrees of complexity can be found in the literature. A survey is presented of the most common ways of simulating the various sections of the process. However, the majority of these models are not suitable for real-time operation. The constraints on processor time and core usage are present in every real-time application, but they are aggravated by the idiosyncrasies of the specific project in hand. Therefore a balance had to be struck between the size and complexity of the model, in which a number of non-linearities are included.

The discretization of the continuous time equations was made using the Z-transform theory. It has the advantage of greatly reducing the computational effort needed, without marked deterioration in the response quality of the model. The initial evaluation of the model was done off-line and the steps are described. Finally, its performance in real-time was tested and some typical responses are shown and discussed. A comparison was also made between the non-linear model and its linearised version.

Chapter 3 gives an account of the development and testing of the steam side of a nuclear plant. A High Temperature Gas-Cooled reactor plant was used, since it is the main type of reactor used in the U.K. This choice also had the advantage that the secondary cycle is the same as that of a conventional plant. So only the control structure had to be changed. The development followed the steps of Chapter 2. The model was made to run both in regulating and non-regulating mode.

It was thought that the inclusion of different types of plant would enhance the flexibility of the simulator. For this reason, a digital hydro-plant model was also developed, as is described in Chapter 4. Its output is the mechanical power. It also uses the same analog representation of the generating unit as the previous two models.

Chapter 5 discusses the operational characteristics of a conventional plant, when it is operated in the variable-pressure mode. A relatively simple control scheme was developed. The response of the model to frequency and demand changes is presented and discussed. This mode of operation was given increased attention by various countries in the last few years.

The software related to these models is discussed in Chapter 6. The structure of the different initialization programs is presented and a comparison of the processor usage by the simulation programs is made.

Finally, in Chapter 7 the conclusions on this work are summarised and some views are given on future development and research work on the simulator.

CHAPTER TWO

CONVENTIONAL STEAM PLANT

2.1 THE PROCESS

The generation of steam to drive a turbine is the most widely used and established method of producing electrical energy. The boiler is the device which turns the water into steam since the first applications. The boilers used in power plants have come a long way as far as their design, size, operating regime and consequent sophistication are concerned[5,6]. The beginning of this century saw a rapid increase in operating steam pressures and temperatures up to 1200 psi and 700°F (700°F reheat)[6]. The capacity of the units built was becoming larger all the time and above 10^6 (lb/hr) the chain grate firing proved to be uneconomical. Therefore pulverised-coal firing was developed and with it came the water-cooled furnaces, both of which gave another boost to the design of larger units. At present, large units of 600-660 MW size, with pressures at the turbine stop valve around 2300 psi and temperatures of 1000-1055°F at the superheater outlet (1005°F at the reheater outlet) are operating and there is no doubt that units above 1000 MW will soon become common.

According to the kind of path which the operating fluid (water and steam) is following into the boiler, three types of units can be distinguished, namely: a) natural circulation, b) re-circulation, and c) once-through. The latter two can also be classified under the heading of "forced circulation systems" (as opposed to the "natural circulation" ones). On the other hand, the first two can be classified under the heading of "drum-type" systems.

2.1.1 Drum-type Boilers

An outline of the main components in a typical unit is shown in Fig. 2.1. On the same figure is shown a (T,S) diagram with the Rankine cycle.

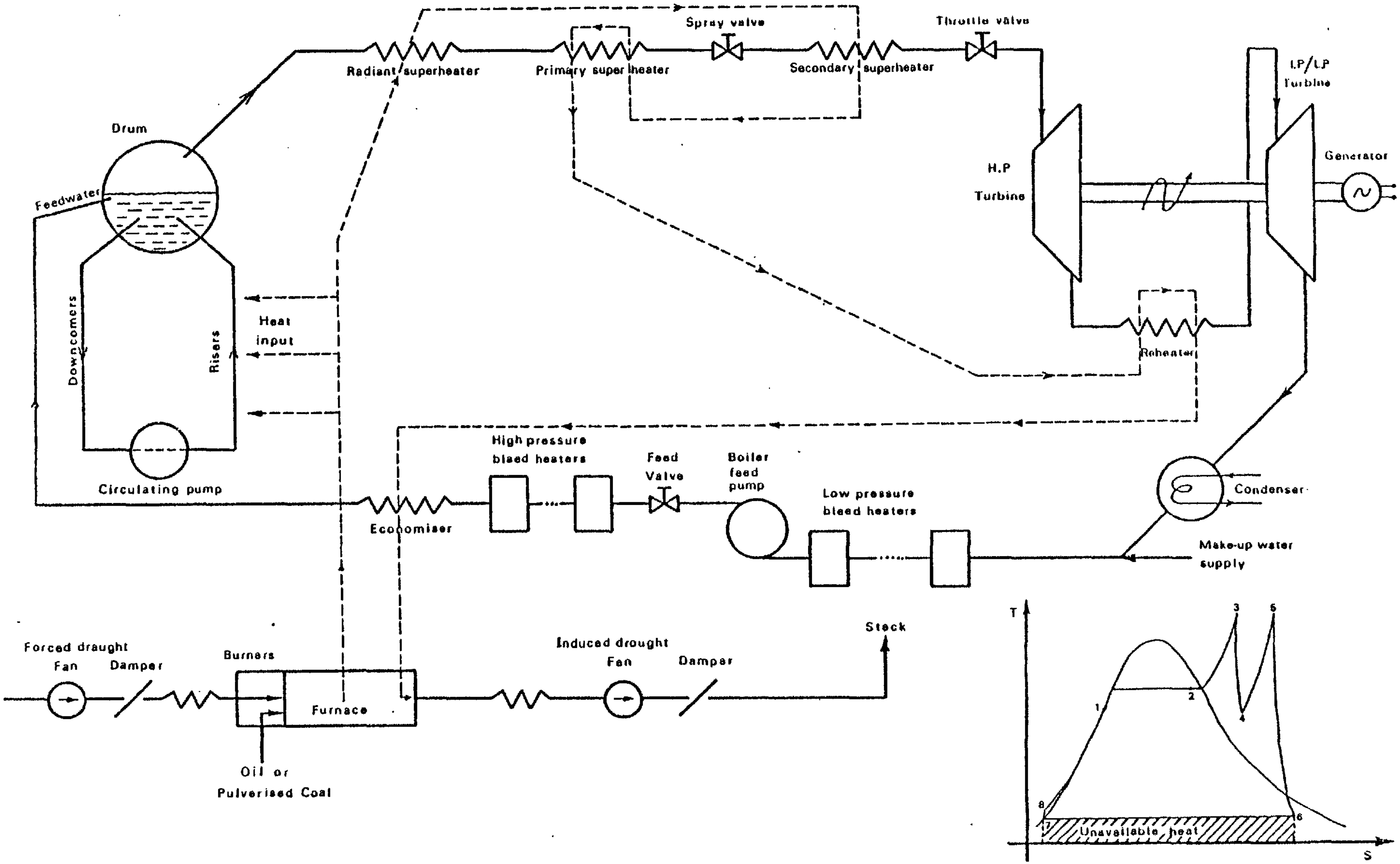

Fig. 2.1 Outline of a typical drum-type boiler unit.

Starting at point 1 on the Rankine cycle, the state of the feedwater going into the drum is saturated liquid and in the drum it coexists with the steam. In general, the water entering the circuit is in excess of the steam produced and therefore a drum is required for the steam separation. In it, the two phases of the fluid coexist. The saturated water goes through the downcomers to the risers, which are tubes heated externally by the furnace. In them, the water starts boiling and the mixture enters again the drum where the steam separation is completed. At this point, the steam is still wet, having, for example, a dryness of 80-90% and this state can be represented by point 2 on the cycle.

There are two ways in which the water from the downcomers can enter the risers: a) through a circulating pump, which pumps it up to the risers, leading to "forced circulation" of the water; and b) without a pump, where the circulation is ensured from the difference in density between the mixture in the risers and the saturated water in the downcomers. This is the case of the so-called "natural circulation", where the circulation increases as the heat input increases. At the same time the friction along the path of the flow increases. Also as the operating pressure increases, the density difference between the two phases decreases. Both these factors reduce the efficiency of the natural circulation system. In general, for pressures above 2900 psi, forced circulation becomes increasingly economical.

The wet steam which leaves the drum enters the superheater (SH) section. There might be different subsections like a radiant SH section, primary SH and secondary SH. In the SH the steam is heated further from heat released by the flue gas, as it passes through. As a result, the steam becomes completely dry, its temperature rising all the time. At the SH output, its state can be represented by point 3 on the cycle. From there the superheated steam enters the HP section of the turbine, where it expands, producing work.

At the output of the HP section of the turbine, the condition of the steam is described by point 4 and at this stage it enters the reheater (RH) section. There it is heated once more by the flue gases up to a temperature more or less similar to the one at the SH output from which (point 5) it enters the IP-LP section of the turbine for the final expansion, thus producing additional work.

The fluid at the turbine output (point 6) is wet steam again, and as such it enters the condenser where heat is rejected, converting it to water (point 7). This goes through the feedwater pump and is compressed to a higher pressure (point 8). From then on, heat is added to the water by the feedheaters (heated with steam extracted at various stages in the turbine) and the economizer (heated by the flue gas before it exits from the stack). This heat brings the water near to saturation and as such it enters the drum, thus completing the cycle.

The furnace can be fired with pulverised-coal, oil or gas. The forced draught fans (Fig. 2.1) provide the necessary air to produce the correct air-fuel mixture for the burners. The induced-draft fans ensure that the pressure in the furnace is kept at a predetermined level.

2.1.2 Once-Through Boilers

Once-through boiler is a forced-circulation system, with the working fluid pumped continuously into the boiler by the feedpump. There is no re-circulation. The fundamental difference between this type of boiler and the drum-type is that here, the heating of water, the steam separation and the superheating take place along the length of the circuit as the fluid goes through it. It can, therefore, be represented as a tube which receives water at one end and produces superheated steam at the other. So drum is not needed, which is an economical advantage. In addition, no pressure restriction is imposed so the boilers of this type can operate at supercritical pressures as well, thus producing greater cycle efficiency. They can also be operated at subcritical pressures.

The feedwater pump is an element of primary importance and its function has to be controlled with precision, because the feedwater flow is a direct function of the load. This means that a once-through boiler can accomplish rapid load changes. This is of great benefit in the effort to match the generation to the demand. On the other hand, the absence of the drum reduces the amount of stored energy in the system. This requires very sophisticated emergency controls, because in the event of feedpump failure the water in the circuit will evaporate very rapidly (e.g. in two minutes).

Once-through boilers are used extensively with large generating units and for this reason they are operated base-loaded most of the time. However, their ability to follow rapid load changes makes them a very useful tool during emergencies.

2.2 MODELLING OF A DRUM-TYPE BOILER

The development of controllers and control techniques for the process of steam generation in power plants requires a good understanding of the mechanisms and dynamics involved and the physical constraints of the operation. Consequently, a mathematical model describing the process or its main characteristics becomes necessary. Chien et al[7] published one of the first comprehensive studies towards this direction and many others followed[8-24].

The main events in the behaviour of a boiler unit can be approximated by non-linear partial differential equations containing partial derivatives of time and space, i.e.

$$f(x,y,z \;\ldots\; \frac{\partial x}{\partial t}, \frac{\partial x}{\partial \ell}, \frac{\partial y}{\partial t}, \frac{\partial y}{\partial \ell}, \;\ldots) = 0 \qquad (2.1)$$

where: x,y,z - functions of t and ℓ,
$(\partial x/\partial t)$- time derivative,
$(\partial x/\partial \ell)$- spatial derivative.

Clearly the solution of a large number of equations of this kind is not an easy task. Enns[9] showed that for flow rate and heat addition transients, the use of a lumped-parameter representation gives almost as good results as the distributed-parameter one (which involves partial differential equations). Therefore, the first simplifying assumption to be made (and which is common to most of the literature) is to consider that the process consists of a number of "lumped" sections (economizer, superheater, reheater, drum, etc.). In each section the properties of the working fluid are assumed to vary only along its length and linearly with space.

Denoting the length of each section as L and x_1, x_2, y_1, y_2, ... the values of the variables x,y,... at the beginning and at the end of the section length L respectively, the partial derivatives can be written as:

$$\left(\frac{\partial x}{\partial \ell}\right) = \frac{x_2-x_1}{L}, \quad \left(\frac{\partial y}{\partial \ell}\right) = \frac{y_2-y_1}{L}, \ldots \tag{2.2}$$

so only ordinary differential equations remain.

The values of x,y,z,... can be chosen at any point along the length L, with the points at the beginning, the end and the middle being the most common. These choices are known as forward, backward and central difference methods of finite representation. The backwards difference method is considered to be the most satisfactory while the forward difference method produces unstable results[9,16] (Chien[7], however, used the second one). So equation (2.1) can be written as:

$$f\left(x_2, y_2, z_2, \ldots, \frac{dx_2}{dt}, \frac{x_2-x_1}{L}, \frac{dy_2}{dt}, \frac{y_2-y_1}{L}, \ldots\right) = 0 \tag{2.3}$$

where: x_i, y_i, z_i are all functions of time only.

In the following, the most significant "lumped parameter" sections of the process are examined.

Economizer

Mass and energy balance equations are written for the economizer section. The water density is considered to be varying only with temperature and not with pressure[16]. Others consider the water incompressible[7,8] or do not include the description of the economizer, claiming that the added complexity to the model is not justified by its inclusion[17]. So the equations are:

Mass balance (fluid) : $(W_{EI}-W_{EO}) = V_E \cdot \frac{d}{dt}(\rho_{EO})$ (2.4)

Energy balance (fluid): $(W_{EI} \cdot h_{EI}+Q_E-W_{EO} \cdot h_{EO}=V_E \cdot \frac{d}{dt}(\rho_{EO} \cdot h_{EO})$ (2.5)

Energy balance (metal): $(Q_{GE}-Q_E) = M_E \cdot C_E \cdot \frac{d}{dt}(T_{EM})$ (2.6)

where : $Q_E = K_E \cdot W_{EO}{}^{0.8} \cdot (T_{EM}-T_{EO})$ (2.7)

Equation (2.7) represents the heat rate transfer from the metal tube to the (turbulent) fluid inside it by convection. It is an empirical expression[25] widely used in the literature.

Downcomers-Risers

For natural or forced circulation it is assumed that no heat is induced on the downcomers, so that boiling takes place only in the risers. For forced circulation it is assumed that there is no mass or energy storage in the downcomer circuit[8,17]. This is not the case for natural circulation[16], although storage can be neglected even here for simplicity.

The total circulating flow can be considered constant in the forced circulation case, with the feedwater flow determining the trend in the drum water level. In the natural circulation case, entrance and exit losses are taken into account. Therefore two sets of equations are:

Forced circulation

Energy balance: $W_D \cdot h_D = (W_D-W_{EO}) \cdot h_{DW}+W_{EO} \cdot h_{EO}$:- for the downcomers (2.8)

Energy balance: $Q_W = W_D \cdot (h_m-h_D)$ – for the risers (2.9)

where: $h_m = x \cdot h_D+(1-x) \cdot h_{DW}$

and: $Q_W = k_{RS} \cdot (T_{RM}-T_{SD})^3$ (2.10)

is the heat rate input from the metal to the boiling water in the riser tubes. Finally:

Energy balance (metal): $(Q_{GW}-Q_W) = M_W \cdot C_W \cdot \frac{d}{dt}(T_{RM})$ (2.11) where it is assumed that the energy added to the fluid by the circulating pumps can be neglected.

Natural Circulation

In this case the difference between the gravity heads (pressure in ft. of standard water) of the downcomers and the risers equals the circulation losses in the system. So:

Momentum equation (downcomers):

$$(P_{DR}-P_{DO})=\underbrace{\left(\frac{f_D L_D W_{DI}^2}{g d_D A_D^2 \rho_{DR}}\right)}_{\text{Pressure loss due to friction}}+\underbrace{\frac{1.W_{DI}^2}{2gA_D^2\rho_{DR}}}_{\text{Entrance loss}}-\underbrace{\rho_{DR}L_D}_{\text{Gravitational head}}+\underbrace{\frac{L_D}{gA_D}\cdot\frac{d}{dt}(W_{DI})}_{\text{Inertia loss}} \qquad (2.12)$$

Mass balance (downcomers):

$$(W_{DI}-W_{DO}) = V_D\cdot\frac{d}{dt}(\rho_{DO}) \qquad (2.13)$$

Energy balance (downcomers):

$$W_{DI}\cdot h_{DR} - W_{DO}\cdot h_{DO} = V_D\cdot\frac{d}{dt}(\rho_{DO}\cdot h_{DO}) \qquad (2.14)$$

and if the downcomer storage volume V_D is considered to be negligible, the last two equations give:

$$W_{DI} = W_{DO}, \qquad h_{DO} = h_{DR}.$$

In a similar fashion the equations for the risers are:

Momentum equation:

$$(P_{DO}-P_{IR})=\left(\frac{f_R L_R W_{RO}^2}{g d_R A_R^2 \rho_{RO}}\right)+\frac{1}{2gA_R^2}\cdot\frac{W_{RO}^2}{\rho_{RO}}+L_R\cdot\left(\frac{\rho_{RO}+\rho_{DO}}{2}\right)+\left(\frac{1\cdot W_{RO}^2}{gA_R^2\rho_{RO}}-\frac{1\cdot W_{DO}^2}{gA_R^2\rho_{DO}}\right)+$$

$$+\frac{L_R}{gA_R}\cdot\frac{d}{dt}(W_{RO}) \qquad (2.15)$$

Pressure loss due to friction + Entrance loss + Gravitational head + Acceleration loss + Inertia loss

Mass balance:

$$(W_{DO}-W_{RO}) = V_R\cdot\frac{d}{dt}(\rho_{RO}) \qquad (2.16)$$

Energy balance:

$$W_{DO}\cdot h_{DO} + Q_W - W_{RO}\cdot h_{RO} = V_R\cdot\frac{d}{dt}(\rho_{RO}\cdot h_{RO}) \qquad (2.17)$$

$$\text{where:} \quad (1/\rho_{RO}) = (x/\rho_{SV}) + ((1-x)/\rho_{DW}) \tag{2.18}$$

$$h_{RO} = x.h_{SV} + (1-x).h_{DW} \tag{2.19}$$

$$\text{and:} \quad Q_W = k_{RS}.(T_{RM} - T_{RO})^3 \tag{2.20}$$

$$\text{Energy balance (metal):} \quad (Q_{GW} - Q_W) = M_W.C_W.\frac{d}{dt}(T_{RM}) \tag{2.21}$$

Drum

Here it is assumed that there is no temperature gradient in the vapour phase and that there is a uniform temperature corresponding to the saturation condition under the drum pressure. Also, there is no temperature gradient in the liquid phase, except through a very thin layer at the liquid surface because of the turbulence in the drum.

The equations of mass and energy conservation can be written either separately for the two phases (water and vapour)[7], or for the drum as a whole[8,17]. With the first approach the phase change mechanism has also to be modelled.

When the drum is treated as a unit and it is assumed that its contents (liquid and vapour) are both at a saturation pressure (P_{SD}) and temperature (T_{SD}), the equations describing it are:

$$\text{Mass balance:} \quad (W_{EO}-W_{SD}) = \frac{d}{dt}\left[(V_{DR}-V_{DW}).\rho_{SD} + V_{DW}.\rho_{DW}\right] \tag{2.22}$$

$$\text{Energy balance:} \quad W_D.h_M-(W_D-W_{EO}).h_{DW}-W_{SD}.h_{SD} = \frac{d}{dt}\left[(V_{DR}-V_{DW}).\rho_{SD}.h_{SD} + V_{DW}.\rho_{DW}.h_{DW}\right] \tag{2.23}$$

For sections like the radiant superheater, primary and secondary superheater and the reheater, the set of the equations describing them has basically the same form. Differences of approach in the formulation of these equations appear in the literature. For example: the energy balance equation can either be described with the "effective mass" principle described by McDonald et al[17], or fluid mass and metal mass can be treated separately. In other words:

$$W_i . h_i + Q - W_o . h_o = \begin{cases} \frac{d}{dt}(M_{ef} . h_o) \\ V . \frac{d}{dt}(\rho_o . h_o) \end{cases}$$

M_{ef} = effective mass
i = input, o = output

In the first case the effective mass is expressed as:

$$M_{ef} = V . \rho_o + M_m . (C_m/\bar{C}) . (T_m/T_o), \qquad m = \text{metal}$$

where: C = heat transfer coefficient.

i.e. it contains the mass of the fluid plus an approximation of the metal mass. Also here, Q is the heat transfer rate from gas to the working fluid and it certainly needs to be expressed appropriately. In the second case, Q is the heat transferred from the metal to the working fluid and so the metal energy balance equation is required as well.

Thomson in his paper[11] introduced the concept of dividing the section into a number of "elemental volumes" and thus being able to obtain the change of the working fluid properties along the section's length. However, this method can be very cumbersome in a plant model where only the overall performance of e.g. the superheater is of interest. It can be very useful when the particular performance of one or two sections is of interest.

On the other hand, division of a section into two "lumped parameter" sections is very common and it can be of some advantage to the performance of the model.

Finally, the existence of radiant SH or secondary SH, horizontal or pendant sections etc. depends on the design of the boiler unit.

The equations for the different sections are presented below:

<u>Radiant Superheater</u>

Pressure drop across the section : $$(P_{SD} - P_{RSHO}) = \frac{f_{RSH} . W_{SD}^2}{\rho_{SD}} \qquad (2.24)$$

Mass balance (vapour) : $$(W_{SD} - W_{RSHO}) = V_{RSH} . \frac{d}{dt} (\rho_{RSHO}) \qquad (2.25)$$

Energy balance (vapour) : $$W_{SD} . h_{SD} + Q_{RSH} - W_{RSHO} . h_{RSHO} = V_{RSH} . \frac{d}{dt}(\rho_{RSHO} . h_{RSHO}) \qquad (2.26)$$

Energy balance (metal) : $(Q_{GRSH}-Q_{RSH}) = M_{RSH}.C_{RSH}.\frac{d}{dt}(T_{RSHM})$ (2.27)

where: $Q_{RSH} = k_{RSH}.W_{RSHO}^{0.8}.(T_{RSHM}-T_{RSHO})$ (2.28)

Primary Superheater

Pressure drop across the section: $(P_{RSHO}-P_{SO}) = \frac{f_{SH}.W_{RSHO}^{2}}{\rho_{RSHO}}$ (2.29)

Mass balance (vapour) : $(W_{RSHO}-W_{SO}) = V_{SH}.\frac{d}{dt}(\rho_{SO})$ (2.30)

Energy balance (vapour) : $W_{RSHO}.h_{RSHO}+Q_{SH}-W_{SO}.h_{SO} = V_{SH}.\frac{d}{dt}(\rho_{SO}.h_{SO})$ (2.31)

Energy balance (metal) : $(Q_{GSH}-Q_{SH}) = M_{SH}.C_{SH}.\frac{d}{dt}(T_{SHM})$ (2.32)

where : $Q_{SH} = k_{SH}.W_{SO}^{0.8}.(T_{SHM}-T_{SO})$ (2.33)

is the heat transfer rate from the metal tube to the steam by convection.

Secondary Superheater

Here a two-section lumped-parameter representation is demonstrated, as well as the principle of the "effective mass". Further assumptions are as follows:

a) The metal mass and the volume are divided equally between the two sections.

b) The steam densities in the two sections can be combined to give an "average" density (ρ_{SS}). This has the effect of reducing the mass balance equations from two to one.

Pressure drop across the section: $(P_{SSI} - P_{T}) = \frac{f_{SS}.W_{SSI}^{2}}{\rho_{SSI}}$ (2.34)

Mass balance (vapour) : $(W_{SSI} - W_{T}) = V_{SS}.\frac{d}{dt}(\rho_{SS})$ (2.35)

Energy balance for the two sections:

$$(Q_{SS}/2)-(h_{SS}-h_{SSI}).W_{SSI} = \frac{M_{SS}}{2}\cdot\frac{d}{dt}(h_{SS}) \qquad (2.36)$$

$$(Q_{SS}/2)-(h_{SSO}-h_{SS}).(\frac{W_{SSI}+W_T}{2}) = \frac{M_{SS}}{2}\cdot\frac{d}{dt}(h_{SSO}) \qquad (2.37)$$

where: $$M_{SS} = \rho_{SS}.V_{SS} + M_{MSS}.(\frac{C_{MSS}}{\bar{C}_{SS}}).(\frac{T_{SSM}}{\bar{T}_{SS}}) \qquad (2.38)$$

is the effective mass and Q_{SS} = the heat transfer rate from the gas to the steam.

Superheater Spray Attemperator

The attemperator is usually situated between the primary and secondary SH sections. Its purpose is to exercise control over the temperature at the SH output. Assuming adiabatic mixing of the two fluids and no pressure drop across the attemperator, the equations describing the process are:

Mass balance: $$W_{SSI} = W_{SO} + W_{SHS} \qquad (2.39)$$

Energy balance: $$W_{SSI}.h_{SSI} = W_{SO}.h_{SO} + W_{SHS}.h_{EO} \qquad (2.40)$$

Reheater

Pressure drop across the section : $$(P_{TO}-P_{RO}) = \frac{f_R.W_{RI}^2}{\rho_{RI}} \qquad (2.41)$$

Mass balance (vapour) : $$(W_{TO}-W_{RO}) = V_R\cdot\frac{d}{dt}(\rho_{RO}) \qquad (2.42)$$

Energy balance (vapour): $$W_{TO}.h_{TO}+Q_{RH}-W_{RO}.h_{RO}=V_R\cdot\frac{d}{dt}(\rho_{RO}.h_{RO}) \qquad (2.43)$$

Energy balance (metal) : $$(Q_{GRH}-Q_{RH})=M_{RH}.C_{RH}\cdot\frac{d}{dt}(T_{RHM}) \qquad (2.44)$$

where : $$Q_{RH} = k_R.W_{RO}^{0.8}.(T_{RHM}-T_{RO}) \qquad (2.45)$$

is the convection heat transfer rate from the tube metal to the steam.

Air-Fuel Input Section

A rather simple system was considered here. Of course, the type of pulveriser which is used, the kind of firing (tangential, front wall, etc.), the kind of control on the air path (i.e. damper control or fan speed control), all affect a great deal the configuration at that part of the plant. A detailed representation of all these would not, however, be justified and so the following is considered:

The amount of coal which goes from the hopper through the feeder to the pulveriser is assumed proportional to the feeder stroke,[17] i.e.

$$W_{FD} = K_F . L_F \tag{2.46}$$

The concentration of fuel in the pulveriser is obviously the difference of the amount of coal going into it and the amount which is coming out. The latter is set to be proportional to the mass of coal stored in the mill at any time. Therefore:

$$\frac{d}{dt}(M_{CR}) = (W_{FD}-W_{OUT}) = W_{FD} - K_{CF}.M_{CR} \tag{2.47}$$

The pulverised coal goes through pipes (representing a delay) to the burners. The dynamics of the burners are neglected. So:

$$\frac{d}{dt}(W_{FI}) = (\frac{1}{T_P}).(W_{OUT}-W_{FI}) \tag{2.48}$$

The amount of air entering through the forced-draught fans consists of the primary air, the secondary air and the excess air. A very common percentage of these quantities could be: 20%, 80% and 8% respectively. Only the primary air goes through the mills and it is used to dry and to lift and transport the pulverised fuel, through the pipes to the burners. There the rest of the air is added and the mixture enters the burners.

The damper and the forced-draught fan dynamics (if that is what the plant is employing) are approximated by a simple lag. Also it is assumed that the input control signal results in a change in the fan's power and generally the power needed by a fan is proportional to the third power of the flow through it. So:

$$\frac{d}{dt}(A) = \left(\frac{1}{T_{AA}}\right).(K_A.L_F - A) \tag{2.49}$$

and $$W_A = W_R.\sqrt[3]{A} \tag{2.50}$$

are the two equations used.

Combustion-Furnace

For the burners the fact is that there is no storage of fuel in them (obviously the situation is different when a stoker furnace is considered). For the air needed for the combustion, it is assumed that the "excess air" controller is perfect and the appropriate amount of primary plus secondary plus excess air is provided through the forced-draught fan. This air goes through the air heaters and enters the burners with a temperature T_A, which is assumed to be constant (ideally it should be). Therefore, in the furnace, just after the burners, the following quantities are defined:

Total gas flow: $$W_{GF} = W_A + W_{FI} - W_{ash} \tag{2.51}$$

Gas temperature: $$T_G = T_A + (W_{FI}.F.n/C_{GF}.W_{GF}) \tag{2.52}$$

where: n = the efficiency of the burner, which is controlled by the excess air controller.

F = the "heating-value" of the fuel used. It can be determined by an analysis of the fuel, which will determine the percentages of the C, H_2, S in the particular sample. An abrupt change in F is reflected at the throttle pressure and it is important that the control system of the boiler can neutralise these changes very quickly.

C_{GF} = the specific heat of the gas; it can be calculated from the specific heats of the combustion products, at the appropriate range of temperature. McDonald et al[17], express the specific heat as a function of the amount of fuel burned, although this kind of representation obviously requires knowledge of the operating characteristic of the particular plant.

Another point of interest here is the possible existence of two furnaces, the superheater and the reheater furnace. In this case, the equations (2.10), (2.11) or (2.20), (2.21) should be written for both furnaces and the heat input to the mixture in the risers (Q_W), should be the sum of the heat outputs of the two furnaces.

Gas-Path

The gas leaving the furnace goes through the various sections of the boiler, releasing gradually its heat. This results in a drop in its temperature, until it finally goes through the stack to the atmosphere.

For the purpose of writing the equations describing these changes the following assumptions can be made:

(a) Radiant heat transfer is assumed for the risers and the radiant superheater.

(b) Convective heat transfer is assumed for the remaining sections.

(c) The inertia and the heat capacitance of the gases is neglected, i.e. the velocity and temperature changes take place instantaneously[10,16,17].

(d) The heat coefficient is assumed to be constant for each section.

So, the heat transfer rates for each section are:

$$Q_{GW} = k_{RW} \cdot (T_G^{\,4} - T_{RM}^{\,4}) \quad - \quad \text{heat transfer from gas to riser metal} \tag{2.53}$$

$$Q_{GRSH} = k_{RSH1} \cdot (T_{out}^4 - T_{RSHM}^4) \quad \text{heat transfer from gas to radiant SH metal} \tag{2.54}$$

$$Q_{GSS} = k_{RSS} \cdot W_G^{\,0.6} \cdot (T_{GSS} - T_{SSM}) \quad \text{heat transfer from gas to secondary SH metal} \tag{2.55}$$

Equation (2.55) will not be used if the concept of the effective mass is employed in the equations for the secondary SH. Because in that case, Q_{SS} will include it.

$$Q_{GSH} = k_{SH1} \cdot W_G^{0.6} \cdot (T_{GSH} - T_{SHM}) \quad \text{- heat transfer from gas to primary SH metal} \qquad (2.56)$$

$$Q_{GRH} = k_{RH} \cdot W_G^{0.6} \cdot (T_{GRH} - T_{RHM}) \quad \text{- heat transfer from gas to reheater metal} \qquad (2.57)$$

$$Q_{GE} = k_{E1} \cdot W_G^{0.6} \cdot (T_{GE} - T_{EM}) \quad \text{- heat transfer from gas to economiser metal} \qquad (2.58)$$

The corresponding equations for the gas temperature "just after" each section, are:

$$T_{out} = T_G - \frac{Q_{GW}}{C_{GF} \cdot W_G} \quad \text{at the furnace output} \qquad (2.59)$$

$$T_{GSS} = T_{out} - \frac{Q_{GSS}}{C_{GSS} \cdot W_G} \quad \text{after the secondary SH} \qquad (2.60)$$

$$T_{GSH} = T_{GSS} - \frac{Q_{GSH}}{C_{GSH} \cdot W_G} \quad \text{after the primary SH} \qquad (2.61)$$

$$T_{GRH} = T_{GSH} - \frac{Q_{GRH}}{C_{GRH} \cdot W_G} \quad \text{after the reheater} \qquad (2.62)$$

$$T_{GE} = T_{GRH} - \frac{Q_{GE}}{C_{GE} \cdot W_G} \quad \text{after the economizer} \qquad (2.63)$$

The equations of the various sections presented so far will be supplemented by the appropriate number of <u>state equations</u> so that the number of equations equals the number of the unknowns in each case. The state equations are relations between quantities such as: pressure, temperature, density, enthalpy, etc. of the working fluid. They can be derived from the steam tables[26,27,28] by approximation inside the appropriate operating "window", defined, for example, between the values of pressure or temperature or both (see Appendix A).

2.3 CHOICE OF MODEL EQUATIONS

It was decided that there would be no linearisation of the equations around an operating point (although this case is examined in Section 2.5.3). Non-linearities like square or cube roots, multiplication of variables, etc. would be allowed in the model. In addition to that, real physical values were used for most of the variables in an attempt to derive the model on the basis of its physical characteristics and not just an input-output model. This gives a better and more realistic understanding of the changes taking place in the actual plant.

Actual operating data to the extent required by the equations presented in the previous section are very difficult to find in the literature. For this reason, the data given in reference 14 were used as a basis for the computation of the steady-state. They correspond to a 200 MW coal-fired drum-type boiler, operating at M.C.R.

The forced-circulation equations of the downcomer-riser section were adopted as being simpler than those of natural circulation and a steady-state was computed for the equations presented in the previous section. The procedure here was to assign the steady-state values to the key variables and then compute the rest of the variables and the constant coefficients as a function of those key variables. As has been already mentioned, a certain number of state equations is necessary. These equations were derived as shown in Appendix A. As a result, the model at this stage consisted of: 20 linear and non-linear ordinary differential equations and 45 non-linear algebraic equations. The equations of the controllers are not included in these figures.

The drum equations (2.22) and (2.23) were combined with the state equation (A.6) and equations (2.8) and (2.9) and they were solved for $\mathring{\rho}_{SD}$ and $\mathring{V}_{DW}$ from the system of equations:

$$(W_{EO}-W_{SD}) = \frac{d}{dt}(\rho_{SD})\cdot\left[V_D-(1-E3)\cdot V_{DW}\right] + \frac{d}{dt}(V_{DW})\cdot\left[EE3-(1-E3)\rho_{SD}\right] \tag{2.64}$$

$$\begin{aligned} Q_W+W_{EO}\cdot h_{EO}-W_{SD}\cdot h_{SD} = {} & \frac{d}{dt}(\rho_{SD})\cdot\left[(2V_D E1)\cdot\rho_{SD}+V_{DW}\cdot\rho_{SD}(2(E2\cdot E3-E1)) + \right. \\ & \left. + V_D\cdot EE1+V_{DW}\cdot(-EE1+E2\cdot EE3+E3\cdot EE2)\right] + \\ & + \frac{d}{dt}(V_{DW})\cdot\left[\rho_{SD}^2\cdot(E2\cdot E3-E1) + \right. \\ & \left. + \rho_{SD}\cdot(-EE1+E2\cdot EE3+E3\cdot EE2)+EE2\cdot EE3\right] \end{aligned} \tag{2.65}$$

The solutions resulted in a third order equation. To investigate further this part of the model, the rest of the drum state equations were used and this system of equations was discretised (see Section 2.4). A Zero-Order Hold approximate discrete integrator was used for this purpose. Lengthy manipulations were required to derive the coefficients of the cubic equations giving ρ_{SD}. It was found that the equation has one real and two complex roots. The real root is of interest and therefore it was taken to be one of the two roots of a quadratic approximation of the cubic equation within a "window" of values of ρ_{SD}. But this approximation proved to be very bad and it was soon abandoned.

The amount of core which the boiler simulation should occupy had to be as small as possible, with the figure of 3k as the absolute maximum. The other restriction is, of course, the computation time. This is a function of the size of the simulation as well as of the kind of computations that have to be performed. At this point it should be noted that the floating point arithmetic is performed by software.

These limiting factors led to the adoption of a much more simplified model, from the original that was envisaged. The first simplification was to drop the reheater section. In fact, in the analog model of the generator[3], the simulation of the prime mover includes the dynamics of the turbine and the reheater (Fig. 2.2a). Furthermore, a digital simulation of the reheater would require for the analog model to be split in the way shown in Fig. 2.2b. Such a scheme was not investigated. But it could certainly present problems of stability, which would perhaps require the reheater part of the program to be run much faster than the rest of the digital simulation.

The air-fuel section equations were retained as they appear on page 35.

If the metal temperatures of all the sections were included in a simplified model, then all equations of the gas-path should be included as well. Therefore only the riser metal temperature is included and the heat transfer equations in the riser section.

Perfect temperature control is assumed at the throttle valve. This makes the equation giving the steam flow at the valve (W_T) independent of the temperature (or the density) of the steam. At the same time the equations of the spray attemperator are not needed any more.

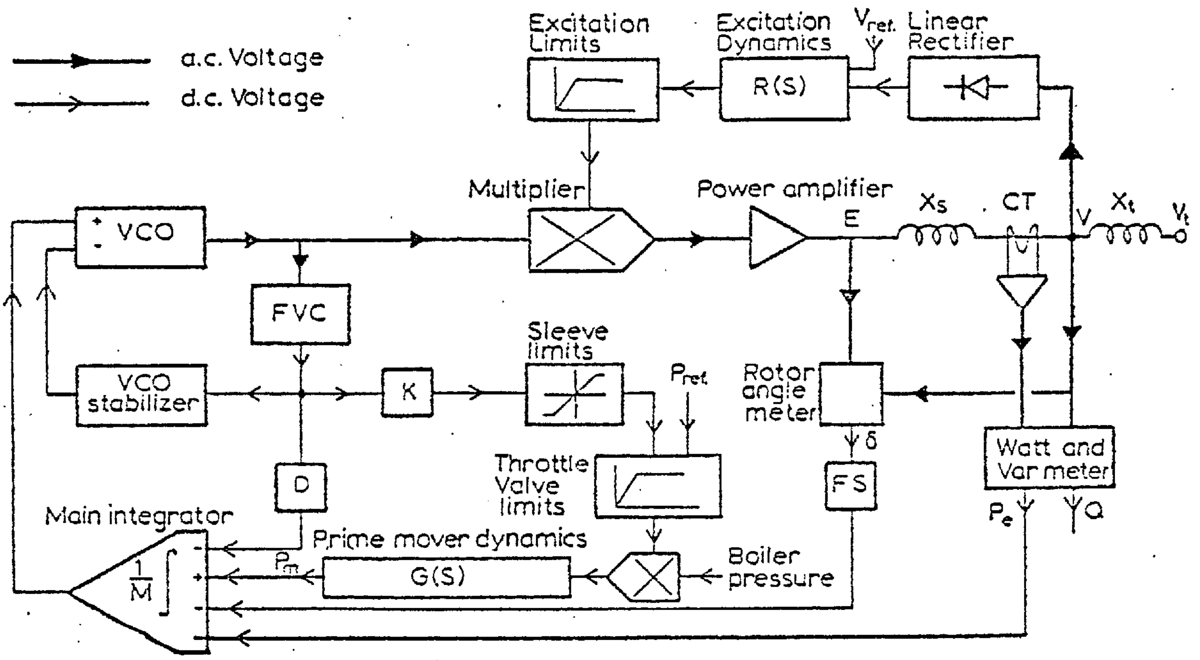

Fig. 2.2a Generating Unit (figure taken from reference 1).

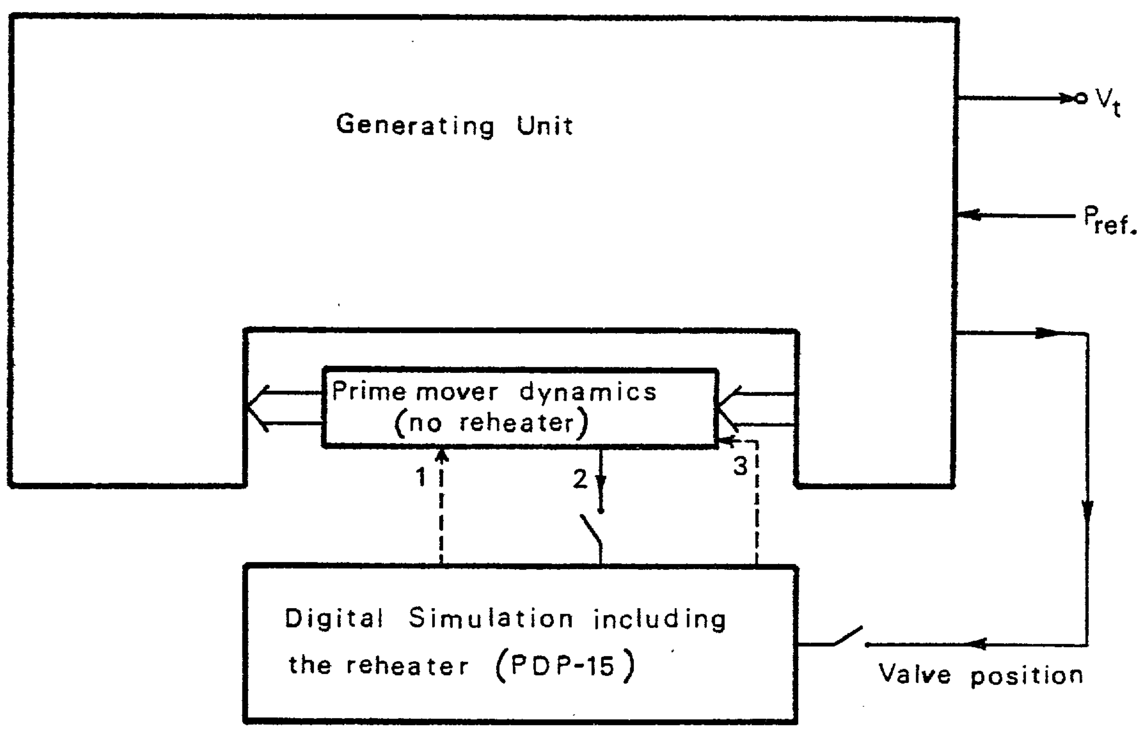

1. Output from reheater simulation to the LP section of the turbine.
2. Input to reheater simulation from the HP section of the turbine.
3. Throttle pressure from the digital simulation to the analog model.

Fig. 2.2b

Radiant and primary SH sections were "lumped" together. Originally it was thought desirable to include a primary and a secondary SH section. But it was found that it would not add too much to the performance of the model and would add another square root in the computation time. So all the three sections were lumped together to form one "superheater" section.

The feedwater section equations were also dropped, because their inclusion would involve computing Q_{GE} and Q_E and this requires the values of the temperatures T_{EM} and T_{EO}. Therefore, perfect feedwater control was assumed. This implies that the drum water level is kept more or less at its target value (so it can be assumed that $(dV_{DW}/dt) = 0.0$) and also that the steam flow out of the drum equals the feedwater flow into the drum ($W_{EO} = W_{SD}$).

From equation (2.64), applying these two simplifications, it can be said that the steam density ρ_{SD} does not change as a result of imbalance between steam and feedwater flow rate. Equation (2.65) indicates that the steam density changes as a result of a change in the rate of firing. Substitution of the appropriate state equations in (2.65) results in the expression:

$$Q_W + W_{SD} \cdot \left[E6 . P_{SD} + EE6\right] = (1/E4) . \frac{d}{dt}(P_{SD}) \cdot \left[E8 . P_{SD} + EE8\right] \qquad (2.66)$$

where: $$E8 = 2.(V_D . E1 + V_{DW} . (E2.E3 - E1))/E4 \qquad (2.67)$$

$$EE8 = -E8.EE4 + (V_D . EE1 + V_{DW} . (-EE1 + E2.EE3 + E3.EE2)) \qquad (2.68)$$

From this equation the drum pressure P_{SD} can be computed as one of the roots of a quadratic equation. Instead, a simpler equation was used (2.81), where the pressure is computed from a first order equation. Both equations result in the same steady-state relations for all of the model variables and from subsequent runs it was found that they gave almost identical transient response to the model.

The equations which were used in the simplified model are presented in Table 2.1. The values of the variables corresponding to the steady-state at M.C.R. and the values of the constants used are shown in Table 2.2.

TABLE 2.1: EQUATIONS USED FOR THE BOILER MODEL

Air-Fuel Section

$$\left.\begin{aligned} W_{FD} &= K_F.L_F \\ \frac{d}{dt}(M_{CR}) &= W_{FD}-W_{OUT} \\ W_{OUT} &= K_{CF}.M_{CR} \\ \frac{d}{dt}(W_{FI}) &= (1/T_P).(W_{OUT}-W_{FI}) \end{aligned}\right\} \text{Fuel input} \qquad \begin{aligned} &(2.67) \\ &(2.68) \\ &(2.69) \\ &(2.70) \end{aligned}$$

$$\left.\begin{aligned} \frac{d}{dt}(A) &= (1/T_{AA}).(K_A.L_F-A) \\ W_A &= W_R.\sqrt[3]{A} \end{aligned}\right\} \text{Air input} \qquad \begin{aligned} &(2.71) \\ &(2.72) \end{aligned}$$

Combustion-Furnace

$$W_{GF} = W_A+W_{FI}-W_{ash} \tag{2.73}$$

$$T_G = T_A+(W_{FI}.F.n/C_{GF}.W_{GF}) \tag{2.74}$$

Drum-Downcomers-Risers

$$Q_W = W_D.(h_m-h_D) \tag{2.75}$$

$$W_D.h_D = (W_D-W_{EO}).h_{DW}+W_{EO}.h_{EO} \tag{2.76}$$

$$h_{SD} = E1.\rho_{SD}+EE1 \tag{2.77}$$

$$\rho_{SD} = (P_{SD}-EE4)/E4 \tag{2.78}$$

$$T_{SD} = E5.\rho_{SD}+EE5 \tag{2.79}$$

$$W_{SD} = \sqrt{F_{SDI}.\rho_{SD}.(P_{SD}-P_T)} \tag{2.80}$$

$$\frac{d}{dt}(P_{SD}) = (1/C_D).(W_D.h_m-(W_D-W_{EO}).h_{DW}-W_{SD}.h_{SD}) \tag{2.81}$$

Superheater

$$\frac{d}{dt}(P_T) = (1/C_{SSH}).(W_{SD}-W_T) \tag{2.82}$$

$$W_T = K_T.A_T.P_T \tag{2.83}$$

Heat Transfer to the Risers

$$Q_W = K_{RS}.(T_{RM}-T_{SD})^3 \tag{2.84}$$

$$Q_{GW} = K_{RW}.(T_G^{\ 4}-T_{RM}^{\ 4}) \longrightarrow T_G \text{ and } T_{RM} \text{ in } (^oK) \tag{2.85}$$

$$\frac{d}{dt}(T_{RM}) = C_M.(Q_{GW}-Q_W) \tag{2.86}$$

TABLE 2.2: STEADY-STATE VALUES OF THE MODEL VARIABLES, CORRESPONDING TO M.C.R. OPERATION

Air-Fuel Section

$W_{FD} = 49.861$ (lb/sec)
$W_{OUT} = 49.861$ (lb/sec)
$W_{FI} = 49.861$ (lb/sec)
$M_{CR} = W_{OUT}/K_{CF}$ (lb)
$W_A = 456.94$ (lb/sec)
$W_{GF} = 500.31907$ (lb/sec)
$A = K_A.L_F$ (1/power)
* $L_F = 10.0$
Ash content = 0.13 (lb/lb)

The values of K_F and W_R are functions of the variables defined already:

$$K_F = W_{FD}/L_F = 4.9861$$
$$W_R = W_A/\sqrt[3]{A}$$
$$W_{ash} = 0.13.W_{FI}$$

The values of K_{CF}, K_A, T_P, T_{AA} are chosen using the rather arbitrary criterion of a reasonable model response:

$K_A = 12.5$
$K_{CF} = 1/35$ (s^{-1})
+ $T_P = 3.5$ (s)
+ $T_{AA} = 30.$ (s)

Combustion-Furnace Section

$T_A = 456.8$ (^oF)
$F = 9762.562$ (Btu/lb)
$C_{GF} = 0.299257$ (Btu/lb $.^oF$)

The following can be computed as functions of the variables already defined:

$T_G = 3,618.7155$ (^oF)
$n = 0.9725$

Drum-Downcomers-Risers-Superheater

$W_{SD} = 348.0$ (lb/sec)
$W_T = 348.0$ (lb/sec)
$\rho_{SD} = 8.498$ (lb/ft^3)
$P_T = 2450.0$ (psia)
* $A_T = 10.0$
$h_{EO} = 611.509$ (Btu/lb)
+ $C_D = 300.0$ (s)
+ $C_{SSH} = 5.85$ (s)

The remaining variables and constants are computed from the equations. Their values are:

$h_{SD} = 1075.49$ (Btu/lb)
$T_{SD} = 675.94$ (^oF)
$P_{SD} = 2653.11$ (psia)
$F_{SDI} = 70.163372$
$K_T = 0.014204081$

Heat Transfer to the Risers

$T_{RM} = 730.22$ (^oF)
$C_M = 1.067058555E-05$ (^oF/Btu)

The remaining variables have the following values:

$Q_W = Q_{GW} = 161464.4832$ (Btu/sec)
$K_{RS} = 1.00961894$
$K_{RW} = 0.617123753E-08$

* Chosen arbitrarily.

\+ Typical values used.

The time constants for the drum (C_D) and the superheater were chosen as: $C_D = 300$ s and $C_{SSH} = 5.85$ s, for the first investigations, but they can be altered to study the response of the model for different values of these time constants.

A block diagram representation of the model described by these equations is shown in Fig. 2.3.

2.4 DISCRETIZATION OF THE MODEL EQUATIONS

To perform a digital simulation of the process described so far, the continuous ordinary differential equations (Table 2.1) had to be converted to equivalent difference equations. For this purpose the Z-transform theory was used. This is the basis of the so-called "operational methods" of digital simulation[29]. Other improved methods such as the IBM method developed by Fowler and Hurt, the discrete compensation method, etc. are not suitable because they require the model to be described by transfer functions with the non-linearities isolated. This is not very easy with the set of equations available.

The model equations involve only first order derivatives and according to the operational methods, the continuous-time integrator (1/s) should be substituted by a chosen discrete integrating operator. There are different discrete operators, each with its advantages and its shortcomings[29,30]. Tustin's operator was chosen originally as it is based on the use of the trapezoidal rule of integration and gives:

$$(1/s)^n \longrightarrow \left[\frac{T(1+z^{-1})}{2(1-z^{-1})}\right]^n , \qquad T = \text{sampling interval} \qquad (2.87)$$

In order to illustrate its application, equations (2.67), (2.68) and (2.69) combined and converted to their discrete equivalents are:

$$s.M_{CR} = W_{FD} - W_{OUT} = K_F.L_F - K_{CF}.M_{CR} \qquad (2.88)$$

Substituting the discrete operator in the place of (1/s), one gets:

$$\left[\frac{2(1-z^{-1})}{T(1+z^{-1})}\right].M_{CR} = K_F.L_F - K_{CF}.M_{CR}$$

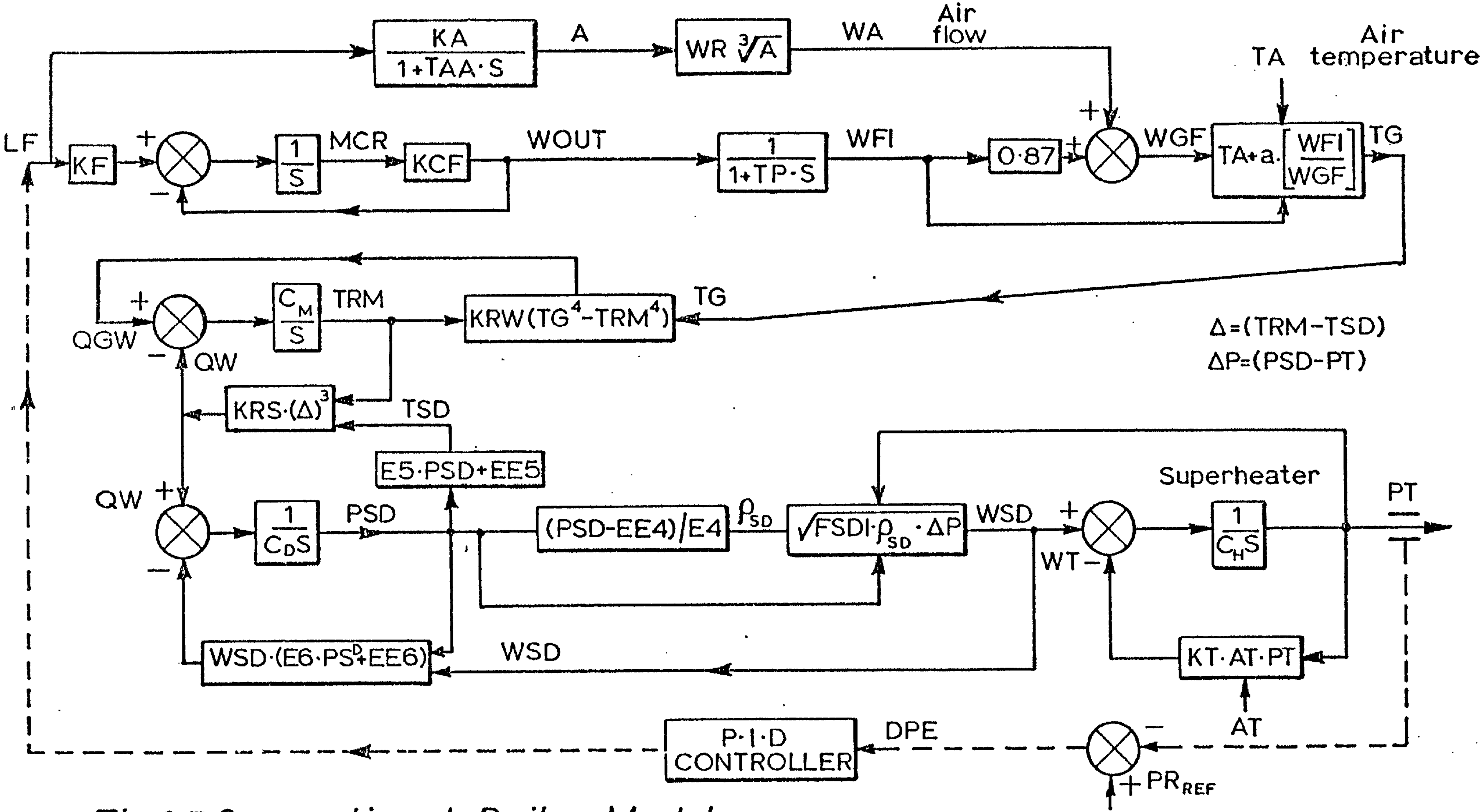

Fig. 2.3 Conventional Boiler Model

or $$2.M_{CR}(K)-2.M_{CR}(K-1) = T.\left[K_F.(L_F(K)+L_F(K-1))-K_{CF}.(M_{CR}(K)+M_{CR}(K-1))\right]$$

or $$M_{CR}(K) = M_{CR}(K-1).\left[\frac{2-T.K_{CF}}{2+T.K_{CF}}\right] + \left[\frac{T.K_F}{2+T.K_{CF}}\right].(L_F(K)+L_F(K-1)) \quad (2.89)$$

From this difference equation one can see that the value of M_{CR} at the "present" sampling instant is a function of: the value of M_{CR} at the "previous" instant and the values of the input or independent variable both at the "present" and "previous" sampling instances. The latter is very important, as will now be explained.

Consider the discretization of the drum and superheater equations as they appear in Appendix B.1. These difference equations have to be put in a programmable or executable order. But as can be seen, this is not straightforward with the equations as they stand. The main (unknown) variables are: $W_T(K)$, $W_{SD}(K)$, $P_T(K)$ and $P_{SD}(K)$ and solving the system of equations (B.1.1) to (B.1.4) would give them expressed in an executable manner. But the difficulty here is the presence of the square root and non-linear terms such as: $W_{SD}(K).P_{SD}(K)$, which make the solution of the system very cumbersome and very expensive in computing time.

For this reason it was decided that the section of the model including the drum-downcomer-riser, superheater and the heat balance in the risers will be discretized using the Z.O.H. (Zero Order Hold) discrete integrator, while the air-fuel section will be discretized using Tustin's operator.

The Z.O.H. is the first-difference technique of approximating a continuous integration process and it is the most elementary operator. Its Z-transform is:

$$(1/s) \longrightarrow \left[\frac{Tz^{-1}}{(1-z^{-1})}\right] \quad (2.90)$$

With the Z.O.H. operator the value of the integral is estimated by using only "previous" values of the variables involved. This is very convenient in helping to place the equations in a programmable order, in other words, to have a physically realizable simulation. The expression (2.90) can also be called an "optimum discrete operator", because it minimizes the "sum of error squared" between the sampled output of the continuous system (continuous integrator) and the output of the discrete system, for a step input[30,31].

The discretization was performed and the equations were arranged in an executable form as in Table 2.3, together with the continuous equations, which they will substitute. In the expression of the heat transfer rate from the gas onto the metal of the risers (Q_{GW}), both T_G and T_{RM} should be expressed in (^oK). Their values are expressed in (^oF) and for the conversion into (^oK) the formula:

$$(^oK) = 0.55555556.(^oF) + 255.372$$

was used. For the throttle pressure control loop a PID controller was used. The conversion from the continuous to its discrete form is shown in Appendix B.2.

2.5 MODEL EVALUATION

Having formed the set of programmable difference equations, a number of runs was made on the CDC 6400 computer. Their purpose was to get an initial assessment of the behaviour of the model, choosing a suitable set of time constants and a proper sampling interval T.

The values of K_A, T_{AA}, K_{CF} and T_P had to be chosen first. With no other source of information available, their values were chosen by trial and error, the criterion being a reasonable response of the model (e.g. when the throttle valve opens, the pressure should drop, etc.). In this way a set of values was found, for which the trend of the various variables, immediately after the introduction of a step input, was in the right direction.

Having done that, the next step was to find the effect on the model of the sampling interval T. The first attempts were made with T = 5 s, but this made the system unsuitable in the sense that the response was becoming unstable even for the smallest step

TABLE 2.3: CONVENTIONAL BOILER MODEL EQUATIONS IN THEIR DISCRETE FORM

Continuous Representation

$$\frac{d}{dt}(M_{CR})=K_F.L_F-K_{CF}.M_{CR} \quad (2.91)$$

$$\frac{d}{dt}(W_{FI})=(1/T_P).(K_{CF}.M_{CR}-W_{FI}) \quad (2.92)$$

$$\frac{d}{dt}(A)=(1/T_{AA}).(K_A.L_F-A) \quad (2.93)$$

$$W_A = W_R.\sqrt[3]{A} \quad (2.94)$$

$$W_{GF} = W_A + 0.87.W_{FI} \quad (2.95)$$

$$\frac{d}{dt}(P_{SD})=(1/C_D).\left[Q_W+W_{SD}.(E6.P_{SD} + EE6)\right] \quad (2.96)$$

$$\rho_{SD} = (P_{SD}-EE4)/E4 \quad (2.97)$$

$$T_{SD} = E5.\rho_{SD} + EE5 \quad (2.98)$$

$$W_{SD}=\sqrt{F_{SDI}.\rho_{SD}.(P_{SD}-P_T)} \quad (2.99)$$

$$\frac{d}{dt}(P_T)=(1/C_{SSH}).(W_{SD}-W_T) \quad (2.100)$$

$$W_T = K_T.A_T.P_T \quad (2.101)$$

$$T_G=T_A+(W_{FI}.F.n/C_{GF}.W_{GF}) \quad (2.102)$$

$$\frac{d}{dt}(T_{RM})=C_M.(Q_{GW}-Q_W) \quad (2.103)$$

$$Q_W = K_{RS}.(T_{RM}-T_{SD})^3 \quad (2.104)$$

$$Q_{GW} = K_{RW}.(T_G{}^4-T_{RM}{}^4) \quad (2.105)$$

where: T_G, T_{RM} are in (^oK)

$$D_{PE} = (P_{SET} - P_T) \quad (2.106)$$

$$L_F=(KPP+\frac{KIP}{s} + KDP.s).D_{PE} \quad (2.107)$$

Discrete Representation

$$ALL = L_F(K) + L_F(K-1)$$

$$M_{CR}(K)=\left[\frac{2-T.K_{CF}}{2+T.K_{CF}}\right].M_{CR}(K-1)+\left[\frac{T.K_{CF}}{2+T.K_{CF}}\right].ALL$$

$$W_{FI}(K)=\left[\frac{2.T_P-T}{2.T_P+T}\right].W_{FI}(K-1) + \left[\frac{T.K_{CF}}{2.T_P+T}\right].(M_{CR}(K)+M_{CR}(K-1))$$

$$A(K)=\left[\frac{2.T_{AA}-T}{2.T_{AA}+T}\right].A(K-1)+\left[\frac{K_A.T}{2.T_{AA}+T}\right].ALL$$

$$W_A(K) = W_R.\sqrt[3]{A(K)}$$

$$W_{GF}(K) = W_A(K)+0.87.W_{FI}(K)$$

$$Z = 1 + (T.E6/C_D).W_{SD}(K-1)$$

$$P_{SD}(K) = \left[P_{SD}(K-1)+(T/C_D).(Q_W(K-1)- W_{SD}(K-1).(EE6-h_{EO}))\right]/Z$$

$$P_T(K)=P_T(K-1)+(T/C_{SSH}).(W_{SD}(K-1)-W_T(K-1))$$

$$R_{SD}(K) =(P_{SD}(K)-EE4)/E4$$

$$T_{SD}(K) = E5.R_{SD}(K) + EE5$$

$$W_{SD}(K) =\sqrt{F_{SDI}.R_{SD}(K).(P_{SD}(K)-P_T(K))}$$

$$W_T(K) = K_T.A_T(K-1).P_T(K)$$

$$Z17 = ((F.n/C_{GF})/W_{GF}(K))$$

$$T_G(K) = T_A + W_{FI}(K).Z17$$

$$T_{RM}(K) = T_{RM}(K-1)+(T.C_M).(Q_{GW}(K-1)-Q_W(K-1))$$

$$Z14 = T_{RM}(K) - T_{SD}(K)$$

$$Q_W(K) = K_{RS}.(Z14.Z14.Z14)$$

$$Z15 = 0.555556\cdot T_G(K) + 255.372$$

$$Z16 = 0.555556\cdot T_{RM}(K) + 255.372$$

$$Q_{GW}(K) = K_{RW}.(Z15^4 - Z16^4)$$

$$D_{PE}(K) = P_{SET} - P_T(K)$$

$$S_E(K) = S_E(K-1) + D_{PE}(K-1)$$

$$L_F(K+1)= KPP.D_{PE}(K)+KIP.S_E(K)+KDP.(D_{PE}(K)- D_{PE}(K-1))$$

input. Further investigation showed that T had to be much smaller than 1 s to produce a stable response. The other two quantities which had a direct effect were the drum and the superheater time constants C_D and C_{SSH}. For example:

For: $T = 0.4$ s, $C_{SSH} = 5.85$ s	and $C_D = 300$ s,	the open-loop response of the model is stable,
	$C_D = 250$ s,	the open-loop response of the model is stable,
	$C_D = 230$ s,	the open-loop response of the model is (just) stable,
	$C_D = 200$ s,	the open-loop response of the model is unstable.

So as the time constant becomes smaller (i.e. the system faster) the response goes unstable and this instability begins at the computation of the pressure P_{SD}. In fact, when the first value of P_{SD} (computed immediately after the introduction of the step input) changes in one direction and the next value of P_{SD} (i.e. the one computed at the next iteration) changes in the opposite direction, the response of the system is unstable for that particular combination of C_D, C_{SSH} and T. The range of values of C_{SSH} is very limited, so its effect on the issue of the stability depends very much on the current value of C_D. Finally, a sampling interval of <u>$T = 0.3$ s</u> was chosen. It gave a stable open-loop response for C_D down to 170 s, with $C_{SSH} = 5.85$ s and a 10% step input in the valve position.

The speed of the response of a conventional steam plant depends, among other things, on the evaporation rate of the boiler and the response of the fuel-feed and firing systems. In the model the two factors are represented by the drum time constant C_D and the fuel-air input time constants. From the range of values appearing in the references 21, 22, 16, 18 and 32 the following three sets of values were used for testing the model:

$$\left.\begin{aligned} C_D &= 300.0 \ \text{s} \\ K_{CF} &= 1/35 \ \text{s}^{-1} \\ T_P &= 3.5 \ \text{s} \\ T_{AA} &= 30.0 \ \text{s} \end{aligned}\right\} \quad \text{For a slow coal-fired unit} \qquad \text{(I)}$$

$$\left.\begin{aligned} C_D &= 250.0 \text{ s} \\ K_{CF} &= 1/20 \text{ s}^{-1} \\ T_P &= 1.5 \text{ s} \\ T_{AA} &= 20.0 \text{ s} \end{aligned}\right\} \quad \text{For a fast coal-fired unit} \qquad \text{(II)}$$

$$\left.\begin{aligned} C_D &= 220.0 \text{ s} \\ K_{CF} &= 1/10 \text{ s}^{-1} \\ T_P &= 0.0 \text{ s} \\ T_{AA} &= 10.0 \text{ s} \end{aligned}\right\} \quad \text{For an oil-fired unit} \qquad \text{(III)}$$

The sets of values presented above were used only for testing the general response of the model. They do not represent constants of a particular steam plant.

The throttle pressure controller was added to the model, as shown in Fig. 2.3. The relation of the controller gains, for each of the three cases, was made by trial and error.

2.5.1 Steady-State Characteristics of the Model

The equations which were used to describe the model and the values (for M.C.R.) assigned to the variables, define the steady-state characteristics of the model. Quantities like T_P, T_{AA}, C_D, etc. affect only the transient response of the model.

Fig. 2.4 shows the closed-loop steady-state characteristics of the model, as functions of a change in the value of the throttle valve opening. This corresponds to a step change in the loading of the unit, with the controllers reacting and after some time bringing the unit to a new steady-state. It was assumed that throughout the range of valve opening the feedback loop keeps the throttle pressure at its set-point.

From these characteristics it can be seen that the changes of steam flow out of the drum and at the valve are directly proportional to the valve opening, as was expected. Another quantity which changes almost linearly is the heat rate input into the risers. This is because its value depends very much on the steam flow into the corresponding piping. The drop in the drum

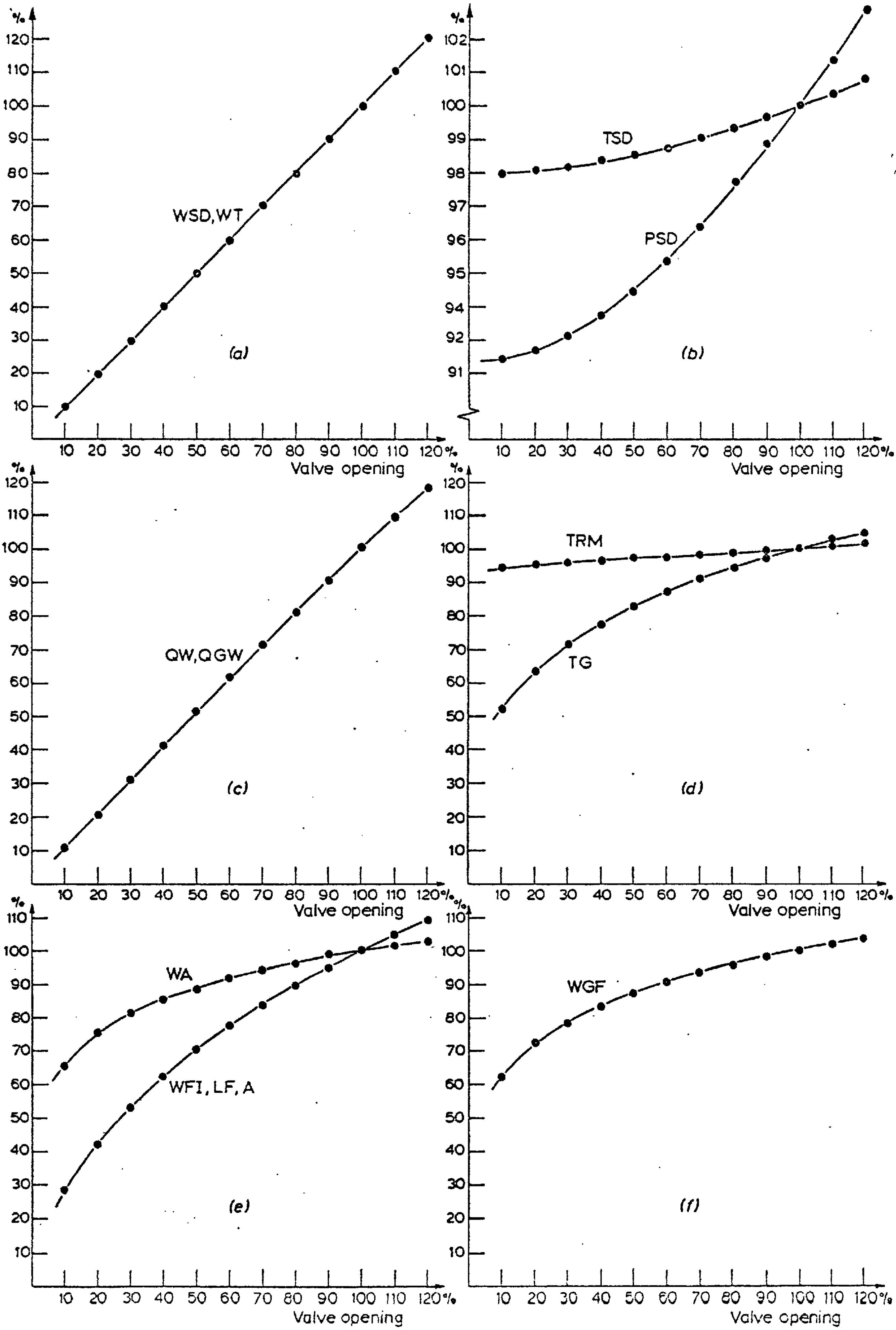

Fig. 2.4 Closed-loop steady-state characteristics of the conventional boiler model.

pressure is only about 6% for 50% valve opening, and this is mainly because the throttle pressure is maintained at its set-point.

The air flow rate and the fuel flow rate (W_A and W_{FI}) are both decreasing. The latter drops more rapidly. However, the air/fuel ratio remains constant because it is controlled throughout the operating range of the unit. The quantity of air in this ratio represents the primary air which goes through the mills. The correct quantity of this air is essential for the efficient operation of the mill. On the other hand, the secondary and the excess air influence the efficient combustion in the burners and the overall quantity of air is determined by the quality of the fuel used. In the model, W_A is the total quantity of air and the primary air is not represented separately.

Another important point is the following: for a new steady-state the value of the furnace gas temperature T_G changes. Therefore, from the equation:

$$(T_G-T_A)/(F.n/C_{GF}) \quad = \quad (W_{FI}/W_{GF})$$

the ratio (W_{FI}/W_{GP}) should change. But if in equation:

$$W_{GF} \quad = \quad 0.87.W_{FI}+W_A$$

where $W_{FI} = K_F.L_F$, the air flow W_A is a function of L_F, such as W_A = const.L_F, then the ratio (W_{FI}/W_{GF}) = const. This means that $W_A = f(L_F)$ must be a function of L_F of higher than first order. Otherwise the new steady-state of the model cannot be computed.

2.5.2 Transient Response of the Model

Open-Loop Response:

Starting from Fig. 2.5, where the model is disturbed by a step increase of 5% in the valve opening, one can observe the following: the steam flow at the valve is reduced initially in a step fashion. This produces an increase in the steam pressure at that point and consequently an increase in the drum

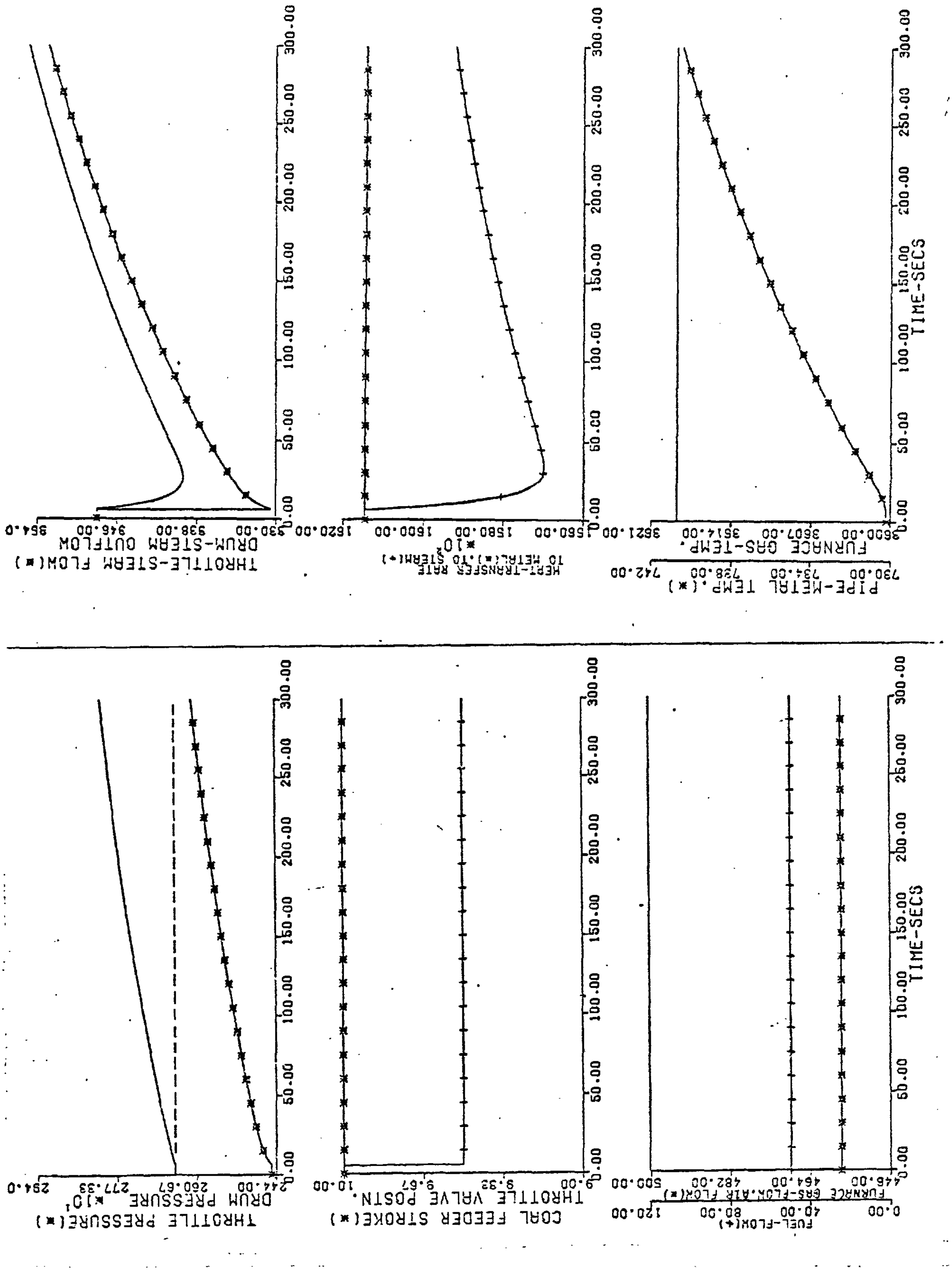

Fig. 2.5: Open-loop response of the conventional boiler model to a 5% step decrease in the valve opening.

steam pressure. The increase in the pressures arrests the drop in the steam flow and both W_{SD} and W_T start rising again. The rise in steam pressure means a rise in steam temperature as well. As a result, the heat transfer rate from the metal tubes to the mixture in the risers begins to fall initially, because it is a function of the difference between the temperatures of the metal tube and the mixture. A fall in the value of Q_W results in an increase in the metal tube temperature because the latter is a function of the difference between Q_{GW} and Q_W. The rise in the metal tube temperature arrests a further fall in the Q_W, which starts rising again.

In Fig. 2.6 the response of the model to an increase of 5% in the valve opening is shown. As expected, it is the opposite of the response in Fig. 2.5.

In Fig. 2.7 is shown the response of the model to a step reduction (5%) in the firing rate. The valve opening remains unaltered. As expected, the fuel flow, air flow and furnace gas flow drop to a new steady-state. This fall is transmitted to the rest of the model variables, through the drop in the furnace gas temperature. As can be seen, it increases slightly at the beginning, but then drops to a new steady-state. This initial increase depends on the time constants of the fuel and air paths, which determine the rate of change in the values of W_{FI} and W_{GF}.

The fall in the furnace gas temperature results in a fall in the heat transfer rate from the gas to the metal of the risers, a fall in their temperature and consequently a fall in the heat transfer rate to the mixture in the risers. Finally this fall is reflected throughout the model and results in a smooth drop in steam pressures and flow rates to reach a new steady-state. In Fig. 2.8 the response of the model to a disturbance to the opposite direction is shown.

Closed-Loop Response:

The closed-loop responses of the model (for the three cases mentioned on page 51) are shown in Figs. 2.9, 2.10 and 2.11. In all

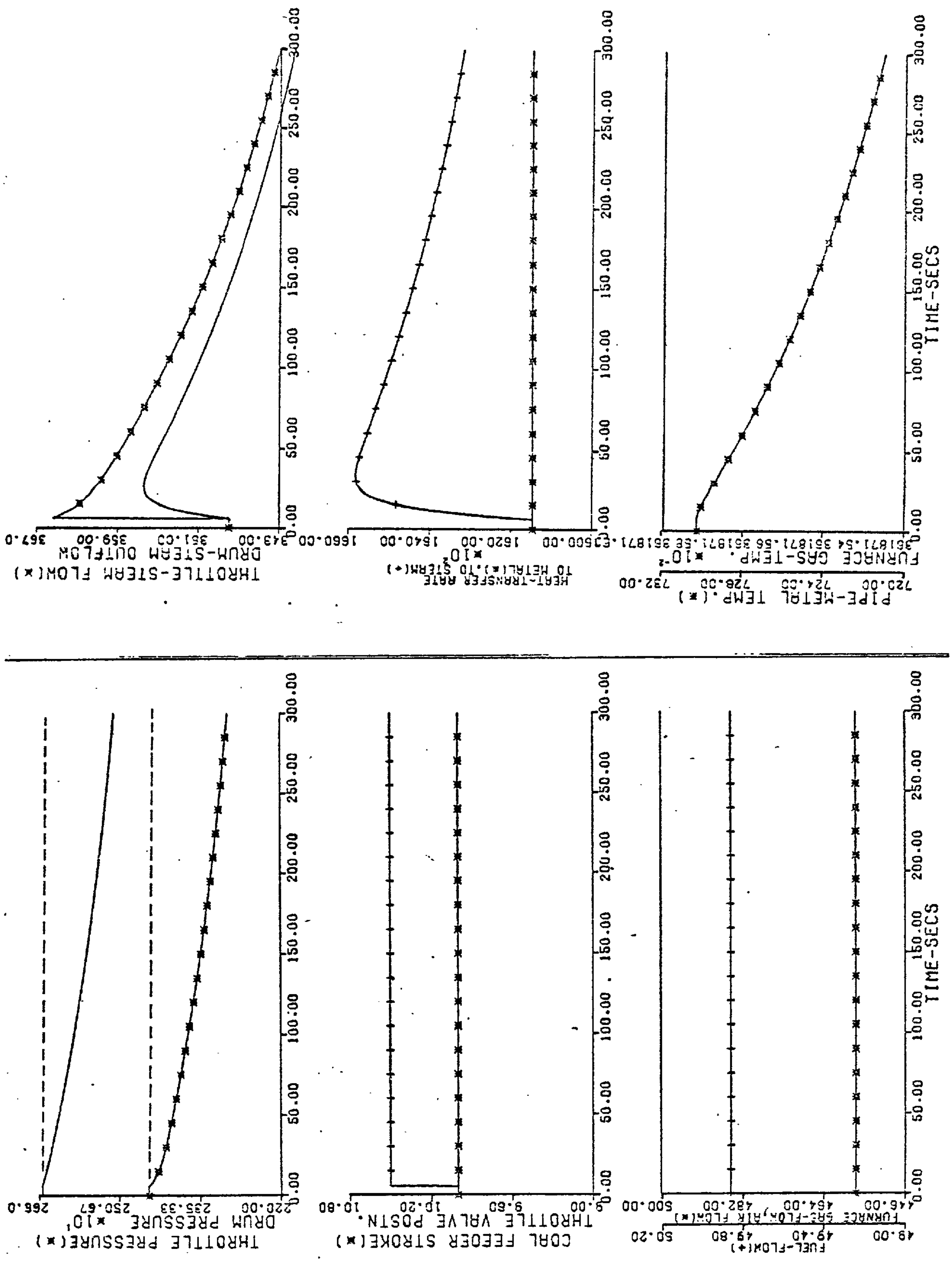

Fig. 2.6: Open-loop response of the conventional boiler model to a 5% step increase in the valve opening.

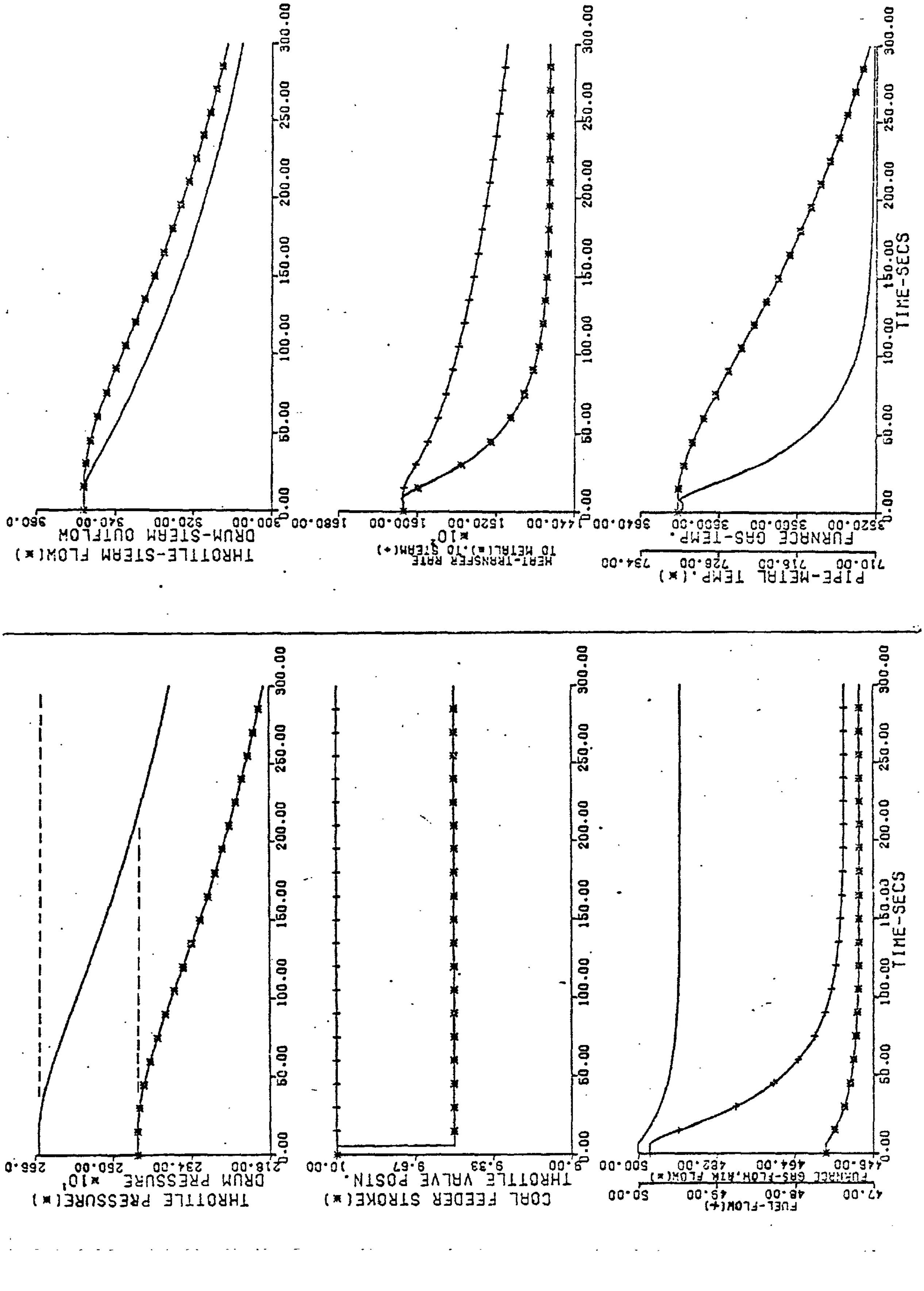

Fig. 2.7: Open-loop response of the conventional boiler model to a 5% step decrease in the firing rate.

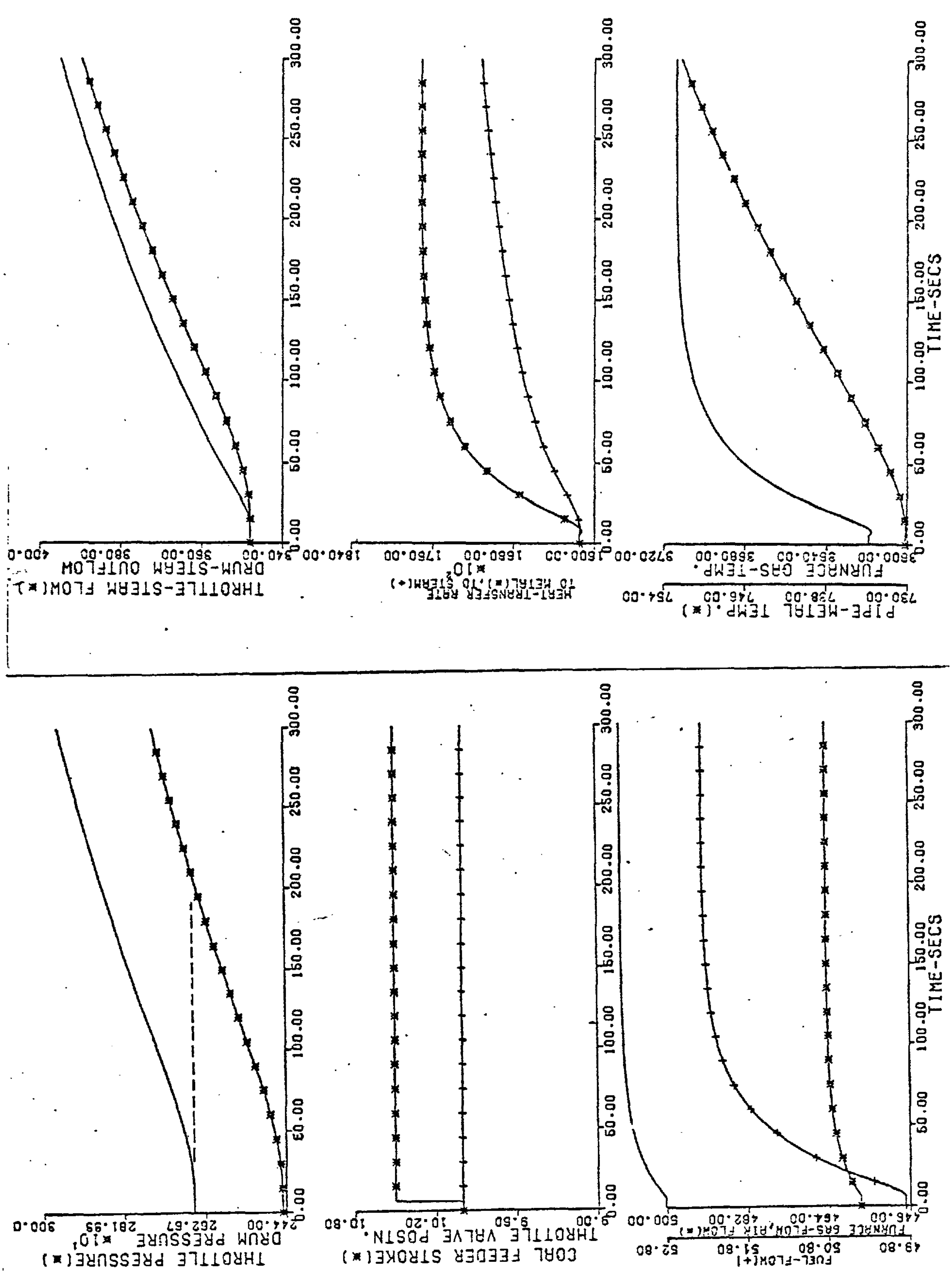

Fig. 2.8: Open-loop response of the conventional boiler model to a 5% step increase in the firing rate.

of them the model starts from its original state, which corresponds to full-load operation. The input disturbance is a step change in the throttle valve opening which decreases by 2% (Figs. 2.9, 2.10, 2.11(b)). As a result, the steam pressure at the valve begins to rise and it is followed by the steam pressure in the drum (Figs. 2.9, 2.10 and 2.11(a)). The steam flow at the valve, after its original drop because of the valve closure, rises again for a while following the rise of the pressure at this point. On the other hand, the steam flow out of the drum keeps falling steadily because it is a function of the difference $(P_{SD}-P_T)$. This difference is becoming smaller after the step input, because the pressure at the valve increases faster than the pressure at the drum since it is nearer to the point of the disturbance. Increase in the drum steam pressure means an increase in the drum steam temperature which results in the heat transfer rate from the tube metal to the mixture to start falling (e).

The initial imbalance between Q_W and the heat going from the furnace gas to the tube metal results in a rise of the tube metal temperature (Figs. 2.9, 2.10 and 2.11(f)). In the meantime, the pressure controller senses the rise of the pressure at the valve and acts to correct the error. This means a reduction in the feeder stroke signal L_F (Figures (b)), which results in a reduction of the fuel and the air entering the burners (Figures (c)). Consequently, the temperature of the furnace gas starts falling (Figures (f)). The heat transfer from the gas to the riser walls is due to radiation (i.e. proportional to T^4), which means that this rate starts falling (Figures (e)). In turn, the metal temperature follows this fall and as a result the heat transferred from the metal to the mixture in the risers drops. This reverses the balance between Q_{GW} and Q_W and so the tube metal temperature begins to fall again (Figures (f)). As a result, the heat transfer rate to the mixture (Q_W) keeps falling.

A reduction in the heat input to the boiler results in a reduction to the pressure in the drum. After a while this reduction in P_{SD} is transmitted through the steam path to the valve (i.e. the superheater output) and so the pressure at this point starts falling again. The controller keeps manipulating the boiler inputs until this pressure assumes its desired value.

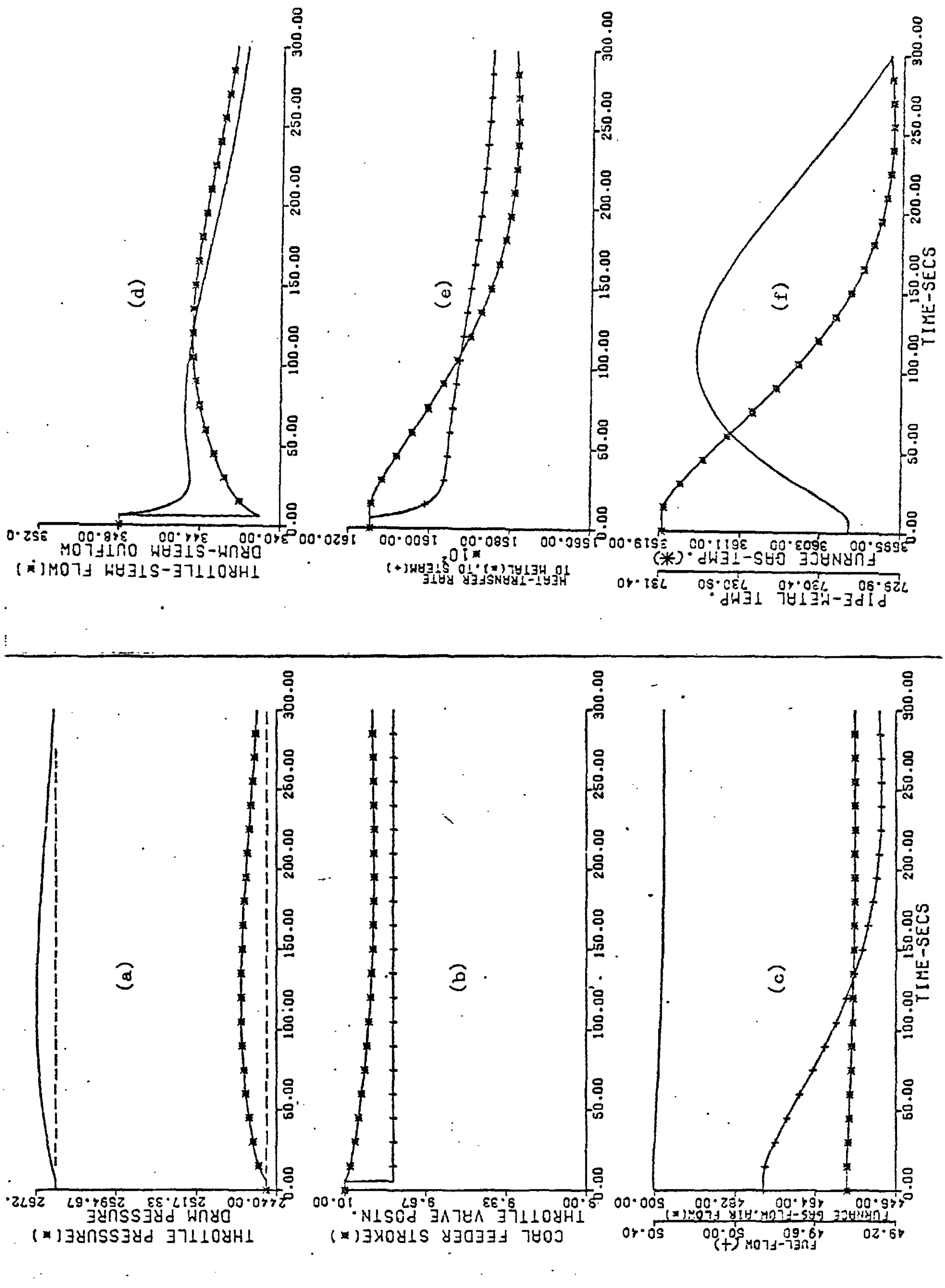

Fig. 2.9: Closed-loop response of the conventional boiler model to a 2% step decrease in the valve opening (drum time constant: 300 s).

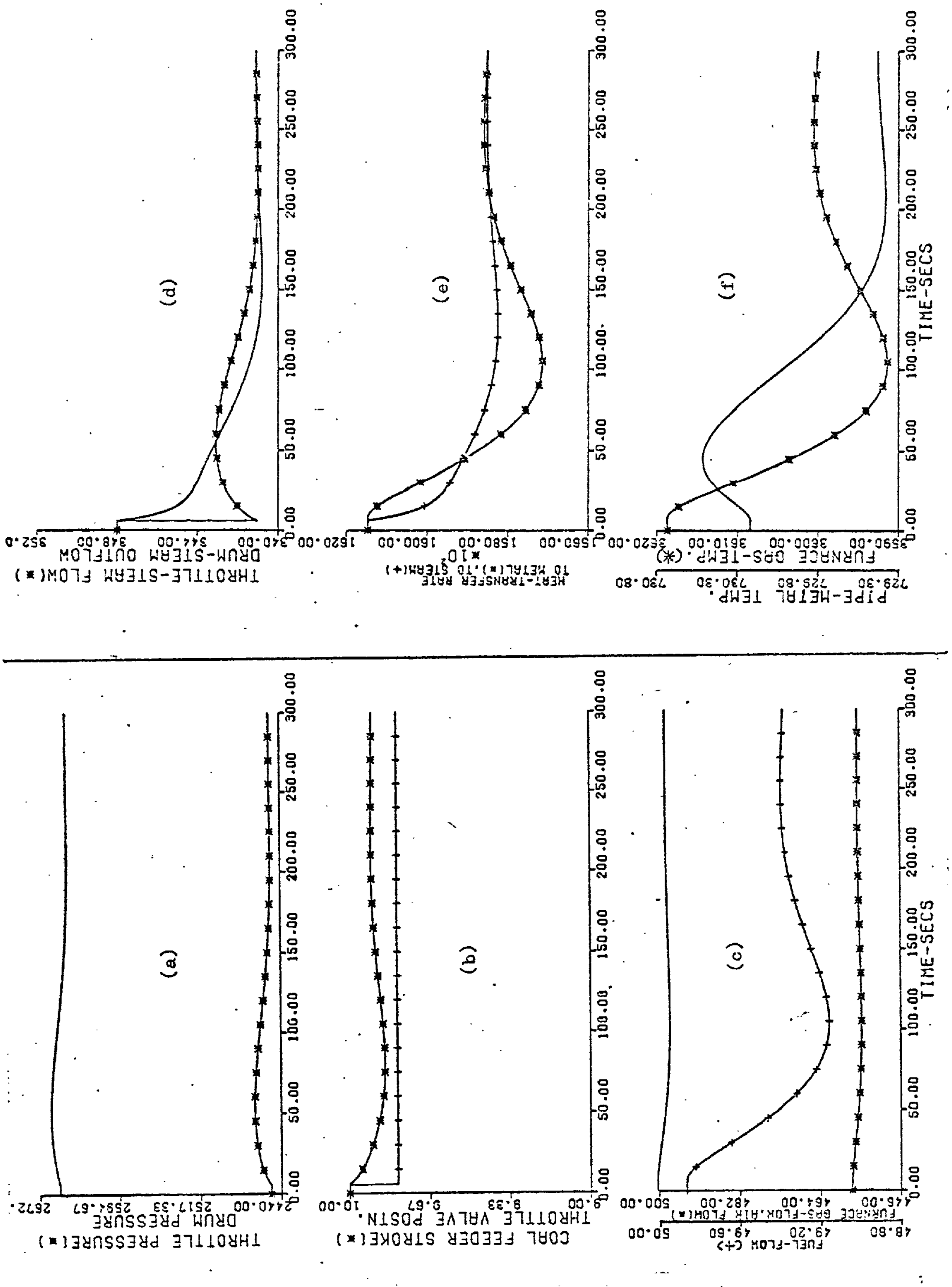

Fig. 2.10: Closed-loop response of the conventional boiler model to a 2% step decrease in the valve opening (drum time constant: 250 s).

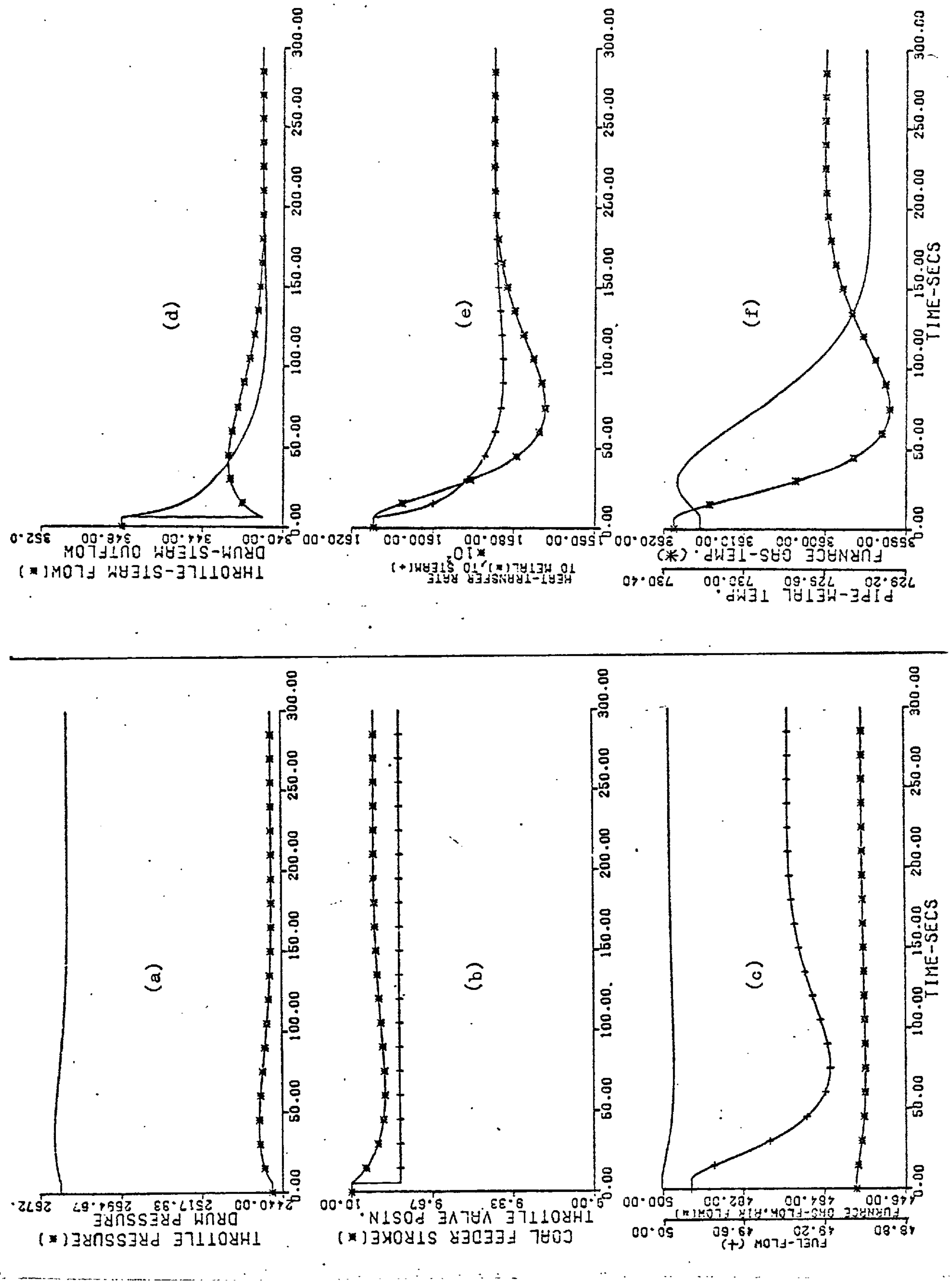

Fig. 2.11: Closed-loop response of the conventional boiler model to a 2% step decrease in the valve opening (drum time constant: 220 s).

It can also be seen in Figs. 2.9, 2.10 and 2.11 that as the time constant of the drum becomes smaller and the time constants of the air and the fuel paths are also becoming smaller, the changes in the control inputs are becoming faster. As a result, the throttle pressure returns faster to its set-point value and the system settles faster to its new steady-state. A more direct comparison of the model response for these three cases can be seen in Figs. 2.12, 2.13 and 2.14. In these, an initial step decrease of 10% was introduced to the valve opening. The system was allowed to settle and then a 10% step increase of the valve opening to its original value was introduced. At this point it should also be mentioned that the closed-loop response of the model with the drum pressure P_{SD} computed from the quadratic equation (2.66) (and with the same controller gains), differs very little from the response of the model presented so far, for which a first order equation is used to compute P_{SD}.

As mentioned in previous sections, the values of the feed-water enthalpy (h_{E0}), air temperature (T_A) and fuel quality (F) were considered to be constant. In order to assess the behaviour of the model to a change in those values, a step reduction of 2% was introduced in all of the three quantities and the open and closed-loop responses were taken for each case.

In Figs. 2.15, 2.16 and 2.17 the open-loop responses are presented. For the disturbances in T_A and F, the response of the model is similar, because it is the change in the heat transfer rate to the riser metal which provokes the change in steam pressures and flow rates. On the other hand, the disturbance in the feedwater enthalpy affects directly the production of steam in the drum and the steam flow rate there. Consequently, it is the heat transfer rate to the mixture in the risers which is affected, increasing suddenly as the steam temperature in the drum drops. From all these disturbances, the one affecting the fuel quality produces the biggest change in the throttle pressure, while the air temperature change affects it on a much lesser scale.

In Figs. 2.18, 2.19 and 2.20 the closed-loop response of the model for the same type of disturbances is shown. These

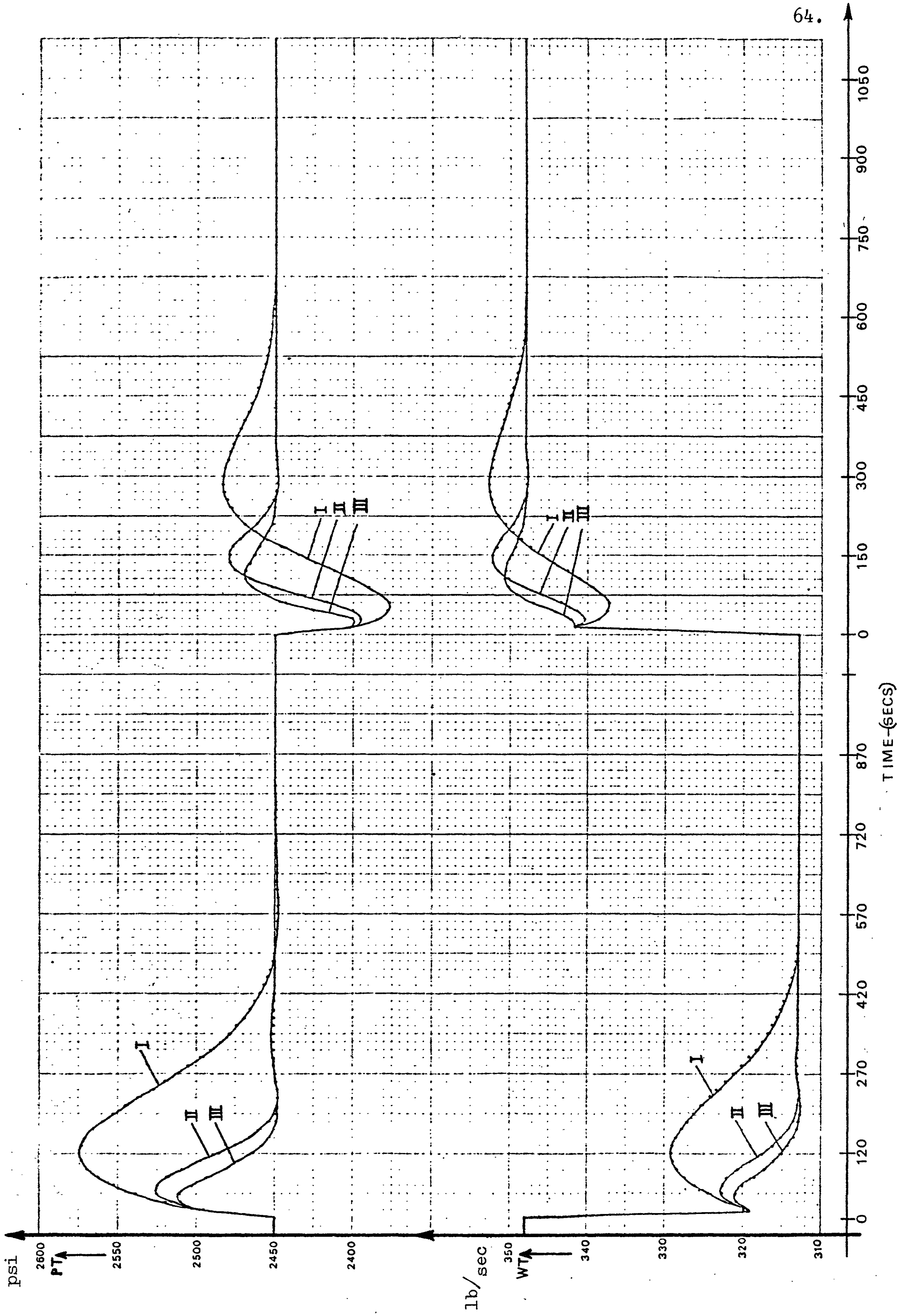

<u>Fig. 2.12</u> Closed-loop response of the conventional boiler model to a double 10% step (decrease/increase) in the valve opening.

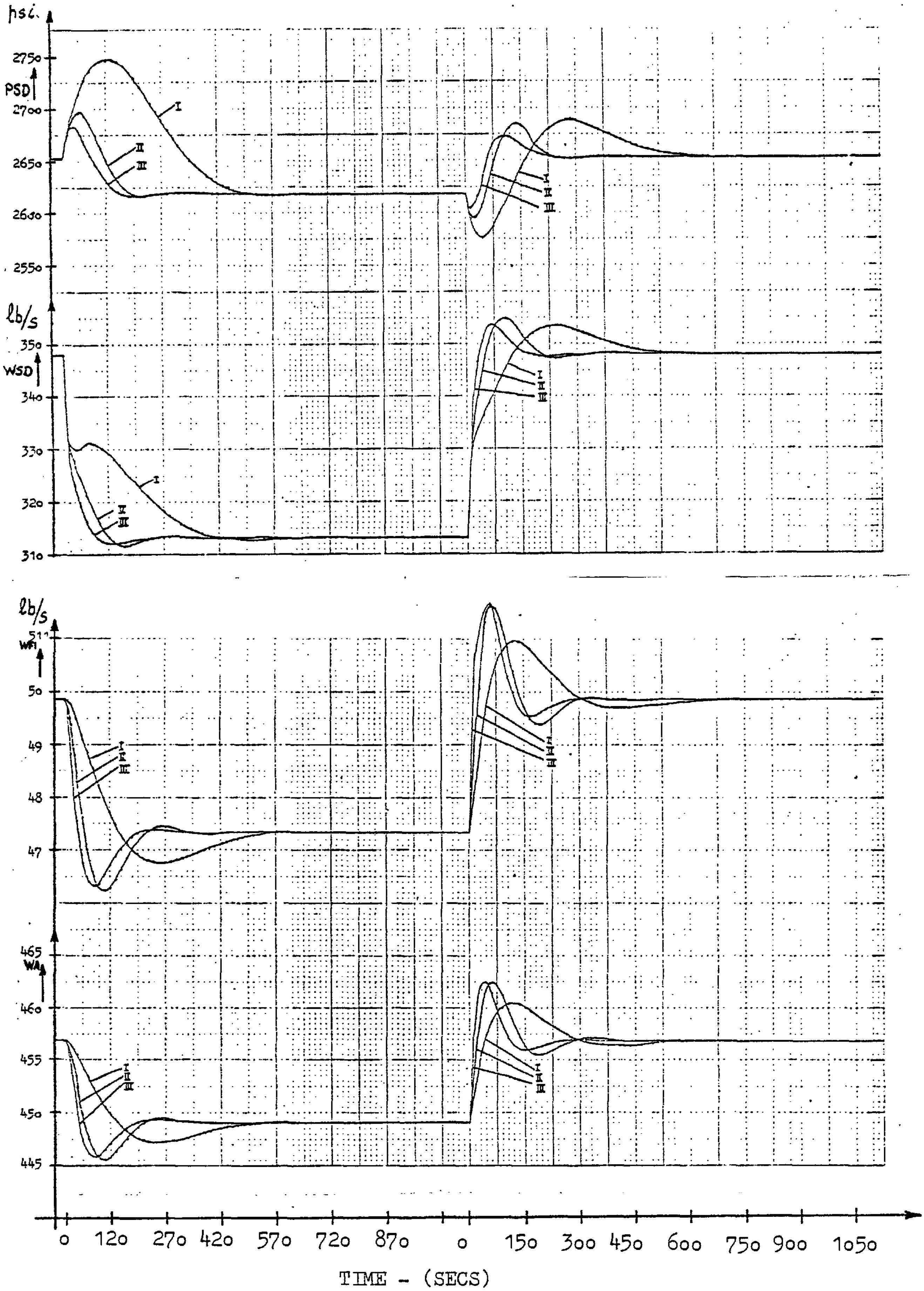

Fig. 2.13 Closed-loop response of the conventional boiler model to a double 10% step (decrease/increase) in the valve opening.

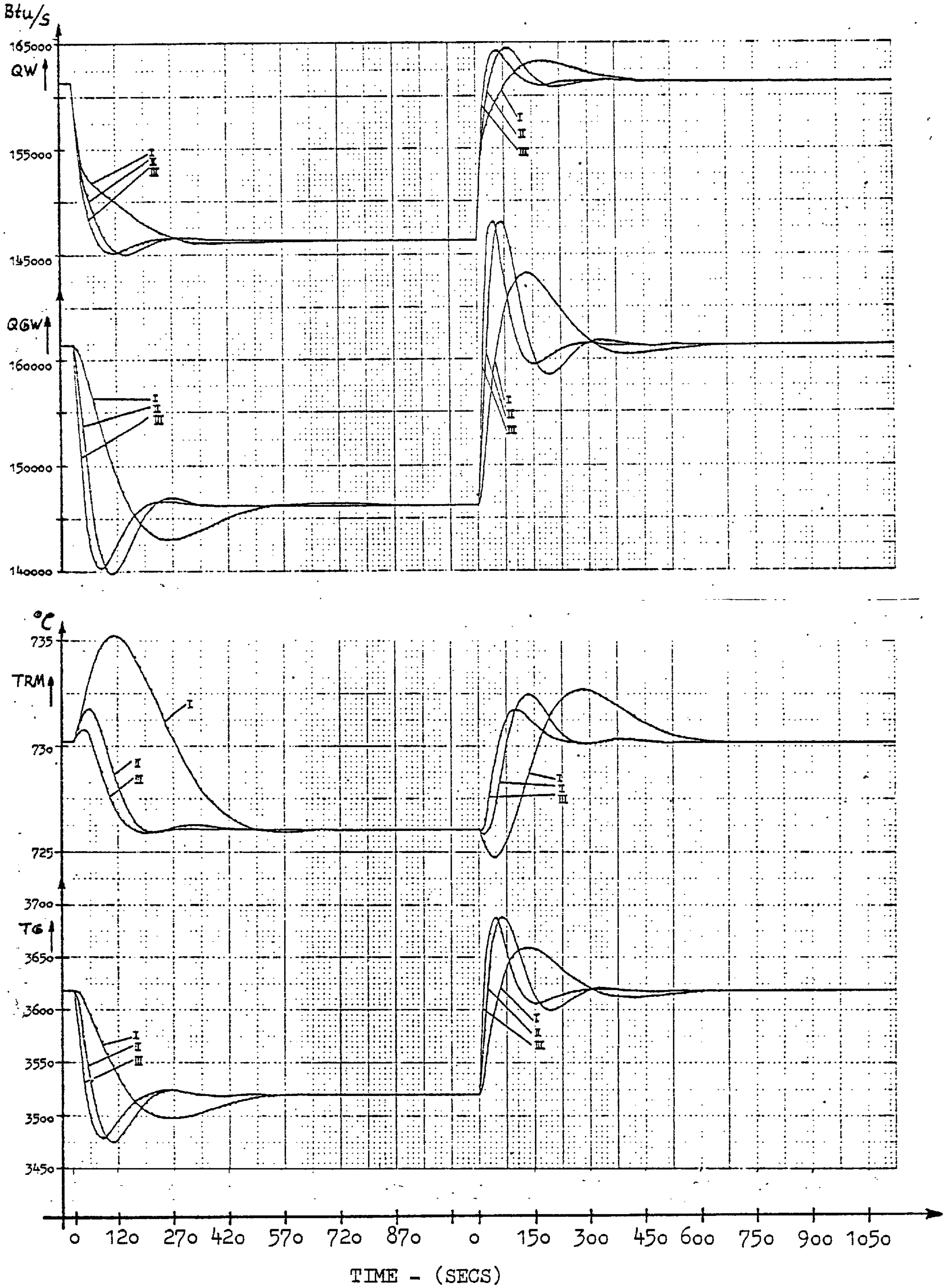

Fig. 2.14 Closed-loop response of the conventional boiler model, to a double 10% step (decrease/increase) in the valve opening.

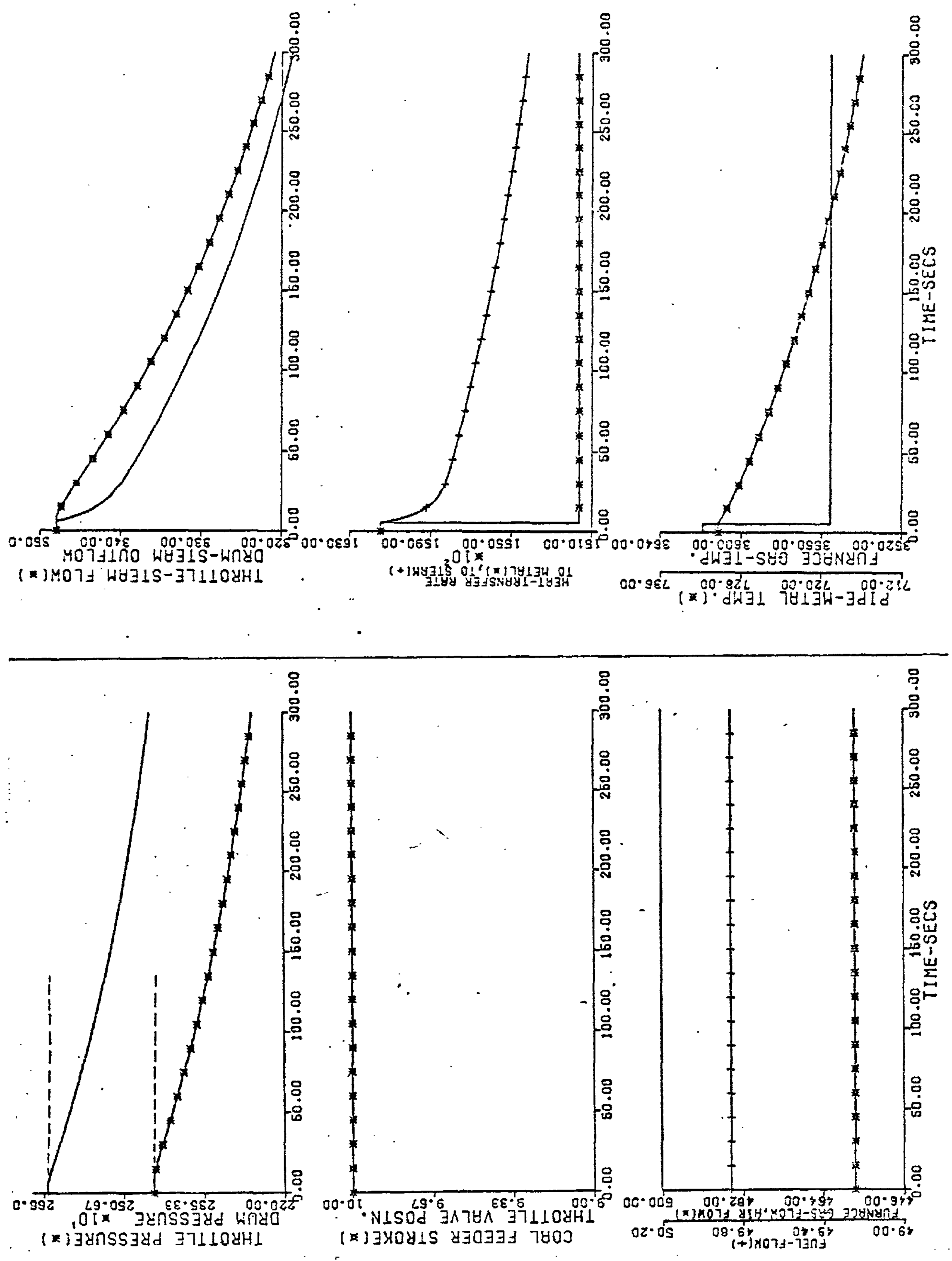

Fig. 2.15: Open-loop response of the conventional boiler model to a 2% step reduction in the fuel quality (F).

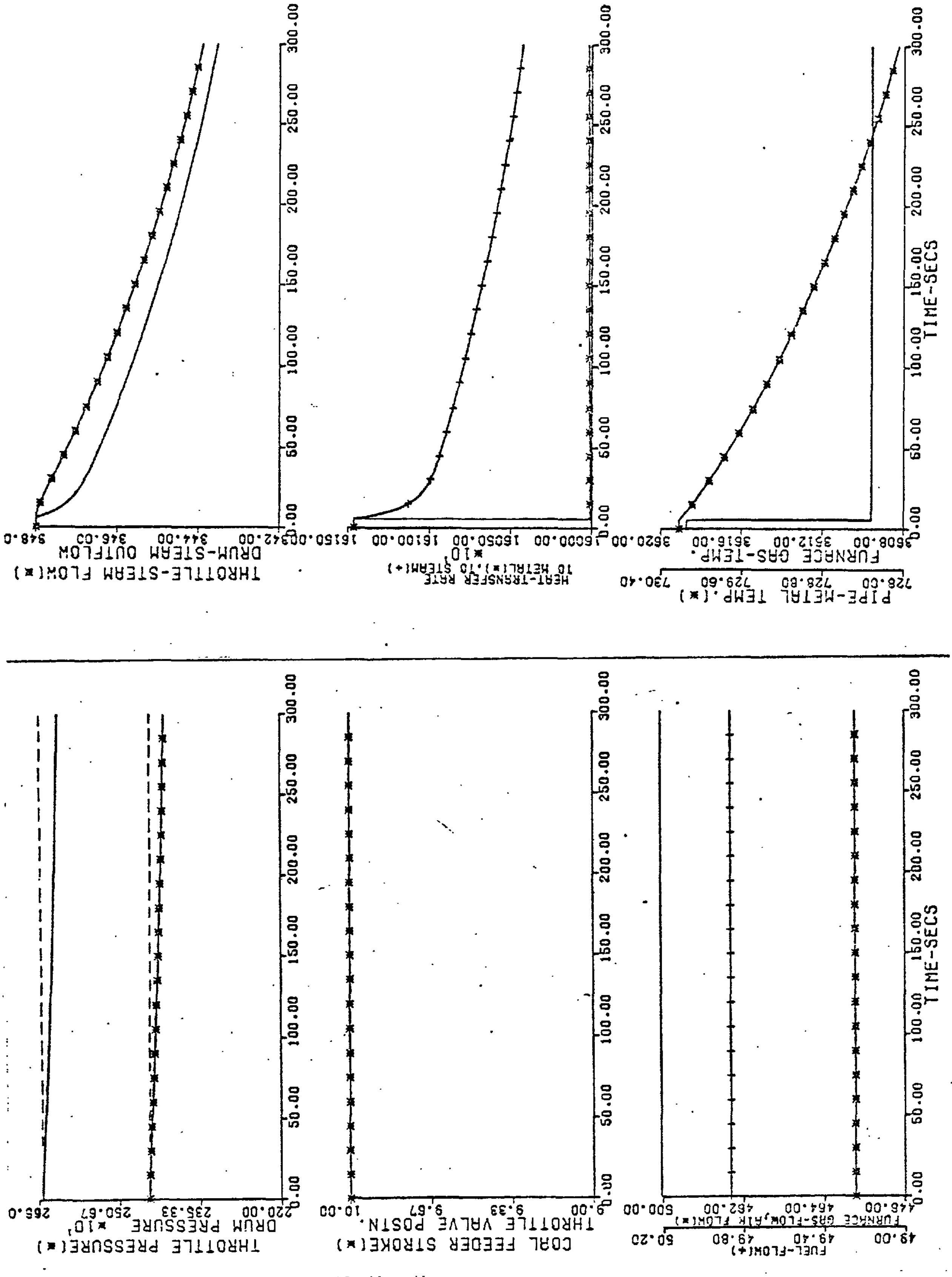

Fig. 2.16: Open-loop response of the conventional boiler model to a 2% step decrease in the air temperature (T_A).

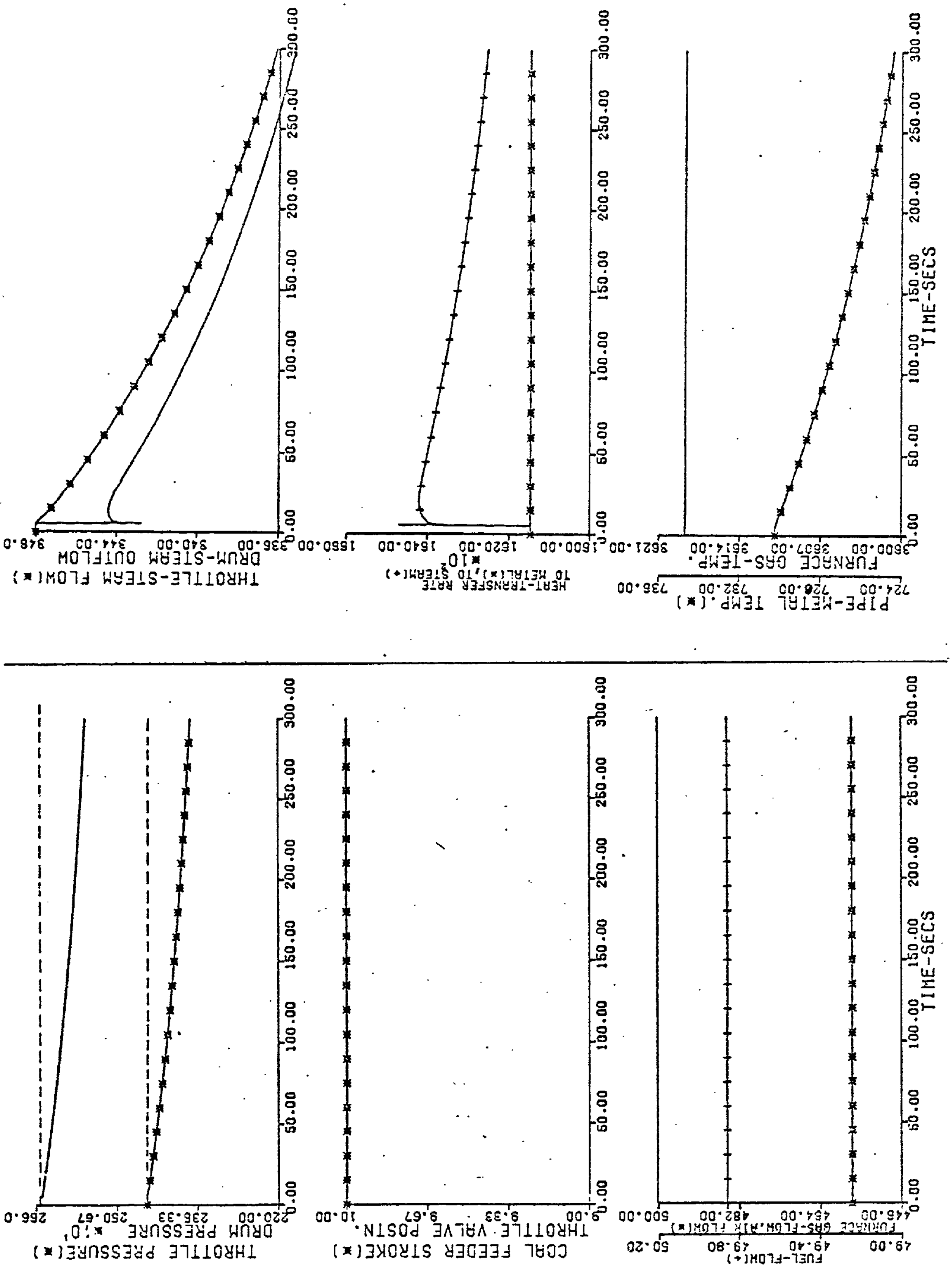

Fig. 2.17: Open loop response of the conventional boiler model to a 2% step decrease in the feedwater enthalpy (h_{E0}).

responses confirm the fact that the greatest effect on the response is caused by the disturbance in the fuel quality. This can be seen by the greater values assumed by the coal-feeder stroke and the fuel and air flow rates.

From the responses shown, it was decided that the model gave a satisfactory representation of the steam generating process of plants with different time constants and that it could be used with confidence as an integral part of the Power Systems Simulator.

2.5.3 The Case for the Once-Through Boiler

The main difficulties in modelling a once-through boiler system arise in the parts where heat exchange takes place. At these sections change of phase of the working fluid takes place, but the boundaries between two phases are not exactly known. This is because the main characteristic of this type of boiler is that the evaporation, superheating, etc. occur along the length of the piping, as the fluid passes through it. So the variables describing the process are functions of at least one space variable (usually the length of the tube), apart from being functions of time. This involves the use of partial differential equations to describe the process. Various techniques are employed and simplifying assumptions made, in order to get rid of the partial differential equations[33-37]. Again, as in the case of drum-type boilers, a rather large number of ordinary differential and algebraic equations, both linear and non-linear, result.

As in the case of the drum-type boiler, a much simpler model would have to be adopted to comply with the limitations imposed by the amount of core and by the sampling interval T for which the model gives a stable response. For this purpose, it was decided that the same model used for drum-type boilers will be used for the once-through with appropriate changes in the fundamental time constants. For example, a simple model representation for a once-through unit is given by Laübli and Fenton[18]. There, a time constant of 115 s is assumed at the steam generation section, for a 575 MW supercritical coal-fired unit. Also, since the control

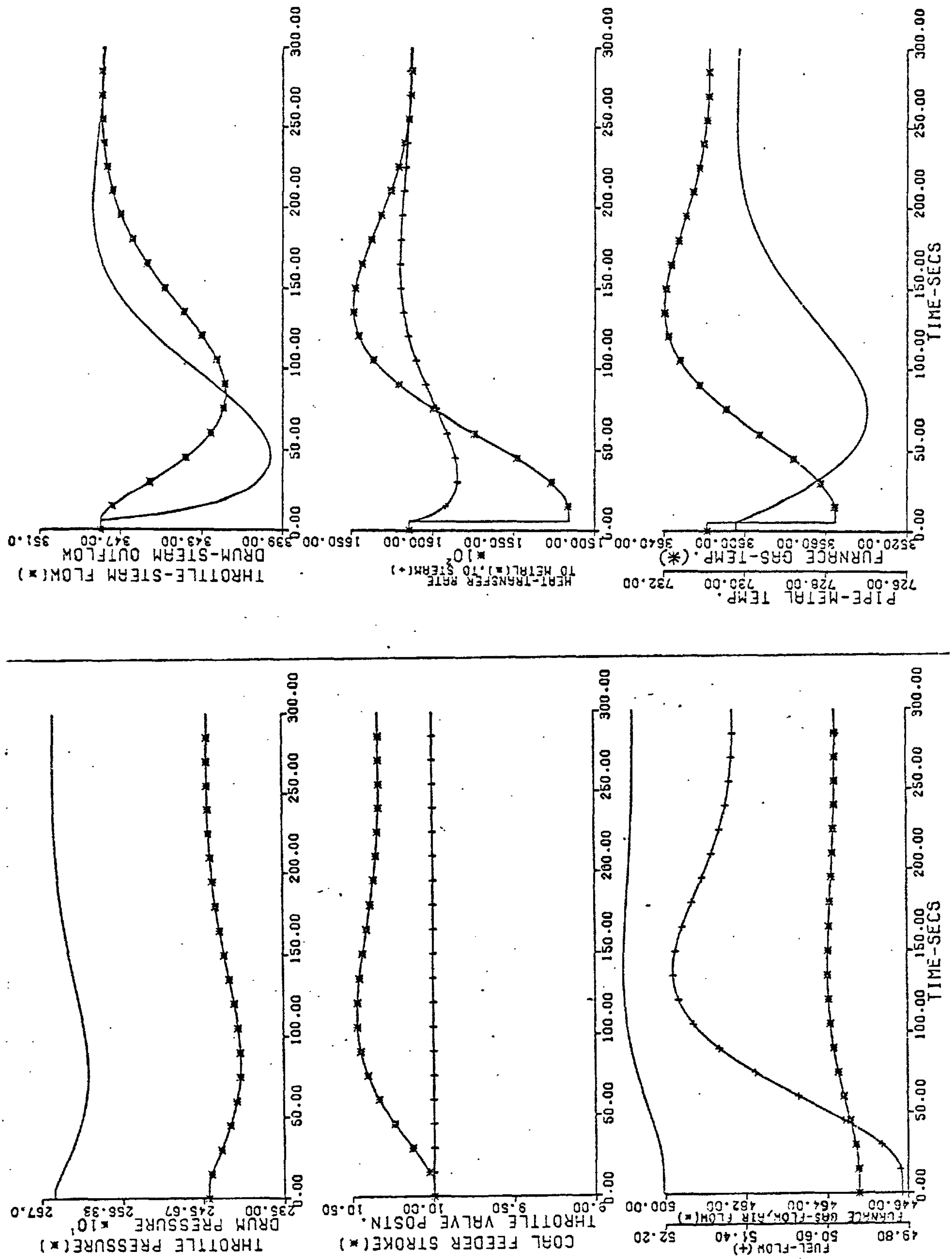

<u>Fig. 2.18</u>: Closed-loop response of the conventional boiler model to a 2% reduction in the fuel quality (F).

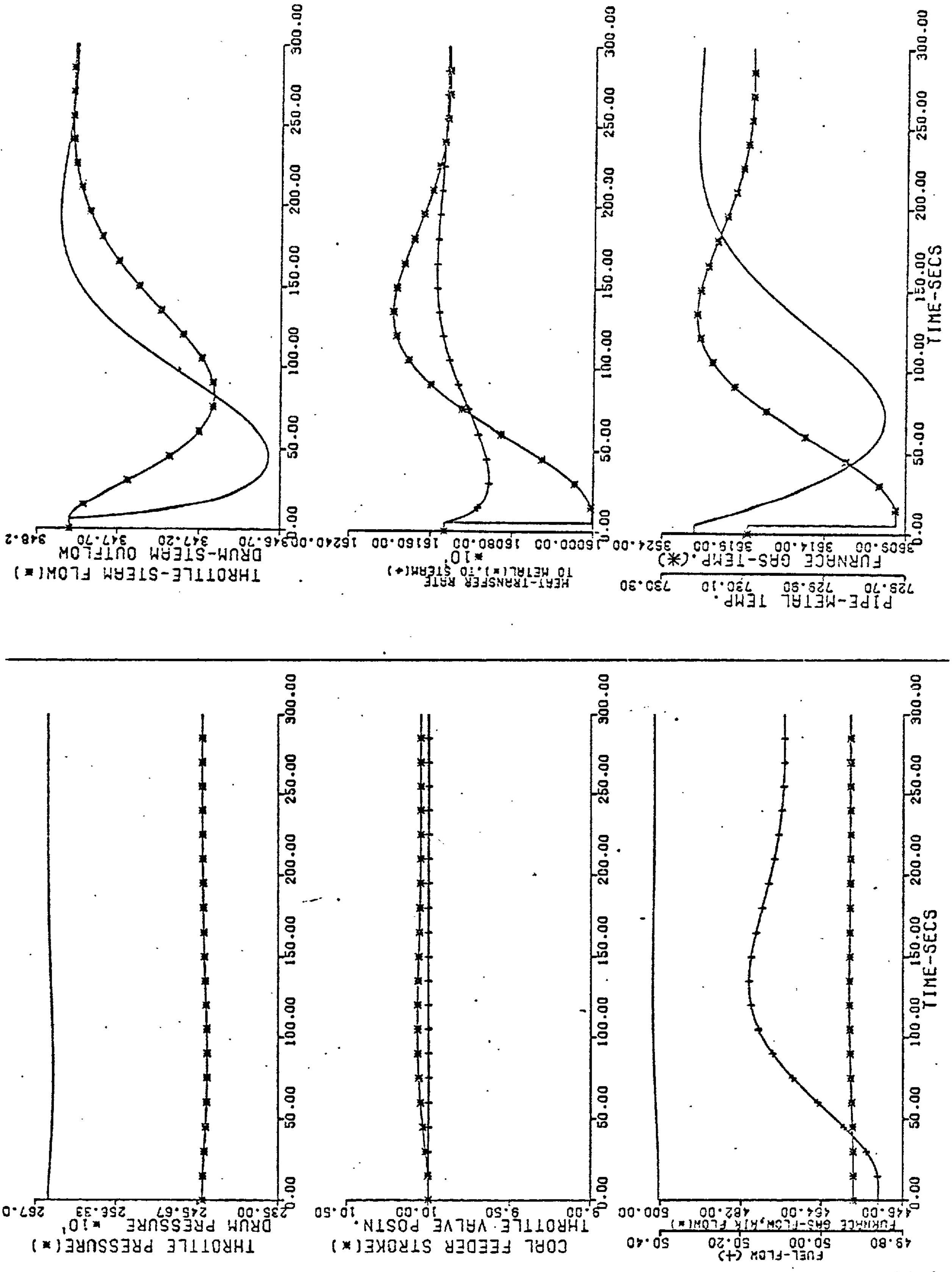

Fig. 2.19: Closed loop response of the conventional boiler model to a 2% reduction in the air temperature (T_A).

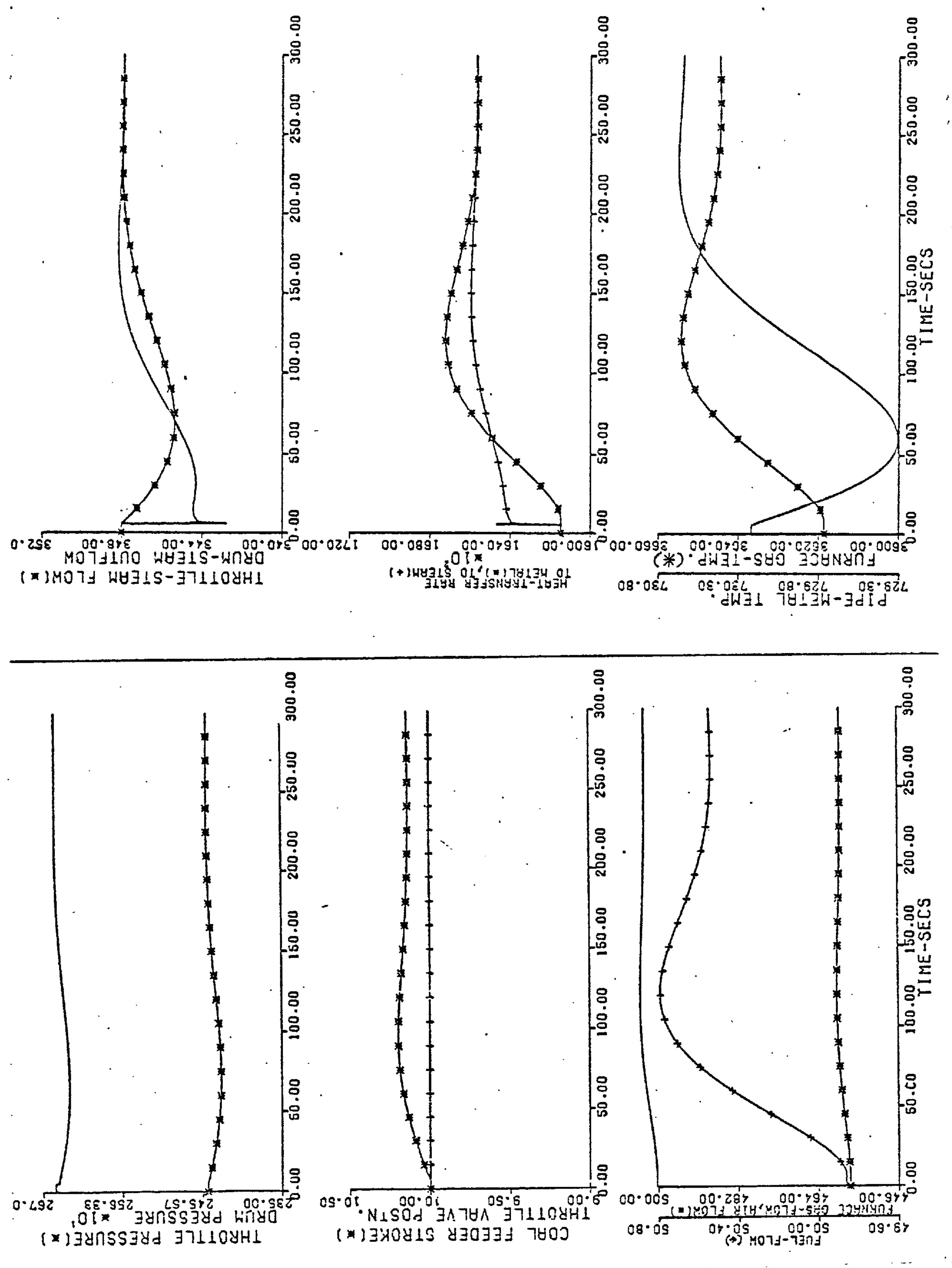

Fig. 2.20: Closed-loop response of the conventional boiler model to a 2% step decrease in the feedwater enthalpy (h_{E0}).

of the feedwater is very important aspect of the operation, the assumption made in the drum-type boiler that $W_{EO} = W_{SD}$ can be dropped here, so the feedwater flow W_{EO} can be used for control purposes.

2.6 REAL-TIME OPERATION OF THE CONVENTIONAL PLANT MODEL

2.6.1 The Operating System

The Real-Time Operating System[38] used on the PDP-15 is called the RSX-15 Phase 1. This is a real-time monitor system designed for handling real-time information in a multi-programming environment. It has a modular construction, which permits its configuration to make the best use of the available hardware and software facilities.

The RSX Executive is the heart of the real-time system. It coordinates all the activities in the system, including the task building, I/O supervision, resource allocation and interactive operator communication.

The RSX-15 utilises two monitors: (a) The Advanced Monitor, and (b) The Real-Time Monitor.

The Advanced Monitor[39] is used for editing, debugging, compiling of programs and for the development of the tasks and the task building. The programs can be written in FORTRAN IV or assembler language. The facilities, mentioned above, are not available in the real-time system. This has the disadvantage that the operator has to change the operating system every time these facilities are needed. On the other hand, the real-time system is faster and more efficient due to the smaller system time overheads.

The Real-Time Monitor supervises and controls the execution of the Real-Time Tasks.

Every program (written either in Fortran or in assembler) has to be converted to a Task to be run in real-time. For this purpose, the binary version of the program and its subroutines is required. Next, the task-builder program is requested and the corresponding task is created, subject to the following information:

- Name of Task,
- Default priority of the Task,
- Partition in the core in which the Task will be run,
- Common blocks used by the Task,
- The resident code, i.e. the programs of the Task thatduring execution will be core-resident (the rest will be disc-resident),
- The structure of the overlaying system.

The task, having been developed, can be stored on a DEC-tape from which it can be installed in the computer, when the real-time system is on.

The TASK BUILDER is a program which utilizes the relocatable binary files, linking them together along with library functions and thus forming an executable task.

The Partition and the COMMON blocks are predetermined in their size and base address. This is done when the real-time system is configured. The SYSTEM CONFIGURATOR is a system task. When it is requested, it allows the user to specify core size, disc size, number of teletypes, clock frequency, partition description, system COMMON block descriptions and a description of peripheral I/O units. The system configuration in its present form is shown on Fig. 2.21a.

The Monitor Console Routine (MCR) is the part of the software which allows the user to interact with the system via the teletype and dynamically alter the operation of the system. The user can install or remove a task, suspend or assume its execution, acquire information about the status of the system, access the contents of any core location, modify them, etc.

This interaction is done by simple commands which, in turn, activate appropriate tasks (called MCR-functions), which perform the requested function. These tasks are normally disc-resident and they are brought in core whenever required.

The scheduling of the real-time tasks is a result of any of the three types of "significant events": (a) the request of the activation of a task, (b) the request of an I/O transfer, or (c) the occurrence of a hardware interrupt.

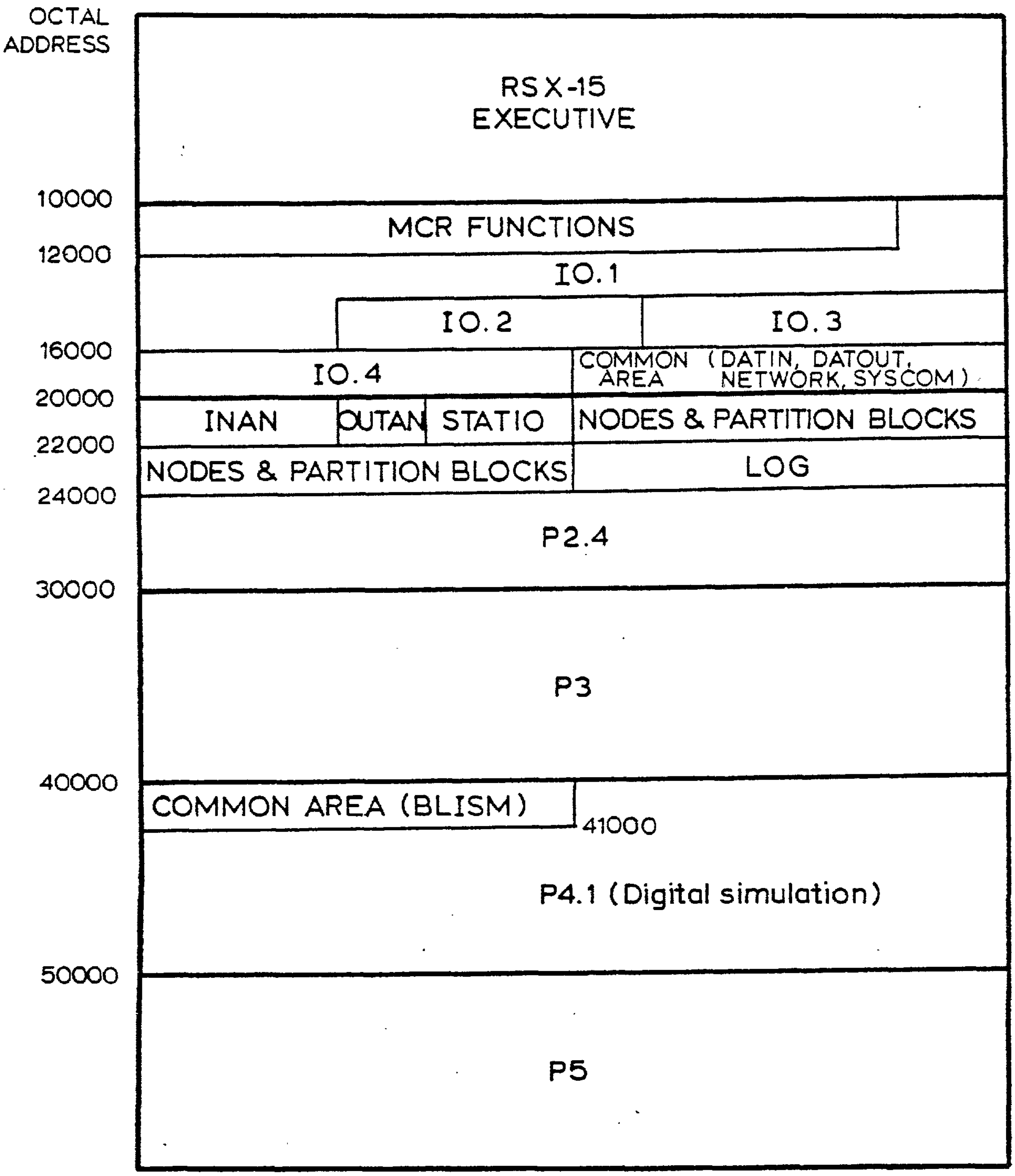

Fig. 2.21a *Core Map*

Fig.2.21b *AUTOMATIC PRIORITY INTERRUPT SYSTEM*

Task Priority Levels	Executive Priority Levels	Hardware Levels
Derived from API Level 7 by the executive 512 ⟶ 1	Exclusive use by the executive	Used by all I/O devices
API LEVELS 7	6 5 4	3 2 1 ϕ
	Increasing Priority ⟶	

There is a priority-ordered list of "Active Tasks" in the system at any time. This list is scanned from high to low priority by the Executive as a result of a significant event occurring. Then, the task with the highest priority is executed.

The operation of the real-time system is based on the Automatic Priority Interrupt (API) structure and the real-time clock which provided the time reference for the scheduling of the various activities. The API includes both hardware and software priority levels. There are eight levels of API; four of them are hardware levels, which are sized to control the I/O devices of the system. Each of these levels can have up to eight device controllers connected to it, so up to 32 devices can be controlled by these four priority levels.

The other four priority levels are software levels assigned to the executive. Levels No. 4 and 6 are used exclusively by the Executive itself. Level No. 5 is not currently used. Under API level No. 7, there are 512 Task priority levels. These are used exclusively for task scheduling and operation. The API structure is shown in Fig. 2.21b.

2.6.2 Conversion of the Model Equations for Real-Time Operation

In Section 2.5 it was shown that the model would give a reasonable response both in open and closed-loop operation. So the next step was to convert the program, which was run on the CDC 6400 computer, into a suitable form which could run on the PDP-15 computer connected to the simulator.

Here, every effort was made to formulate the program in a way which would give the maximum possible savings in storage and computation time, for obvious reasons. Therefore simplifications and approximations were adopted when it was required. In Table 2.4 the difference equations (run on the CDC 6400) and the same equations with the form they assume in the real-time version, are presented. The following are the main points of interest concerning their conversion:

TABLE 2.4 CONVENTIONAL BOILER MODEL EQUATIONS IN THEIR REAL-TIME FORM

Discrete Representation	Real-Time Representation
$ALL = L_F(K) + L_F(K-1)$	$ALL = A_{LF}(I) + A_{LF1}(I)$
$M_{CR}(K) = \left[\frac{2-T.K_{CF}}{2+T.K_{CF}}\right].M_{CR}(K-1) + \left[\frac{T.K_F}{2+T.K_{CF}}\right].ALL$	$A_{MCR}(I) = C(I,1)*A_{MCR}(I)+C(I,2)*ALL$ $A_{LF1}(I) = A_{LF}(I)$
$W_{FI}(K) = \left[\frac{2.T_P-T}{2.T_P+T}\right].W_{FI}(K-1) + \left[\frac{T.K_{CP}}{2.T_P+T}\right].(M_{CR}(K)+M_{CR}(K-1))$	$W_{FI}(I) = C(I,3)*W_{FI}(I) + +C(I,4)*(A_{MCR}(I)+A_{MCR1}(I))$ $A_{MCR1}(I) = A_{MCR}(I)$
$A(K) = \left[\frac{2.T_{AA}-T}{2.T_{AA}+T}\right].A(K-1) + \left[\frac{K_A.T}{2.T_{AA}+T}\right].ALL$	$A(I)=C(I,5)*A(I)+C(I,6)*ALL$
$W_A(K) = W_R.\sqrt[3]{A(K)}$	For: $A(I) \leqslant 69.741515$, then: $W_A(I)=218.0-(A(I)*2.342549026)$ For: $A(I) > 69.741515$, then: $W_A(I)=286.0-(A(I)*1.36752004)$
$W_{GF}(K) = W_A(K)+0.87.W_{FI}(K)$	$W_{GF}(I)=W_A(I)+0.87*W_{FI}(I)$
$Z = 1 + (T.E6/C_D).W_{SD}(K-1)$	$Z = 1+C(I,7)*W_{SD}(I)$
$P_{SD}(K) = [P_{SD}(K-1)+(T/C_D).(Q_W(K-1)- -W_{SD}(K-1).(EE6-h_{EO}))]/Z$	$P_{SD}(I)= [P_{SD}(I)+C(I,8)*(Q_W(I)- -W_{SD}(I)*C(I,9))]/Z$
$P_T(K)=P_T(K-1)+(T/C_{SSH}).(W_{SD}(K-1)- -W_T(K-1))$	$P_T(I)=P_T(I)+C(I,10)*(W_{SD}(I)-W_T(I))$
$R_{SD}(K) =(P_{SD}(K)-EE4)/E4$	$R_{SDX} = (P_{SD}(I)-EE4)/E4$
$T_{SD}(K) = E5.R_{SD}(K)+EE5$	
$W_{SD}(K)=\sqrt{F_{SDI}.R_{SD}(K).(P_{SD}(K)-P_T(K))}$	$W_{SD}(I)=\sqrt{F_{SDI}*R_{SDX}*(P_{SD}(I)-P_T(I))}$
$W_T(K) = K_T.A_T(K-1).P_T(K)$	$W_T(I) = (A_T/GSCAL(I))*P_T(I)$
$Z17 = ((F.n/C_{GF})/W_{GF}(K))$	
$T_G(K) = T_A + W_{FI}(K).Z17$	$T_G(I) = T_A+C(I,11)*(W_{FI}(I)/W_{GF}(I))$
$T_{RM}(K)=T_{RM}(K-1)+(T.C_M).(Q_{GW}(K-1)- -Q_W(K-1))$	$T_{RM}(I) = T_{RM}(I)+C(I,12)*(Q_{GW}(I)-Q_W(I))$
$Z14 = T_{RM}(K) - T_{SD}(K)$	$Z14 = T_{RM}(I)-(E5*R_{SDX}+EE5)$
$Q_W(K) = K_{RS}.(Z14.Z14.Z14)$	$Q_W(I) = K_{RS}*(Z14*Z14*Z14)$
$Z15 = 0.555556\cdot T_G(K) + 255.372$	$Z15A = 0.555556\cdot T_G(I)+255.372$
$Z16 = 0.555556\cdot T_{RM}(K)+ 255.372$	$Z16A = 0.555556\cdot T_{RM}(I)+255.372$
	$Z15 = Z15A.Z15A$
	$Z16 = Z16A.Z16A$
$Q_{GW}(K) = K_{RW}.(Z15^4-Z16^4)$	$Q_{GW}(I) = K_{RW}.((Z15.Z15)-(Z15.Z15))$
$D_{PE}(K) = P_{SET}-P_T(K)$	$S_E(I) = S_E(I) + D_{PE}(I)$
$S_E(K) = S_E(K-1)+D_{PE}(K-1)$	$D_{PE}(I) = P_{SET} - P_T(I)$
$L_F(K+1)= KPP.D_{PE}(K)+KIP.S_E(K)+ + KDP(D_{PE}(K)-D_{PE}(K-1))$	$A_{LF}(I) = KPP(I).D_{PE}(I)+KIP(I).S_E(I)+ + KDP(I).(D_{PE}(I)-D_{PE}(I))$
	$D_{PE1}(I) = D_{PE}(I)$

(a) As mentioned in Section 2.4, the air-fuel section equations were discretized with the use of Tustin's operator. As a result both quantities X(K) and X(K-1) are needed in the same equation. This situation arises for three variables: L_F, D_{PE} and M_{CR}. In all three cases it was decided to introduce three more variables designated: L_{F1}, D_{PE1}, M_{CR1}, which would contain the value of the last iteration, i.e. X(K-1). This could be avoided, but in so doing, three more floating point multiplications would be added to the computation time.

(b) The computation of the air flow W_A involved the computation of a cubic root. This would take a very long time to be performed; for this reason, this cubic root equation was approximated by two straight line segments. This approximation is shown in Fig. 2.22, together with the equations of the straight lines used. By so doing, the maximum number of operations would be one arithmetic if-statement, one multiplication and one addition (floating point both of them).

(c) The use of the X(I) representation of the variables enables the use of the same equations (in a do-loop) to represent as many different boiler units as required. For the Power Systems Simulator, this is six.

(d) The constants designated C(I,12) are precalculable. Their computation is performed in a separate program (initialization program). The use of the variable (I) here, as well as in the representation of the P I D controller gains, gives the opportunity for each of the six units to have different operating characteristics.

(e) The valve position A_T was not dimensioned as $A_T(I)$, because this quantity is "read" from the analog part of the simulator for every unit separately (i.e. every time the do-loop in the real-time program starts from the beginning).

(f) The variables R_{SD} and T_{SD} although dimensioned in the common block, can be used without their X(I) representation in the program. This is possible because they are direct functions of $P_{SD}(I)$. By so doing, the space they occupy in the common block can be used for other purposes.

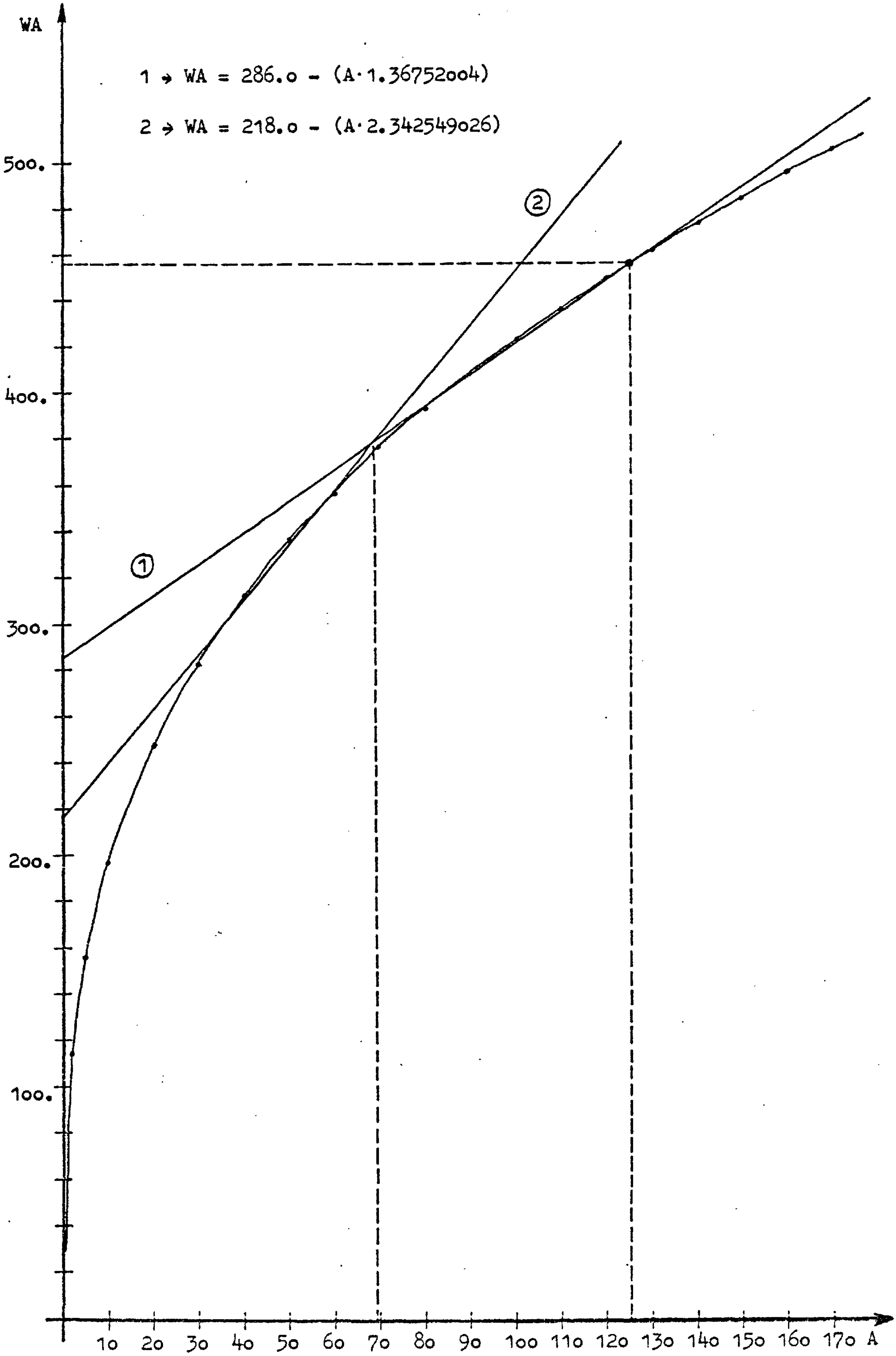

Fig. 2.22 Straight-line approximation of the equation: $W_A = W_R . \sqrt[3]{A}$

For the "real-time" version equations, as they are presented in Table 2.4, the number of operations needed is:

Floating Point Multiplications	:	31
Floating Point Divisions	:	4
Floating Point Additions	:	27
Square Root	:	1

In the actual program there are some more operations needed for various purposes, but the basic functions of the program are: to read in the valve position of the simulated unit, perform the simulation of the plant dynamics and output the throttle pressure at the valve to the analog part of the simulator.

2.6.3 Response of the Conventional Boiler Model working in Real-Time

The configuration shown in Fig. 2.23 was set up on the simulator and the boiler simulation program was initialized (for two conventional units) in order to assess its behaviour under real-time conditions. The loads are programmable sinks of in-phase current and sinks or generators of quadrature current, as mentioned in Section 1.3. A load simulation program was developed by Mogridge[43]. In this the trend changes, the load characteristics and randon fluctuations are modelled. Therefore any of the five loads can be made to change in any way desired by the simulator user.

The system was allowed to settle and then disturbances were introduced, namely manual increases or decreases to the speeder gear setting of unit no. 1. As a result, the valve opening changes and this upsets the pressure at this point. The P I D controller reacts and tries to reduce the pressure error by changing the firing rate of the boiler.

During these tests, the circuit-breaker 14 was closed, i.e. the whole system was connected to the infinite bus, which has the frequency of the mains. It is this frequency that is shown in the Figures 2.24 to 2.29.

The responses were taken for the three cases mentioned in Section 2.5, i.e. for the model with different drum time constants.

In Figs. 2.24 and 2.25 the response of unit 1 is shown to step changes in the valve position, in both directions (drum time

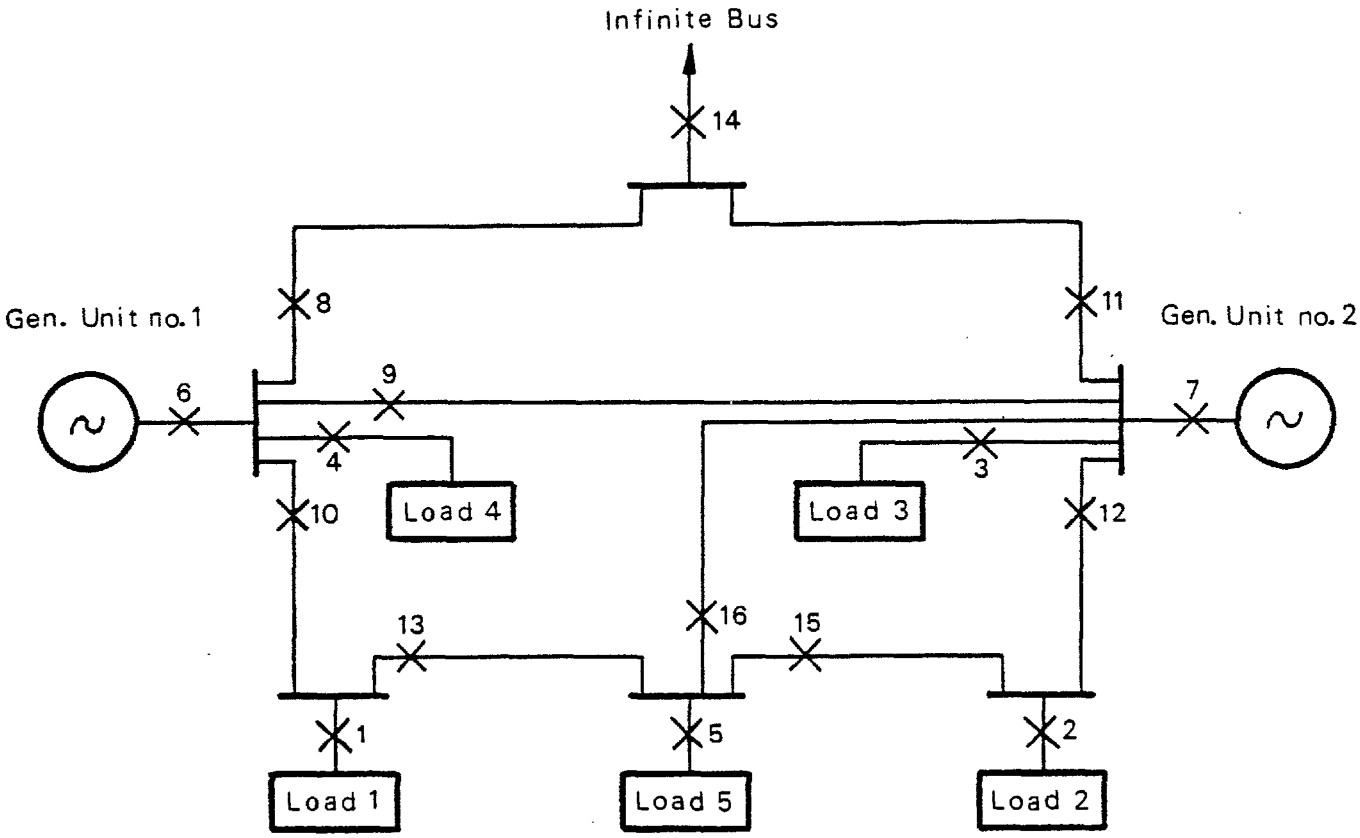

FIG. 2.23 Power system configuration used for testing the digital plant models.

constant C_D = 300 s). In Fig. 2.24 the throttle pressure is brought back to its set point value in about 11 minutes. This time should be shorter, but as can be seen the valve position drops further below the value of the original step change and this results in a further increase of pressure. The rest of the variables change in an appropriate fashion.

In Figs. 2.26 and 2.27 the response of the same unit is shown, when the drum time constant is 250 s. In Figs. 2.28 and 2.29 the time constant is 220 s. As was expected, the response of the boiler is faster and the overshoot of the pressure is smaller.

For another test, the system was disconnected from the infinite bus and it was left to settle. Then, a step increase of about 0.3 p.u. was introduced into load no. 1. In Fig. 2.30 the responses of the main variables of interest for the simulation are shown. With the introduction of the step, the frequency dropped very fast to 48.2 Hz in about 5 s. Then the governors reacted and arrested this fall. From the responses of the valve positions of the two units

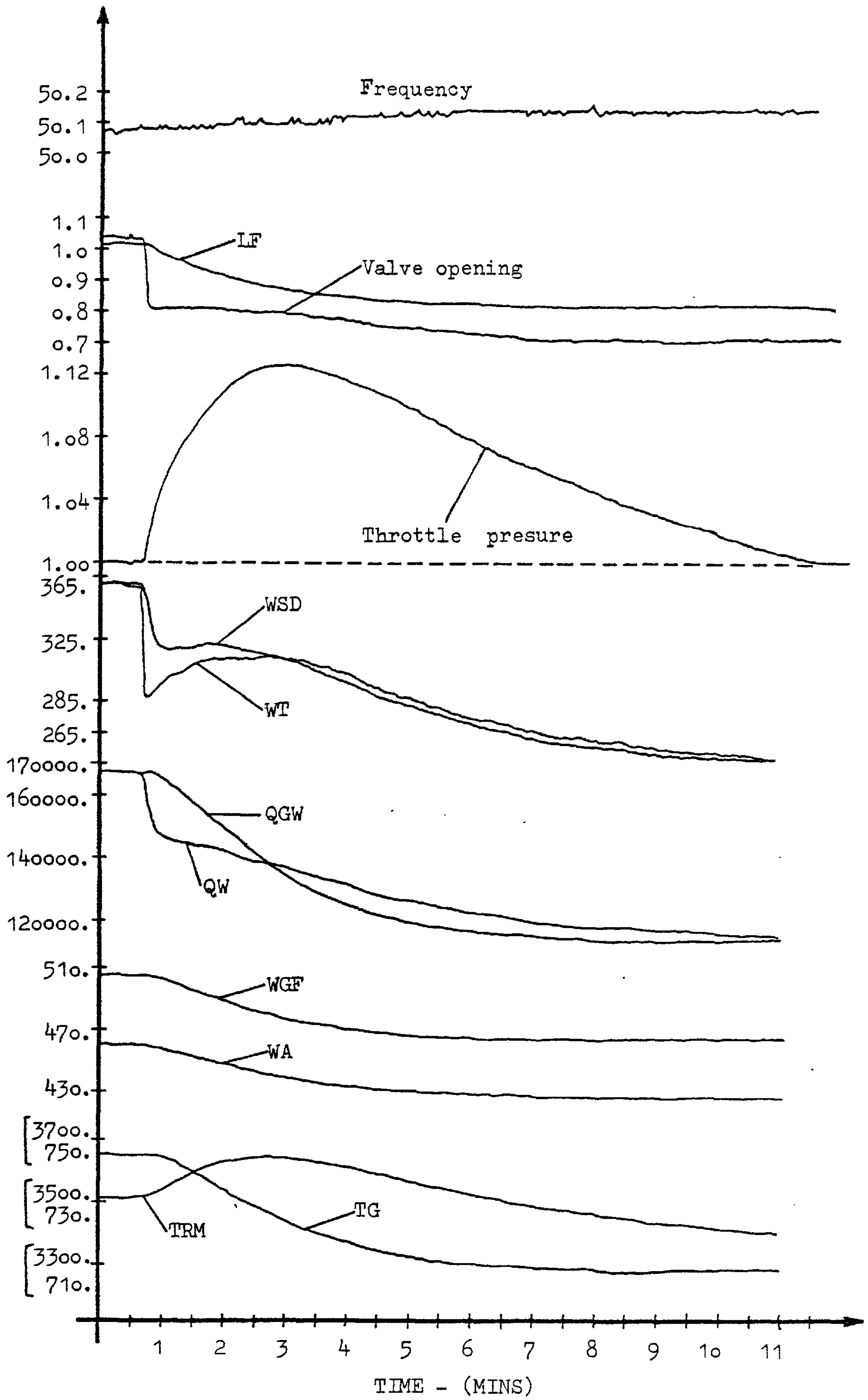

Fig. 2.24 Closed-loop response of the conventional boiler model running in real-time, to a 25% initial step decrease in the valve opening. Drum time constant: 300 s.

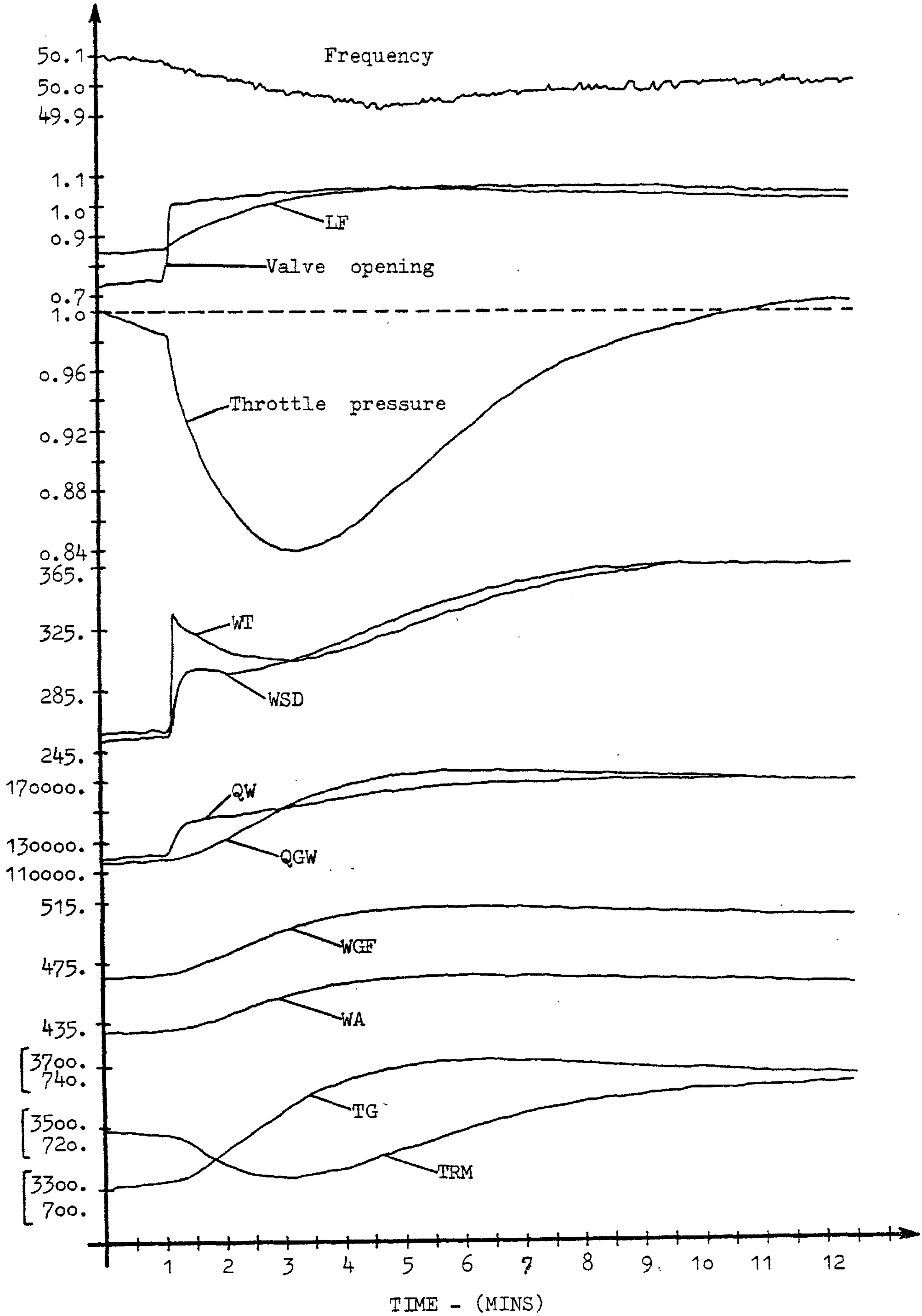

Fig. 2.25 Closed-loop response of the conventional boiler model running in real-time, to a 25% initial step increase to the valve opening. Drum time constant: 300 s.

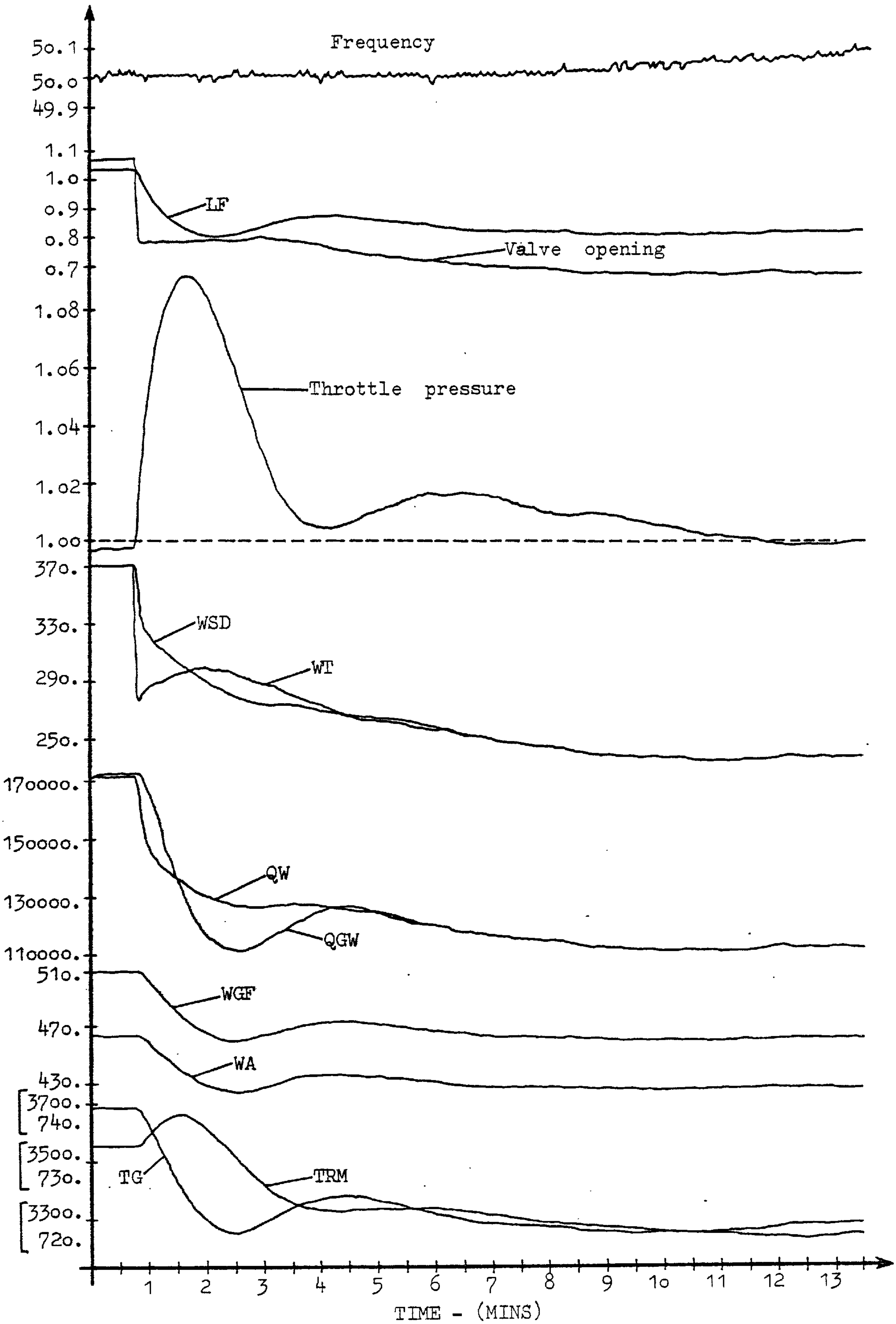

Fig. 2.26 Closed-loop response of the conventional boiler model running in real-time, to a 29% original step decrease in the valve opening. Drum time constant: 250 s.

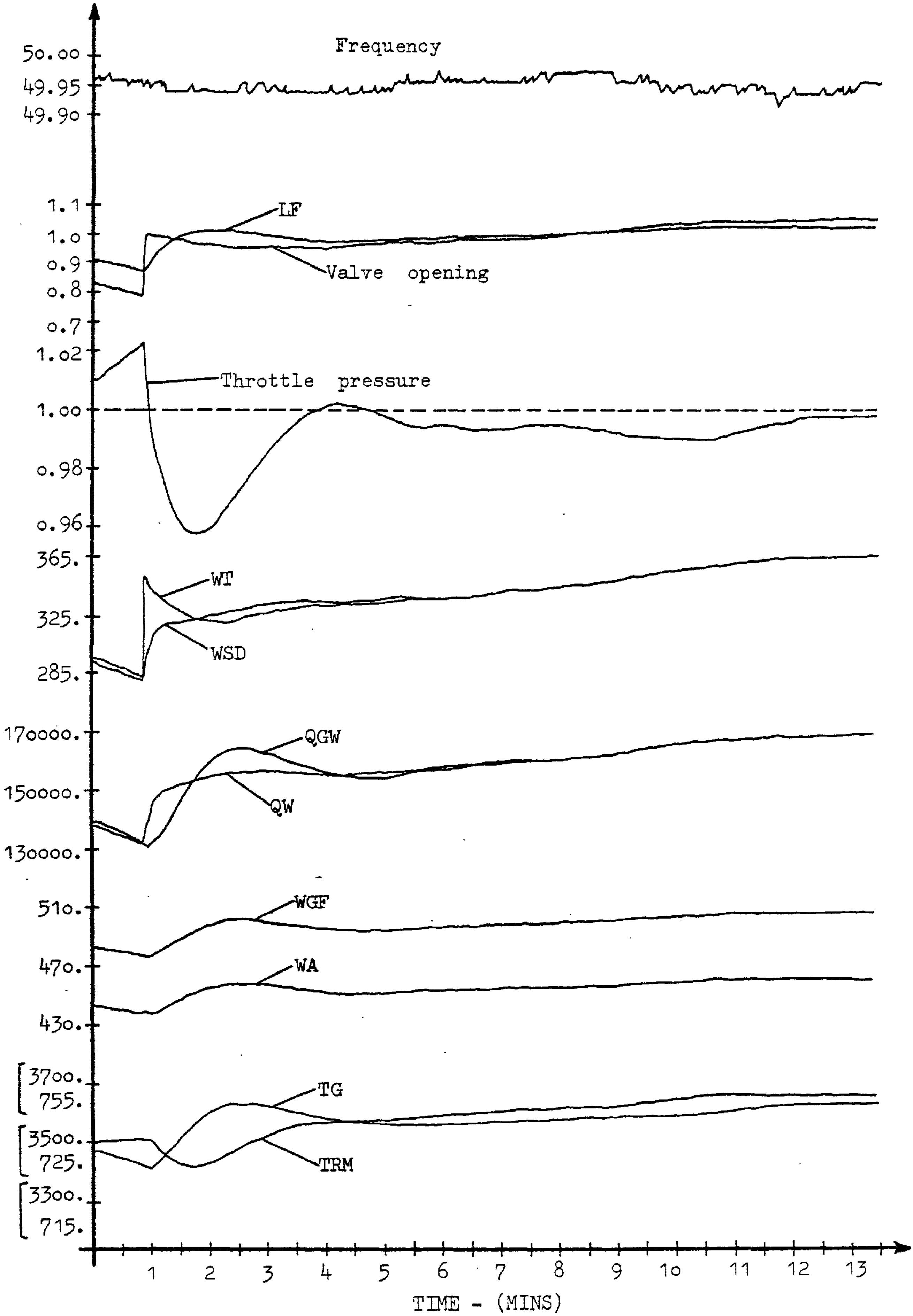

Fig. 2.27 Closed-loop response of the conventional boiler model running in real-time, to a 20% original step increase in the valve opening. Drum time constant: 250 s.

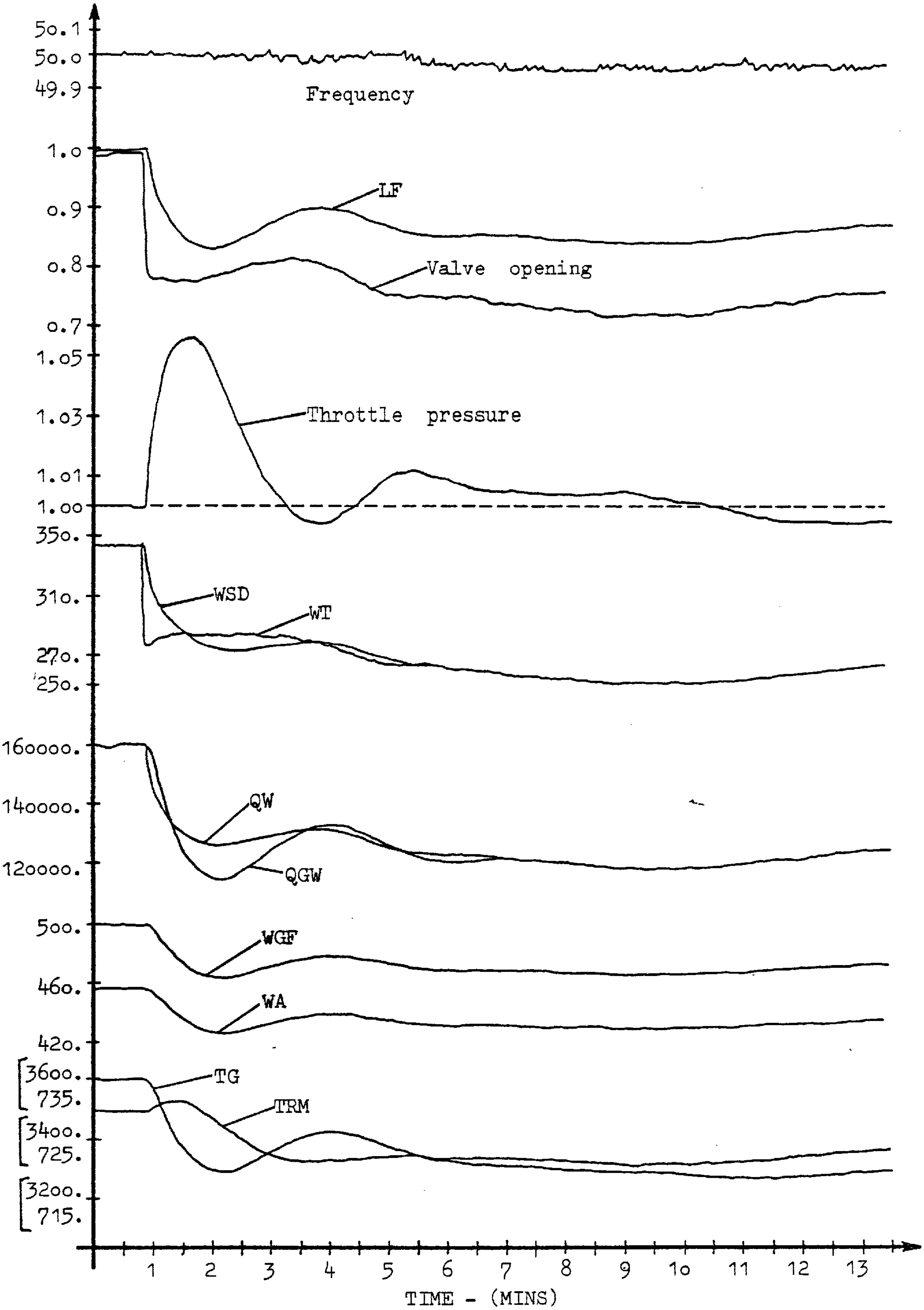

Fig. 2.28 Closed-loop response of the conventional boiler model running in real-time, to a 22% original step decrease in the valve opening. Drum time constant: 220 s.

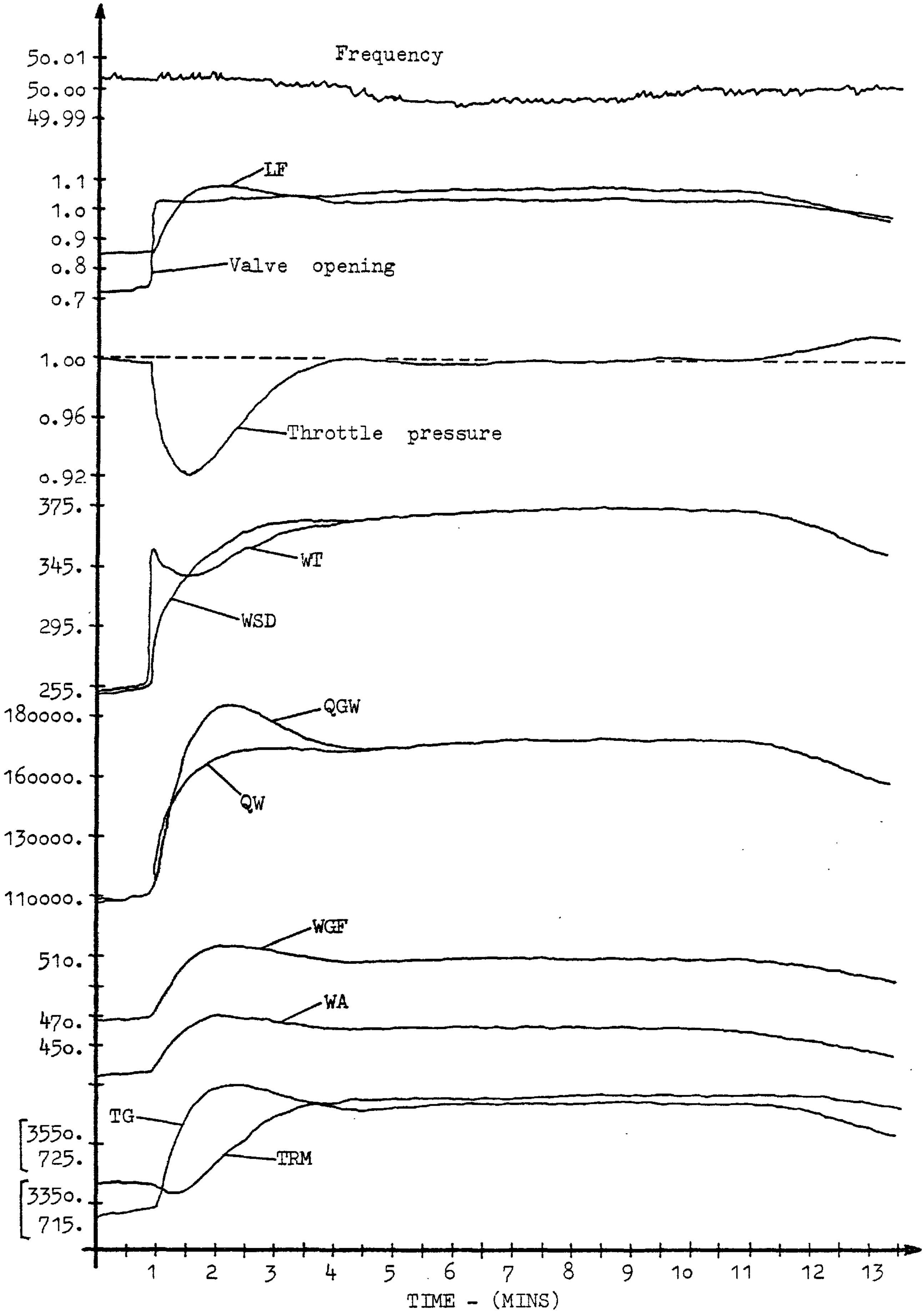

Fig. 2.29 Closed-loop response of the conventional boiler model running in real-time to a 29% original step increase in the valve opening. Drum time constant: 220 s.

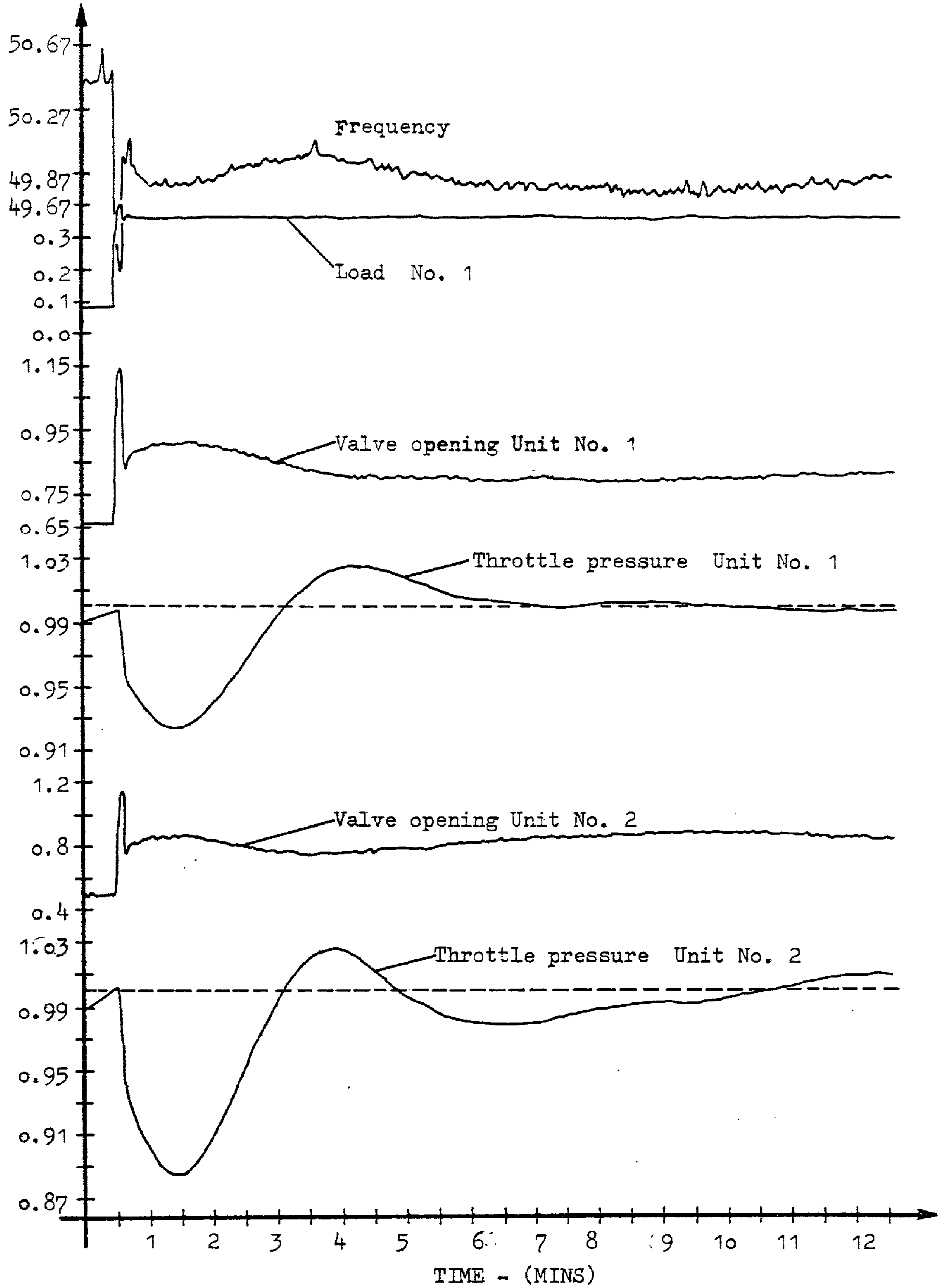

Fig. 2.30 Response of the isolated system (Fig. 2.23) to a 0.3 p.u. step increase in Load 1. The conventional boiler model is driving both generating units (drum time constant: 250 s for both units).

it can be said that the governors overreact to the changes in frequency and in fact bring it up again (point (a) on the frequency curve). By that time, the change in the valve position has affected the boilers and the pressure begins to drop, bringing down with it the frequency (point (b) on the frequency curve). After that, the frequency is mainly affected by the changes in the throttle pressure and it more or less follows the two pressure curves.

Therefore it is concluded that the response of the boiler simulation running in parallel with the analog part of the simulator is very satisfactory.

2.7 LINEARISATION OF THE CONVENTIONAL BOILER MODEL

For comparison purposes, the model equations (Table 2.3) were linearised around the steady-state point corresponding to full-load operation. The linearisation is shown in Appendix D.

The six linear model equations are shown in state space form on Table 2.5, together with the arithmetic values for T = 0.3 s. The eigenvalues of the system matrix are:

$$\left.\begin{array}{l} -0.0285714 \\ -0.285714 \\ -0.0333333 \\ -3.522304 \\ -0.141237829 \\ -0.0031465441 \end{array}\right]$$

and they are all stable. Also, the first three are the diagonal elements (1,1), (2,2), (3,3) of the system matrix.

For the discretization of the system equations, both the Tustin and the Z.O.H. approximate integrating operators were used, as follows:

- Using the Tustin operator the system equations become:

$$s\underline{X} = A.\underline{X} + B.\underline{u} \quad \text{or} \quad \left[\frac{2(1-z^{-1})}{T(1+z^{-1})}\right]\underline{X} = A.\underline{X} + B.\underline{u}$$

$$\underline{X}(K) = \left[I-(T/2).A\right]^{-1}\cdot\left[I+(T/2).A\right].\underline{X}(K-1)+\left[I-(T/2).A\right]^{-1}\cdot\left[B.(T/2)\right]\cdot .(\underline{u}(K)+\underline{u}(K-1))$$

$$
\begin{bmatrix} \dot{M}_{CR} \\ \dot{W}_{FI} \\ \dot{A} \\ \dot{P}_{SD} \\ \dot{P}_{T} \\ \dot{T}_{RM} \end{bmatrix}
=
\begin{bmatrix}
-K_{CF} & 0 & 0 & 0 & 0 & 0 \\
(K_{CF}/T_P) & (-1/T_P) & 0 & 0 & 0 & 0 \\
0 & 0 & (-1/T_{AA}) & 0 & 0 & 0 \\
0 & 0 & 0 & (K11+K12.K16) & (K12.K17) & K13 \\
0 & 0 & 0 & (K16/C_{SSH}) & K14 & 0 \\
0 & K34 & K33 & K31 & 0 & K32
\end{bmatrix}
\begin{bmatrix} M_{CR} \\ W_{FI} \\ A \\ P_{SD} \\ P_{T} \\ T_{RM} \end{bmatrix}
+
\begin{bmatrix}
K_F & 0 \\
0 & 0 \\
(K_A/T_{AA}) & 0 \\
0 & 0 \\
0 & K15 \\
0 & 0
\end{bmatrix}
\begin{bmatrix} L_F \\ A_T \end{bmatrix}
$$

$$
A=\begin{bmatrix}
-.2857E-01 & 0 & 0 & 0 & 0 & 0 \\
.8163E-02 & -.2857E+00 & 0 & 0 & 0 & 0 \\
0 & 0 & -.3333E-01 & 0 & 0 & 0 \\
0 & 0 & 0 & -.3401E+01 & .1325E+01 & .2975E+02 \\
0 & 0 & 0 & .1656E+00 & -.1707E+00 & 0 \\
0 & .9858E-01 & -.1311E-01 & .6466E-02 & 0 & -.9527E-01
\end{bmatrix},
\quad
B=\begin{bmatrix}
.4986E+01 & 0 \\
0 & 0 \\
.4167E+00 & 0 \\
0 & 0 \\
0 & -.5949E+01 \\
0 & 0
\end{bmatrix}
$$

TABLE 2.5: LINEARISED CONVENTIONAL BOILER MODEL IN STATE SPACE FORM

or $\underline{X}(K) = AD.\underline{X}(K-1)+BD.(\underline{u}(K)+\underline{u}(K-1))$ (2.108)

where AD and BD are the discrete system matrices.

- Using the Z.O.H. operator, one gets:

$$s\underline{X} = A.\underline{X} + B.\underline{u} \quad \text{or} \quad \left[\frac{1-z^{-1}}{T.z^{-1}}\right]\underline{X} = A.\underline{X} + B.\underline{u}$$

$$\underline{X}(K) = \left[I + T.A\right].\underline{X}(K-1) + \left[T.B\right].\underline{u}(K-1)$$

or $\underline{X}(K) = AD.\underline{X}(K-1) + BD.\underline{u}(K-1)$ (2.109)

The system matrices of the discrete systems (i.e. AD and BD) for the two cases are shown in Table 2.6 for a sampling interval T = 0.3 s. Also the eigenvalues of the system matrix AD, for the two cases, are shown for the same value of T.

Both sets contain stable eigenvalues (i.e. inside the unit circle). Computation of the eigenvalues for different values of the sampling interval T, showed that:

(a) Using Tustin's operator, the discrete system eigenvalues are stable for values of T even up to T = 2 s.

(b) Using the Z.O.H., the eigenvalues become unstable for $T > 0.55$ s.

So the superiority of Tustin's operator for larger sampling intervals T is confirmed.

In Fig. 2.31, the closed-loop steady-state characteristics of this linear model are shown, in comparison with the characteristics of the non-linear model. As can be seen, the characteristics are straight lines, departing very little from the operating point around which the linearisation was performed. The linear model is therefore unsuitable for accurate responses to large input disturbances, away from the point of linearisation. In fact it was confirmed that the response of the linear model to a 2% step change in the valve position was almost the same as the response of the non-linear model, but this was not the case for bigger step inputs.

TABLE 2.6: DISCRETE-TIME REPRESENTATION OF THE LINEARIZED BOILER MODEL

A) Using the Tustin approximate discrete integration:

$$\underline{X}(K) = AD.\underline{X}(K-1)+BD.\left[u(K)+u(K-1)\right] \text{ , where}$$

$$AD = \begin{bmatrix} .9915E+00 & 0 & 0 & 0 & 0 & 0 \\ .2338E-02 & .9178E+00 & 0 & 0 & 0 & 0 \\ 0 & 0 & .9900E+00 & 0 & 0 & 0 \\ .1013E-03 & .8312E-01 & -.1147E-01 & .3324E+00 & .2582E+00 & .5862E+01 \\ .2455E-05 & .2014E-01 & -.2778E-03 & .3228E-01 & .9563E+00 & .1420E+00 \\ .3419E-04 & .2804E-01 & -.3869E-02 & .1274E-02 & .2469E-03 & .9774E+00 \end{bmatrix}$$

$$BD = \begin{bmatrix} .4965E+01 & 0 \\ .5830E-02 & 0 \\ .4146E+00 & 0 \\ -.2136E-02 & -.7680E+00 \\ -.5176E-04 & -.5819E+01 \\ -.7207E-03 & -.7343E-03 \end{bmatrix}$$

The eigenvalues of AD are:

.3086045030E+00
.9990564821E+00
.9914651494E+00
.9178082192E+00
.9585076936E+00
.9900497512E+00

B) Using the Z.O.H. approximate discrete integrator:

$$\underline{X}(K) = AD.X(K-1)+BD.u(K-1) \text{, where:}$$

$$AD = \begin{bmatrix} .9914E+00 & 0 & 0 & 0 & 0 & 0 \\ .2449E-02 & .9143E+00 & 0 & 0 & 0 & 0 \\ 0 & 0 & .9900E+00 & 0 & 0 & 0 \\ 0 & 0 & 0 & -.2021E-01 & .3975E+00 & .8924E+01 \\ 0 & 0 & 0 & .4969E-01 & .9488E+00 & 0 \\ 0 & .2957E-01 & -.3932E-02 & .1940E-02 & 0 & .9714E+00 \end{bmatrix}$$

$$BD = \begin{bmatrix} .1496E+01 & 0 \\ 0 & 0 \\ .1250E+00 & 0 \\ 0 & 0 \\ 0 & -.1785E+01 \\ 0 & 0 \end{bmatrix}$$

The eigenvalues of AD are:

-.5669130051E-01
.9142857143E+00
.9990560367E+00
.9914285714E+00
.9576286511E+00
.9900000000E+00

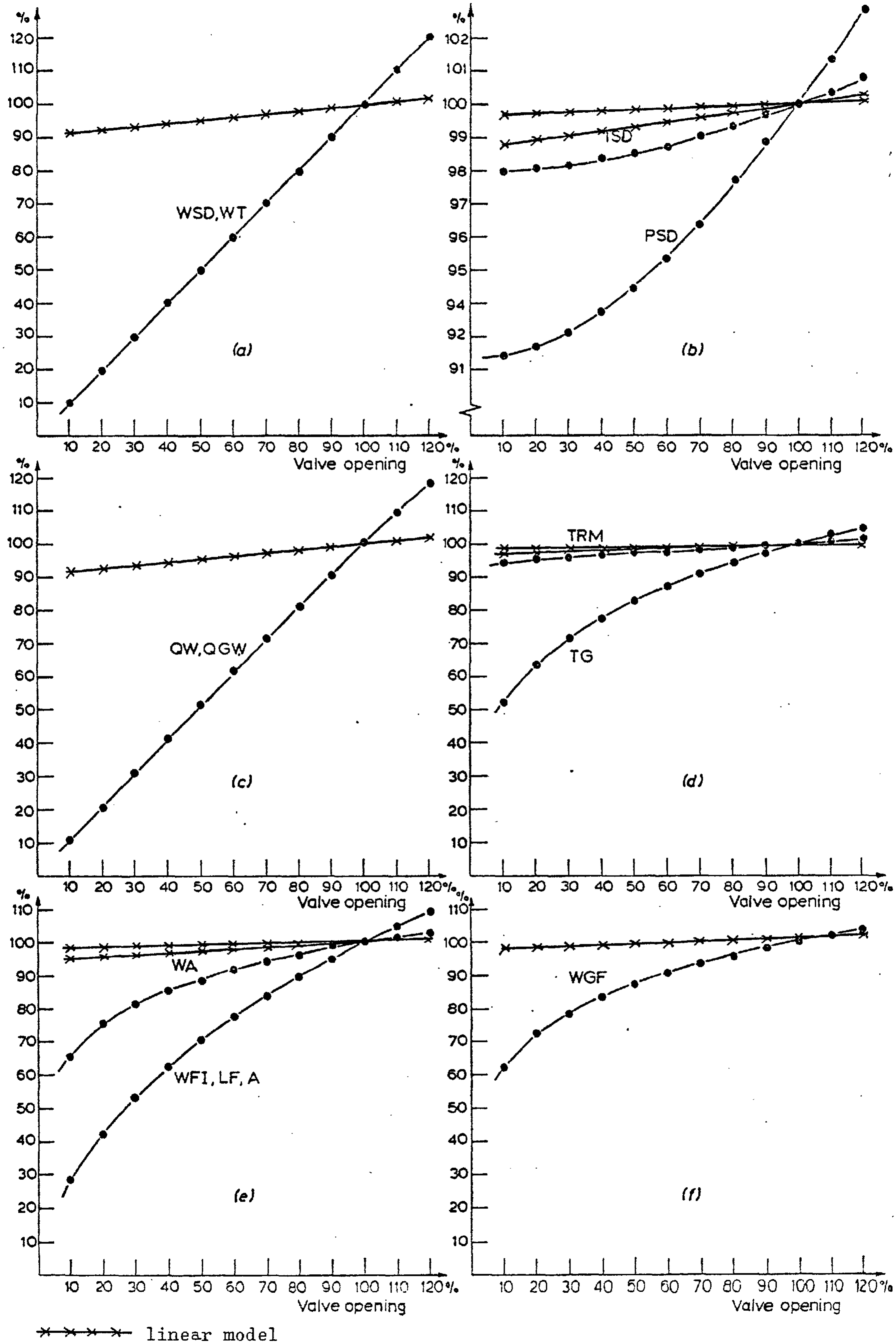

Fig. 2.31 Comparison of the steady-state characteristics of the non-linear and linearised models.

Comparing the linearised to the non-linear representation of the model, from the point of view of the number of operations needed when the model runs in real-time, the situation is as follows:

	Linearised version	Non-linear version
Multiplications	34	34
Divisions	0	4
Additions	31	27
Square Roots	0	1

So the only advantage of the linearised version, from this point of view, is the saving of the computation of the square root. Indeed this computation takes up something around 1-1.5% of the system's time. But the linear system is unsuitable for large disturbances away from its initial steady-state.

CHAPTER THREE

NUCLEAR PLANT

3.1 THE PROCESS

Nuclear power plants are being introduced in increasing numbers around the world towards the goal of cheaper and more dependable production of electricity. The process can be divided generally into the following sections: the reactor section, where the reaction products heat up the fuel elements and the moderator; the coolant circulation section, where the coolant absorbs the heat of the core and the steam-generation section, where the coolant heat is released to evaporate the liquid in this section (Fig. 3.1).

The circuit of the coolant flow is called primary circuit, while the circuit of the steam flow is called the secondary circuit. Various types of reactors have been developed over the past two or three decades. They were used as pilot plants initially and the most successful of them were employed in commercial power plants.

The Boiling Water Reactor (B.W.R.) is the simplest of them. It uses light water both as coolant and as moderator. A conventional single-pressure heat cycle can be used in the secondary circuit, since the steam pressure can be raised to a considerable level (e.g. 900-950 psig). A disadvantage of this design is that the steam and the water could become radio-active and contaminate the turbine, because the same water goes to the turbine as well. So particular care must be taken during the design of the unit to minimise this risk. Another type of "water-reactor" uses heavy water as a moderator (H.W.R.).

The Pressurised-Water Reactor (P.W.R.) uses ordinary water under pressure as coolant. The pressure is sufficient to suppress any boiling. The coolant water goes through heat exchangers where it releases its heat, thus producing steam in the secondary circuit. So here the fluids in the two circuits are different and there is no direct contact between them.

The Gas-cooled Reactor (G.R.) uses gas as coolant (e.g. helium, carbon dioxide, air, etc.), while the moderator is usually

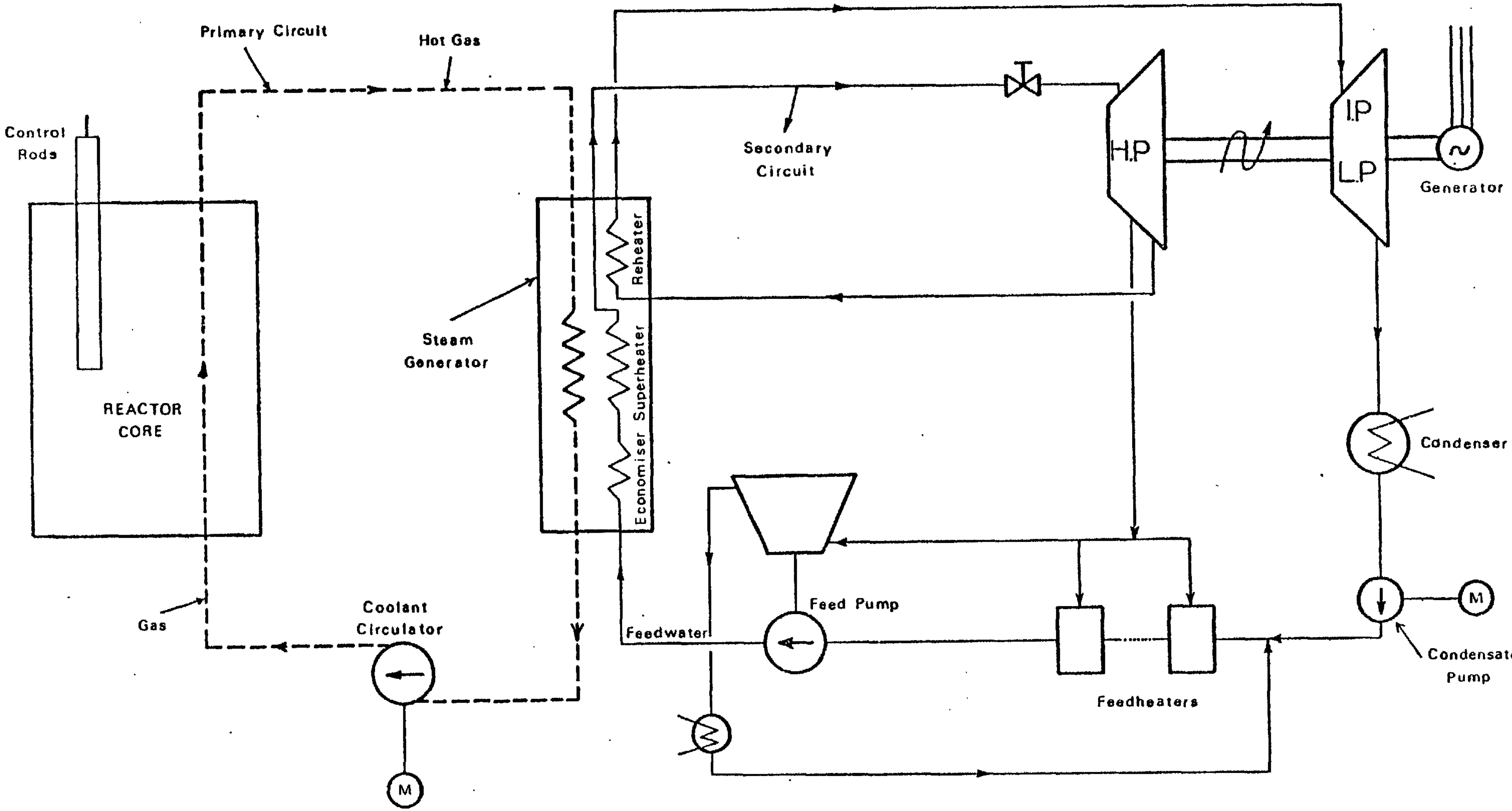

Fig. 3.1 Schematic diagram of a nuclear generating plant.

graphite, berylium, berylium oxide or an organic liquid.

Much of the effort in nuclear power engineering is directed towards finding ways and means of subtracting the maximum power from the reactor, with the minimum temperature drop at the heat transfer surfaces. Low steam temperature means lower steam cycle, i.e. lower efficiency. The temperatures of steam associated with these reactor designs are of the order 350-400°C. One way of getting round this problem is the use of dual-pressure steam cycles, where the steam is generated in two separate feedwater circuits but in the same heat exchanger[5]. A technique like this can raise the efficiency of the cycle up to 40%. In a further advance, liquid metal-steam binary cycles are claiming efficiencies up to 50-51% [44].

A parallel improvement towards increased cycle efficiency has come with the High-Temperature gas-cooled Reactor (H.T.R.). The movement began in the U.K. with helium-graphite reactor development[45], the fuel being uranium or thorium[46,47]. The advantage of this design is the high gas outlet temperature 700-780°C. This means that the generation of steam can be made at present-day standard conditions of pressures and temperatures and so have a high cycle efficiency.

Other more advanced designs are in development, such as the gas turbine H.T.R., where the coolant helium directly drives gas turbines in parallel loops, and the gas-cooled fast reactor, where the fuel rods are cooled by pressurised helium[45].

Fast reactors are so-called because the reaction in them is sustained by high energy (fast) neutrons, in contrast with the thermal reactors (low energy neutrons). Every high energy neutron can produce more than two neutrons in the reaction, in which case more fissionable material is produced than consumed. This phenomenon is called "breeding" and the reactor "Breeder Reactor". The obvious advantage of this type is that with the existing world resources of uranium, power can be produced (and plutonium) for hundreds of years. The United Kingdom, France, Germany, U.S.S.R. are at late stages of the construction of commercial breeder reactors in the range of 1200-1500 MW despite the controversy about the safety of their operation.

3.2 CHOICE OF A MODEL

As in the case of the conventional boiler model, the requirement of a program which will occupy very little space in the computer and which can be executed very fast, calls again for a very simple model to represent a nuclear plant. An additional reason is that this model should be incorporated in the same program with the conventional boiler model. More details will be given in Chapter 6.

For this purpose, a high temperature gas-cooled reactor plant was assumed. The dynamics of the reactor part were ignored, and it was assumed that the control of this part is perfect. For the steam generation side, the equations of the drum-downcomers, risers and superheater used in the conventional boiler model were retained in this model as well. The equations are presented on the left-hand side of Table 3.1. In equation (3.1) the term expressing the quantity of heat input by the feedwater ($W_{EO}.h_{EO}$) was separated from the steam flow W_{SD} and can be used as a controlling input.

The control strategies used in a nuclear plant vary according to the type of the reactor and perhaps the special requirements of the particular power plant. For example, for an H.T.R. with a high and always negative temperature coefficient of the reactivity, it is possible to control the reactor output by varying only the speed of the gas circulators[48,49]. Another scheme uses the primary gas flow to control the throttle pressure, while the steam temperature is controlled by the control rods and the gas outlet temperature by the feedwater flow[47].

The scheme that was adopted in the model is the following[46,50]: the pressure of the steam at the throttle valve is controlled by adjusting the feedwater flow rate. For this purpose the throttle pressure error is formed (Equation (3.12)) and this goes through a P I D controller. The controller output together with the flow rate out of the steam generator, form the FW flow rate, as shown in Equation (3.11). This scheme is very simple and it only indicates the principal effect that the feedwater flow can have in keeping the throttle pressure at its desired level. The feedwater enthalpy is assumed to be constant.

TABLE 3.1: NUCLEAR PLANT MODEL EQUATIONS

Continuous-time representation		Discrete-time representation
		$Z=1+(T.E66/C_D).W_{SD}(K-1)$
$\frac{d}{dt}(P_{SD})=(1/C_D).\left[Q_W+W_{EO}.h_{EO}-W_{SD}.E66.P_{SD}+EE66)\right]$	(3.1)	$P_{SD}(K)=\left[P_{SD}(K-1)+(T/C_D).(Q_W(K-1)+W_{EO}(K-1).h_{EO}-W_{SD}(K-1).EE66)\right]/Z$
$\frac{d}{dt}(P_T)=(1/C_{SSH}).(W_{SD}-W_T)$	(3.2)	$P_T(K)=P_T(K-1)+(T/C_{SSH}).(W_{SD}(K-1)-W_T(K-1))$
$R_{SD} = (P_{SD} - EE4)/E4$	(3.3)	$R_{SD}(K) = (P_{SD}(K) - EE4)/E4$
$T_{SD} = E5.R_{SD} + EE5$	(3.4)	$T_{SD}(K) = E5.R_{SD}(K) + EE5$
$W_{SD} = \sqrt{F_{DSI}.R_{SD}.(P_{SD} - P_T)}$	(3.5)	$W_{SD}(K) = \sqrt{F_{DSI}.R_{SD}(K).(P_{SD}(K)-P_T(K))}$
$W_T = K_T.A_T.P_T$	(3.6)	$W_T(K) = K_T.A_T\ (K-1).P_T(K)$
$\frac{d}{dt}(T_{RM}) = C_M.(Q_{GW} - Q_W)$	(3.7)	$T_{RM}(K) = T_{RM}(K-1)+(T.C_M).(Q_{GW}(K-1)-Q_W(K-1)$
$Q_W = K_{RS}.(T_{RM} - T_{SD})^3$	(3.8)	$Z14 = (T_{RM}(K) - T_{SD}(K))$
$XX = 11.97777781 \cdot A_T + 112.22222$	(3.9)	$Q_W(K) = K_{RS}.((Z14.Z14).Z14)$
$Q_{GW} = XX.(T_{CG} - T_{RM})$	(3.10)	$XX = 11.97777781 \cdot A_T(K-1) + 112.222222$
$W_{EO} = W_{SD} + CC$	(3.11)	$Q_{GW}(K) = XX.(T_{CG} - T_{RM}(K))$
$D_{PE} = P_{SET} - P_T$	(3.12)	$D_{PE}(K) = P_{SET} - P_T(K)$
$\left(\frac{CC}{D_{PE}}\right) = (P - I - D)$	(3.13)	$S_E(K) = S_E(K-1) + D_{PE}(K-1)$
		$CC = KPP.D_{PE}(K) + KIP.S_E(K) + KDP.(D_{PE}(K) - D_{PE}(K-1))$
		$W_{EO}(K) = W_{SD}(K) + CC$

The temperature of the metal tubes in which the water/steam mixture flows, is determined by the balance of the heat rate released by the coolant and the heat rate absorbed by the water in the secondary circuit (Equation (3.7)). Again for the heat transfer into boiling water the cubic equation (3.8) was used. For the heat released from the coolant to the tubes carrying the steam/water mixture, heat transfer by pure convection was assumed. The heat transfer is assisted by the temperature difference between the coolant outlet temperature (T_{CG}) and the temperature of the tube metal.

At this point it is assumed that the control system in the reactor side keeps T_{CG} constant. This means that the power extracted from the reactor is proportional to the coolant flow. In the model, the power from the reactor is represented by the heat transfer rate Q_{GW} from the coolant to the secondary circuit. Therefore, this was set proportional to the coolant flow by inserting the term XX in Equation (3.10). This term varies linearly with the throttle valve opening (Equation (3.9)) which, in turn, expresses the load demand from the nuclear plant. The coolant flow is, of course, proportional to the load (with T_{CG} = constant).

Other control loops, usually included in a plant of this kind, are assumed to be working perfectly. For example, the reheater outlet temperature is controlled by the control rods, while the reheater inlet temperature by cold steam spraying. But because of the simplicity of the model these loops cannot be included. The gains for the P I D controller, which give a reasonable response, were determined by trial and error.

The model, in block diagram form, is shown in Fig. 3.2.

3.3 MODEL EVALUATION

3.3.1 Steady-State Characteristics of the Nuclear Plant Model

It is assumed that the initial steady-state of the model is the one corresponding to full-load operation. For this reason

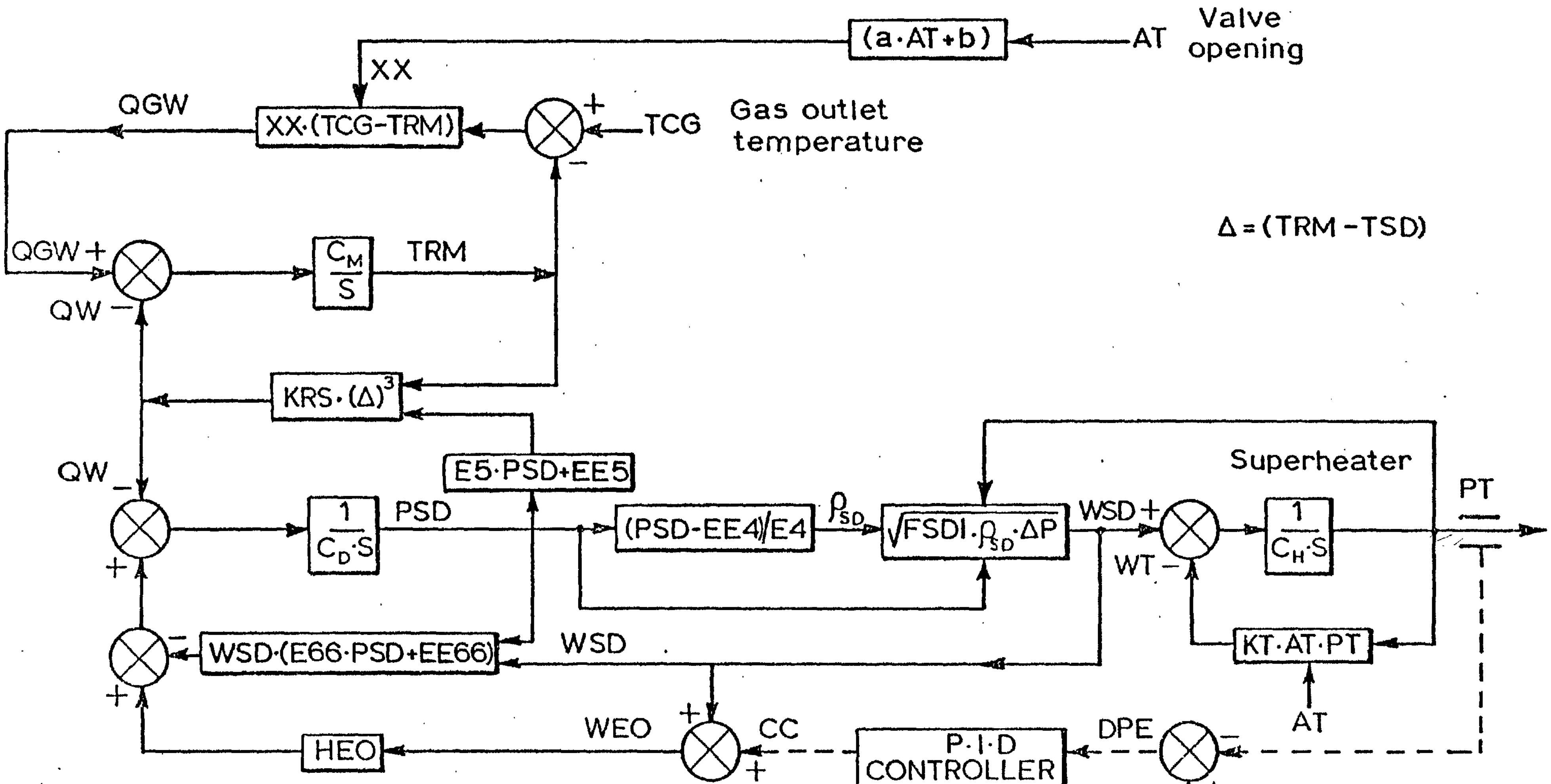

Fig.3.2 Nuclear Plant Model

the main variables have the same values as for the conventional plant, i.e. the ones presented in Table 2.2. The new quantities appearing in this model can be computed as a function of the main variables, and their values are:

$$\left.\begin{aligned} XX &= 232.0 \\ CC &= 0.0 \end{aligned}\right] \quad \text{for the full-load conditions}$$

Again it is assumed that the plant starts from the full-load conditions and goes to a new steady-state as a result of the change in the throttle valve opening, while the pressure controller keeps the throttle pressure at its desired value. So with the new values of the valve opening and the pressure reference known, the new steady-state can be computed from the model equations as shown in Appendix E.1.

The closed-loop steady-state characteristics of the most important variables are shown in Fig. 3.3. As expected, the steam flows at the valve and at the evaporator output change in direct proportion with the valve opening (Fig. 3.3(a)). The steam pressure at the evaporator (P_{SD}) does not change too much, as a result of the throttle pressure being kept constant at its predetermined level. The steam temperature (T_{SD}), as a linear function of P_{SD}, changes in a similar fashion to P_{SD}. Interesting is the characteristic of the feedwater flow. It settles at a level always lower than that of W_{SD}. By so doing it reduces the amount of energy going in the evaporator (i.e. $W_{EO}.h_{EO}$), so that it cancels the tendency of the pressure to rise (as a result of a reduction in the load demand), thus keeping P_T at the desired level. Below 50% loading, this characteristic is obviously unrealistic, the reason being that a nuclear plant is very unlikely to be operated below 50% and also a minimum amount of feedwater flow has to be maintained for safety reasons. But, as has been mentioned, this control scheme is very simple and cannot be expected to respond well over every load range. Finally, the input power from the reactor, which can be represented by Q_W and Q_{GW} and the coolant flow (represented by XX) are changing in the same fashion, i.e. linearly with the valve opening (see Equation (3.9)).

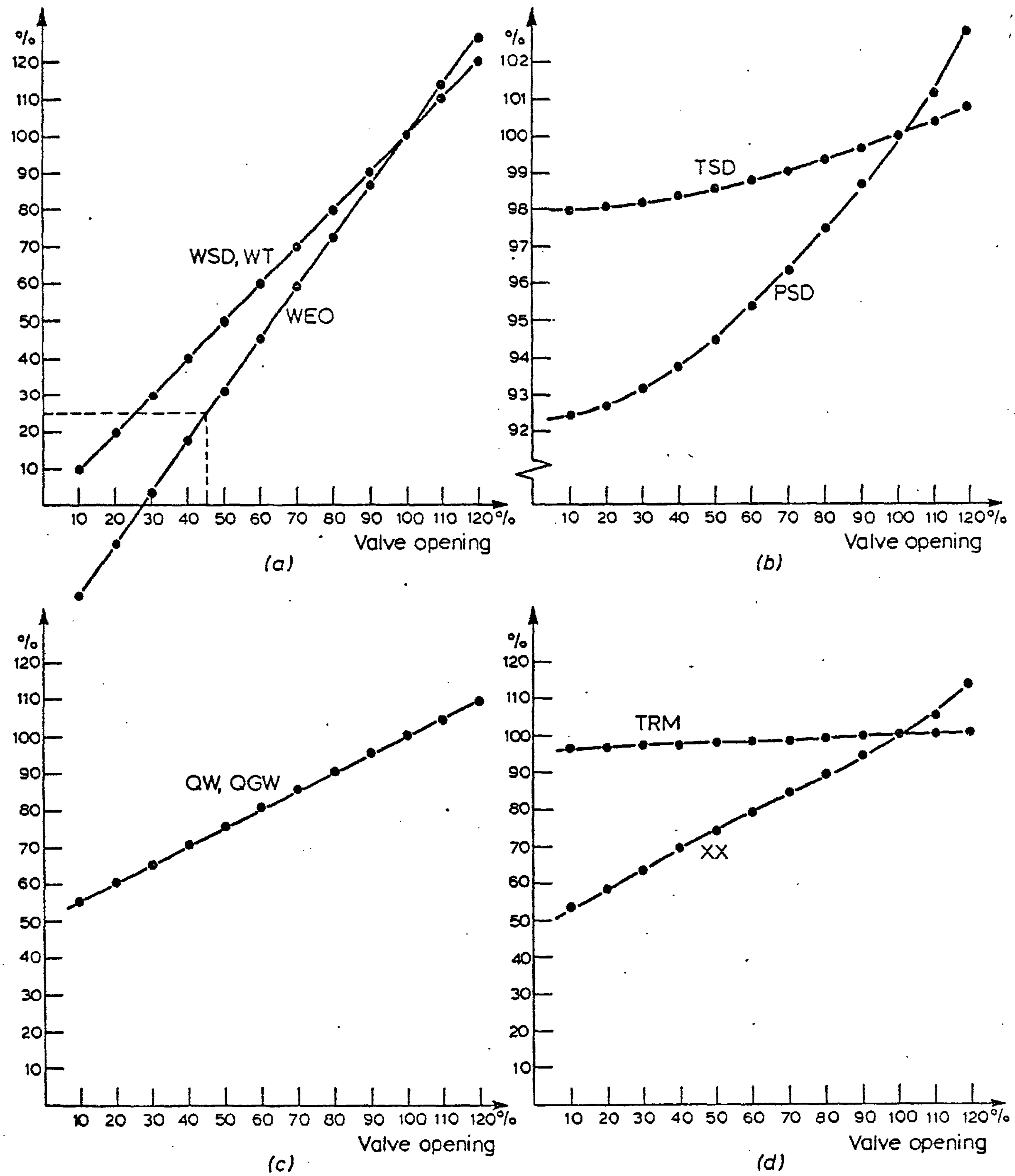

Fig. 3.3 Closed-loop steady-state characteristics of the nuclear plant model.

3.3.2 Discretization and Transient Response of the Nuclear Plant Model

As in the case of the conventional plant model (Section 2.4), the Z.O.H. approximate discrete integrator was used to discretize the continuous-time equations of the model. The corresponding difference equations are shown alongside the continuous ones in Table 3.1.

In this form, the equations were run on the CDC 6400 in order to assess the open and closed-loop response of the model. In Fig. 3.4 is shown the response of the model to a 5% step reduction in the valve opening, with the feedback loop (which determines the feedwater flow) open. So the feedwater is always the same as the steam flow out of the evaporator (W_{SD}). As can be seen, the throttle pressure and the steam pressure at the evaporator, begin to rise and eventually they settle to higher values. The heat transfer rate to the evaporator metal (from the gas coolant), experiences a step decrease, because it is directly proportional to the coolant flow and this, in turn, to the valve opening. The metal temperature of the heat exchanger starts rising until the balance of the heat transfer rates is established again. For the same type of disturbance, when the feedwater controller is connected, i.e. the loop is closed and $W_{EO} = W_{SD}+CC$, the response of the model is shown in Fig. 3.5. In this figure the feedwater flow drops below the level of the steam flow out of the evaporator. As a result, the heat input to the evaporator is smaller and this forces its pressure (and consequently the pressure at the valve) to start falling again, until P_T goes back to its desired value. Also, the heat transfer rate from the coolant into the evaporator drops to a lower level because it is proportional to the load demand.

An attempt was made to get the response of the model, with the feedwater control loop determining directly the feedwater flow, i.e. with W_{EO} = CC (and not $W_{EO} = W_{SD}+CC$). With this kind of loop open, obviously the feedwater flow remains unchanged at its "full load" value. As a result, the response of the model to a step change in the valve opening was found to be unstable. With the loop closed, it was very difficult to choose the controller gains such as to

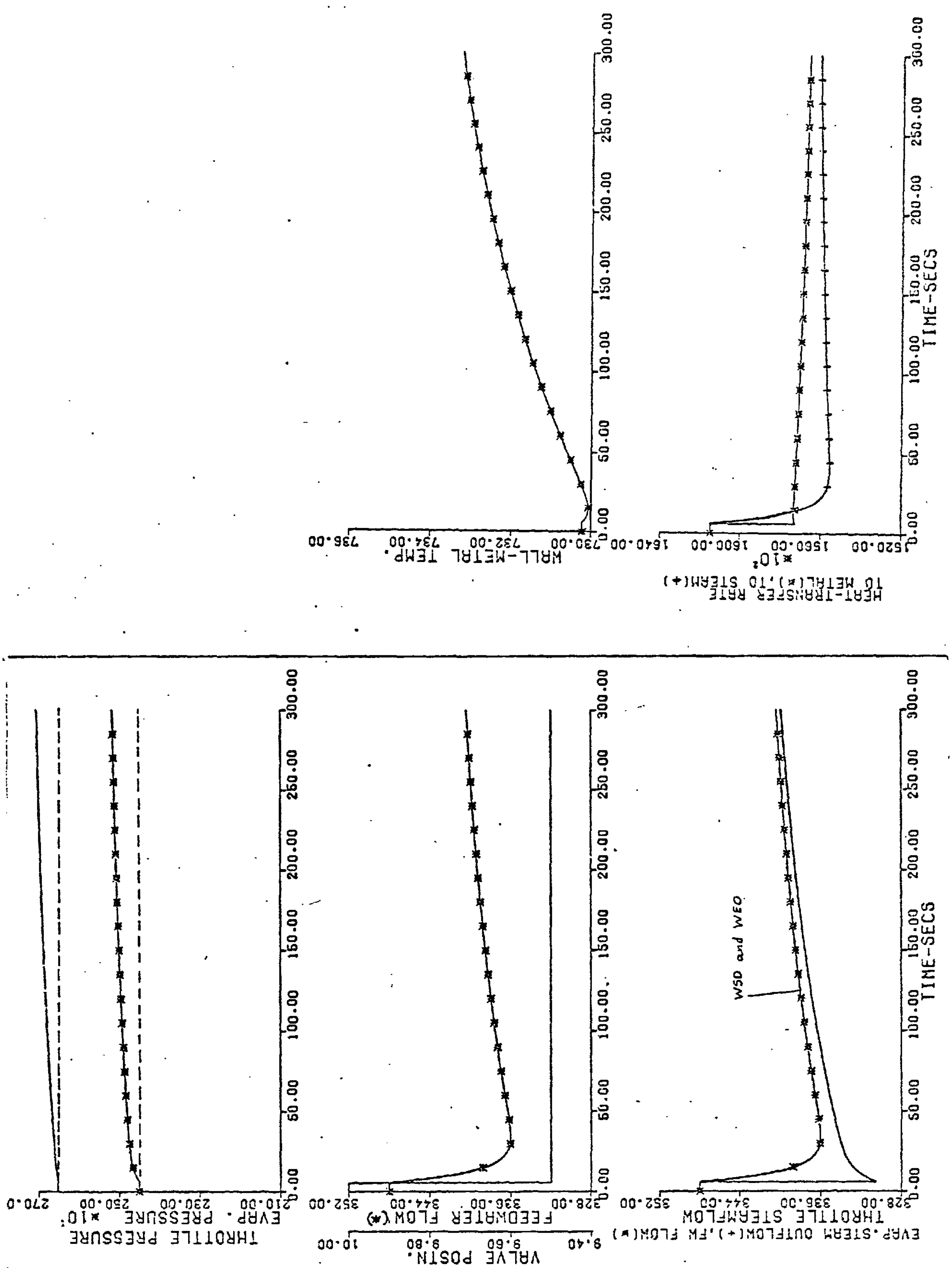

Fig. 3.4 Open-loop response of the nuclear plant model, to a 50% step decrease in the valve opening.

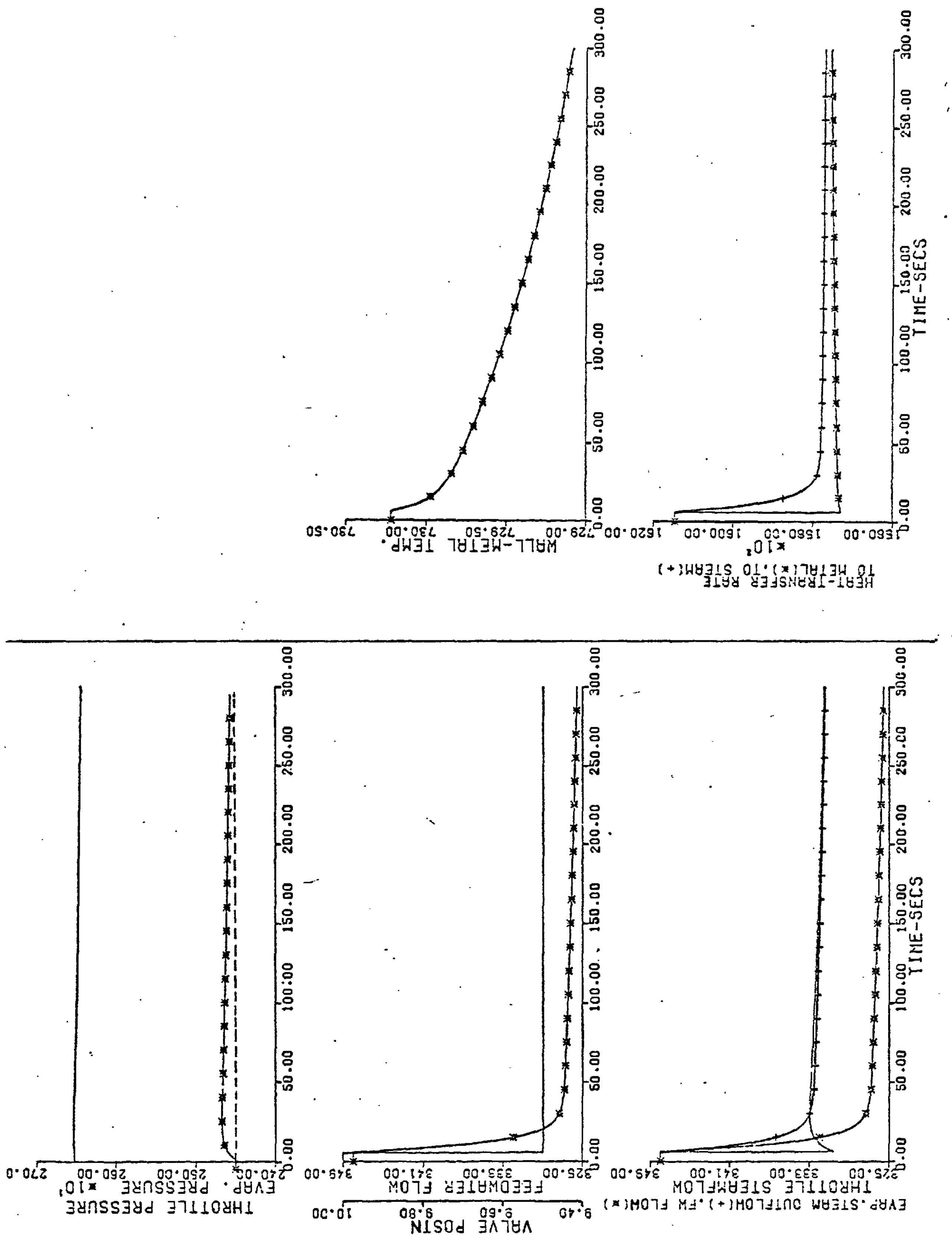

<u>Fig. 3.5</u>: Closed-loop response of the nuclear plant model to a 5% step decrease in the valve opening.

obtain a reasonable response. So this scheme was not examined further. However, this emphasises the fact that the feedwater flow and its control must be balanced against the steam production at the evaporator, this balance being the indication of safe operation of the plant.

3.4 REAL-TIME OPERATION OF THE NUCLEAR PLANT MODEL

The conversion of the discrete-time program to a version suitable for running in real-time on the PDP-15, followed the same pattern as in the case of the conventional steam plant model (see Section 2.4). Both versions are presented in Table 3.2.

The number of operations involved is:

Floating point	Multiplications	:	19
Floating point	Divisions	:	2
Floating point	Additions	:	20
Square Roots		:	1

Because of the high capital cost of the nuclear plants, they are normally used to cover base load operating at the highest possible output for maximum efficiency. This means no participation in system secondary (or supplementary) control, and often no primary (governor) control. However, most of the nuclear plants have a significant load-following capability, which is not only a result of a negative temperature coefficient, but also of the control techniques employed [46,47,51]. Therefore the decision on the mode of operation of the plant is based mainly on economics and the constraints imposed by features like the wear of the fuel elements when they are subjected to continuous changes of power, etc.

Non-Regulating Plant:

For the case where the plant is operating in a non-regulating mode, its output changes only when the frequency drops to a level where it results in a drop in the output of the plant's auxiliaries. For this reason an auxiliary output/frequency characteristic was specified[52] as shown in Fig. 3.6.

TABLE 3.2: NUCLEAR PLANT MODEL EQUATIONS IN THEIR REAL-TIME FORM

Discrete-Time Representation	Real-Time Representation
$Z = 1+(T.E6/C_D).W_{SD}(K-1)$	$Z = 1 + C(I,7).W_{SD}(I)$
$P_{SD}(K)= [P_{SD}(K-1)+(T/C_D).(Q_W(K-1)+ +W_{EO}(K-1).h_{EO}-W_{SD}(K-1)EE66)]/Z$	$P_{SD}(I)= [P_{SD}(I)+C(I,8).(Q_W(I)+ +W_{EO}(I).h_{EO}-W_{SD}(I).EE66)]/Z$
$P_T(K)=P_T(K-1)+(T/C_{SSH}).(W_{SD}(K-1)- - W_T(K-1))$	$P_T(I) = P_T(I)+C(I,10).(W_{SD}(I)-W_T(I))$
$R_{SD}(K) = (P_{SD}(K)-EE4)/E4$	$R_{SD}(I) = (P_{SD}(I) - EE4)/E4$
$T_{SD}(K) = E5.R_{SD}(K) + EE5$	$T_{SD}(I) = E5.R_{SD}(I) + EE5$
$W_{SD}(K) = \sqrt{F_{SDI}.R_{SD}(K).(P_{SD}(K)-P_T(K))}$	$W_{SD}(I) = \sqrt{F_{SDI}.R_{SD}(I).(P_{SD}(I)-P_T(I))}$
$W_T(K) = K_T.A_T(K-1).P_T(K)$	$W_T(I) = K_T.A_T.P_T(I)$
$T_{RM}(K) = T_{RM}(K-1)+(T.C_M).(Q_{GW}(K-1)- - Q_W(K-1))$	$T_{RM}(I) = T_{RM}(I) + C(I.12).(Q_{GW}(I) - - Q_W(I))$
$Z14 = (T_{RM}(K) - T_{SD}(K))$	$Z14 = (T_{RM}(I) - T_{SD}(I))$
$Q_W(K) = K_{RS}.((Z14.Z14).Z14)$	$Q_W(I) = K_{RS}.((Z14.Z14).Z14)$
$XX = 11.97777781 \cdot A_T(K-1)+112.22222$	$XX = 11.97777781 \cdot A_T+112.22222$
$Q_{GW}(K) = XX.(T_{CG} - T_{RM}(K))$	$Q_{GW}(I) = XX.(T_{CG} - T_{RM}(I))$
$D_{PE}(K) = P_{SET} - P_T(K)$	$S_E(I) = S_E(I) + D_{PE}(I)$
$S_E(K) = S_E(K-1) + D_{PE}(K-1)$	$D_{PE}(I) = P_{SET} - P_T(I)$
$CC = KPP.D_{PE}(K)+KIP.S_E(K) + + KDP.(D_{PE}(K) - D_{PE}(K-1))$	$CC = KPP(I).D_{PE}(I) + KIP(I).S_E(I) + + KDP(I).(D_{PE}(I) - D_{PE1}(I))$
$W_{EO}(K) = W_{SD}(K) + CC$	$D_{PE1}(I) = D_{PE}(I)$
	$W_{EO}(I) = W_{SD}(I) + CC$

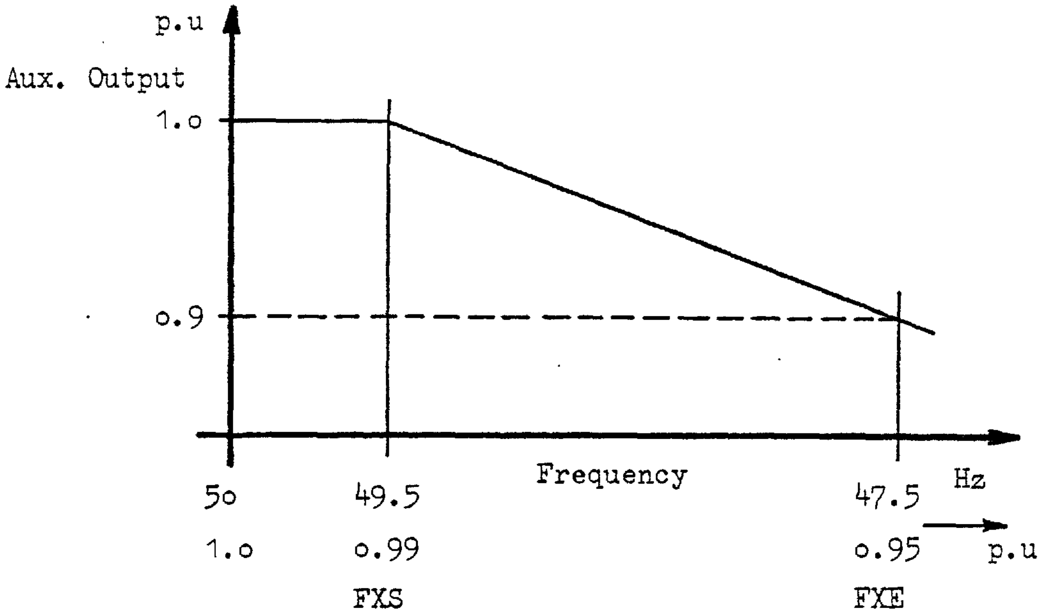

FIG. 3.6 Auxiliaries output/frequency characteristic.

From a frequency FXS downwards, the output of the auxiliaries drops linearly from 1.0 p.u. down to 0.9 p.u. The slope of the characteristic is obviously: (1-0.9)/(FXS-FXE). Normally one would not expect the frequency of the system to stay for long periods of time below 49 Hz. But even during a short period it is essential that the loading of the nuclear plant should not be above the capacity of the auxiliaries at that particular time.

So for operation at reduced frequency the simulation program "reads in" the current value of the system frequency, compares it with the value of FXS and if necessary adjusts the position of the speeder gear according to the auxiliary output/frequency characteristic shown above.

It must be noted here that the valve opening is determined only by the speeder gear since the governor is used only as an overspeed safety mechanism.

Regulating Plant:

In the case where the nuclear plant is taking part in frequency regulation, then the scheme employing the auxiliary output/ frequency characteristic is no longer relevant. Therefore the valve opening is determined by the position of the governor and the power demands set by the speeder motor.

3.4.1 Response of the Model Operating in Real-Time

The responses of the nuclear plant model running in real-time on the PDP-15 were taken for the cases of the plant operating in the non-regulating mode and in the regulating mode. They are presented below:

Regulating Plant Response:

For this purpose, the power system configuration shown in Fig. 2.23 was set up on the simulator. The circuit breaker no. 14 was open, i.e. the system was not connected to the infinite bus. The system was allowed to settle and then a change of 0.43 p.u. was introduced on load 1. The response of the two units is shown in Fig. 3.7. The two governors respond very quickly to arrest the fall of the frequency resulting in both valve positions overshooting by about 100% above the new steady state, which they eventually assume. The steam pressures at the valves follow the changes very quickly and drop by about 5% and 6% respectively, before this fall is arrested by the pressure controller. The pressure is back within 1% of its set value in about 7 minutes from the start of the disturbance.

The response of the two valve positions was a bit oscillatory in this particular test and this resulted in a slightly bumpy response for the pressures. But the overall characteristics of the model response can be seen very clearly.

The controller gains were: KPP = 0.3, KIP = 0.00032, KDP = 0.1. With the possibility of choosing them during the initialisation of the simulation, they can be varied until the desired response is achieved. For example, when KPP is changed to 0.4, the response of the throttle pressure is quicker for the same step input to the model, as can be seen in Fig. 3.7.

Non-Regulating Plant Response:

For this purpose, the signal from the governor to the valve was disconnected (see Fig. 2.2a - generating unit) in unit no. 2. As

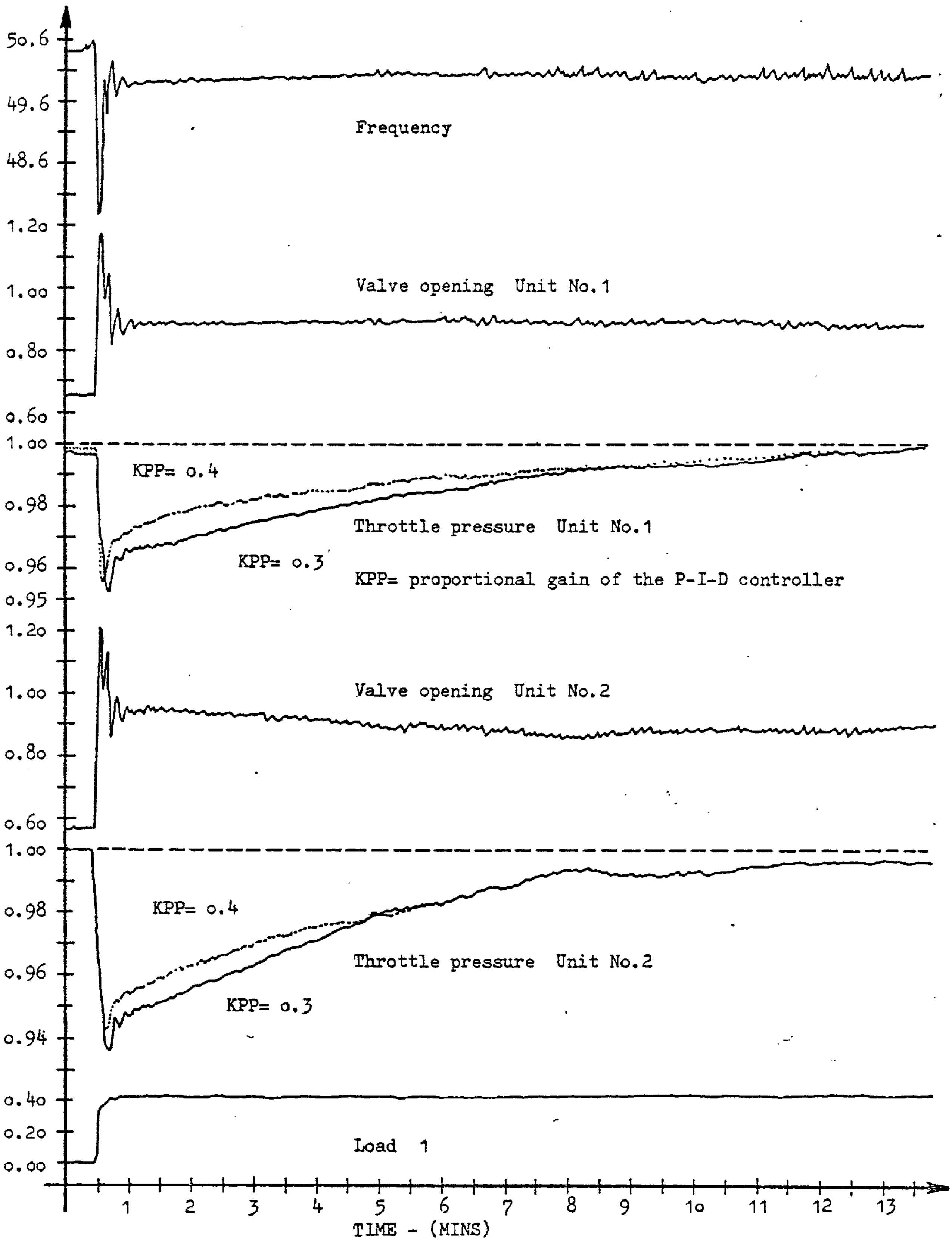

Fig. 3.7 Nuclear plant model response in real-time, to a step increase in Load 1.

a result, the valve opening was determined only from the speeder motor position. This was adjusted so as to give a valve opening of 100%.

As mentioned in Section 3.4, for the auxiliaries output/frequency characteristic the values of FXS = 49.5 Hz and FXE = 47.5 Hz were chosen. These might not represent the values which will be used in a real plant. But they were chosen for test purposes, i.e. to introduce a significant change in the operating point of the model. Otherwise the frequency of the system would have to be lowered (e.g. to 46 Hz) and this would cause many of the variables to saturate.

The response of the non-regulating unit to a frequency fall is shown in Fig. 3.8. The system frequency is originally around 50 Hz, when an increase in load 1 is taking place. As a result, the frequency falls to a new level, around 48.0-48.5 Hz. This frequency is "read in" every time the plant simulation program is executed (i.e. every 300 ms) through a first order digital filter of the form:

$$Y(K) = a \,.Y(K-1) + b.X(K) \tag{3.14}$$

where: $a = e^{-\tau/T}$ and $a + b = 1.0$

and: τ = the sampling interval (in this case 300 ms),
T = the filter time constant.

For the test shown in Fig. 3.8, $a = 0.7$ and $b \doteq 0.3$. The filter was used to smooth slightly the frequency readings since, from these readings, the desired plant output is computed (from the auxiliary output/frequency characteristic). This desired output is compared to the actual one, and, if different, a signal (voltage) is directed to the raise/lower pulse integrator, which opens or closes the valve accordingly.

Because the raise/lower pulse generator is active most of the time, in one or the other direction, the valve position oscillates around a certain level, as can be seen in Fig. 3.8. The same sort of behaviour is displayed by the steam flow at the valve (W_T), because it is a direct function of the valve position. The

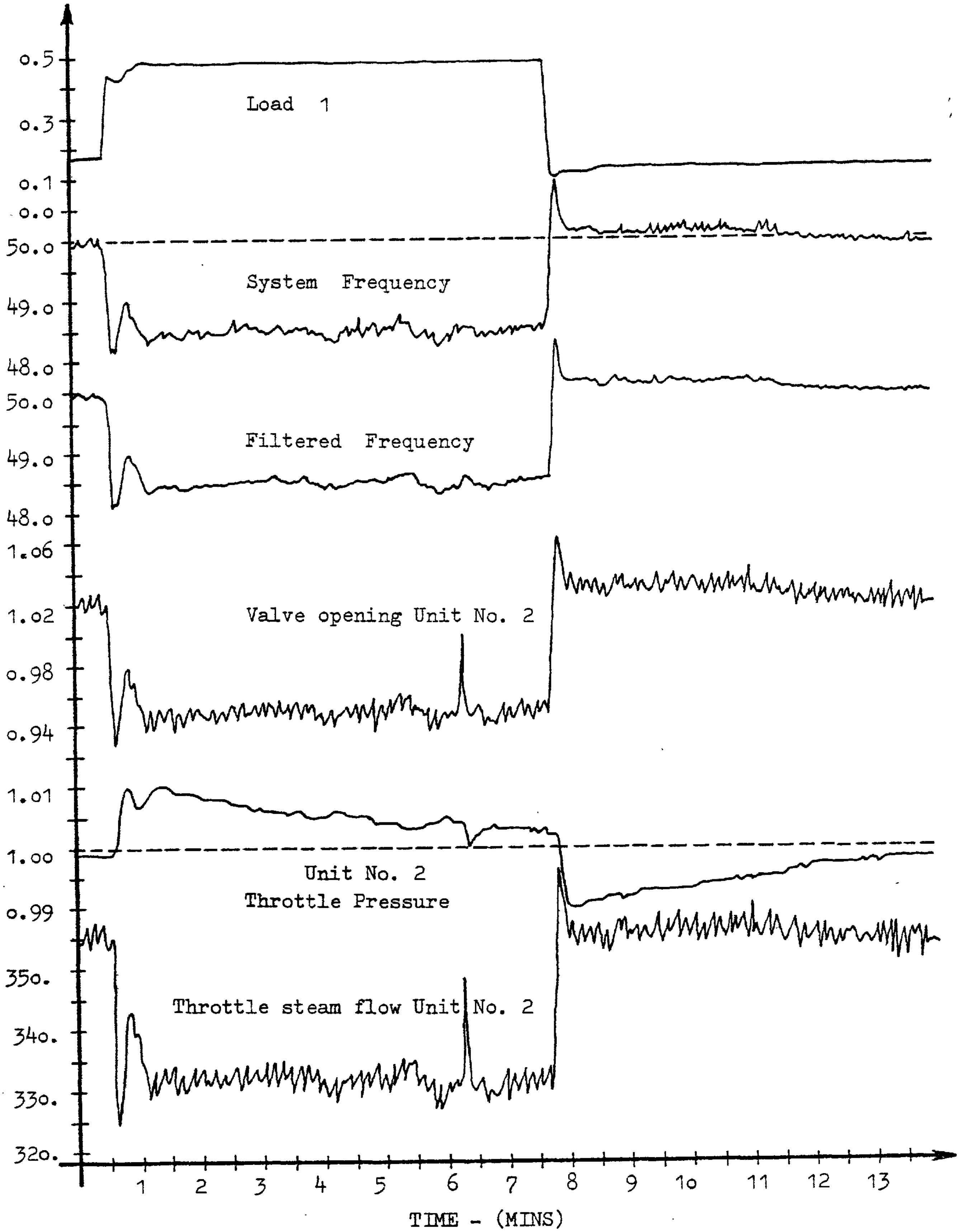

Fig. 3.8 Real-time response of the nuclear plant model operating in the non-regulating mode, to a change in frequency (i.e. change in the output of the axiliaries).

steam pressure at the valve behaves as expected, rising when the valve closes and dropping when it opens. The product of: (steam flow) x (pressure) represents the power going into the turbine.

In conclusion, it can be said that the "non-regulating" model displays the desired behaviour, considering its simplicity. The overall response would be made smoother with some more filtering of the frequency reading and a better voltage input to the raise/lower pulse generator. This voltage determines the rate of change of the output of the pulse generator and a better choice for that can only be made by trial and error.

CHAPTER FOUR

HYDRO PLANT

4.1 THE PROCESS

In a hydro plant, the potential energy of the mass of water contained in a reservoir is transformed to kinetic energy, as the water is carried through a conduit to a water turbine (at a lower level). The kinetic energy is transformed to mechanical power through the turbine, which in turn drives a generator for the production of electrical energy.

A typical cross-section of a hydro plant is shown in Fig. 4.1. The water is gathered in the upper reservoir as a result of rainfall on the catchment area or a river discharge into it. The reservoir is usually natural and it requires the construction of a dam to block the passage of water at one end of it, so as to form a basin. It can also be artificial, but on a much smaller scale. From there, the water is brought to the water turbine, which is located at a lower ground elevation. The distance between the reservoir and the power house can vary from a few meters to several kilometers. In the latter case, a tunnel is needed which will bring the water just above the power house. From there it is carried through one or several penstocks to the different turbine units. The presence of a long power tunnel makes necessary the construction of a surge tank. Its function it to relieve the pressure on the penstock, tunnel and the turbine. This build-up of pressure is a result of the deceleration of the water column, due to a decrease in the valve opening. The surge tank is located preferably on high ground in order to reduce the height of the tower to be constructed. At the lower end of the penstock is the valve, which determines the amount of water entering the turbine section and thus the power produced. From the turbine the water goes through the draft tube and it is discharged to the lower reservoir. A relief valve is often incorporated into the penstock, just before the turbine inlet. It allows the water in the penstock between the surge tank and the turbine to be diverted from the turbine, in response to rapid closing of the gates. This reduces the pressure created by the deceleration of

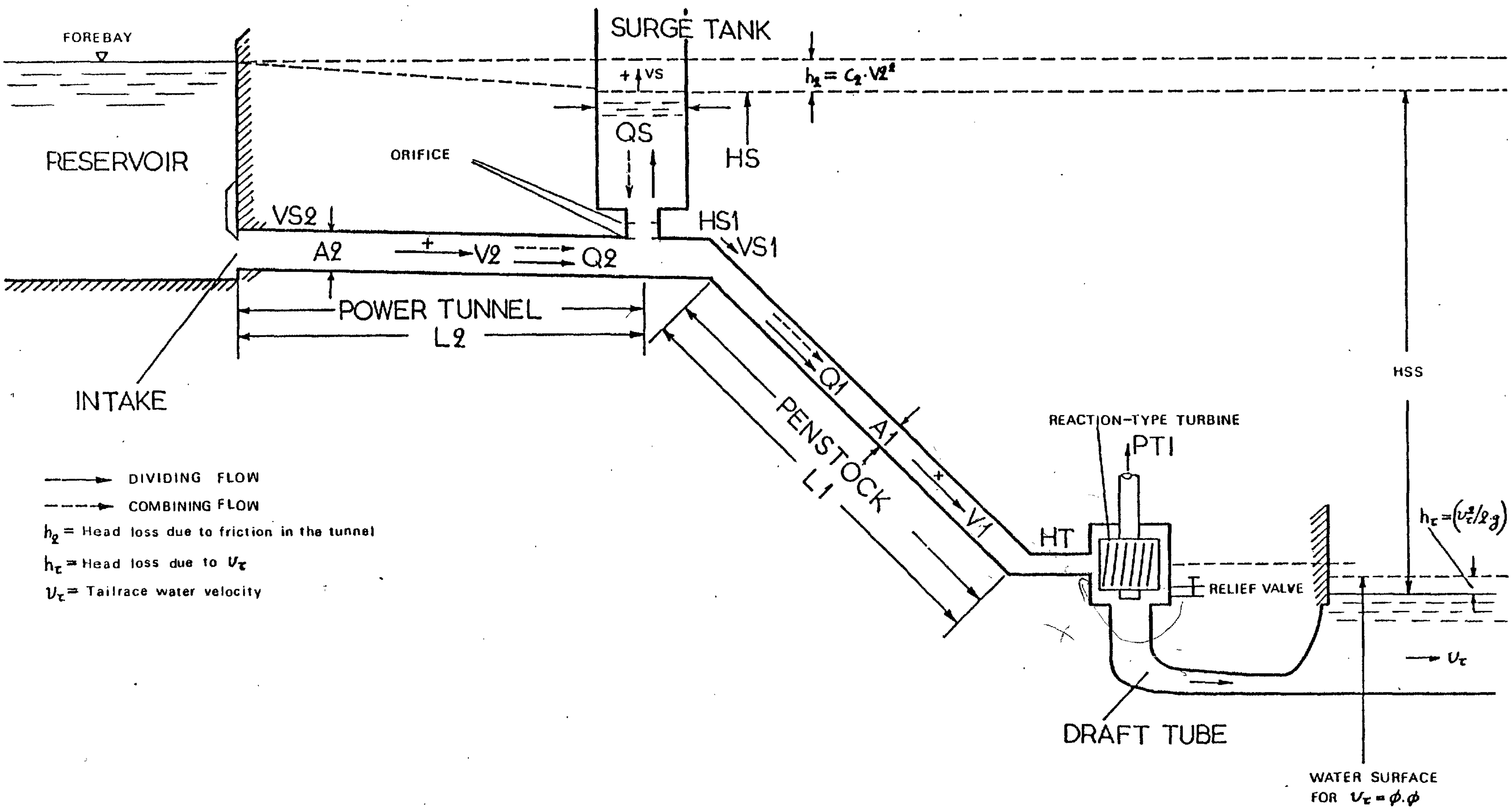

Fig. 4.1 Hydro Plant cross-section.

the water column in the penstock. So by its action the relief valve assists the surge tank and helps to reduce the oscillations of the water level due to a sudden closing of the gates.

The difference in elevation between the water level in the reservoir and the turbine or the tailwater level, called the "operating head", together with the flow of the water in the conduit, determines the power which can be produced by the particular unit. The power may be developed from the water by its weight, its pressure, its velocity, or a combination of any or all three. Therefore, the hydraulic turbines may be classified accordingly[53,54]:

<u>The impulse turbine:</u>

Here all the available head (i.e. the potential energy) is converted into kinetic energy through one (or several) nozzles, forming a jet(s). This jet discharges freely under atmospheric pressure into the wheel housing and thus it sets the runner in motion by acting against bowl-shaped buckets which only partly fills. After that, the water runs freely in the tailrace.

The representative type of impulse turbine is the Pelton-type turbine. This is usually employed with heads above 800 ft ("high-head" hydro plants) since as mentioned, it converts the available head into kinetic energy. It can, however, be used at lower head depending on the particular circumstances.

<u>The reaction turbine:</u>

Here all the water passage is filled with water (i.e. there is a closed-conduit system, as opposed to the free-surface flow of the impulse-type machines). The water enters the turbine casing at a relatively low speed where only a small part of the available head is converted into kinetic energy. The rest remains as a pressure head, which varies along the water passage. Therefore most of the power is produced from the difference in pressure acting on the front and the back of the runner blades. The rest is due to the velocity of the water mass. The water having gone through the runner buckets, discharges into the draught tube (see Fig. 4.1). The draught tube passage lies below the free surface of the tailrace. The shape of the tube is one of gradually increasing cross-section. Therefore the velocity of the water is reduced, the average pressure head at the discharge is increased and so the back pressure, against which runner discharges, is reduced. As a result, the pressure difference between the front and the back surfaces of the runner increases, thus producing more power.

The two characteristic types of reaction turbines are the Francis turbine and the propeller-type turbine, the latter being primarily represented by the Kaplan machine which is an adjustable-angle blade machine. The Francis turbines are used mainly for medium head projects, although they have been used up to 2200 ft. head[53]. The Kaplan-type machines are more suitable for low head plants, below 300 ft.

Pumped-Storage Plant:

There are several types of pumped-storage schemes, the most common being the recirculating or pure pumped storage[53]. It performs the basic function of a hydro plant, with the additional capability of pumping the water from the lower reservoir back to the upper reservoir and so the same water can be used again for generation. Depending on the particular characteristics of the site, the scheme might require a power tunnel and surge tank or only a penstock. Both tunnel and penstock have to be designed for two-directional flow. Usually tunnels seem to be preferred to exposed penstocks for pumped-storage applications. Obviously in any hydro scheme and especially in pumped-storage, it is desirable that the length of the power tunnel is as small as possible. This greatly reduces the capital cost because it also eliminates the need for a surge tank. The ratio (head/distance between the reservoirs) is an index which generally indicates the "pumped-storage" characteristic of the site; the smaller the ratio, the poorer the characteristic (from the point of view of increased construction costs and longer time to accelerate the water column over a long length of conduit).

The water flow in both directions demands a special arrangement of machines in the power house. The most frequently used arrangement in most pumped-storage projects until the late sixties, was the separate pump and turbine assemblies, both in the U.S.A.[55] and in Europe. However, the trend today seems to be towards reversible pump/turbine hydraulic machines. The main advantage of using these is the elimination of the separate machine and the space for its accommodation. The disadvantages are that to change the operating mode, the machine rotation has to be reversed and that their design gives at present a limit of operation under 550 m head.

The construction of a hydro plant usually requires a high capital cost, mainly because of the civil engineering work involved. But the operating costs are small and the efficiency very high. In addition, the contribution of the hydro-sets to the frequency regulation of the network and their ability to pick up the peak loads very quickly, make them an invaluable tool in the everyday running of the power system. Recently the pumped-storage schemes gained increased popularity with their ability to rapidly change their operating mode and take over in the event of the loss of a large unit of conventional or nuclear plant[56,57]. They can also be kept as a "spinning reserve" by either using a very small amount of water or using compressed air (spinning in the air). In this case they can be run up to full load in only a few seconds. In the following sections, the development of a model for a typical hydro plant will be presented.

4.2 CHOICE OF A MODEL

Because of lack of comprehensive data for a specific (typical) hydro plant, the data concerning the Appalachia hydroelectric plant were used. The main sources of information were references nos. 53, 58 and 59. The variables used are depicted in Fig. 4.1, to which reference will be made very frequently in what follows.

A first assumption was that the upper reservoir would be considered large. So the change of the water level in it can be neglected in comparison to the total head.

The most fundamental characteristic of the operation of the hydro plant is what is commonly known as the "water hammer phenomenon". This is the phenomenon of the change in pressure above or below the value that it had during the last steady-state of the system, at the entrance to the turbine and along the conduit, up to the surge tank and the reservoir. It is obviously a transient phenomenon and it takes place during the transition of the system from one steady-state to another. Its source is a change in load demand required from the plant, which means a change in the water flow through the conduit system to the turbine input. This is accomplished by a change of the control valve (gate) position at the entrance of the turbine. To follow the occurrence of this phenomenon, let it be assumed that the hydro plant operates at a specific steady-state when a decrease in generation is required. The valve opening at the entrance to the turbine is thus decreased in a step or other fashion. This action results, obviously, in a deceleration of the water along the conduit system and an increase in pressure at the valve. This positive pressure change travels backwards along the conduit, compresses the water and stretches the conduit shell. This wave is reflected at the upper end of the conduit (surge tank and/or reservoir) and the resulting negative pressure change travels downwards to the valve, where it is reflected back and the procedure is repeated. Therefore a standing wave develops along the conduit , if the friction opposing the flow is neglected. A change in the valve opening towards the other direction produces the same phenomenon, with the difference that the immediate effect is a decrease in pressure at the valve, instead of an increase.

The pressure of the water-hammer phenomenon is one of the basic considerations in the design of the plant and it also affects its performance, from the point of view of supplying the demanded load without many fluctuations. However, the oscillations in the pressure at the turbine input act unfavourably towards this goal. For this reason special devices, like the relief valve, the surge tank and the hydrogovernor are used to reduce the oscillations and the time interval over which they continue (after the change in the valve position).

The mathematical analysis of the water-hammer in a simple conduit, taking into account the compressibility of the water column and the elasticity of the pipe-line appears in many publications with various degrees of complexity[53,54,58,60,61,62]. The derivation of the equations describing the phenomenon involves partial differential equations and with friction neglected, the water-hammer effect in uniform conduit is described by the equations:

$$\boxed{\frac{\partial V}{\partial X} = -Q\,\frac{\partial H}{\partial t}} \qquad \text{Hydraulic Continuity Equation} \qquad (4.1)$$

$$\boxed{\frac{\partial V}{\partial t} = -g\,\frac{\partial H}{\partial X}} \qquad \text{Force Equation (Newton's } 2^{nd} \text{ Law)} \qquad (4.2)$$

where: V = the velocity of the fluid in the tube,
H = the head at the point (x,t) along the tube,
g = acceleration of gravity (32.2 ft/sec^2),

and: $$Q = \left[\frac{1}{K} + \frac{D}{d.E}\right].w \qquad (4.3)$$

where: K = voluminal modulus of elasticity of water in compression (lb/in^2),
D = the internal diameter of the pipe (in),
d = thickness of the pipe walls (in),
E = modulus of elasticity of the pipe material (lb/in^2),
w = weight of 1 ft^3 of water in lb (62.42763 lb/ft^3),
X = a point of observation of the wave along the length of the tube, at time t.

Equations (4.1) and (4.2) have the standard form of the wave propagation along a transmission line, and in this case represent the "pressure wave" which is propagated up the penstock to the forebay with a velocity of:

$$\alpha = \sqrt{g/Q} \quad \text{(ft/sec)}, \qquad (4.4)$$

or

$$\alpha = \frac{4675}{\sqrt{1 + (\frac{K.D}{E.d})}} \quad \text{(ft/sec)} \qquad (4.5)$$

For steel pipes, common in practice, it becomes:

$$\alpha = \frac{4675}{\sqrt{1 + (\frac{D}{100.d})}} \quad \text{(ft/sec)} \tag{4.6}$$

For a pipe concreted in solid rock, the fraction: (k.D/E.d) becomes infinitesimal and α gets a limiting value of: α = 4675 (ft/sec), this being the velocity of sound in the water.

There are different ways of solving the two equations (4.1) and (4.2). The approach which uses the Laplace Transforms of the partial differential equations of the flow (described in Ref. 57) was adopted. It ends up with two equations relating the head (H) and the volumetric flow (Q) at any point x along the conduit, to the same quantities at a specific point, where the conditions (H,Q) are known. If these two locations are considered to be the beginning and the end of the conduit, then the two equations take the following form:

$$H_L = \text{sech}(T_e s).H_\emptyset - (\frac{\alpha}{g.A}).(\tan h(T_e s)).Q_L - k_1|Q_L|Q_L \tag{4.7}$$

$$Q_\emptyset = \cos h(T_e s).Q_L + (\frac{g.A}{\alpha}).(\sin h(T_e s)).H_L \tag{4.8}$$

where:
- T_e = elastic time of the tunnel = (L/α),
- s = the Laplace operator,
- L = indicates the end of the tunnel,
- $\emptyset$ = indicates the beginning of the tunnel.

The term $k_1|Q_L|Q_L$ in the force equation (4.7) represents the losses due to friction.

From these two equations, it is obvious that for very accurate studies of the water behaviour in the tunnel, hyperbolic expressions are necessary. But for studies where less accuracy is required, an approximation which reduces computation time is often enough to reveal the basic characteristics of the process.

Therefore the first order approximation of equations (4.7) and (4.8) was taken, from the Taylor series of the hyperbolic functions, as follows:

$$\cos h(T_e s) = 1 + T_e^2 s^2 + T_e^4 s^4 + \ldots \quad \approx 1 \Rightarrow \sec h(T_e s) = 1/\cos h(T_e s) \approx 1$$

$$\sin h(T_e s) = T_e s + T_e^3 s^3 + T_e^5 s^5 + \ldots \quad \approx T_e s$$

$$\tan h(T_e s) = (\sin h(T_e s)/\cos h(T_e s)) \quad \approx T_e s$$

Substitution of these expressions in (4.7) and (4.8) gives:

$$H_L = H_\emptyset - \left(\frac{\alpha}{g.A}\right).(T_e s)Q_L - k_1|Q_L|Q_L \qquad (4.9)$$

$$Q_\emptyset = Q_L + \left(\frac{g.A}{\alpha}\right).(T_e s)H_L \qquad (4.10)$$

<u>For the penstock</u> (Fig. 4.1), application of (4.9) and (4.10) gives respectively:

$$\frac{d}{dt}(V_1) = \left(\frac{g}{L_1}\right).\left[H_{S1} - H_T - C_1V_1^2\right] \quad \text{Force Equation} \qquad (4.11)$$

$$\frac{d}{dt}(H_T) = \left(\frac{\alpha_1^{\,2}}{g.L_1}\right).\left[V_{S1} - V_1\right] \quad \text{Continuity Equation} \qquad (4.12)$$

and:
$$C_1 = \frac{fL_1}{2.D_1.g} \qquad (4.13)$$

where: f = coefficient of frictional resistance. It is dimensionless and can be easily derived from the Darcy-Weisbach or the Scobey formulae[53].

<u>For the power tunnel</u>, these equations take the form:

$$\frac{d}{dt}(V_2) = \left(\frac{g}{L_2}\right).\left[H_R - H_{S1} - C_2V_2^2\right] \quad \text{Force Equation} \qquad (4.14)$$

$$\frac{d}{dt}(H_{S1}) = \left(\frac{\alpha_2^{\,2}}{g.L_2}\right).\left[V_{S2} - V_2\right] \quad \text{Continuity Equation} \qquad (4.15)$$

and again:
$$C_2 = \left(\frac{fL_2}{2.D_2.g}\right) \qquad (4.16)$$

<u>Surge Tank</u>

The main designs for the surge tank are the: simple surge tank, the restricted-orifice tank and the differential surge tank. Their general forms are shown in Fig. 4.2.

In the simple tank, the riser has to have sufficient cross section to permit the free flow of water into the main compartment of the tank. The build-up of the head due to acceleration or deceleration of the water in the conduits is very slow and it follows the build-up of the water level in the tank. It can be shown that the volume required in a tank of this type is large and so its construction more expensive.

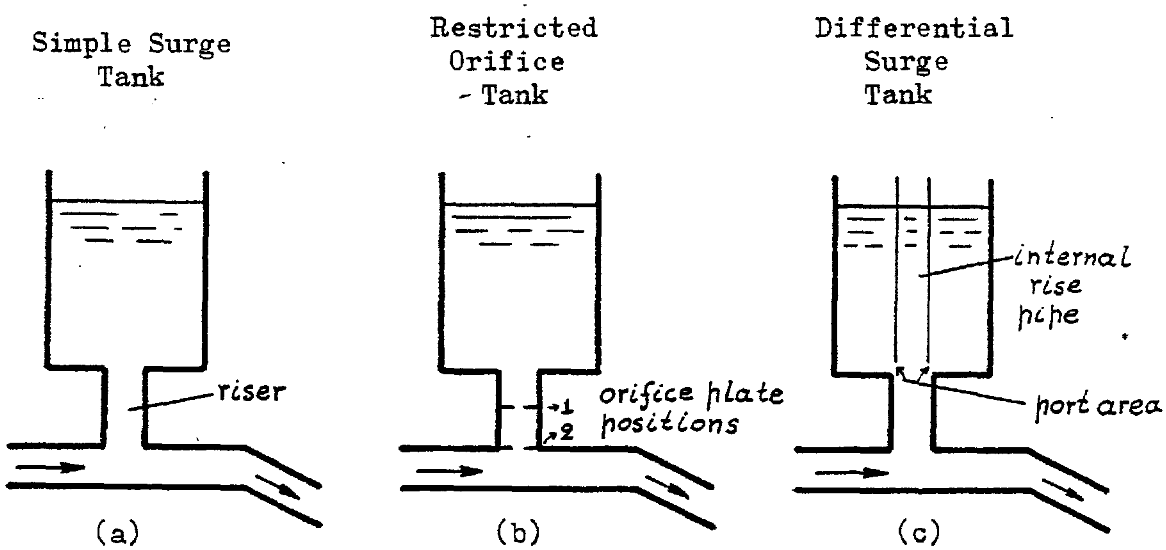

Fig. 4.2 Surge tank designs.

In the differential surge tank, the main feature is the additional internal riser. Its diameter is smaller than the normal riser and so it leaves an annular area (port area) from which the main tank can fill with water. The advantage over the simple tank is the faster build-up of the head inside the internal riser, which makes the reaction of the whole tank faster. This results in a considerable saving of construction costs, because a smaller tank diameter is needed.

The equations describing the flows in the differential tank are[63]:

$$\frac{d}{dt}(H_r) = (1/A_r).\left[(V_u.A_u - V_d.A_d) - \underbrace{C_r\sqrt{H_r - H_s}}_{\text{flow into the main tank}} - \underbrace{C_o.(H_r - H_{cr})^{3/2}}_{\text{water spilled over the riser crest}}\right] \qquad (4.17)$$

$$\frac{d}{dt}(H_s) = (1/A_S).\left[C_r.\sqrt{(H_r-H_s)} + C_o.(H_r-H_{cr})^{3/2}\right] \qquad (4.18)$$

where: H_{cr} = internal riser crest height,
H_r = water level in internal riser,
C = discharge coefficient,
H_s = water level in main tank.

and the indices: u = upstream from tank,
d = downstream from tank.

Finally, in the orifice surge tank, the main feature is an additional restriction which is installed between the conduit and the tank (Fig. 4.2(b)). The performance of the tank depends on the opening of the orifice. The opening completely blocked, eliminates the surge tank. The opening unrestricted represents the case of a simple surge tank. When the gates are suddenly closed, the surplus of the decelerating water will be throttled as it passes through the orifice and so a head loss will take place, in addition to the build-up of the retarding head. The orifice plates can be in different positions as is shown in Fig. 4.2(b). Yu-Tek Li[64] gives a detailed study of the performance of the tank with different combinations and shapes of the orifice plate.

The restricted-orifice design enjoys increased popularity because it has several advantages over the differential tank design[64]. Most important of them are the fact that it is more economical to build and that the size and location of the orifice can be easily changed to accommodate better performance under various operating conditions. In reference 65 is justifiably suggested that, especially in this type of surge tank, the power tunnel is not completely isolated from the pressure waves and that a considerable portion of the overpressure is transmitted to the power tunnel. This is taken into account by equation (4.14), where the "input disturbance" is H_{S1}, i.e. the head at the base of the surge tank.

For the junction at the surge tank base, the continuity of flow is:

$$A_2.V_2 - 2.A_1.V_{S1} = A_S.\frac{d}{dt}(H_S) = Q_\phi \qquad (4.19)$$

The presence of two penstocks is the reason for the term: $2.A_1.V_{S1}$. In this equation the term (A_S/A_2) can be seen as the time constant of the oscillation of the water level in the surge tank (H_S). So as this ratio increases, the period of the oscillations becomes longer.

The flow through the orifice can be expressed as[64,65]:

$$H_{S1} = H_S \pm KK.(Q_\emptyset)^2, \quad \begin{array}{l} + \text{ for } Q_\emptyset > 0 \text{ (i.e. inflow)} \\ - \text{ for } Q_\emptyset < 0 \text{ (i.e. outflow)} \end{array} \tag{4.20}$$

where: $$KK = (1/2g).\left[\frac{1}{cA_o} - \frac{1}{A_S}\right]^2, \text{ and} \tag{4.21}$$

c = coefficient of contraction of the orifice,

A_o = cross section of the orifice.

The head loss due to the flow through the orifice, is $\Delta h = (H_{S1}-H_S)$. At a steady-state operation obviously $H_{S1} = H_S$ and $Q_\emptyset = 0.0$.

The turbine

From Bernoulli's theorem, the relation between the head and the velocity of the water at a certain position along the conduit is of the form:

$$H = \text{const.}(V)^2 \tag{4.22}$$

At the entrance of the turbine the flow depends also on the gate opening so this has to be incorporated into the expression shown above. This is done by taking into account that a decrease in the gate opening results in an increase of the head at the turbine entrance. So the relation (4.22) becomes:

$$H_T = K_1.(V_1/G)^2 \tag{4.23}$$

In this expression the "speed-effect" can be included[66], to formulate the final head at the turbine entrance. This is the effect on the head of the difference between the actual turbine speed from the synchronous one. But during regulating action it can be assumed that the deviation of the turbine speed from normal is small (it must be if the regulation is effective) and so the speed can be included in the constant K_1.

The equation (4.23) has the disadvantage of giving infinite head H_T, when the gate valve is closed, i.e. G becomes zero. In order to overcome this, another expression was adopted in which G is not in the denominator:

$$H_T = H_S - KKA.G + KKB.V_1 \qquad (4.24)$$

In this expression the quantities G and V_1 have the same effect on H_T when, for example, they are decreased suddenly in value. Both constants KKA and KKB are positive.

Finally the power input to the machine is proportional to the flow of water into it and the available head at the turbine entrance, i.e.

$$P_{TI} = K_P.V_1.H_T \qquad (4.25)$$

Governor

It is well known that when the gates close, the desired effect of a reduction in input power cannot be realized immediately because of the inertia of the water column in the conduit. In fact the immediate effect of this action is the opposite of the desired direction. The faster is the change in the gate position, the more the system tends initially towards the wrong direction. Therefore the governor, which is responsible for the changes in the gate position, must incorporate some means of reducing this effect.

This means is a dashpot in the feedback loop of the servomotor, which in effect produces a signal which is proportional to the rate of change of the servomotor position. This signal is called temporary droop (T.D.), in contrast to the permanent droop (P.D.), i.e. the standard feedback signal which is proportional to the position of the servomotor. The T.D. provides sufficient damping to the system by not allowing the servomotor position to change very fast. On the other hand the P.D. ensures that a permanent change in the turbine speed causes a permanent alteration in the servomotor position, as well as responding to the speeder gear (demand) signal for a change of load under steady-state conditions.

The hydrogovernor representation which was adopted in this study was the standard IEEE representation of mechanical hydraulic governor widely used in the literature[66,67,68,69]. The corresponding equations are:

$$C_p = \sigma . G \qquad \text{permanent droop} \tag{4.26}$$

$$C_T = \left[\frac{\delta . s T_R}{1 + s T_R}\right] . G \qquad \text{transient droop} \tag{4.27}$$

and:

$$CC = C_P + C_T$$

$$D_{PE} = D_N - CC + P_{ref} \qquad \text{error signal} \tag{4.28}$$

$$R = \left[\frac{(1/T_G)}{1 + s T_P}\right] . D_{PE} \qquad \text{rate of change of servomotor position} \tag{4.29}$$

$$G = (1/s) . R \qquad \text{servomotor position} \tag{4.30}$$

and the symbols can be found in the nomenclature.

The continuous equations which were used in the hydro model are shown on Table 4.1. The restricted orifice surge tank representation was used in preference to the differential tank. Another point is that equation (4.15) was not used because the velocity of the water at the intake is not needed by the rest of the equations.

Finally, a block diagram representation of the model is shown in Fig. 4.5.

TABLE 4.1: HYDRO PLANT MODEL EQUATIONS

Continuous time representation		Discrete-time representation
		$VV_1 = V_1(K-1).V_1(K-1)$
$H_T = H_S - KKA.G + KKB.V_1$	(4.31)	$H_T(K)=H_S(K-1)-KKA.G(K-1)+KKB.V_1(K-1)$
or: $H_T = K_1(V_1/G)^2$	(4.32)	or: $H_T(K)=(K_1.VV_1)/(G(K-1).G(K-1))$
$\frac{d}{dt}(V_1)=(\frac{g}{L_1}).\left[H_{S1}-H_T-C_1V_1^2\right]$	(4.33)	$V_1(K)=V_1(K-1)+((T.g)/L_1).\left[H_{S1}(K-1)-H_T(K)-C_1.VV_1\right]$
$\frac{d}{dt}(V_2)=(\frac{g}{L_2}).\left[H_R-H_{S1}-C_2V_2^2\right]$	(4.34)	$VV_2 = V_2(K-1).V_2(K-1)$
$A_S.\frac{d}{dt}(H_S)=A_2.V_2-2.A_1.V_{S1}=Q_\emptyset$	(4.35)	$V_2(K)=V_2(K-1)+((T.g)/L_2).\left[H_R-H_{S1}(K-1)-C_2.VV_2\right]$
$V_{S1}=V_1+(\frac{gL_1}{\alpha_1^2}).\frac{d}{dt}(H_T)$	(4.36)	$QQQ=(T.A_2/A_S).V_2(K-1)-(2.A_1.T/A_S).V_1(K-1)-(2.A_1.g.L_1/\alpha_1.\alpha_1.A_S).(H_T(K)-H_T(K-1))$
$H_{S1} = H_S \pm KK.(Q_\emptyset)^2$	(4.37)	$H_S(K) = H_S(K-1)+QQQ$
$P_{TI} = K_P.V_1.H_T$	(4.38)	$H_{S1}(K)=H_S(K)\pm(\frac{A_S}{T})^2.KK.(QQQ.QQQ)$
		where: + is used when $QQQ > 0$
		− is used when $QQQ < 0$
		$P_{TI}(K) = K_P.V_1(K).H_T(K)$
$D_{PE} = D_N - CC + P_{ref}$	(4.39)	$D_{PE}(K) = D_N - CC(K-1) + P_{ref}$
$\frac{d}{dt}(R) = (1/T_P).\left[\frac{D_{PE}}{T_G} - R\right]$	(4.40)	$R(K)=\left[\frac{(T/T_G)}{T+2.T_P}\right].\left[D_{PE}(K-1)+D_{PE}(K)\right] - \left[\frac{T-2.T_P}{T+2.T_P}\right].R(K-1)$
$\frac{d}{dt}(G) = R$	(4.41)	$G(K)=G(K-1)+(T/2).(R(K)+R(K-1))$
$\frac{d}{dt}(CC)=(1/T_R).\left[\sigma.G+T_R.(\sigma+\delta).R - CC\right]$	(4.42)	$CC(K)=C8.G(K)+C9.G(K-1)-C10.CC(K-1)$
		where: $C8=(\sigma.T+2((\sigma+\delta).T_R))/(T+2T_R)$
		$C9=(\sigma.T-2.((\sigma+\delta).T_R))/(T+2.T_R)$
		$C10=(T-2.T_R)/(T+2.T_R)$

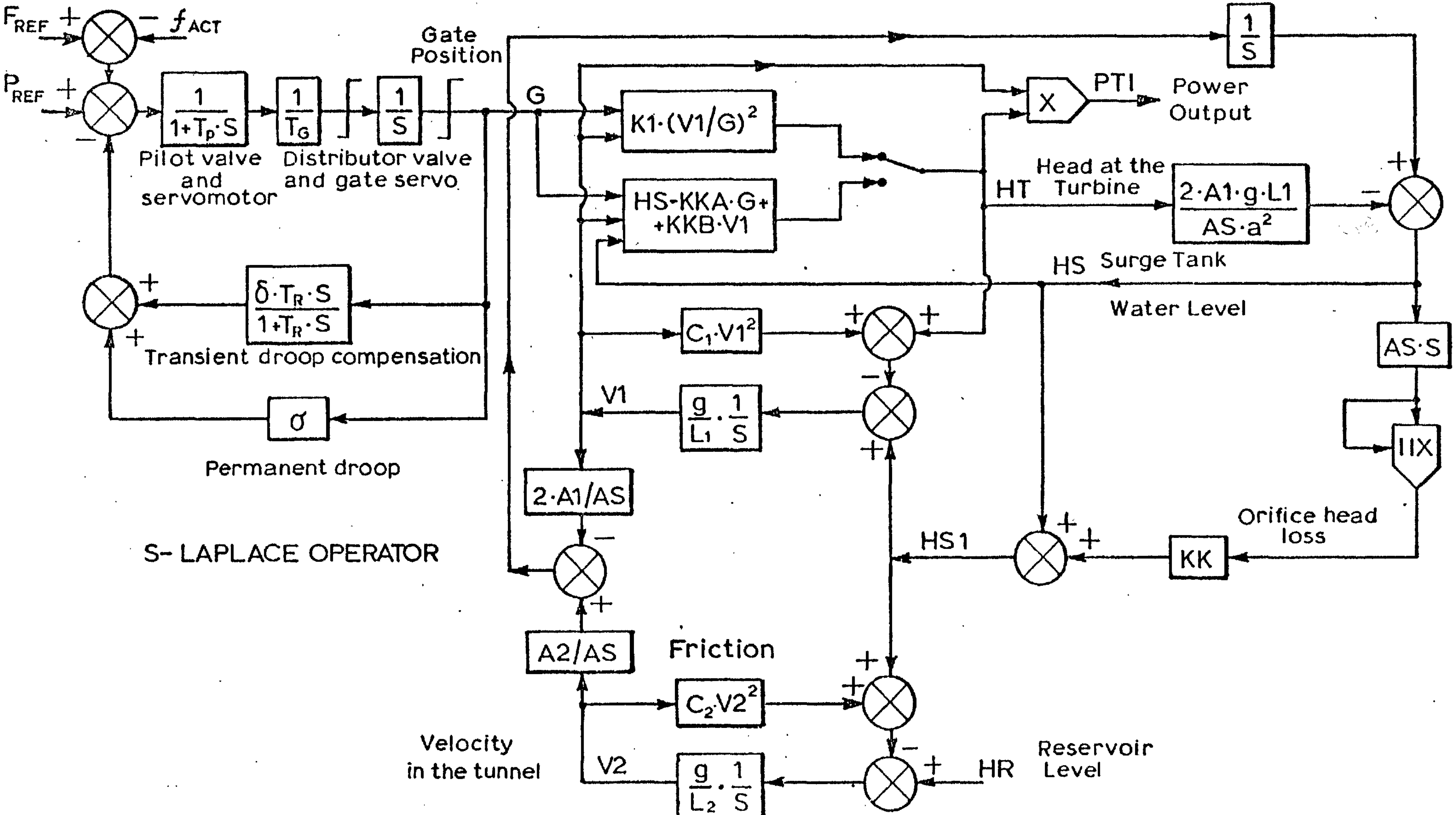

Fig. 4.3 Hydro-Plant Model

4.3 STEADY-STATE CHARACTERISTICS OF THE HYDRO MODEL

4.3.1 The Plant

The original steady-state from which the investigation started was considered to be that corresponding to full-load operation. The numerical values for the main variables and the other parameters of the model for this study are presented in Appendix F.1.

A change in the full-load steady-state can be initiated by a change in the speeder gear (a change in demand) or by fluctuation in the system frequency which in turn affects the rotational speed of the machine. Assuming that the frequency is 50 Hz and knowing the new load demand, the new steady-state of the plant can be computed from the equations presented in Table 4.1. This computation is shown in Appendix F.2.

Using these equations, the steady-state characteristics of the various quantities of the model were plotted as functions of the control valve position, G. In Fig. 4.4(a), the turbine output/ valve opening characteristic is shown for the model using equation (4.32). It is compared with the corresponding characteristics for the Appalachia hydro plant, for the prototype and for the model used in the studies presented in Reference 58. The actual numbers for these characteristics were taken from Fig. 4, p. 406 of the reference mentioned above. Considering that a first order approximation was used for the model in Fig. 4.3, the characteristic shown in Fig. 4.4(a) is not out of proportion.

In Fig. 4.4(b) comparison is made between the same kind of characteristics for the model and the Appalachia plant for the cases where one only and both units were in operation. The data for the Appalachia characteristic were taken from Fig. 5 in reference 58. Again it can be said that the model is not very far from the real plant characteristic.

The possibility of producing this characteristic closer to the real-life one was investigated. In Fig. 4.4(c) the two cases where the friction losses are given by: C_V and $C_V^{1.5}$ are compared with the normal case considered so far. From this can be seen that

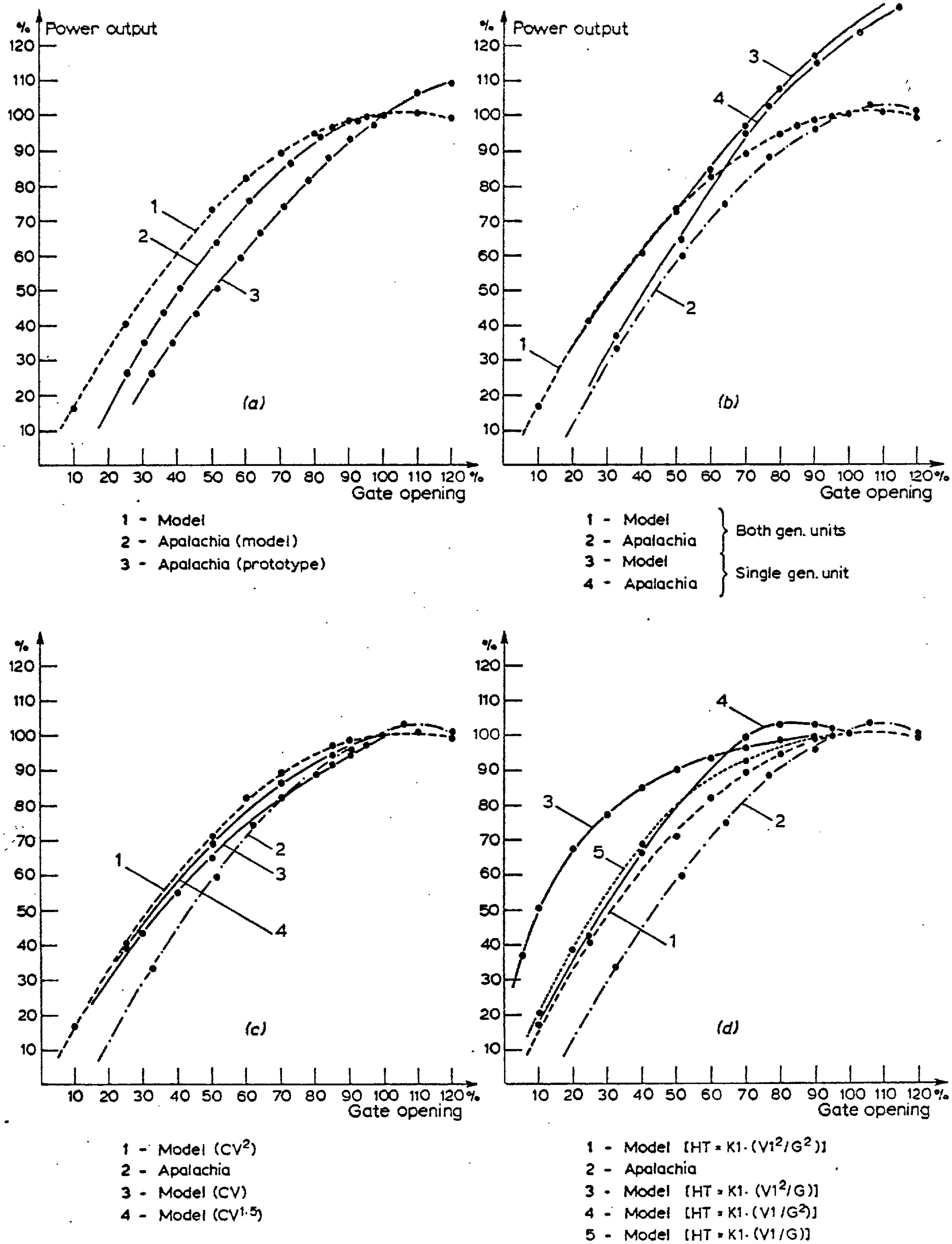

Fig. 4.4 Mechanical Power/Valve Opening (closed-loop) steady-state characteristics for different cases and operating conditions of the hydro plant model.

as the exponent drops, the characteristic is moving downwards. Both characteristics are nearer the Appalachia characteristic in the range from 100 to 85% of the valve opening, but then move away from it and approach the model characteristic.

In Fig. 4.4(c) the two characteristics (Appalachia and model) are compared with similar curves derived from the model equations with the friction losses given by $C_V{}^2$, while the turbine entrance head is given by the following expressions:

(a) $H_T = K_1.(V_1)^2/G$

(b) $H_T = K_1.(V_1)/G^2$

(c) $H_T = K_1.(V_1)/G$

As can be seen, all of them are on the left-hand side of the model characteristic, so they do not introduce any improvements.

When equation (4.31) is used to compute the turbine entrance head (H_T), then the form of the characteristic depends on the values of the constants KKA and KKB. With KKA = 500, the output/valve opening characteristic for three different values of KKB is shown in Fig. 4.5a. As the value of the KKB increases, the power output for 100% valve opening increases, taking values from zero to above 100%. Obviously the output is 100% for only one value of KKB. In this case it is KKB = 28.125.

In Fig. 4.5(b) a comparison is made between the characteristic of the Appalachia plant and the model,with equations (4.31) and (4.32) for the pairs (KKA = 500, KKB = 28.125) and (KKA = 2500, KKB = 146.546). As KKA increases in value, the characteristic goes nearer to the one of the Appalachia generator and away from the model characteristic. This happens in the region between 100% and 40% of the valve opening. Below 40% the two characteristics merge, although they remain below the one corresponding to the model. So from the steady-state point of view the use of equation (4.31) gives an improvement over the use of (4.32) as far as the power output/ valve opening characteristic is concerned.

The steady-state characteristics of the water velocity in the conduit, the head in the turbine entrance and the head at the surge tank as functions of the valve opening are shown in Fig. 4.5(c) and (d) for the cases where:

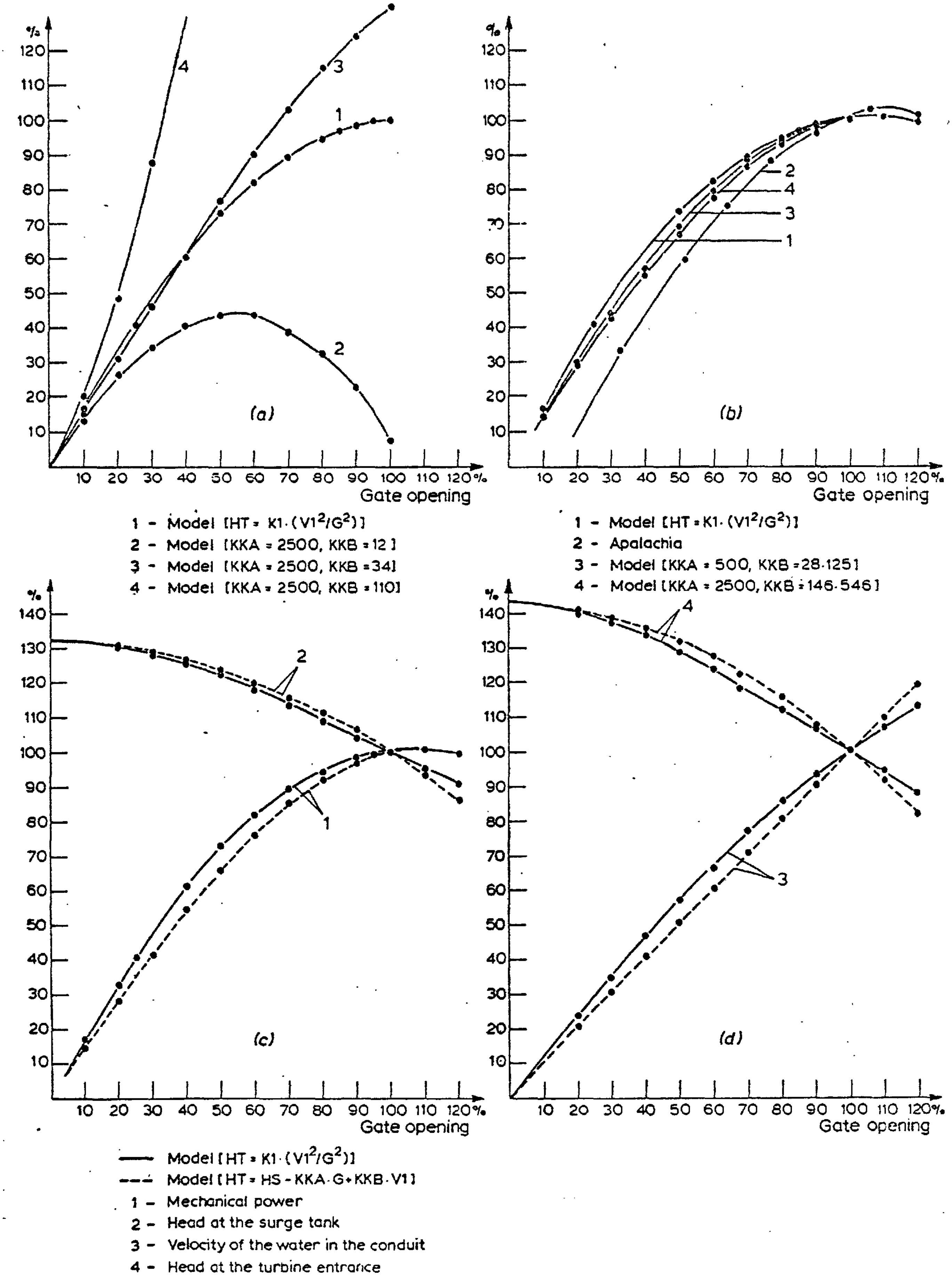

Fig. 4.5 (a), (b): Mechanical Power/Valve Opening steady-state characteristics for different configurations of the hydro plant model.

(c), (d): Steady-state characteristics of the two versions of the hydro plant model.

$$H_T = K_1.(V_1/G)^2$$

and $$H_T = H_S - KKA.G + KKB.V_1,$$

for: KKA = 2500. and KKB = 146.546.

4.3.2 The Governor

There are no non-linearities (like dead band, etc.) included in the governor equations (Table 4.1), therefore there is a direct steady-state relationship between the speeder gear setting P_{ref} and the valve position G. If the 1 p.u. value of the valve position is 1.0 and the frequency error is $D_N = 0.0$, then the corresponding value of the speeder gear setting is $P_{ref} = 0.04$. These are the values adopted in the model.

T_G is called the gate opening time, i.e. the time in seconds, for a 1 p.u. change in frequency to produce 1 p.u. gate opening (typical value chosen, $T_G = 0.2$).

The gate closing time, i.e. the time required for the gate to go from fully open to fully closed moving with maximum velocity has a typical range of values: 5–10 s. If the closing time is represented by T_C, then it is related to the opening time by:

$$T_G = \delta . T_C$$

where: δ = the p.u. speed deviation required to saturate the pilot valve[68]. Typical value $\delta = 0.04$ p.u.

Finally, the frequency or speed error is defined as:

$$D_N = N_{ref} - N_{act}$$

or: $$D_N = F_{ref} - f_{act} = (50 - f_{act})$$

4.4 TRANSIENT RESPONSE OF THE HYDRO MODEL

The continuous-time equations of the model (shown on Table 4.1) were converted to their discrete-time form. For the hydro governor discretization Tustin's approximate discrete integrator was used, while for the rest of the equations the Z.O.H. operator was employed. For this purpose, the same considerations as for the conventional steam model were taken and they will not be repeated here. The resulting difference equations are presented on Table 4.1.

4.4.1 The Plant Response without the Governor

Many runs (on the CDC 6400) were made without the orifice and the hydro governor equations, in order to assess the behaviour of the model. It soon became apparent that A_S should have a value of at least 3000 in order to get a response of the surge tank water level comparable to that of the actual plant.

With the orifice equations included, the response of the model was investigated for the case where a complete gate closure is taking place within 5 s, as was suggested in reference 59. This corresponds to a 6% change every 0.3 s. In Figs. 4.6 and 4.7 the responses are shown for the cases where equations (4.32) and (4.31) were used respectively, for an 18% change in gate position within 0.9 s. For both cases the gate closure produces a sharp increase in the head at the turbine entrance and as a result the mechanical power changes in a similar way. The water level in the tank obviously begins to rise and reaches the quarter cycle in about 6.7 mins. (which is about the same as in reference 59). In Figures 4.6 and 4.7(b), the time scale is 5 mins. and as can be seen the level approaches its first peak. The velocity of the water in the penstock begins to drop steadily up to a point and then starts rising slowly. The velocity of the water in the tunnel begins to drop, as it should do. Its change is very smooth, which indicates that the surge tank provides an effective screen protection to the tunnel from the water hammer effect. It is possible, however, that with more detailed representation of the plant, the pressure waves transmitted to the tunnel would have been more evident.

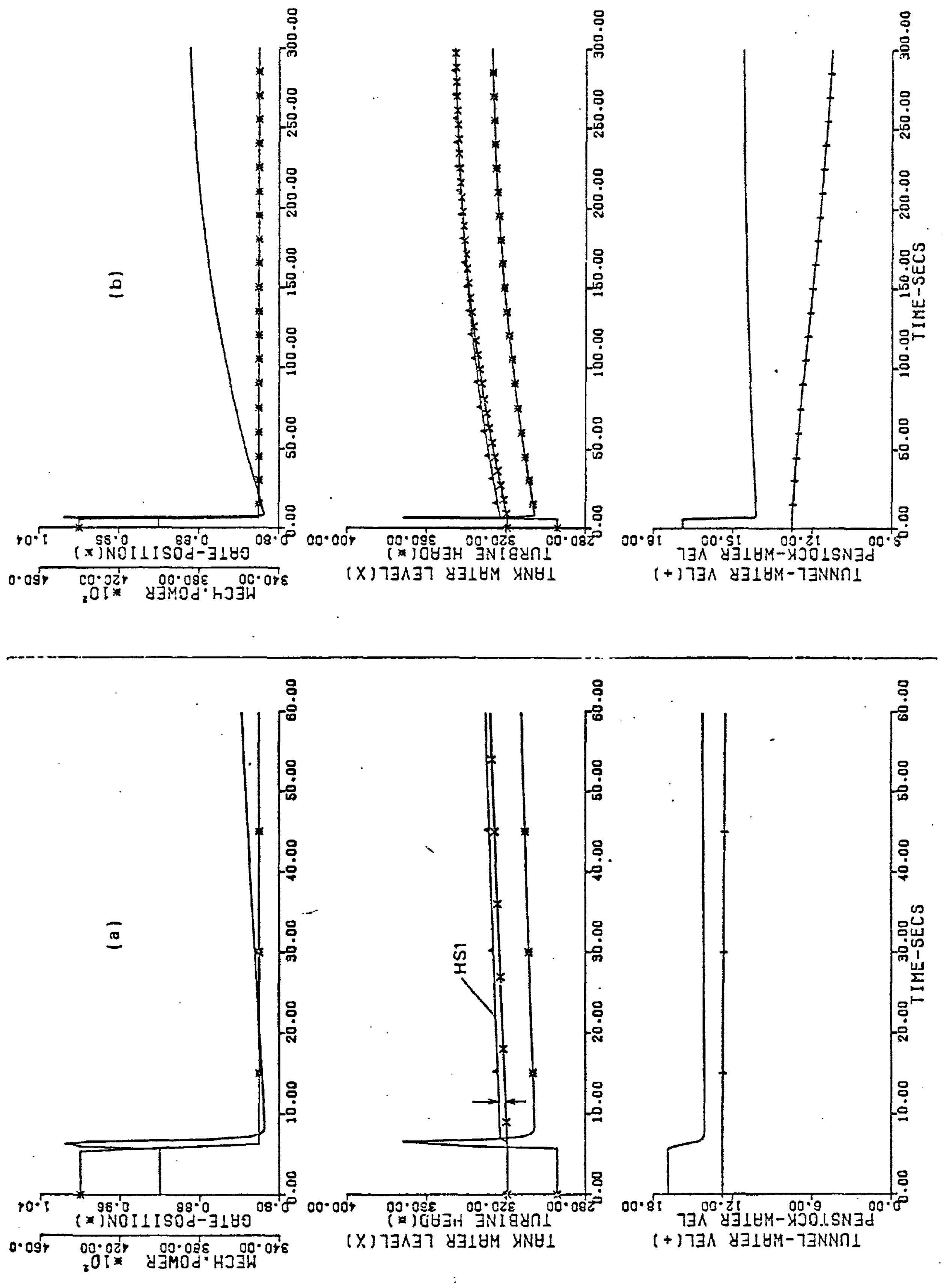

Fig. 4.6: Hydro model response to an 18% decrease in the valve opening within 0.9 s $\left[H_T = K_1 . (V_1/G)^2\right]$.

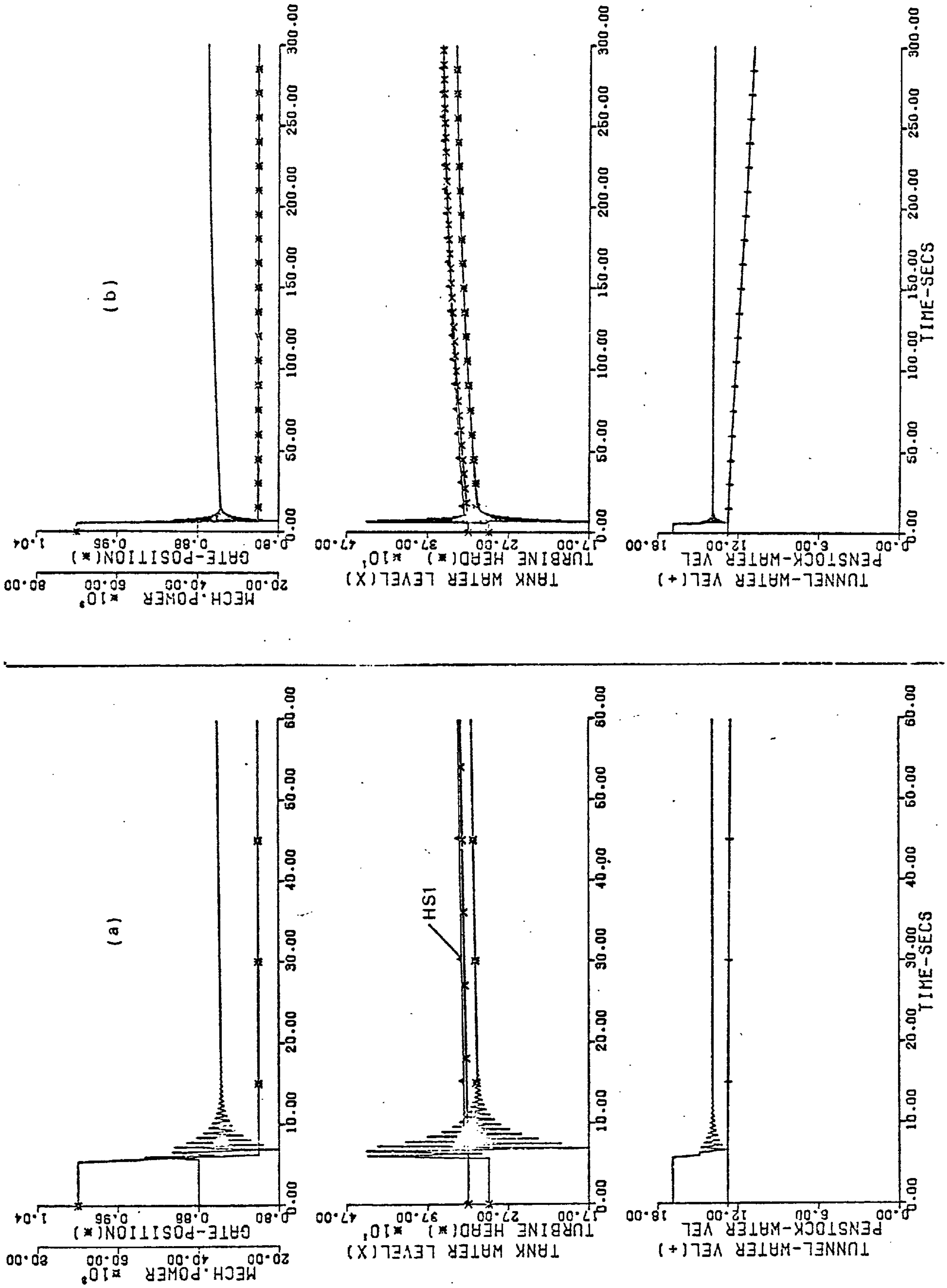

Fig. 4.7: Hydro model response to an 18% decrease in the valve opening within 0.9 s $\left[H_T = H_S - KKA.G + KKB.V_1\right]$.

During attempts to get the model response for greater changes in the valve position, it was found that below the value of $G \simeq 0.24$ (24% valve opening), the smallest change in the value of G resulted in instability when the equation (4.32) was employed for the computation of the turbine entrance head. The reason is that as G became very small, even a small change in its value resulted in a very big change in H_T, which eventually became greater than H_{S1} and made V_1 negative. Therefore the problem with equation (4.32) arises not only when G becomes zero (as was mentioned in Section 4.2) but it starts long before that. This, of course, does not happen when the expression (4.31) is used.

In Figs. 4.8 and 4.9 the response of the model is shown when equation (4.32) is used and when a 54% gate closure and 54% gate opening is introduced within 2.7 s in both cases. In fact the response is stable for similar gate opening changes down to 30%, but below that the response becomes unstable. An interesting aspect which can be seen in these figures is the initial large difference between the values of H_S and H_{S1}. This confirms the fact that the effect of the orifice equations becomes significant when large changes in the valve position and consequently large disturbances are introduced into the model. In such cases the head lost due to the throttling becomes more evident (compare it with Fig. 4.6). Also in reference 64 it is shown that the head loss at the orifice is greater in combining flow (flow out of the surge tank) than in dividing flow (flow into the tank). This is confirmed from Figs. 4.8 and 4.9(a), where at t = 20 s the head loss due to throttling was 29.53 (ft) for the dividing flow (Fig. 4.8) and 32.28 (ft) for the combining flow (Fig. 4.9). Yu-Tek Li[64] showed that the orifice coefficient KK (equation (4.37)) is not constant throughout the flow envelope (it decreases as the ratio (Q_S/Q_1) decreases). This fact has not been taken into account in the model.

In Figs. 4.10 and 4.11, the response of the model is shown when equation (4.31) is used and when a 100% (within 5 s) change in the gate opening in both directions is introduced.

Both responses are stable. The effect of the orifice throttling is evident. In Fig. 4.10(a) after 15 s H_T becomes equal to H_{S1}, because by that time both G and V_1 are almost zero, as

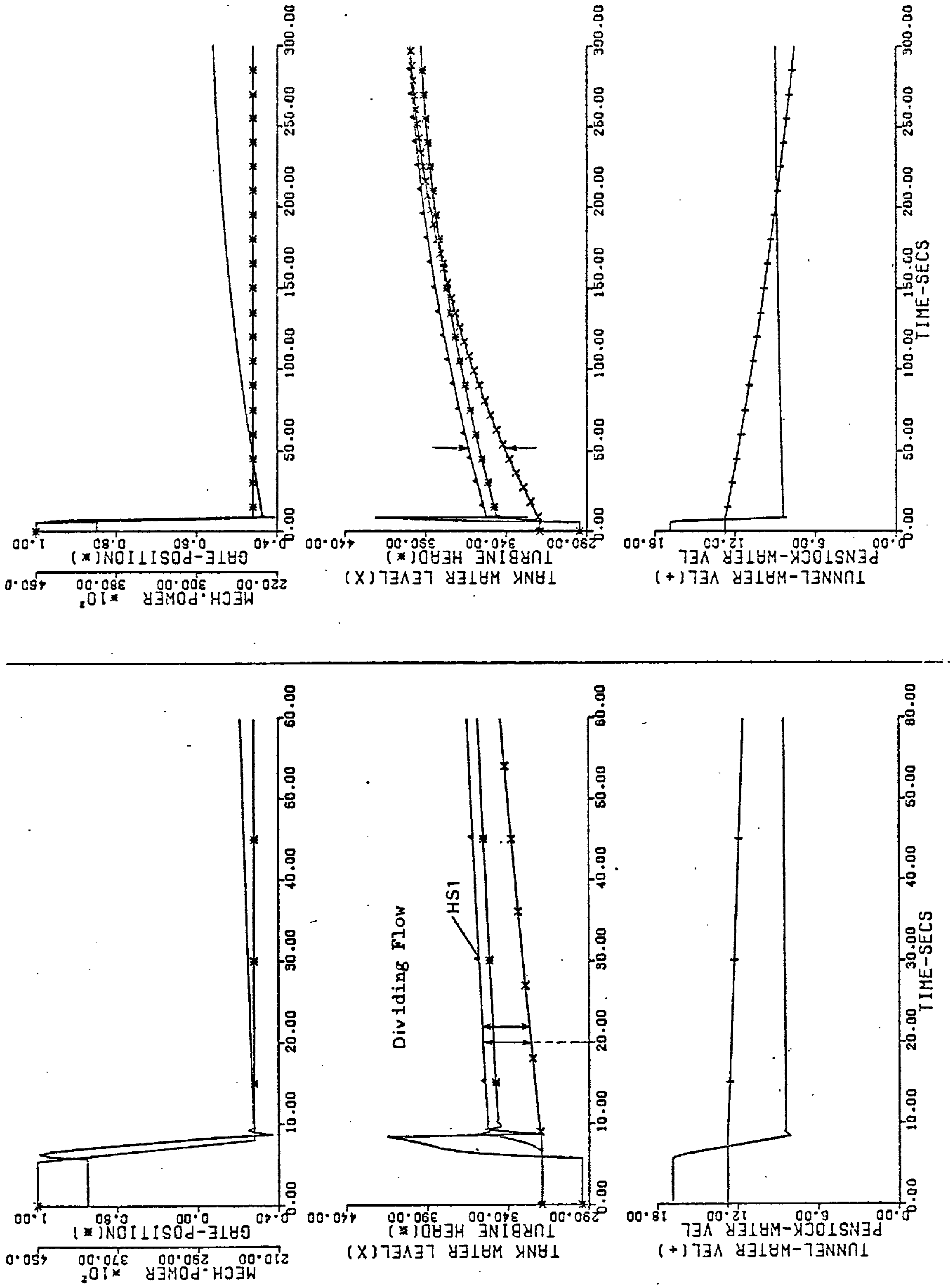

Fig. 4.8: Hydro model response to a 54% decrease in the valve opening within 2.7 s $\left[H_T = K_1.(V_1/G)^2\right]$.

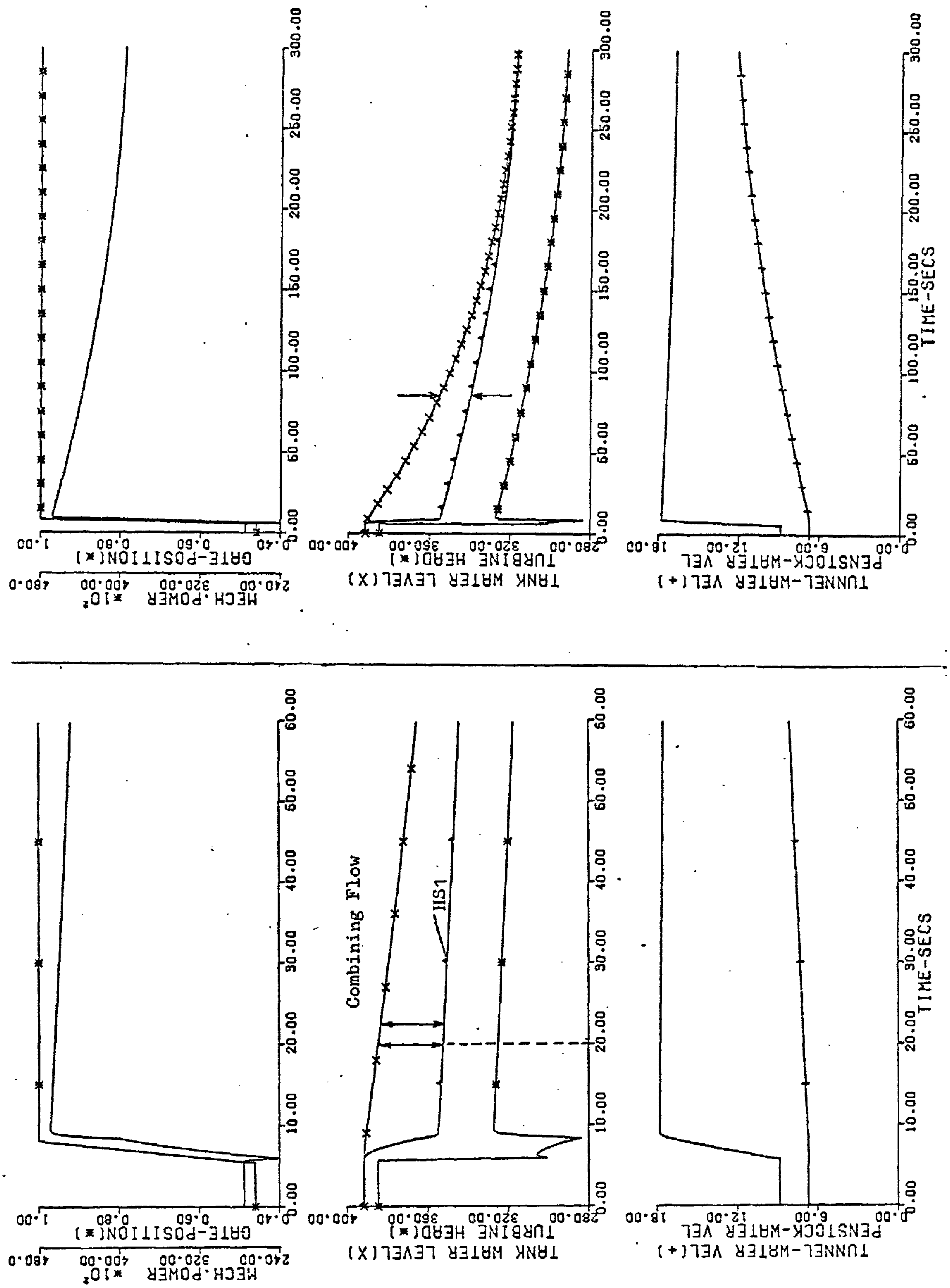

Fig. 4.9: Hydro model response to a 54% increase (from 46% to 100%) in the valve opening, within 2.7 s $\left[H_T = K_1.(V_1.G)^2\right]$.

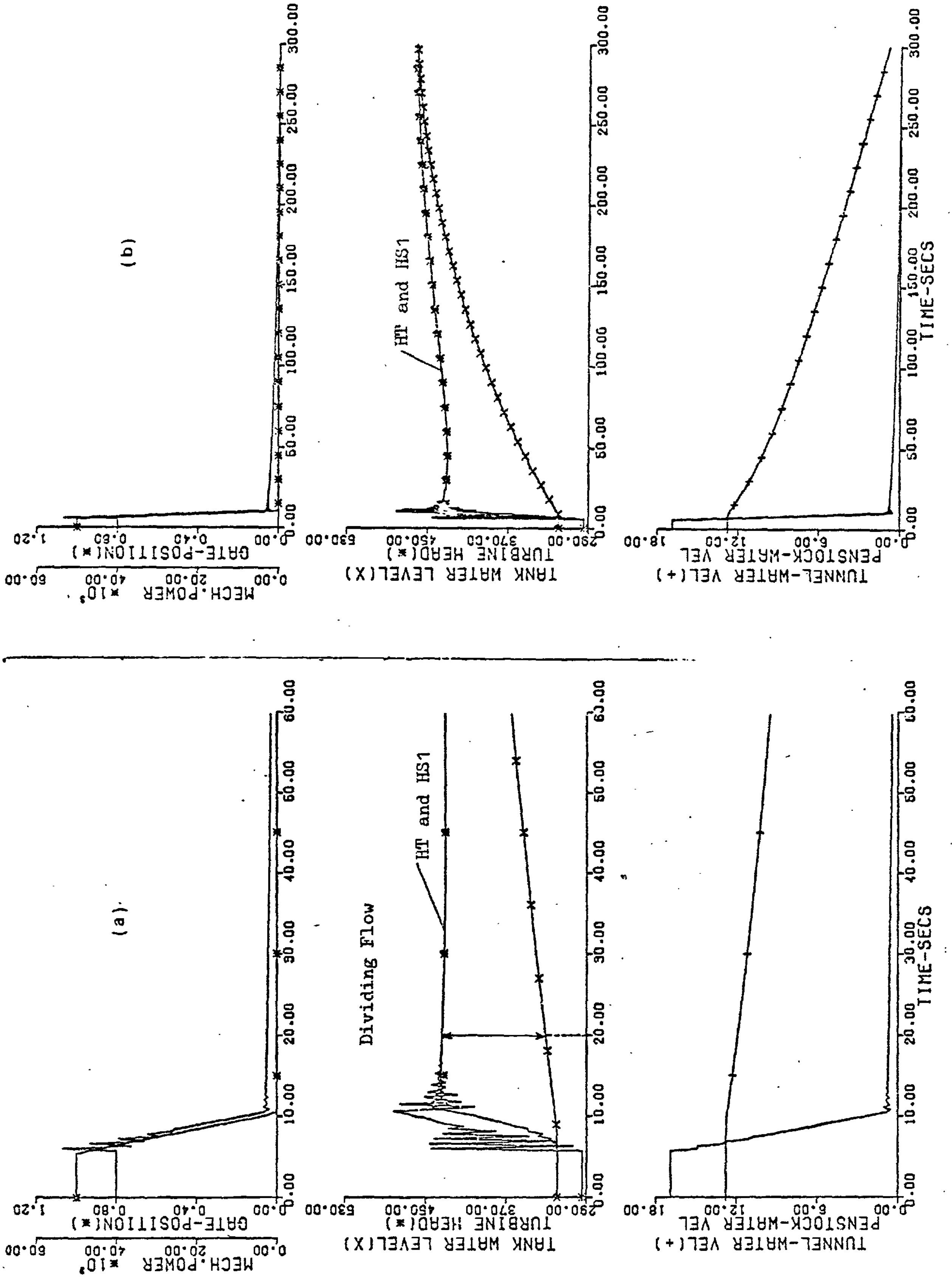

Fig. 4.10: Hydro model response to a 100% decrease in the valve opening within 5 s $[H_T = H_S - KKA.G + KKB.V_1]$.

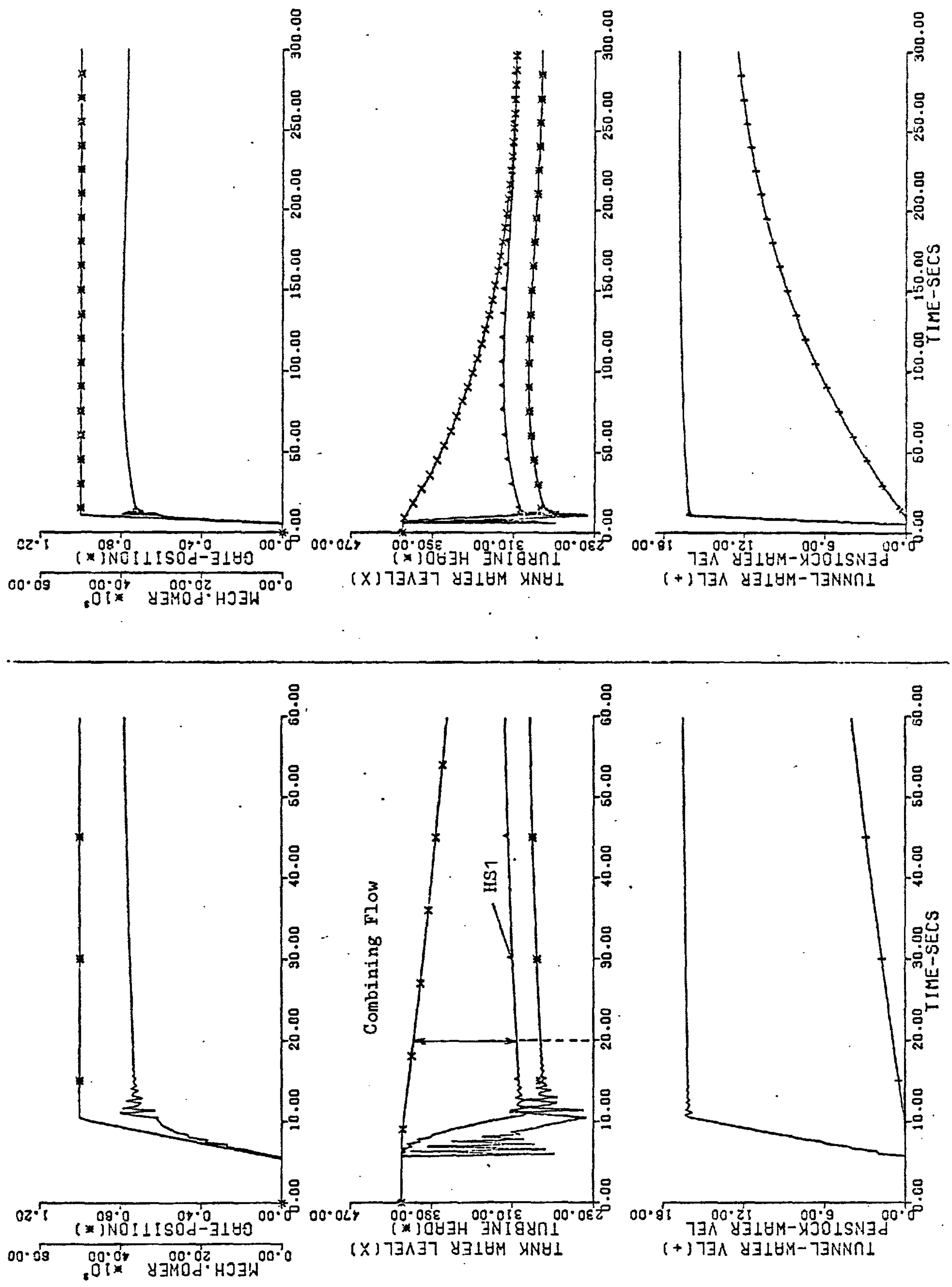

Fig. 4.11: Hydro model response to a 100% increase in the valve opening within 5 s $[H_T = H_S\text{-}KKA.G\text{+}KKB.V_1]$.

expected from equation (4.31). The time to quarter cycle is about 6 mins. In Fig. 4.11 the quarter cycle is reached in about 5.75 mins (quarter cycle is the term used for the time required by the water level in the tank to reach its first peak).

The response of the hydro model when using both equations (4.31) and (4.32)

Here the case was investigated for expression (4.31) being used to compensate for the bad properties of the equation (4.32), for values of valve position below 30%. For this purpose a criterion had to be established for the changeover from one expression to the other. After some study of the model response with different combinations of criteria, it was decided that:

(a) The criterion for the changeover from (4.32) to the expression (4.31), when the gate is closing, should be the velocity of the water in the penstock (V_1). The actual valve position was not chosen as the criterion, because as was mentioned earlier in this section, one cannot specify exactly one value of G where the instability occurs. Much depends on the way the valve position changes, i.e. if it changes fast or slowly. In other words, for a fast change in G, instability might occur long before G takes a value around 20%. On the other hand, when G changes slowly it might reach 20-22% without any signs of instability, although not below that figure.

(b) The criterion for the changeover from (4.31) to the expression (4.32) when the gate is opening should be the actual valve position signal G. This was chosen for two reasons: (i) after $G = 0.2$, the expression (4.32) can be used (when the gate is opening), and (ii) the way the velocity V_1 changes when the model starts from $G = 0.0$ and equation (4.31) is used, is not the same as the way V_1 changes when the model starts from $G = 0.2$ and the equation (4.32) is used. So it would be very difficult to establish a single value for V_1 to cover both cases.

A large number of test runs was made on the CDC 6400 to choose suitable values for V_1 and G which would give the smoothest changeover. It was found that the oscillations of the main variables were smaller for bigger values of G and smaller values of V_1. A reasonable compromise seemed to be the choice of the following values:

VV = 4.0 (ft/sec),
GG = 0.31 p.u.

In Figs. 4.12 and 4.13, the response of the model is shown when the scheme discussed above was employed. In Fig. 4.12 the gate opening is reduced from full-open to zero within 5 s. As can be seen, the power output drops almost at the same rate as the gate opening. Again, after the first 10-15 s the value of the head at the turbine entrance becomes almost equal to the head at the base of the surge tank (H_{S1}), because of the form of equation (4.31). Comparing their response to that where only equation (4.31) was used (shown in Fig. 4.10), there is a much smoother operation during the first 10 s. After that the two responses are almost identical, as one could expect, since by then the value of V_1 is below 4.0 (ft/sec) and so the model has switched to equation (4.31).

In Fig. 4.13 the response of the model is shown after a full-load acceptance has been carried out by opening the gate within 5 s. Again the response of variables like the power output, the head at the turbine entrance, the water level in the tank, etc. is reasonably smooth.

In Fig. 4.14 the water level oscillations in the surge tank are shown for a load rejection test and a load acceptance test, both carried out within 5 s. The responses shown are for the case where only equation (4.31) was used and for the case where both equations (4.31) and (4.32) were used, for comparison purposes. For the load rejection test, Fig. 4.14(a), the responses for the two cases are almost identical and it is very difficult to distinguish between them. This is obviously because V_1 drops very quickly below the value of 4.0 (ft/sec) and so the model switches to the use of the equation (4.31). Comparing this response to those presented in references 53 and 59 for the Appalachia plant (for the main tank), it gives almost identical results.

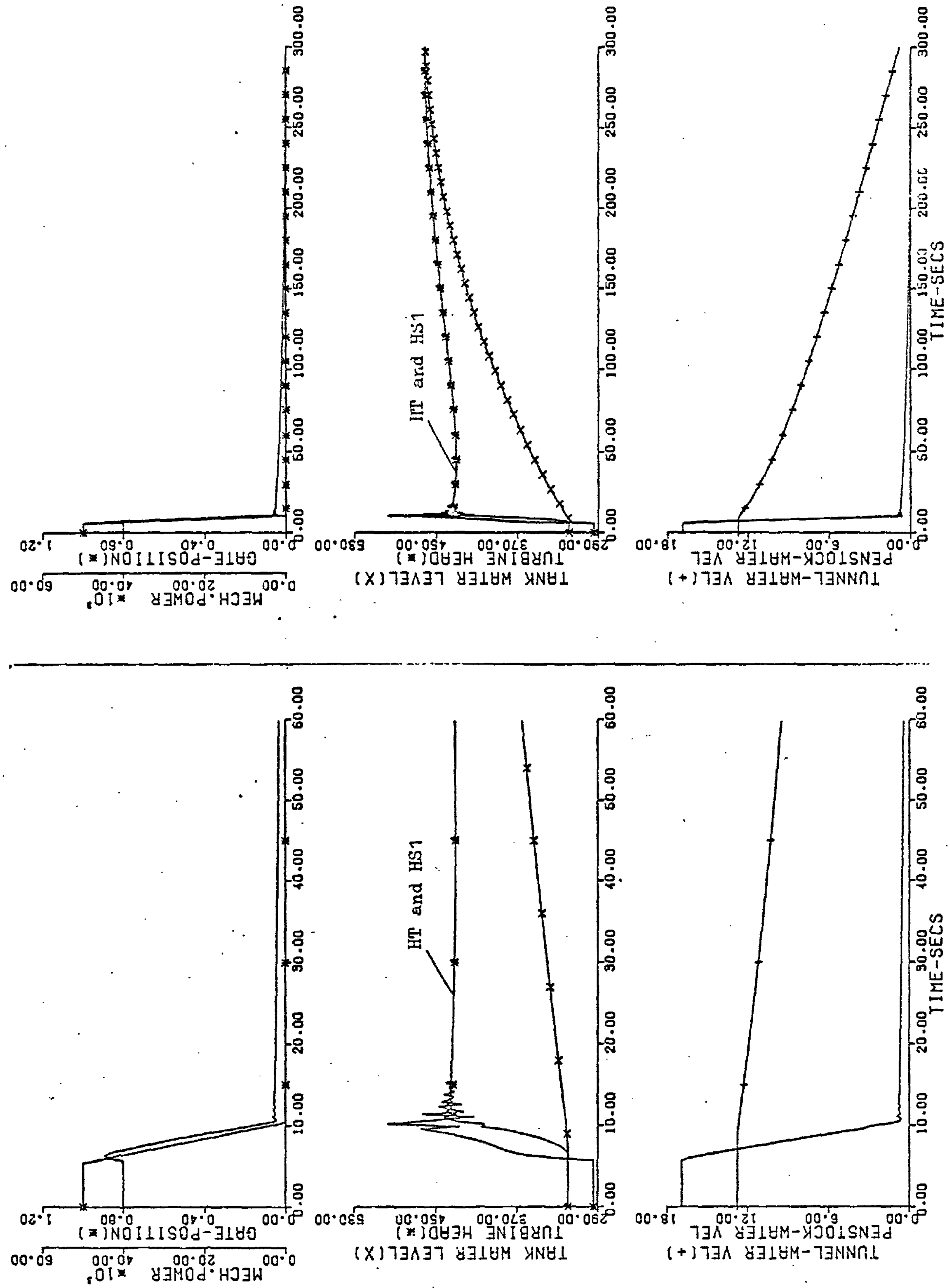

<u>Fig. 4.12:</u> Hydro model response to a 100% decrease in the valve opening within 5 s (both expressions for H_T were used).

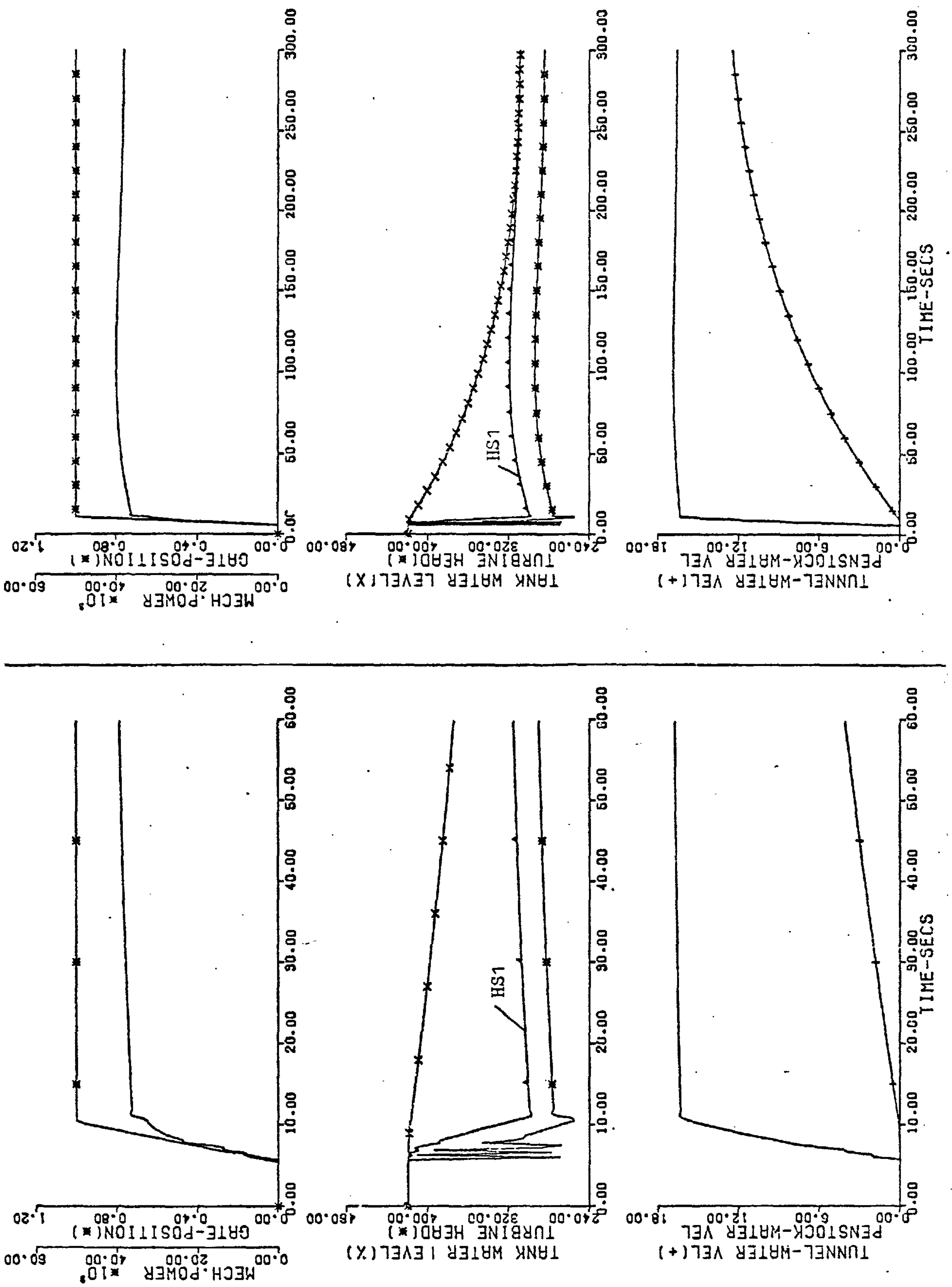

Fig. 4.13: Hydro model response to an increase in the valve opening from zero to 100% within 5 s (both expressions for H_T were used).

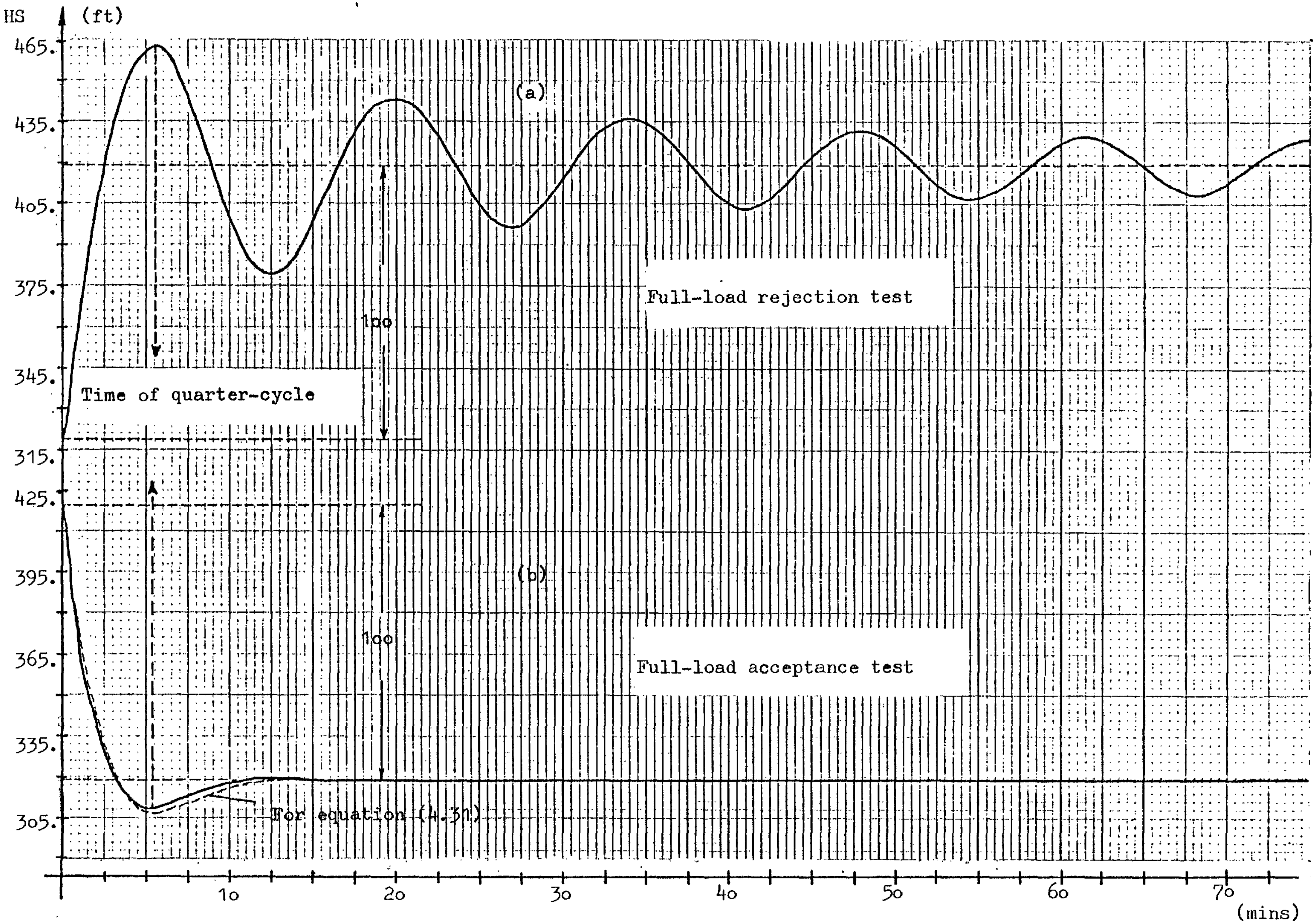

Fig. 4.14 Full-load rejection and full-load acceptance response oscillations in the surge tank. In both cases the full gate opening changed within 5 s.

For the load acceptance test, the responses for the two cases differ slightly during the first 10 minutes, but not in a fundamental way. Again this response is almost identical to the corresponding response in references 53 and 59 (for the main tank).

In conclusion it can be said that the scheme which utilizes both expressions (4.31) and (4.32) for the computation of the head at the turbine entrance, gives a reasonable representation of the hydro plant along its full operating envelope, considering that the model is only a first order approximation.

4.4.2 The Governor Response

The parameter values which were used in the governor equations are shown in Table F.1. The response of the governor to a step input is shown on Fig. 4.15.

On Fig. 4.15(a) a step in the speeder gear setting brings the gate from fully open to completely closed. As can be seen, the absence of transient droop makes the response much faster. In fact, 10 s after the introduction of the step, the gate position is only 6% away from that requested, while for the response with the transient droop the same figure is 66%. This demonstrates the necessity and the function of the transient droop because without it, the very fast change of the gate position would produce a very large change in the flow in the conduit. This would mean an oscillatory output for the hydro plant. The governor response to a step in the opposite direction is shown in Fig. 4.15(b).

The same type of response as (a) and (b) can be produced by a step change of the frequency or speed error, D_N, by an amount equal to σ (in p.u.).

From the other parameters, an increase in the value of T_R makes the response of the system slower and the same effects have similar changes in T_G and T_P.

Here it must also be noted that the governor mechanism cannot distinguish between an error signal created because of speeder gear action or because of change in the turbine speed.

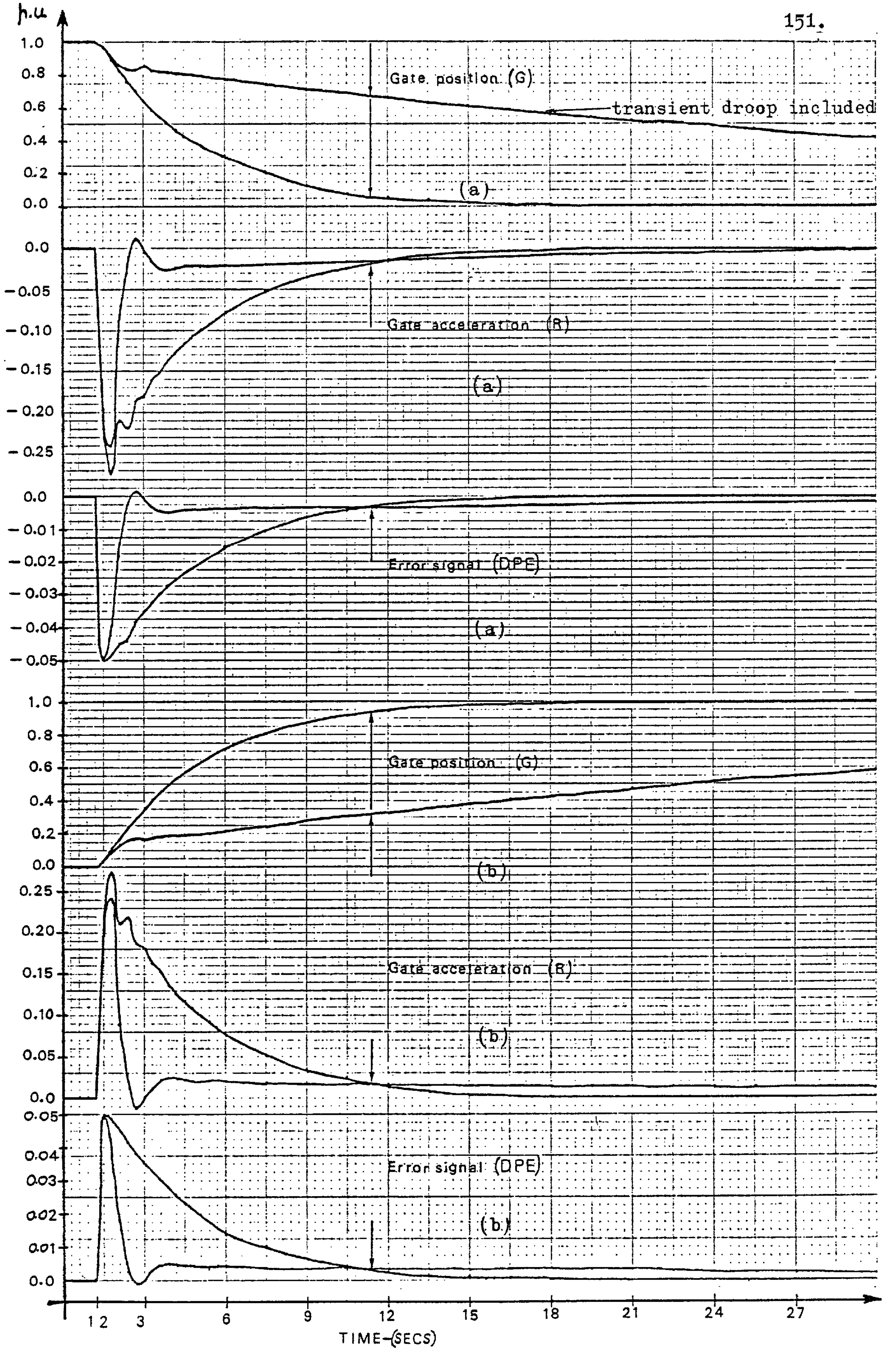

Fig. 4.15 Governor response to a 100% step change in its input (P_{ref}) in both directions: (a) to close the gate, (b) to open the gate.

4.4.3 The Hydro Model Response with the Governor included

The hydraulic-mechanical governor equations presented in Table 4.1 were added into the model and its response was taken for step changes in the governor input (P_{ref}).

In Fig. 4.16 the response is shown to a step decrease of the P_{ref}, from 100% to 50% loading. Obviously the response is much more smooth just after the introduction of the disturbance, because the change in the gate position is slower. Otherwise the response of the variables is as expected. So is the response in Fig. 4.17 where the opposite kind of disturbance is introduced. In both of them the power output follows the form of change of the gate opening. This is characterised by a quick change within the first 1-2 s and a slower change after that point. In this second part of the response, the effect of the transient droop becomes more pronounced.

The same kind of disturbances are shown on Figs. 4.18(a) and (b), this time with the model using only expression (4.31) for the computation of H_T. In this case, the disturbance causes a more violent change in the head at the turbine entrance and hence in the power output. In fact, P_{TI} reaches the full output mark for the first time after about 45 s.

In Figs. 4.19 and 4.20 the response of the model is shown when both expressions (4.31) and (4.32) are used for computing H_T. A 100% step change in the governor input is introduced in both directions. In Fig. 4.19, the moment at which the model switches from equation (4.32) to (4.31) can be seen. The effect is a few oscillations in H_T and V_1 and in turn, to the power output, but this effect is very small. From this point onwards the response carries on normally.

In Fig. 4.20, the interchange of the expressions takes place much earlier and its effect is much worse on the response of the power output. For the simular disturbances in Figs. 4.12 and 4.13 (where the governor equations are not present), the effect of the interchange on the power output response cannot be seen separately because the interchange takes place very shortly after the disturbance and any oscillations are contained within the oscillations due to the input disturbance.

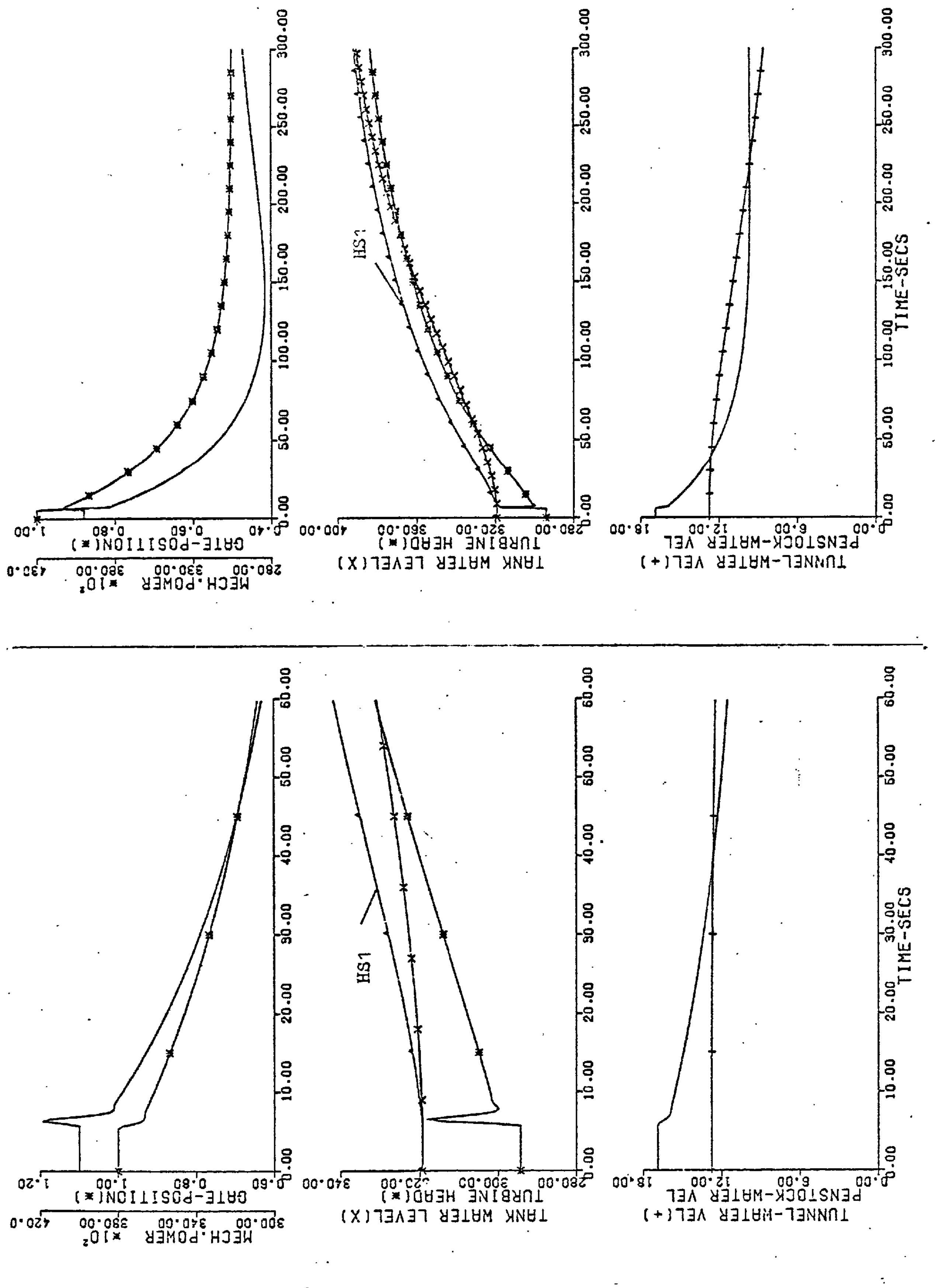

Fig. 4.16: Hydro model response (with the governor equations included) to a step decrease in P_{ref} from 100% to 50% $\left[H_T=K_1.(V_1/G)^2\right]$.

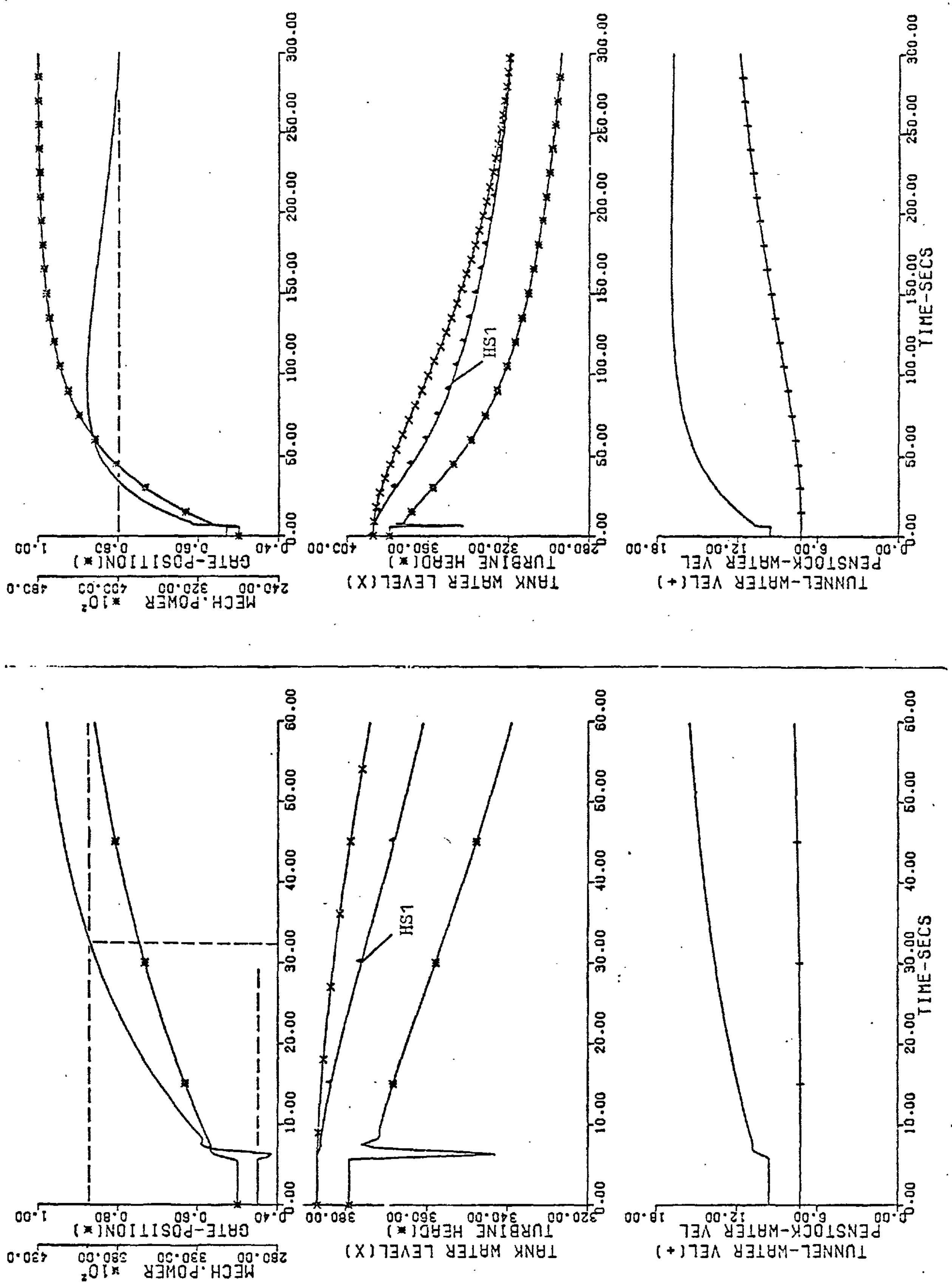

Fig. 4.17: Hydro model response (with the governor equations included) to a step increase in P_{ref} from 50% to 100% $\left[H_T=K_1.(V_1/G)^2\right]$.

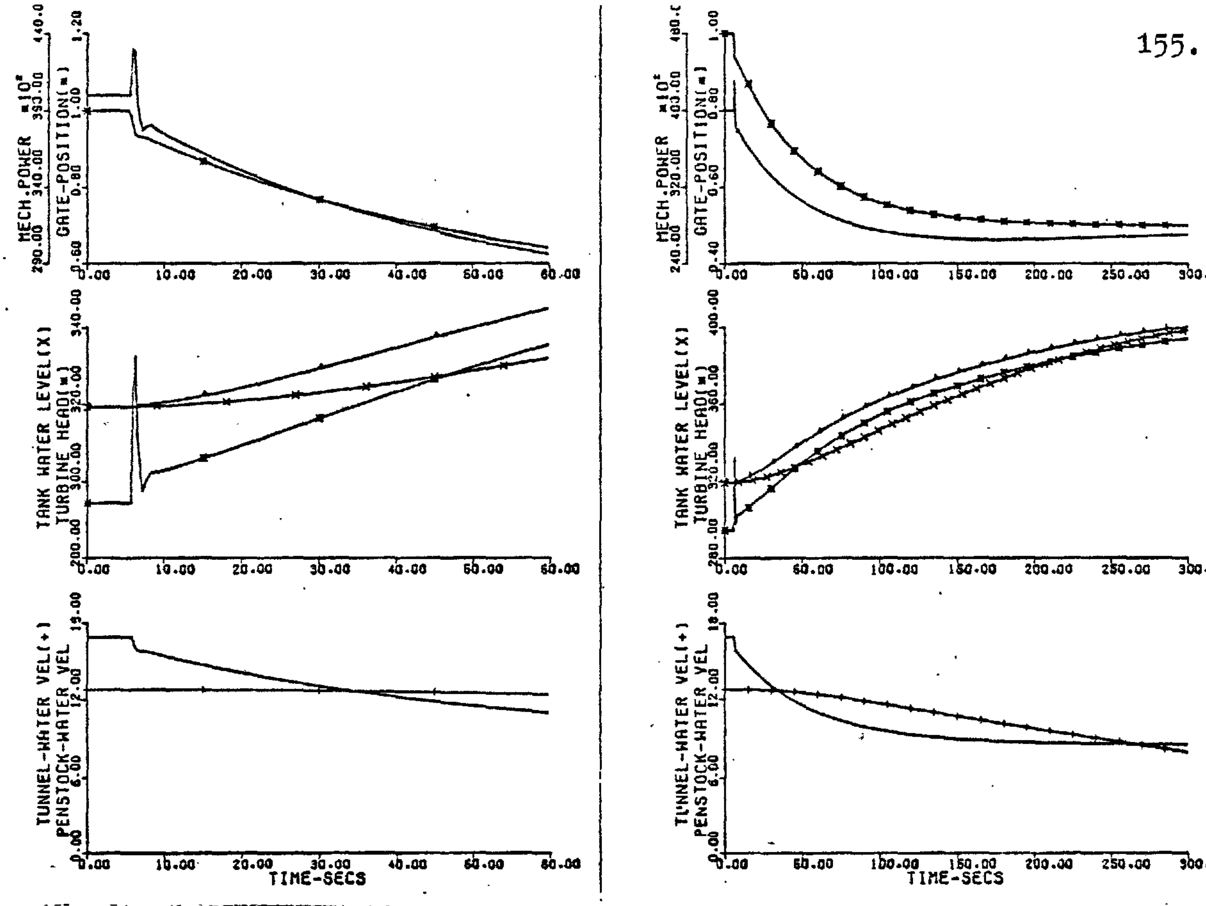

Fig. 4.18a Hydro model response (with the governor eqns. included) to a a step decrease in P_{ref}, from 100% to 50% ($H_T=H_S-KKA.G+KKB.V_1$).

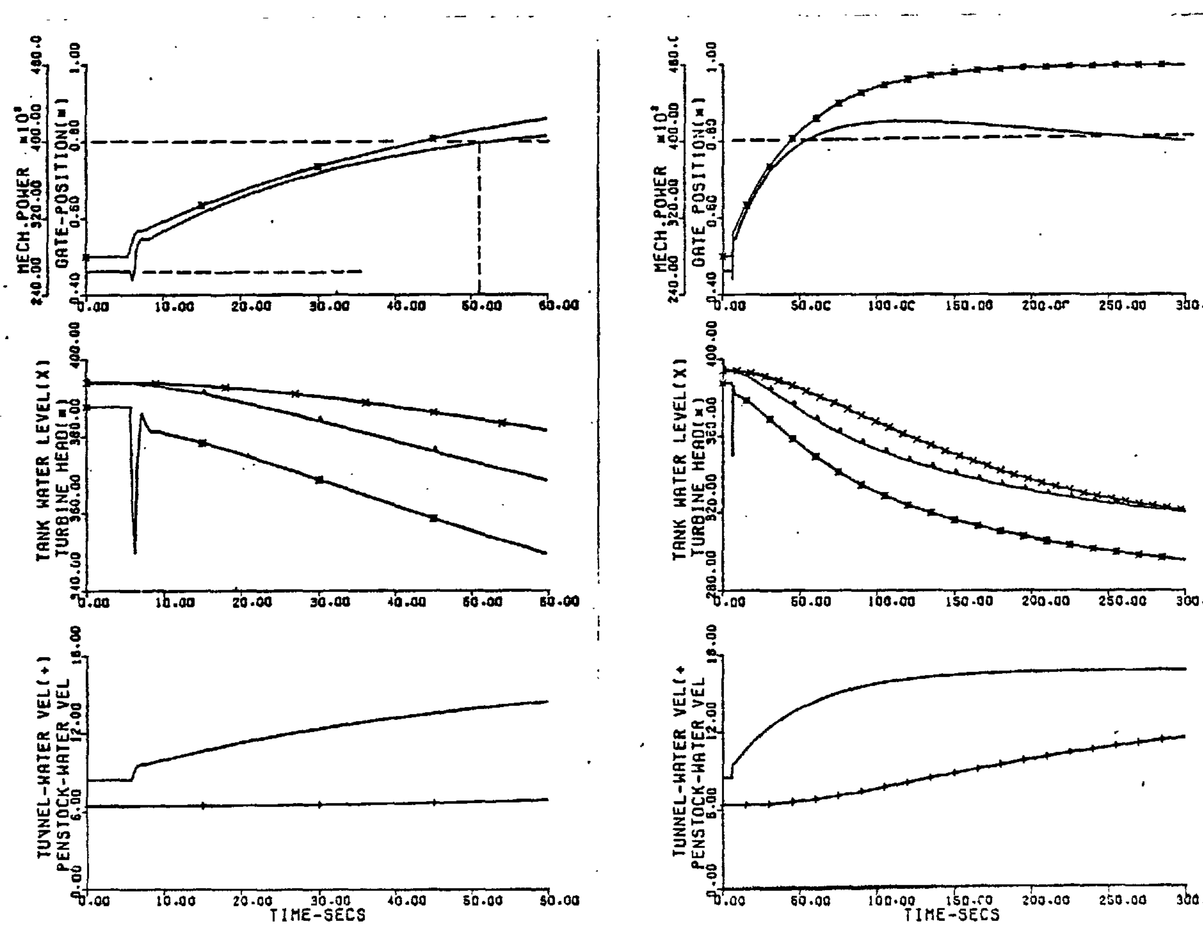

Fig. 4.18b Hydro model response (with the governor eqns. included) to a step increase in P_{ref}, from 50% to 100% ($H_T=H_S-KKA.G+KKB.V_1$).

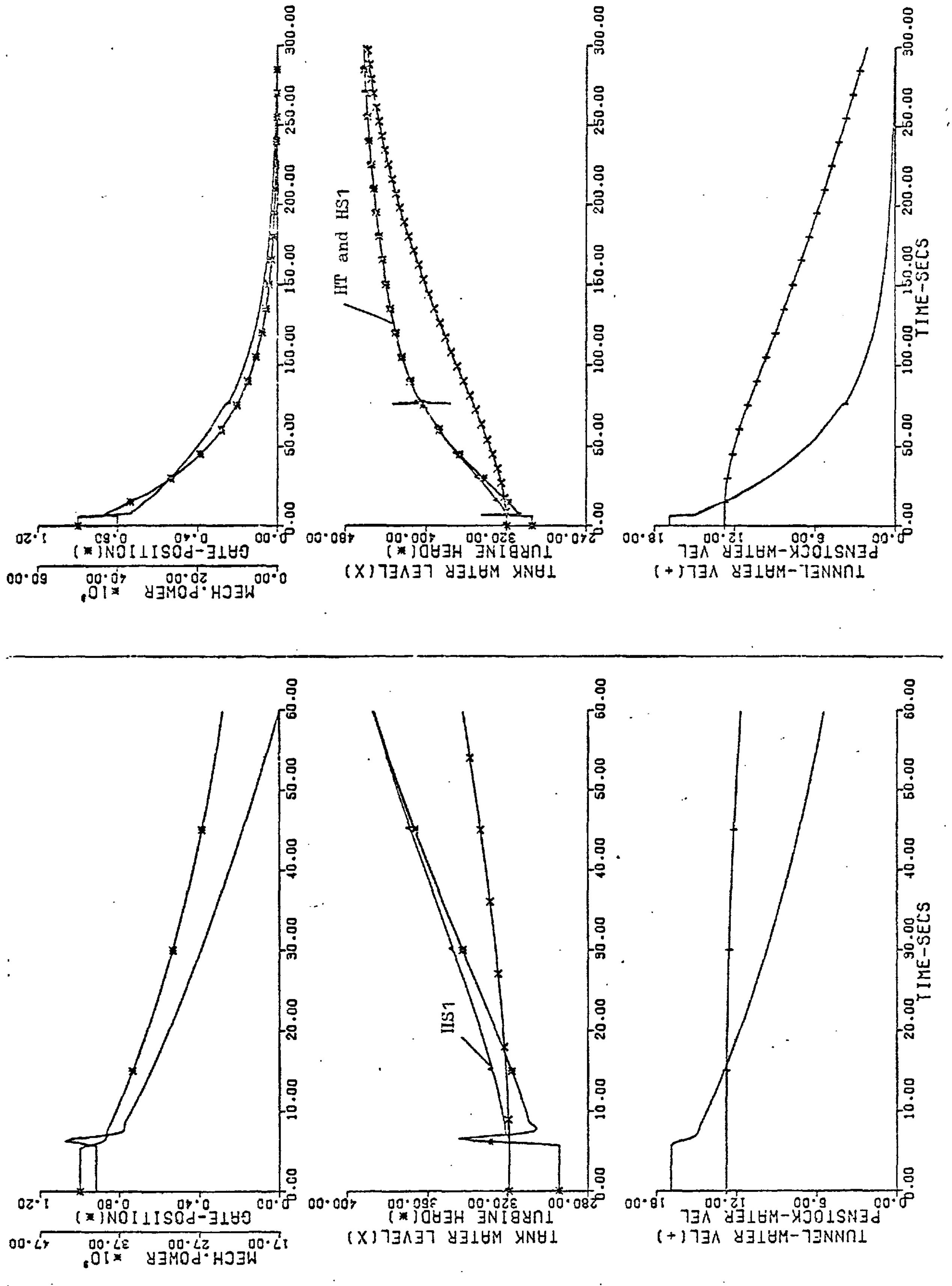

Fig. 4.19 Hydro model response (with the governor equations included) to a step decrease in P_{ref} from 100% to zero (both expressions for H_T were included).

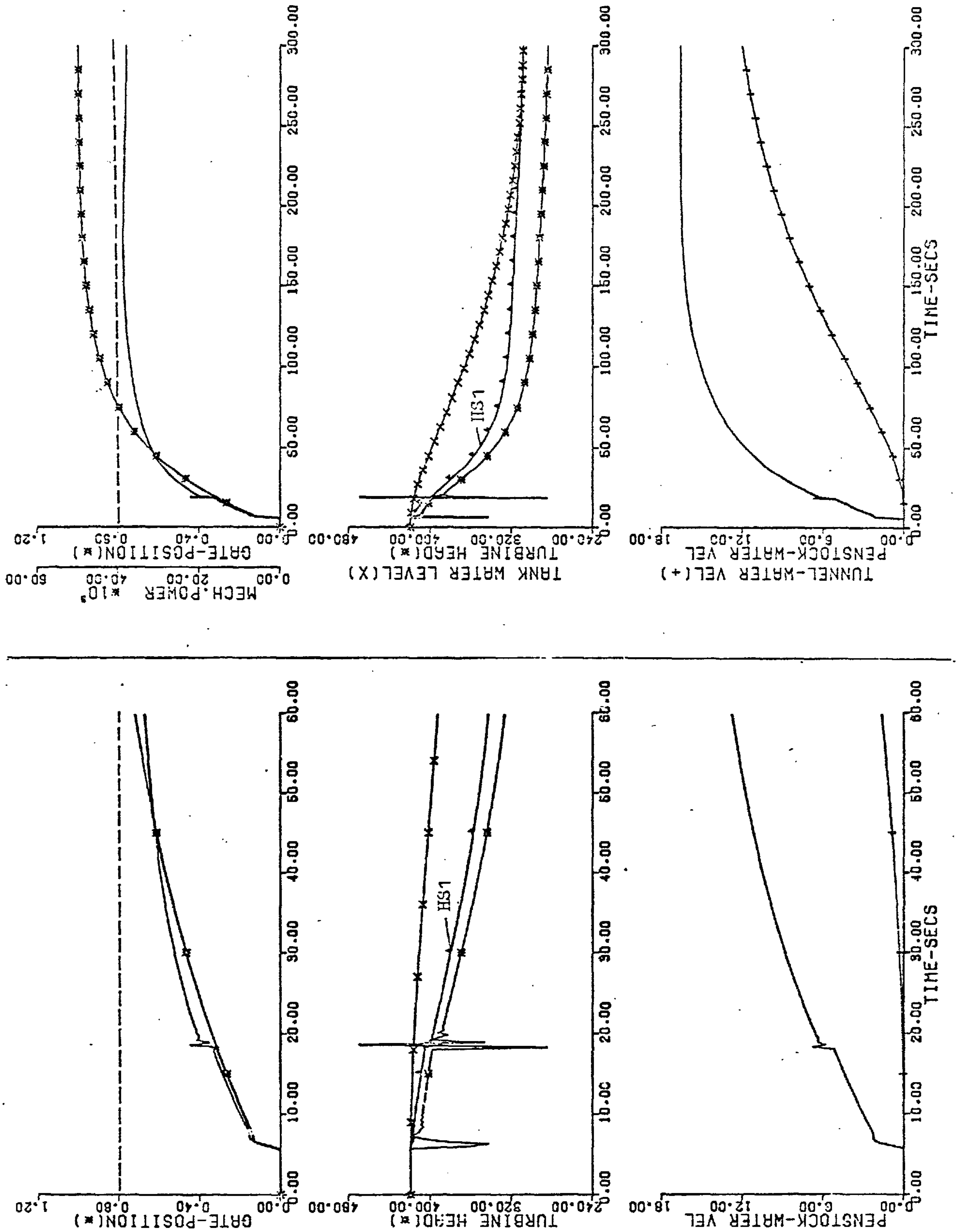

<u>Fig. 4.20</u>: Hydro model response (with the governor equations included) to a step increase in P_{ref} from zero to 100% (both expressions for H_T were used).

This abrupt change in V_1 (and consequently in the power output), takes place (with less oscillations) throughout the range of G. This is because the velocity of the water at the turbine entrance changes in the same pattern, but in the case where only the expression (4.31) is used, it remains always at a lower level than that for the case when only the expression (4.32) is used. Obviously in the end, V_1 assumes the same value in both cases.

The only way to avoid completely this sudden change, is obviously to use only the expression (4.31). Finally, it is again stressed that the form of the response depends also on the way the valve opening changes.

In Figs. 4.21 and 4.22, a 100% step input into the governor is introduced, into both directions again. Only the expression (4.31) is used for H_T. As can be seen, the responses in Figs. 4.19, 4.20 and 4.22 are more or less the same, the only difference being this "bump" in the case where both expressions are used for the computation of H_T.

In Fig. 4.23 the oscillations in the surge tank are shown for a load rejection and a load acceptance test. The difference between this and the similar response in Fig. 4.14 is that the presence of the governor results in a slower rate of change in the valve position. This in turn makes the water level in the tank reach its first peak slightly later than in Fig. 4.14 (about 30 s and 1 min. later).

4.5 LINEAR APPROXIMATION OF THE HYDRAULIC MODEL

For comparison purposes, a linear approximation of the hydraulic model as it appears in reference 62 was examined. In this work, the derivation of the model is based on the assumptions that the surge tank may be considered as an infinite reservoir and that the friction losses in the penstock are proportional to the fluid flow. Also the changes in the turbine torque and flow are expressed as a linear function of changes in fluid head, turbine valve opening and shaft speed. These assumptions are valid in the area around the system equilibrium.

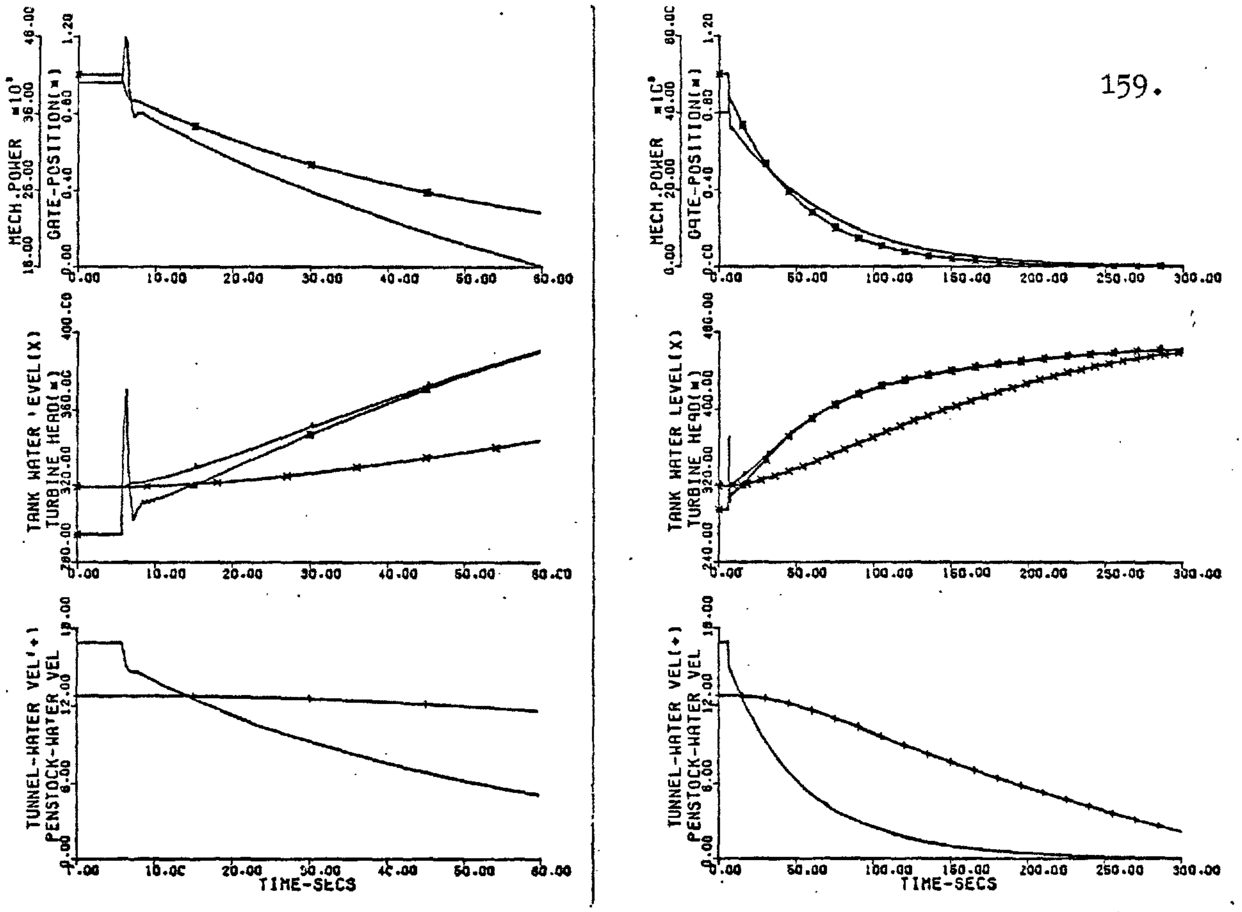

Fig. 4.21 Hydro model response (with the governor equns. included) to a step decrease in P_{ref}, from 100% to zero.

$[H_T = H_S - KKA.G + KKB.V_1]$

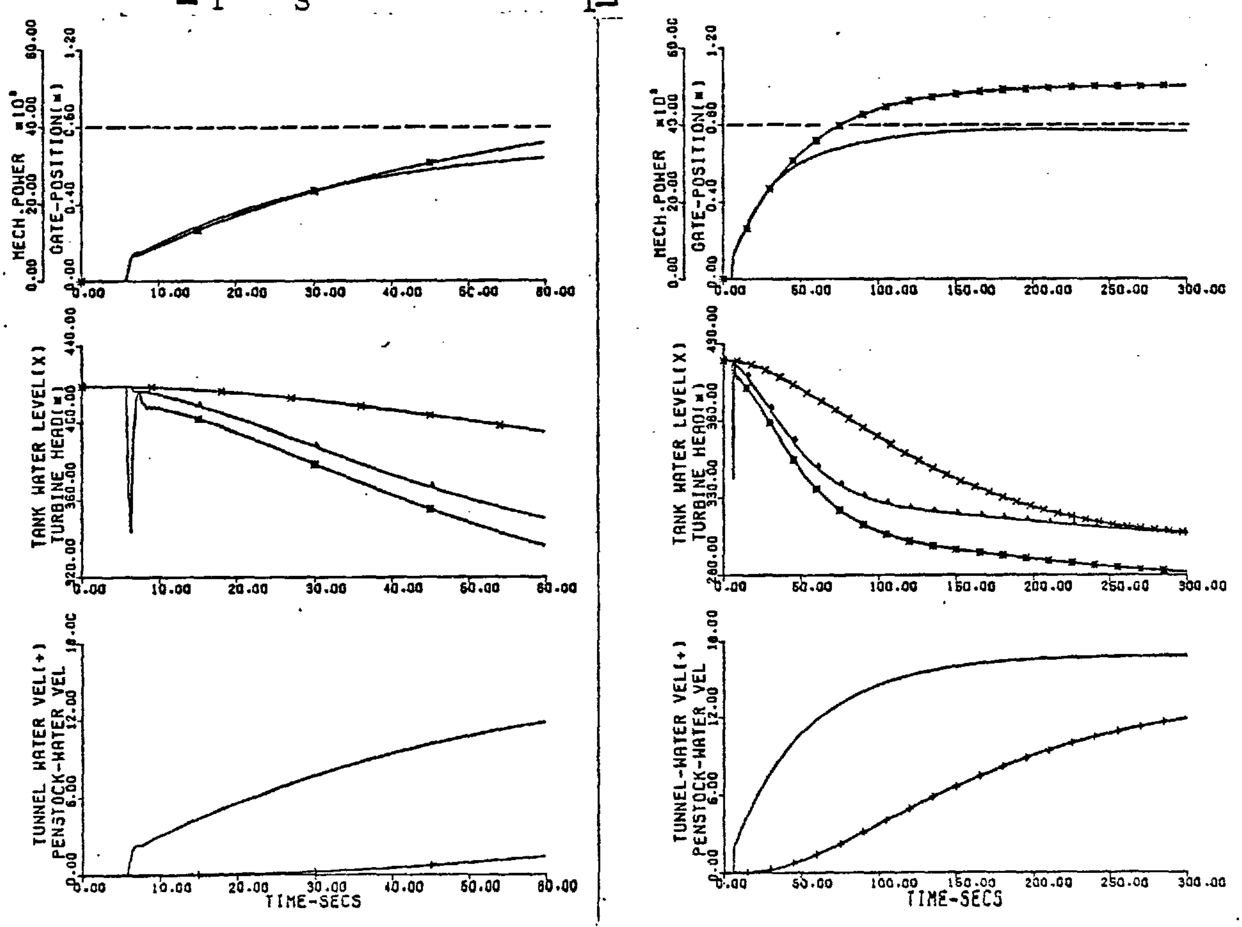

Fig. 4.22 Hydro model response (with the governor equns. included) to a step increase in P_{ref}, from zero to 100%.

$[H_T = H_S-KKA.G+KKB.V_1]$

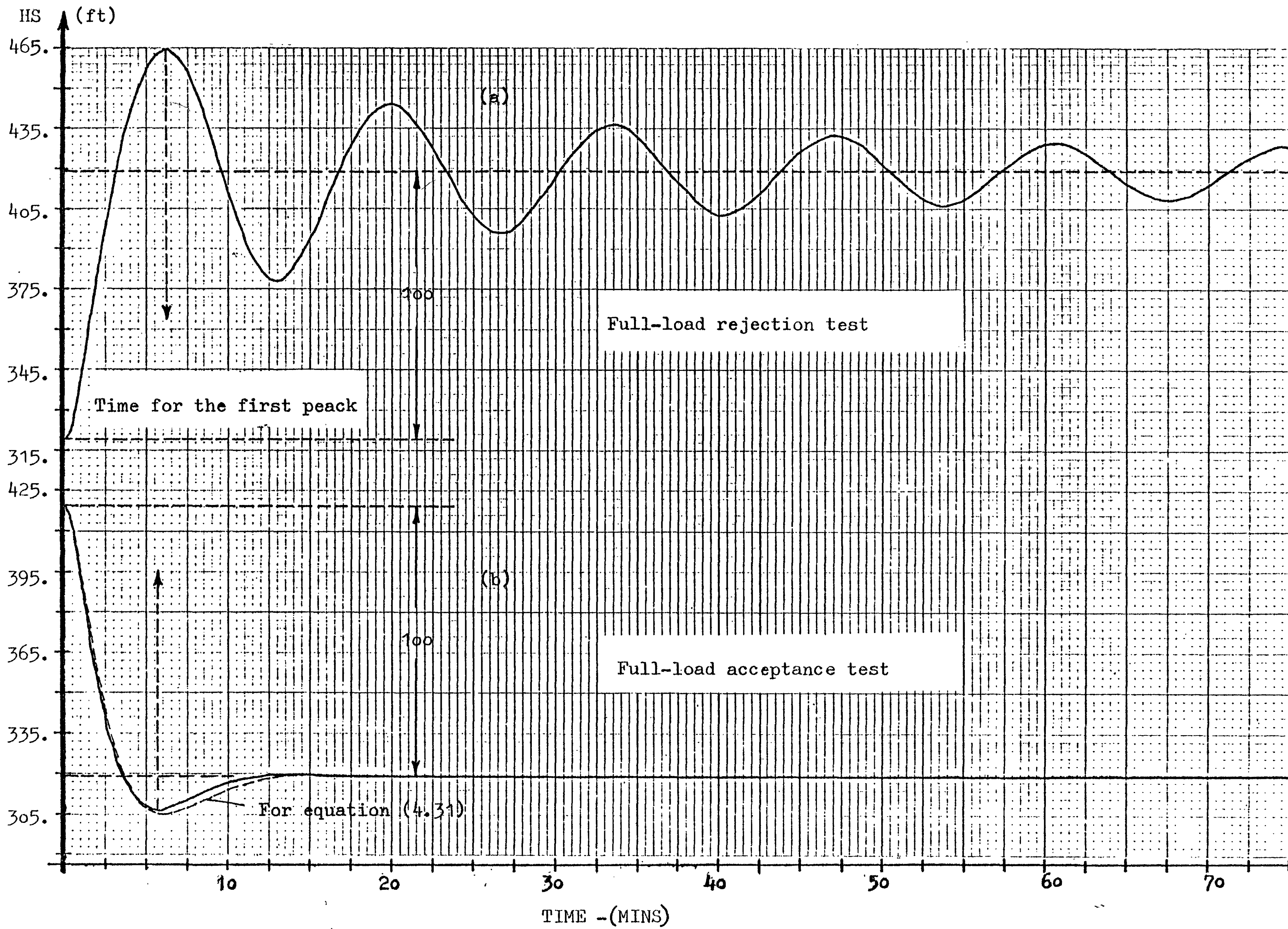

Fig. 4.23

Full-load rejection and full-load acceptance response oscillations in the surge tank. The step change was introduced to the governor input P_{ref}.

Starting again from the two basic expressions (4.1) and (4.2) they end up with the dynamic relationship between the small p.u. changes in the valve opening and the turbine torque. This relationship is of the form:

$$\frac{P_M(s)}{G(s)} = \frac{a_{23} + (a_{11}.a_{23} - a_{21}.a_{13}).Z.\tan h(W)}{1 + Z.a_{11}.\tan h(W)} \qquad (4.43)$$

where:

$$Z = (\alpha_1/g.A_1).(Q1_\phi/H_{T\phi})$$

$$W = T_e.(\frac{\Delta H_T.g}{V_1.L_1} + s) = (F + T_e.s)$$

$$D = Z.(a_{11}.a_{23} - a_{21}.a_{23})$$

$$E = Z.a_{11}$$

$$a_{11} = (\partial Q/\partial H_T)$$

$$a_{21} = (\partial M/\partial H_T)$$

$$a_{23} = (\partial M/\partial G)$$

$$a_{13} = (\partial Q/\partial G) \qquad M = \text{torque}$$

The equation (4.43) is called the "exact" expression of the dynamic relation between P_M and G. The partial derivatives are not constant in reality and so this expression is a non-linear one. But for simplicity a_{ij} is assumed constant for the area around the system equilibrium; therefore (4.43) becomes linear.

From this "exact" expression, by expanding the tan $h(T_e.s)$ term, one can take the first, second and third order approximate expressions; they are:

<u>First order approximation:</u>

$$\frac{P_M(s)}{G(s)} = \frac{a_{23} + (a_{11}.a_{23} - a_{13}.a_{21}).Z.W}{1 + Z.a_{11}.W} \qquad (4.44)$$

<u>Second order approximation:</u>

$$\frac{P_M(s)}{G(s)} = \frac{a_{23}.(1 + W^2) + Z.(a_{11}.a_{23} - a_{13}.a_{21})}{(1 + W^2) + Z.a_{11}.W} \qquad (4.45)$$

Third order approximation:

$$\frac{P_M(s)}{G(s)} = \frac{a_{23}.(1 + W^2) + Z.(a_{11}.a_{23} - a_{13}.a_{21}).(W + (W^3/6))}{(1 + W^2) + Z.a_{11}.(W + \frac{W^3}{6})} \quad (4.46)$$

Setting the derivatives equal to zero, the steady-state characteristic of these relations can be taken:

"Exact" expression:

$$P_{M_{ss}} = G_{ss}.\left[\frac{a_{23}+\tan h(F).D}{1 + \tan h(F).E}\right] \quad (4.47)$$

$$= k_E.G_{ss}$$

First order approximation:

$$P_{M_{ss}} = G_{ss}.\left[\frac{a_{23} + F.D}{1 + F.E}\right] \quad (4.48)$$

$$= k_{1A}.G_{ss}$$

Second order approximation:

$$P_{M_{ss}} = G_{ss}.\left[\frac{a_{23}.(1+F^2)+FD}{1 + F^2 + F.E}\right] \quad (4.49)$$

$$= k_{2A}.G_{ss}$$

Third order approximation:

$$P_{M_{ss}} = G_{ss}.\left[\frac{a_{23}.(1+F^2)+D.(F+(F^3/6))}{1+F^2+E.(F+(F^3/6))}\right] \quad (4.50)$$

$$= k_{3A}.G_{ss}$$

These relations show that the power output or torque/valve opening characteristic is a straight line with about 50^0 slope. This is clearly not the case for the real plant, where the characteristic is of the form shown in Fig. 4.4(b).

The transfer functions (4.43), (4.44), (4.45) and (4.46) were converted to their discrete-time form, with the use of the Tustin discrete approximate integrator. The corresponding relations are:

"Exact expression:

$$P_M(K) = (1/A_1).\left[-A_\emptyset.P_M(K-T_1)+B_1.G(K)+B_\emptyset.G(K-T_1)\right] \qquad (4.51)$$

where:

$$\begin{aligned} A_\emptyset &= (1-E).(1 - \tan h(F)) \\ A_1 &= (1+E).(1 + \tan h(F)) \\ B_\emptyset &= (a_{23} - D).(1 - \tan h(F)) \\ B_1 &= (a_{23} + D).(1 + \tan h(F)) \\ T_1 &= (2.T_e)/T \end{aligned}$$

For $T_e = 0.3$, the sampling interval T was chosen as $T = 0.3$ in order to make $T_1 = 2$.

First order approximate expression:

$$P_M(K) = (1/A_1).\left[-A_\emptyset.P_M(K-1) + B_1.G(K) + B_\emptyset.G(K-1)\right] \qquad (4.52)$$

where:

$$\begin{aligned} A_\emptyset &= (1 + E.F).T - 2(E.T_e) \\ A_1 &= (1 + E.F).T + 2(E.T_e) \\ B_\emptyset &= (a_{23} + D.F).T - 2(D.T_e) \\ B_1 &= (a_{23} + D.F).T + 2(D.T_e) \end{aligned}$$

Second order approximate expression:

$$P_M(K) = (1/A_2).\left[-A_1.P_M(K-1)-A_\emptyset.P_M(K-2)+B_2.G(K)+B_1.G(K-1)+B_\emptyset.G(K-2)\right] \qquad (4.53)$$

where:

$$\begin{aligned} A_\emptyset &= 4a_2-2a_1.T+a_o.T^2, & B_\emptyset &= 4b_2-2b_1.T+b_o.T^2 \\ A_1 &= -8a_2+2.a_o.T^2, & B_1 &= -8b_2+2b_o.T^2 \\ A_2 &= 4a_2+2a_1.T+a_o.T^2, & B_2 &= 4b_2+2b_1.T+b_o.T^2. \end{aligned}$$

and:

$$\begin{aligned} a_2 &= T_e^2, & b_2 &= a_{23}.T_e^2 \\ a_1 &= T_e.(2.F+E), & b_1 &= T_e.(2.a_{23}.F+D) \\ a_o &= 1+F^2+E.F, & b_o &= a_{23}.(1+F^2)+D.F \end{aligned}$$

Third order approximate expression:

$$P_M(K) = (1/A_3).\,[-A_2.P_M(K-1)-A_1.P_M(K-2)-A_\emptyset.P_M(K-3)+$$
$$+B_3.G(K)+B_2.G.(K-1)+B_1(K-2)+B_\emptyset.G(K-3)] \qquad (4.54)$$

where:
$$A_\emptyset = -8a_3+4a_2T-2a_1T^2+a_oT^3, \quad B_\emptyset = -8b_3+4b_2T-2b_1T^2+b_oT^3$$
$$A_1 = 24a_3-4a_2T-2a_1T^2+3a_oT^3, \quad B_1 = 24b_3-4b_2T-2b_1T^2+3b_oT^3$$
$$A_2 = -24a_3-4a_2T+2a_1T^2+3a_oT^3, B_2 = -24b_3-4b_2T+2b_1T^2+3b_oT^3$$
$$A_3 = 8a_3+4a_2T+2a_1T^2+a_oT^3, \quad B_3 = 8b_3+4b_2T+2b_1T^2+b_oT^3$$

and:
$$a_3 = (E.T_e^{\,3}/6), \qquad b_3 = (D.T_e^{\,3}/6)$$
$$a_2 = (T_e^{\,2} + \frac{E.F.T_e^{\,2}}{2}), \qquad b_2 = (a_{23}.T_e^{\,2}+(D.F.T_e^{\,2}/2))$$
$$a_1 = (2.F.T_e+E.T_e+(E.F^2.T_e/2)), \quad b_1 = (2.a_{23}.F.T_e+D.T_e+(D.F^2.T_e/2))$$
$$a_o = (1+F^2+E.F+(E.F^3/6)), \quad b_o = (a_{23}+F^2.a_{23}+D.F+(D.F^3/6))$$

The responses of these transfer functions were taken with and without the governor equations. They are compared with the corresponding of the non-linear model (Table 4.1).

In Fig. 4.24 the response of the turbine output is shown when a full gate closing takes place within 5 s. The response of the linear transfer functions differs from the non-linear representations, mainly in the way they behave just after the introduction of the disturbance. In fact, the temporary increase in power is much bigger in the case of the non-linear model. After that, the response of the non-linear model drops faster towards the new steady-state, but after 10-15 iterations (i.e. 3-4.5 s) the responses of the linear models catch up.

The same pattern can be observed in Fig. 4.25, where the gate is fully opened within 5 s. The response of the linear versions are more or less similar but with opposite sense to the responses in Fig. 4.24.

In Figs. 4.26 and 4.27, the governor equations are included and the disturbance is a step change in the governor input (P_{ref}).

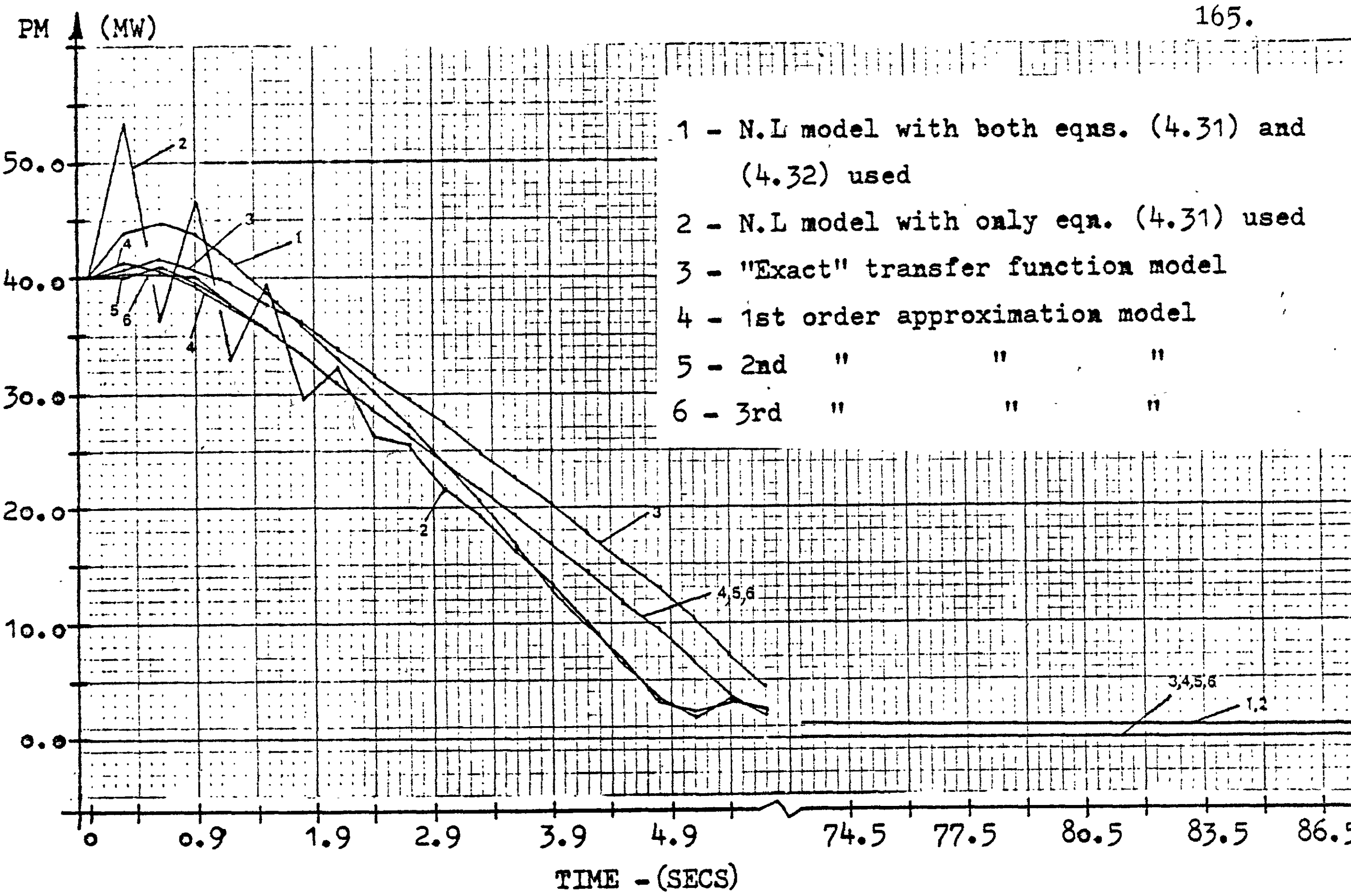

Fig. 4.24 Turbine power response to a decrease in the valve opening from 100% to zero, within 5 s (no governor eqns. present).

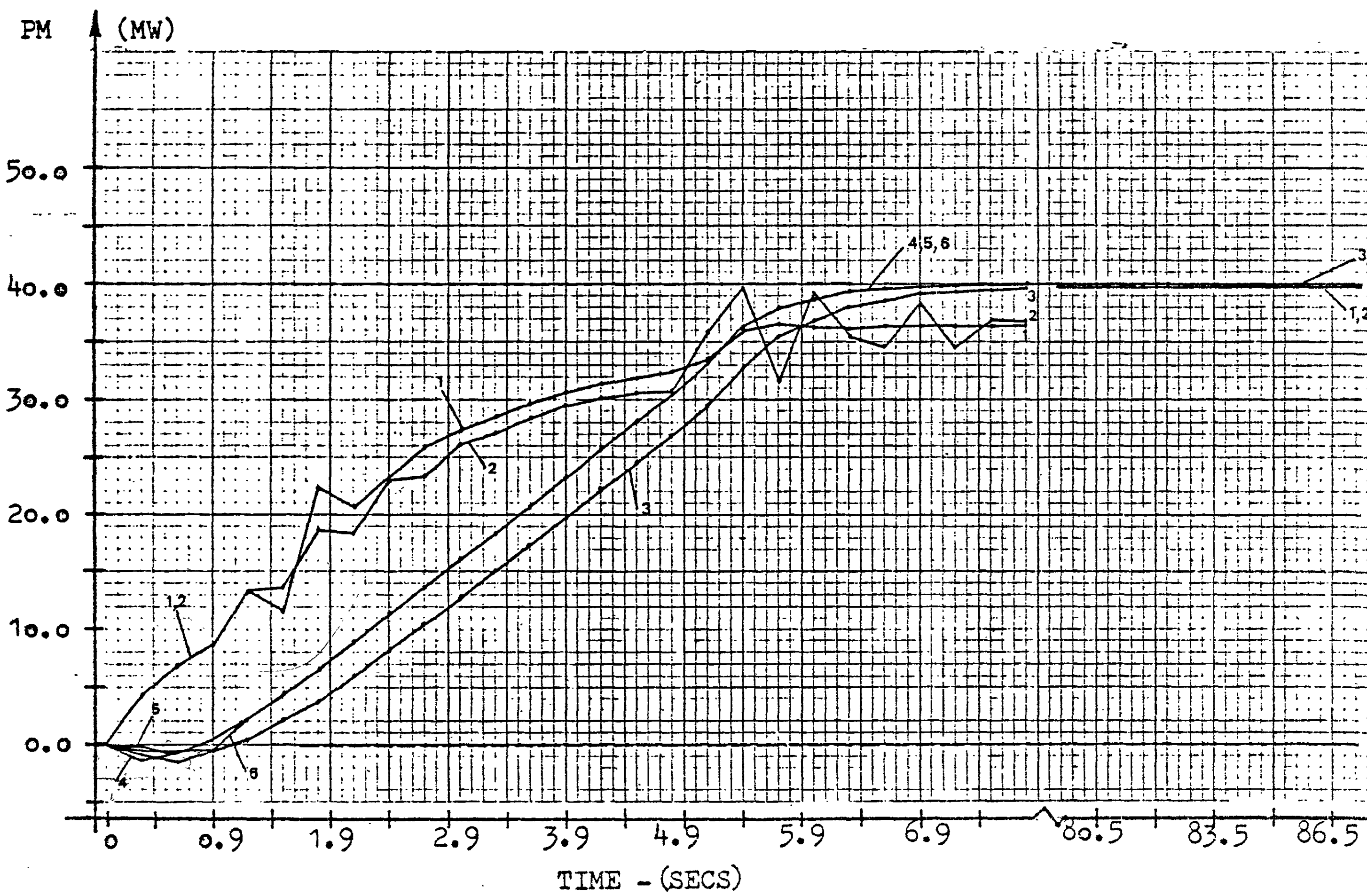

Fig. 4.25 Turbine power response to an increase in the valve opening from zero to 100%, within 5 s (no governor eqns. present).

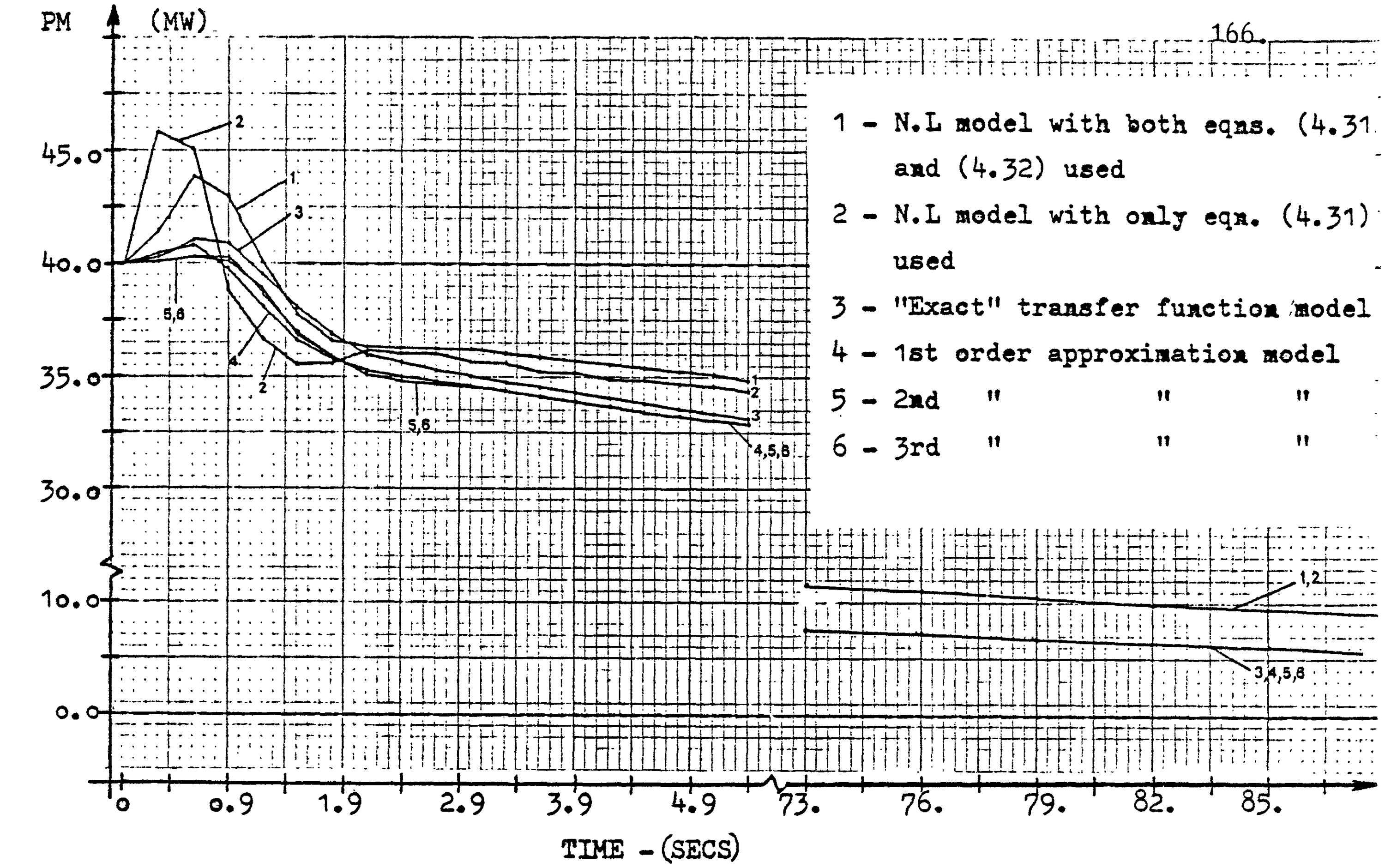

Fig. 4.26 Turbine power response to a step decrease in the governor input, from 100% to zero.

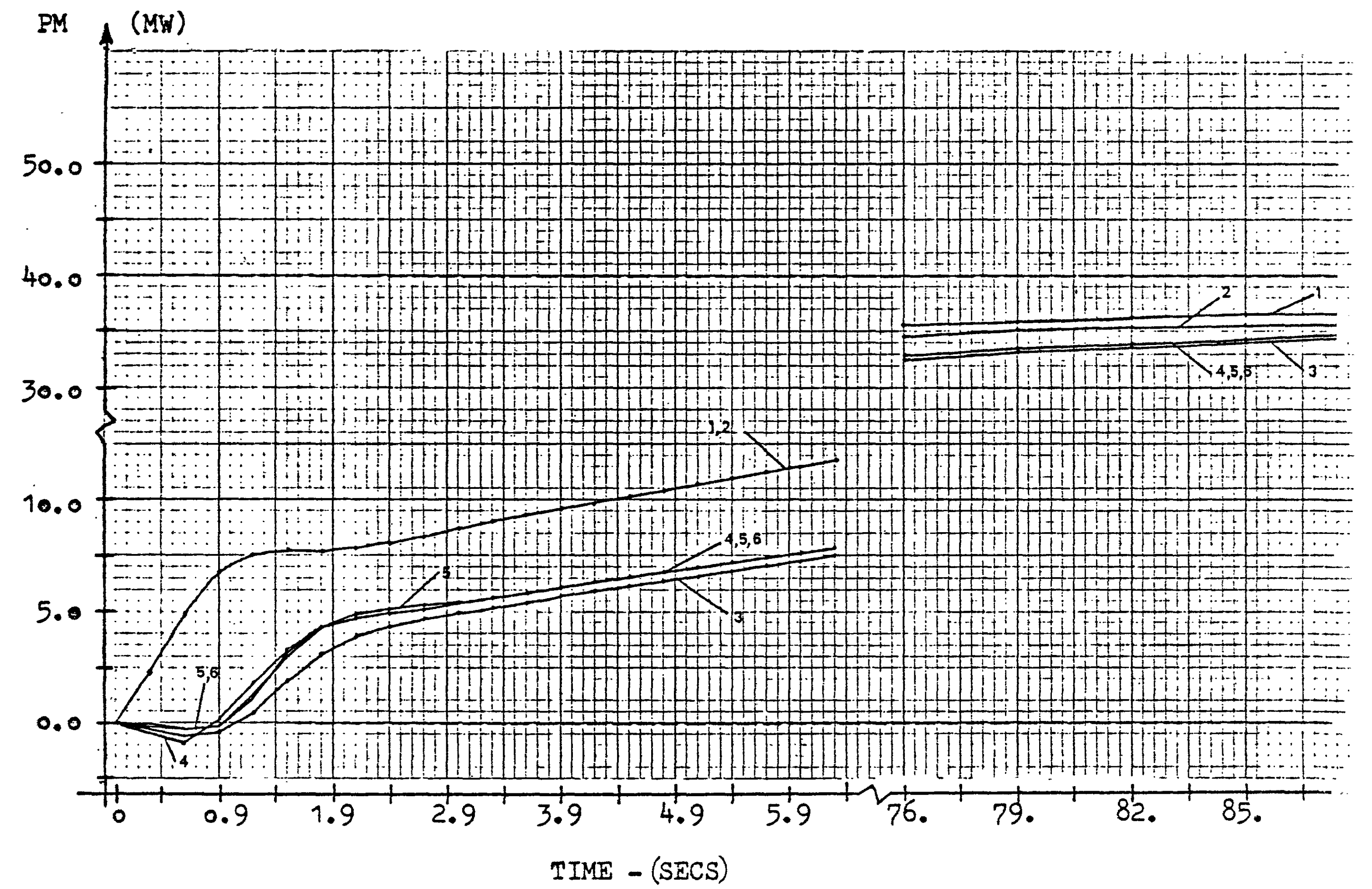

Fig. 4.27 Turbine power response to a step increase in the governor input, from zero to 100%.

Obviously the response here is slower, but the difference between linear and non-linear model responses is again the overshoot in the power response.

In conclusion it can be said that the presence in the model of some non-linearities makes the response more realistic. The choice between the two depends as always on what is the purpose of the simulation. It was felt that a non-linear representation is needed if the hydro plant model was to be used in the simulator with other plant.

4.6 REAL-TIME OPERATION OF THE HYDRO PLANT MODEL

The discrete-time equations of the hydro model shown in Table 4.1 were converted to a form suitable for running in real-time on the PDP-15. These two versions of the model equations are shown in Table 4.2. The precalculable constants stored in the common block BLSIM as well as others stored as data in the simulation program are shown in Appendix F.3.

Because of the modular construction of the generating units, the prime mover dynamics can be disconnected from the unit and the mechanical power to the main integrator (Fig. 2.2a) can be supplied by another source, in this case the output of the (digitally simulated) hydro model.

The power system configuration shown in Fig. 2.23 was used again, with the tie-line not connected (circuit breaker no. 14 open). The generating unit no. 1 was driven by a conventional plant and unit no. 2 by a hydro plant. The steady-state condition of the system was disturbed by a step change in Load 1, as can be seen in Fig. 4.28. The system frequency drops abruptly. The two governors (simulated in analog form for unit no. 1 and digitally for unit no. 2) react to the frequency change and open the valve and the gate of the two plants respectively. The response of the hydro unit is the purpose of this test and, as can be seen, the gate response is rapid in the first few seconds. Then the transient droop of the governor comes into effect and slows down this change. The water level in the surge tank drops smoothly and the pressure head at the turbine

TABLE 4.2: HYDRO PLANT MODEL EQUATIONS IN THEIR REAL-TIME FORM

Discrete-time representation

$$W_1 = V_1(K-1).V_1(K-1)$$

$$H_T(K)=H_S(K-1)-KKA.G(K-1)+KKB.V_1(K-1)$$

or

$$H_T(K) = (K_1.W_1)/(G(K-1).G(K-1))$$

$$V_1(K)=V_1(K-1)+((T.g)/L_2).\left[H_{S1}(K-1)- - H_T(K)-C_1.W_1\right]$$

$$W_2 = V_2(K-1).V_2(K-1)$$

$$V_2(K)=V_2(K-1)+((T.g)/L_2).(H_R-H_{S1}(K-1) - C_2.W_2)$$

$$QQQ = (T.A_2/A_S).V_2(K-1)-(2.A_1.T/A_S).V_1(K-1)-(2.A_1.g.L_1/\alpha_1.\alpha_1.A_S).(H_T(K)-H_T(K-1))$$

$$H_S(K) = H_S(K-1) + QQQ$$

$$H_{S1}(K) = H_S(K)\pm(\frac{A_S}{T})^2.KK.(QQQ.QQQ)$$

where: + is used when $QQQ > 0$

- is used when $QQQ < 0$

$$PTI(K) = K_P.V_1(K).H_T(K)$$

$$D_{PE}(K) = D_N - CC + P_{ref}$$

$$R(K)=\left[\frac{(T/T_G)}{T+2.T_P}\right].(D_{PE}(K)+D_{PE}(K-1))- -\left[\frac{T-2.T_P}{T+2.T_P}\right].R(K-1)$$

$$G(K)=G(K-1)+(T/2).(R(K)+R(K-1))$$

$$CC(K)=C8.G(K)+C9.G(K-1)-C10.C_C(K-1)$$

Real-time representation

$$W_1 = V_1(I)*V_1(I)$$

$$H_T(I)=H_S(I)-KKA*G(I)+KKB*V_1(I)$$

or

$$H_T(I) = (C(I,12)*VV_1)/(G(I)*G(I))$$

$$QQQ = CE2*V_2(I)-CE3*V_1(I)-CE1*(H_T(I)- - H_{T1}(I))$$

$$H_{T1}(I) = H_T(I)$$

$$V_1(I)=V_1(I)+CTI*(H_{S1}(I)-H_T(I)-C(I,1)*W_1)$$

$$W_2 = V_2(I)*V_2(I)$$

$$H_S(I) = H_S(I) + QQQ$$

$$H_{S1}(I) = H_S(I)\pm C(I,11)*(QQQ.QQQ)$$

where: + is used when $QQQ > 0$

- is used when $QQQ < 0$

$$PTI(I) = C(I,7)*V_1(I)*H_T(I)$$

$$D_{PE}(I) = D_N - CC(I) + P_{ref}$$

$$R(I) = C(I,3)*(D_{PE}(I)+D_{PE1}(I)- -C(I,4)*R(I))$$

$$D_{PE1}(I) = D_{PE}(I)$$

$$G(I) = G(I)+CT3*(R(I)+R_1(I))$$

$$R_1(I) = R(I)$$

$$CC(I)=C(I,3)*G(I)+C(I,9)*G_1(I)- -C(I,10)*CC(I)$$

$$G_1(I) = G(I)$$

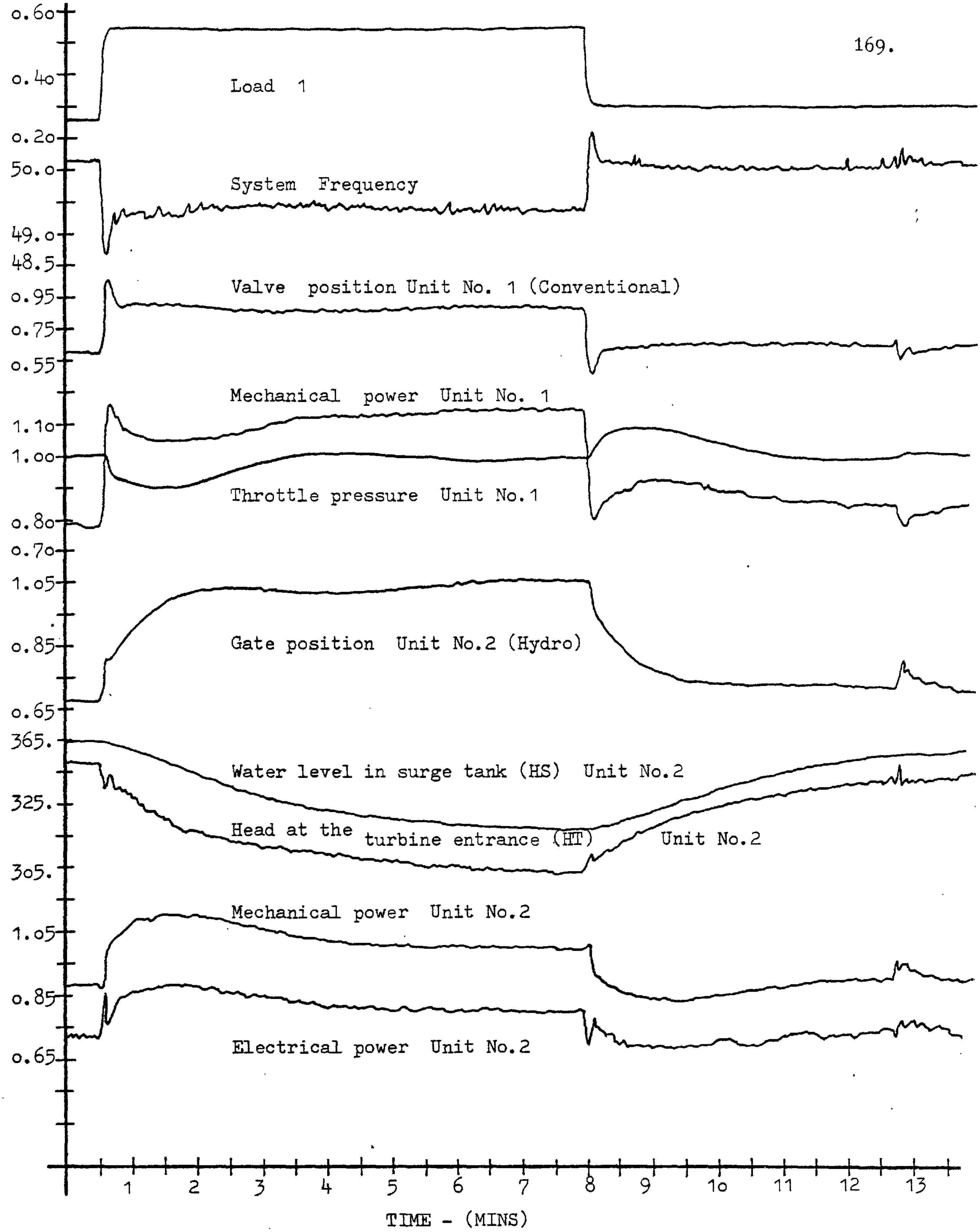

Fig.4.28Real-time response of the Hydro plant model (Unit No.2),to a step change in load

entrance does the same with a few oscillations. The initial change of H_T results in the inevitable "bump" towards the wrong direction of the mechanical power of the turbine, which afterwards increases to a new level. The electrical power output increases originally, as the system inertia supplies the required energy (at the expense of the frequency). It drops as the frequency begins to rise again; following this short period the electrical power begins to rise steadily, but this time the required energy is supplied by increased production by both units.

Load 1 changes in the opposite direction, after about 7.5 mins of the first change and the response of the two plants follows suit. The two spikes in this part of the response are a result of a bad frequency reading by the program.

In Fig. ~~4~~5.29 the response of the hydro model is shown when the gate opening is increased from 20% to 100% in about 7 s. The governor is by-passed. The system starts from an equilibrium, where the bulk of the power is supplied by the conventional plant with the hydro plant operating at about 27% of its full output. The load demand increases (load 1) and as the frequency begins to fall, the hydro plant is brought to full output in about 10 secs. In this way this plant now supplies most of the power needed and the governor of the conventional plant closes the valve and the output of this plant is reduced.

The frequency increases above 51 Hz because of the excess power supplied to the system. The gate of the hydro plant is constantly at 100% opening during the 7 mins after the command was issued for it to open. During this time interval the hydro governor was by-passed and the plant was not taking part in frequency regulation. After this time interval the governor is switched in. As can be seen, it immediately begins to reduce the gate opening, because the system frequency is far above 50 Hz. At this stage both plants participate in the frequency regulation.

In Fig. 4.30 the response of the hydro model is shown when the gate is completely closed by an action which by-passes the governor. In this case, the system starts from a state where the hydro plant operated at about 50% of its output. The load demand

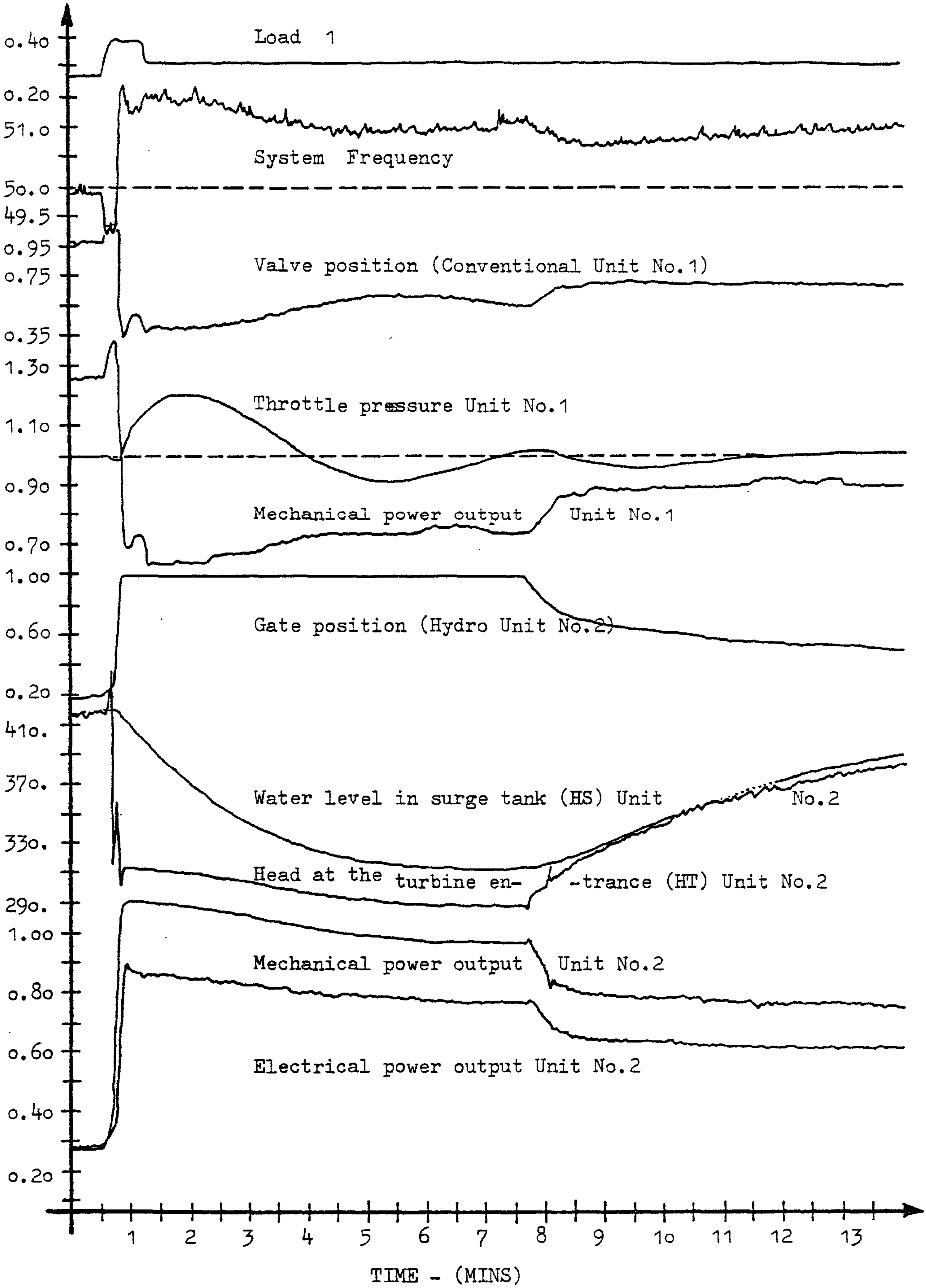

Fig. 4.29 Hydro-model response (in real-time) to a fast opening of the gate, with the governor by-passed.

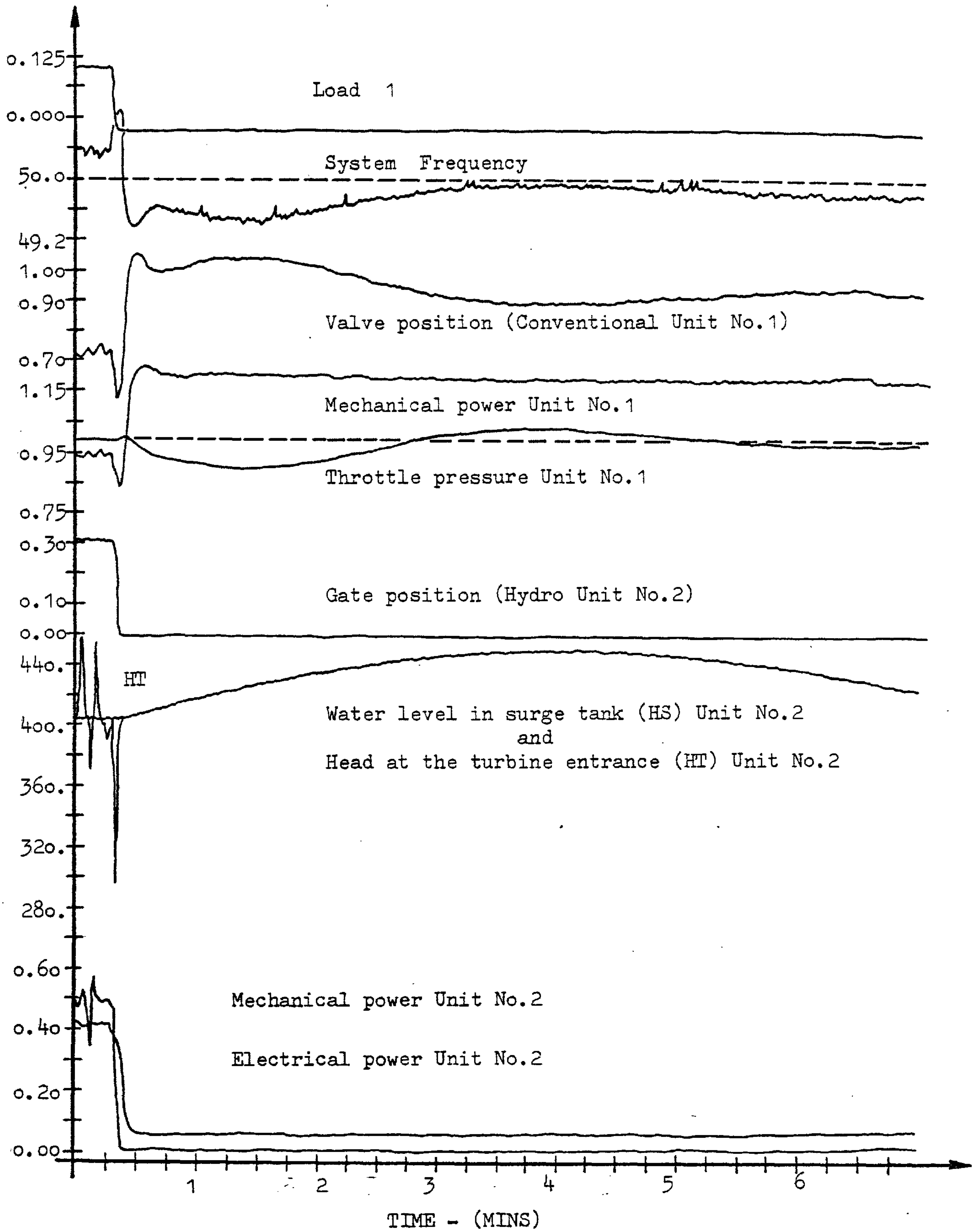

Fig. 4.30 Hydro-model response (in real-time) to a fast closure of the gate, with the governor by-passed.

drops suddenly. The frequency begins to increase. At this moment the command to the gate to close is given and the opening goes from about 30% to zero, within 1.5 s. The mechanical power follows this fall. The frequency drops below 50 Hz originally and remains there for some time, while the throttle pressure of the conventional plant is below its set point. After that, the frequency moves nearer the 50 Hz mark. The pressure head at the turbine entrance and the water level in the surge tank assume almost identical values (after the gate closure). That is because the former is computed by equation (4.31) in which both the gate position and the water velocity in the penstock are almost zero. The electrical power output is not completely zero, because deliberately the mechanical power input was not allowed to assume a zero value.

In conclusion, it can be said that, with the three tests shown in Figs. 4.28, 4.29 and 4.30 the hydro model can operate in real-time in conjunction with the generator (analog) model and give a reasonably acceptable response.

CHAPTER FIVE

VARIABLE PRESSURE STEAM PLANT

5.1 INTRODUCTION

During the last decade, more and more large conventional and nuclear units came into operation in the electric utilities and the trend for units of even higher capacity continues. Although most of the nuclear units have reasonably good load-following capabilities, it is often desirable to operate them base loaded. Hydro plants and pumped-storage plants may not be available or have enough capacity to supply the peak loads of the daily load curves, which do not seem to become smoother. For these reasons there is a growing need for the big conventional units to take part in supplying the peak loads. This means operation at low load for increasing periods of time and even overnight or weekend shutdown.

This kind of operation sets a number of requirements such as: fast start-up of the unit, low start-up losses, good heat rate at low loads, fast load changes, minimum wear of the unit's components, high availability.

The mode of operation which can meet most of these requirements satisfactorily is called: variable-pressure operation or sliding-pressure operation or pressure-governing. In this, the steam pressure is varied to change unit output, while the valves remain (ideally) wide open. This means that the governor does not act on them in response to small frequency changes but only as an overspeed trip mechanism.

This principle of operation is used extensively in the Federal Republic of Germany[70], but it also has begun to spread in the U.S.A.[71-73] and other countries.

The basic operating modes of a boiler-turbine-generator unit can be derived from the simplified expression giving the unit's power output (P_{out}). This is mainly proportional to the steam flow and therefore to the pressure (P_T) and the valve opening (A_T), i.e.:

$$P_{out} \simeq \text{steam flow rate} \simeq (A_T . P_T) \text{ in p.u.} \qquad (5.1)$$

So the way the steam flow changes determines the operating mode of the unit. On Table 5.1 various operating modes are presented[70,71]. On this table a controlled-variable is a variable which is kept to a desired value by a controller. A variable which changes freely does so under the influence of one or more of the system inputs (frequency, firing rate, etc.).

5.2 VARIABLE-PRESSURE OPERATIONAL CHARACTERISTICS

Theoretical analysis and on site experiments were carried out by many researchers in the industry, for the assessment of the characteristics and the feasibility of this method of operation[70-78]. Reviewing this work, some of the main features of the sliding-pressure operation are presented below.

In the case of constant-pressure (CP) operation with nozzle group control, as the load drops, the pressure at the HP section outlet drops and so does the temperature at the reheater inlet. This results in a reduced efficiency of the HP section[70,77]. The changes in temperature are extended along the steam circuit. So a limit is placed on the rate of output change to ensure that the turbine is not exposed to extensive thermal stresses and differential expansions. Final SH and RH temperatures can change by 100-160^{o}F and 20-50^{o}F respectively over the load range[70,73,74], depending on the design of the turbine. Also as the steam flow (i.e. the load) drops, fewer nozzles in the HP section are active and thus fewer blades on the turbine wheel have to cope with the increasing load (this is not the case for the IP-LP sections). Consequently the design and the construction of this part must be different to cope with stresses three or four times the normal[70,71,74].

In the case of variable-pressure (VP) operation with nozzle group control, the pressure at the input of the HP section changes in direct proportion to the load. Therefore the enthalpy difference converted to mechanical power by the HP section remains essentially constant over the entire load range. Consequently the efficiency of the turbine is improved at low loads and also the restrictions on the rate of output changes imposed by the temperature change on the

TABLE 5.1

TABLE 5.1 Basic operating modes of a boiler-turbine generator set $[P_{out} = AT \cdot PT]$

	Controlled variable		Variable changing freely	Means of varying the steam flow into turbine		Mode of control		
	Boiler	Turbine		Varying the admission flow area	Varying the main steam pressure at the inlet of the blading....			
(a)	PT	P_{out}	AT	.... of the blading in the first (HP) stage	—	Nozzle group control for constant-pressure operation	Boiler-following	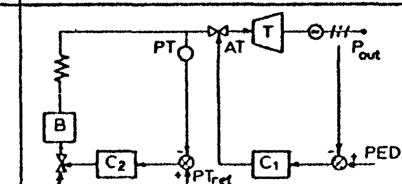
				....by throttling action of the control valves	—	Throttling control for constant-pressure operation		
(b)	P_{out}	PT	AT	.... of the blading in the first (HP) stage	—	Nozzle group control for constant-pressure operation	Turbine-following	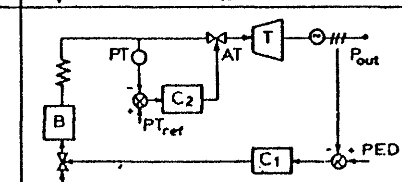
				....by throttling action of the control valves	—	Throttling control for constant-pressure operation		
(c)	AT	P_{out}	PT	—	.... by varying the pressure supplied by the boiler	Valve position controlled (boiler) variable pressure operation		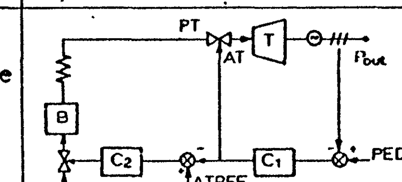
(d)	P_{out}	AT	PT	—	"	"		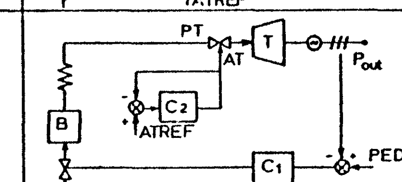
(e)	PT	P_{out}	AT	—	The pressure set-point is proportional with the load	Pressure controlled (boiler) sliding pressure operation ✱ When the pressure set-point = const., this is a case identical with *(a)*		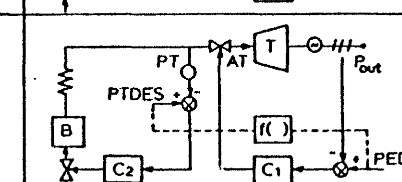

PT_{ref} = Pressure set-point, ATREF = Valve opening set-point, PTDES = Desired pressure level, PED = Desired unit output turbine are eliminated. Restrictions on the rate of change of the saturation temperature are imposed now on the boiler, but they are much less severe than those of the turbine. The SH and the RH outlet temperatures can be held constant down to 25% and 50% respectively[73].

In the case of CP operation with throttling control, the temperature drop across the HP section is not so big. Therefore the performance of this unit is reasonable, although at low loads there is an increased drop in temperature at the HP inlet due to the increased throttling[70].

Another feature of the VP operation concerns the feedpump. As the pressure drops following the load, the pressure of the feedwater also drops, the pump loading decreases and thus the power required to drive it. However, the efficiency does not drop significantly[70,71]. For motor or turbine-driven pump there is a gain over the power consumed as the load drops. But the overall gain is bigger in the case of a low-loss speed control when a turbine drive is employed.

Equally, if not more, important are the operational characteristics of the VP mode during the unit start up[70,71,75,76,77]. Since the unit can operate at low loads, the steam pressure and temperature can be brought very quickly to match those of the turbine casing. In contrast, under CP operation full-load conditions must be achieved for the steam. This is a time-consuming procedure and involves considerable losses.

A requirement for this independent start for the boiler is the by-pass system. A system of piping by-passes the HP and the IP-LP sections of the turbine. It is designed so that it can accommodate full-load operation of the boiler. Thus in the case of full-load rejection, the boiler can continue its normal operation and so it can be put again on-line in very short interval.

The fact that high temperatures can be kept at low loads (as mentioned earlier) contributes to a slow cooling down of the various sections. So after an overnight shutdown the unit can be run up to load quickly next morning.

From the maintenance point of view, operation at lower than the designed pressure reduces the stresses and improves the life of the RH and SH tubes. Together with the reduced thermal stresses on the turbine, there is a considerable improvement in the availability of the whole unit. Overall heat rate improvements of the order of 3-5% at low loads have been reported[77,78].

5.2.1 The Control Aspect of the Variable-Pressure Operation

For a plant designed to operate with VP, the methods of controlling temperatures, flows, water levels, etc. in the boiler unit are essentially the same as in the case for CP operation. Three-term feedwater controllers, desuperheating, burner tilting, gas recirculation, forced and induced draft fans for air flow and furnace pressure control, all do the same work[72,73]. The basic difference is in the control of the unit's output.

From equation (5.1) the straightforward way of controlling the output is to keep the valve fully opened and vary the boiler pressure according to the output requirements. This is called "pure sliding-pressure" mode of control, or "passive pressure governing". It has, however, the obvious disadvantage of slow response, because the output changes only in response to a change in the firing rate. No use is made of the unit's stored energy.

A modification to this concept aimed at improving the response is achieved by keeping the valve less than fully open during normal operation (pre-throttling). If an increase in the output is required, the valve opens to assist the rate of response (using the boiler's stored energy) and drops back to its set-point when the pressure rises enough to support the increase in load.

Pre-throttling obviously has an adverse effect on the cycle efficiency at low loads. A trade-off must be made between speed of response and loss in efficiency. Units with low storage and fast firing controls (e.g. oil-fired once-through units) can achieve high rates of response up to 10-12% min[70,71]. Overfiring is also used to compensate for the initial sluggish response of the boiler.

Other modifications to the pure sliding-pressure operation can be done by: introducing a by-pass valve around the HP stage to the LP stages or throttling the steam going into the HP feed-heaters.

In both cases more steam is injected into the IP-LP stages, speeding up the response of the unit[70]. Different methods of control are favoured by various designs of boiler and turbine.

The cases (c), (d) and (e) on Table 5.1 represent three ways of controlling the output of a VP unit. For the first two, the boiler inputs are activated in response to the deviation of the valve opening from its set-point. In (e) the pressure error activates the boiler input. Here the pressure set-point is a function of the desired output. In the cases (c) and (e) the turbine is load-controlled, while in (d) the boiler is load-controlled. For this reason, case (d) gives clearly an inferior response to frequency regulation, as does the turbine-following mode of control for CP operation (case (b)).

5.3 CHOICE OF MODEL AND ITS STEADY-STATE CHARACTERISTICS

The boiler model for CP operation was described by the set of equations shown in Table 2.1. The VP operation affects very little the temperature of the water entering the economizer[78]. So the feedwater enthalpy (h_{E0}) can be assumed constant as on Table 2.1. The entering air temperature (T_A) is independent of the type of operation, so again it is assumed constant. The state equations for the drum (2.77), (2.78) and (2.79) are valid for a change in drum pressure down to 40% of its full-load value. The pressure drop due to friction along the steam path is almost proportional to the load[70] and not to the square of it as in the case of CP operation. Therefore the square root in equation (2.30) was cancelled. The rest of the equations in Table 2.1 were left unchanged.

To compute the state of the model at any point along its operating range, the values of the valve opening and the pressure at this point are needed. At the new steady-state, the steam flow W_T should be equal to the unit's desired output. If the valve opening is also known, then the pressure can be computed from equation (5.1). Based on this principle the closed-loop steady-state characteristics can be computed and they are shown in Fig. 5.1.

As can be seen in Fig. 5.1(a), when pre-throttling is used the pressure/load characteristic is higher. Also, if the output exceeds

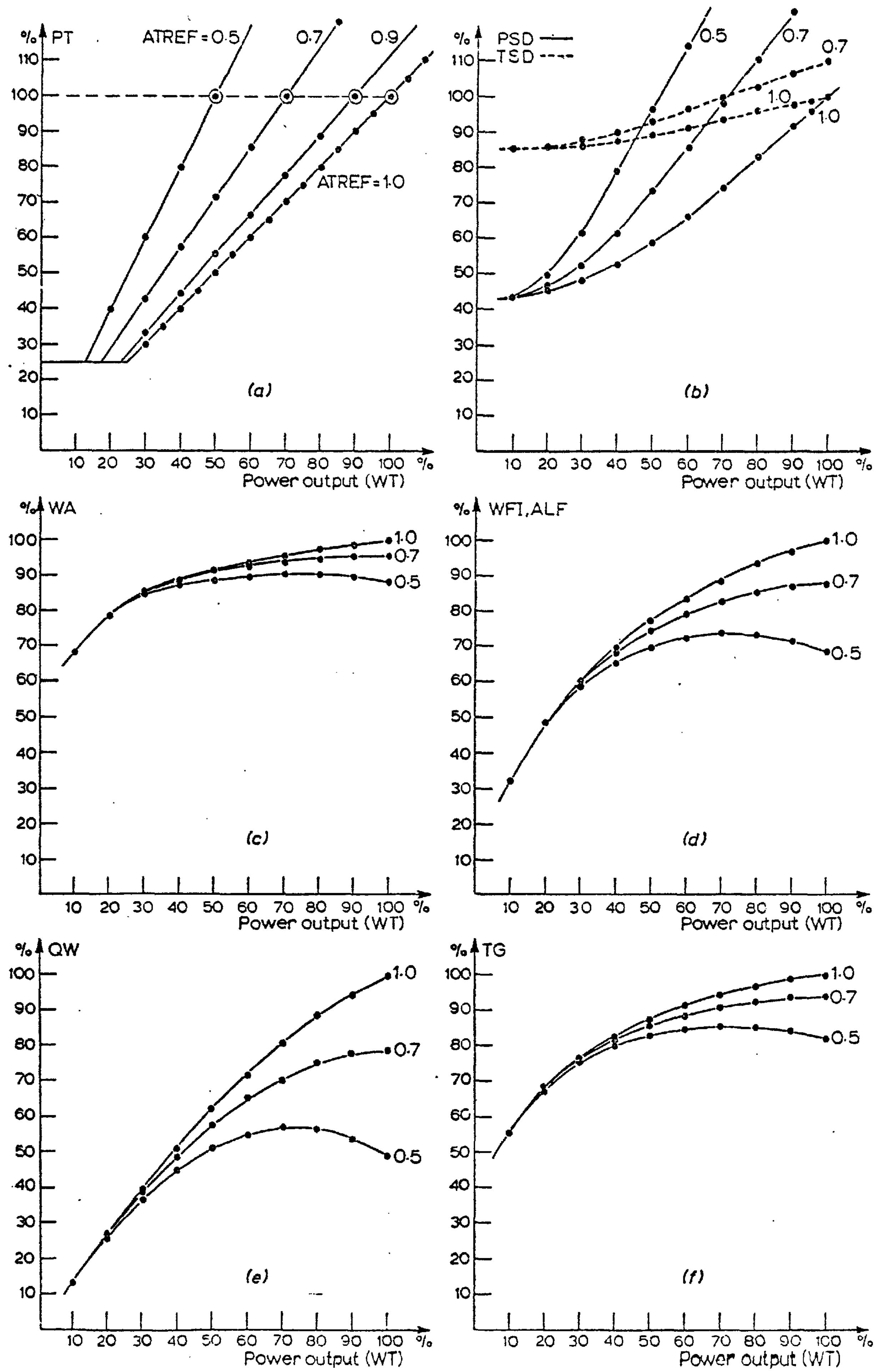

Fig. 5.1 Closed-loop steady-state characteristic of the sliding-pressure boiler model.

the desired valve opening (both expressed in p.u.), the pressure must be greater than its value corresponding to full-load. The gas temperature in the furnace (T_G) and the drum steam temperature (T_{SD}) drop only between 15 and 20% for 30% load. This is in agreement with the practice (i.e. low temperatures can be kept at low loads), as mentioned in Section 5.2.

5.4 THE CONTROL SYSTEM USED IN THE MODEL

It was assumed that the variable-pressure unit has a load-controlled turbine and a pressure-controlled boiler. This is the case (e) on Table 5.1. For this mode of control, the unit's desired output must be known in order to compute the pressure set-point (from equation (5.1)) as mentioned in Section 5.3. The valve is not fully open. When an increase in output is required, the valve opening will increase initially to assist the response of the unit. When the pressure has increased sufficiently, the valve will return back to its set-point. Therefore, the form of response of the generating unit is greatly influenced by the way the valve changes and a rather sophisticated algorithm is needed for that. A much simpler scheme was employed in the model; it is shown in Fig. 5.2.

When the unit does not take part in frequency regulation, it responds only to changes in demand, introduced manually or by an automatic load despatching algorithm. The value of the total demand is divided by the valve opening set-point to give the pressure set-point. The pressure error goes through a P I D algorithm to produce the firing rate demand. At the same time, the valve can be adjusted to assist the unit's response. This adjustment is implemented as follows: the demand signal goes through a first order lag, thus producing a desired or ideal response of the steam flow into the turbine (WTI). This is compared with the actual steam flow (W_T). The difference between these two is shaped by another simple lag. Its output is added to the nominal valve set-point (ATREF) and so a new "transient" set-point is created. The difference between this and the actual valve opening produces raise or lower pulses, which vary the valve opening through the speeder gear. In this way, the steam flow during the transient is forced to follow the desired response WTI.

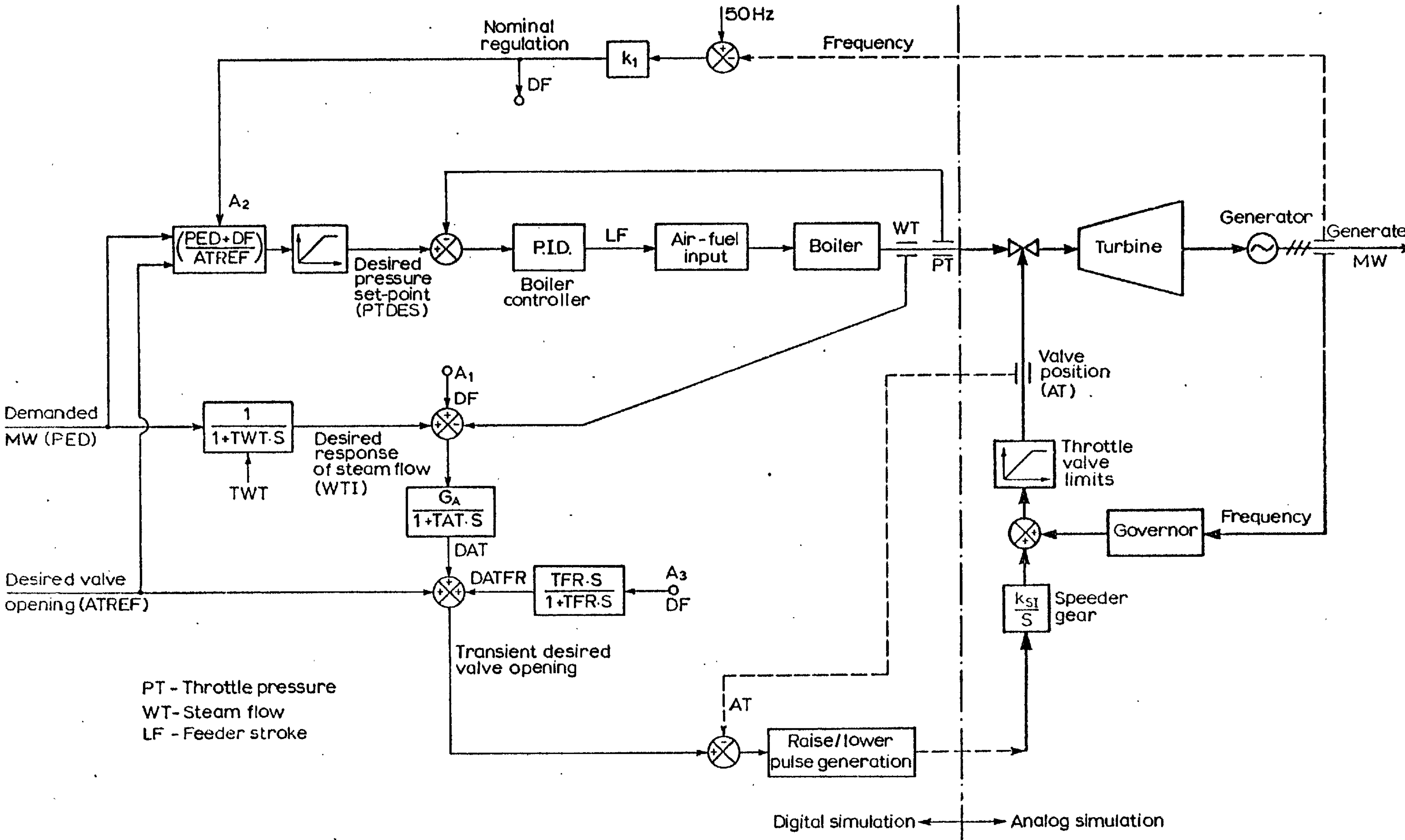

Fig. 5.2 The control scheme of the sliding-pressure boiler model.

After the transient, the valve opening returns to ATREF.

Another mode of operation is to keep the demand signal constant and allow the unit to respond only to frequency changes. Two cases can be distinguished here:

(1) the governor is acting on the valve normally, as it does for a CP unit, and

(2) the governor is made insensitive to frequency changes of $\pm$ 0.5 Hz, for example, and acts with 4% droop outside this limit.

In the first case, for a frequency drop, the governor will open the valve to supply the additional demand. At the same time a signal to return the valve to its set-point (with speeder motor action) will start acting. This is because PED and therefore WTI in Fig. 5.2 are unchanged, while the actual steam flow W_T has increased. This is the turbine-following mode of control (case (b) on Table 5.1). It gives a good balance between the boiler and the turbine, but very poor balance between generation and demand. In addition there is no change in the boiler input.

To rectify this situation, the frequency error is multiplied by a 4% droop, thus forming a nominal regulation signal DF. This is fed into three parts in the control system (Fig. 5.2). In point A_1 it modifies appropriately the WTI so as to prevent initially the speeder motor from returning the valve to its set-point and allow it to do so, when the pressure has changed by the proper amount corresponding to the frequency change. The introduction of DF in point A_2 is responsible for changing the boiler input and thus the pressure P_T. At the point A_3, the signal DF goes through a transient term which can be used to assist the overall response, by selecting the time constant, TFR.

In the case where the governor does not respond to frequency changes, the valve opening is changed only by the speeder gear. The control scheme is the same as in the first case.

5.5 REAL-TIME RESPONSE OF THE VARIABLE-PRESSURE BOILER MODEL

The power system configuration shown in Fig. 2.23 was used again to study the operation of the VP model in real-time. Both generating units were driven by this boiler model. First the response to frequency changes was investigated. The governor was assumed to act on the valve in the usual way, in other words it was not restricted to react only to large frequency deviations. Then the response of the model to large changes in output was studied.

5.5.1 Response to Frequency Changes

In Fig. 5.3 the response of the two units is shown to changes in frequency. The system is disconnected from the infinite bus. The set-point for the valve opening is 80%. The demand remains unchanged for each unit at 70%. The frequency of the system increases as a result of a change in Load 1. This drops just above 0.1 p.u. in about 3 s. The governors of both units respond immediately by closing the valves. The electrical output follows this change very closely. If the control mechanism was allowed to bring the valve back to its set-point straightaway, the electrical output would follow and it would begin to increase again. But as was described in Section 5.4, a transient set-point is created for the valve opening, with the injection of the signal DF at the points A_1 and A_3 of the control scheme shown in Fig. 5.2. As a result, the valve opening is kept at its new value for a period of time. This time interval was around 1 min. for the response shown in Fig. 5.3. During this time, the boiler pressure drops to a new level determined by the new load demand. After that, the valve opening is allowed to return to its set-point. The same features can be observed on the response, for a disturbance in the opposite direction.

The speeder motor responds to raise/lower pulses. For a valve opening error greater than 10% the pulse initiates a change of approximately 16%/min with no action taken when the error is smaller than 0.8%. Obviously such a scheme cannot give a particularly smooth response of the valve, but it was found to be an acceptable compromise.

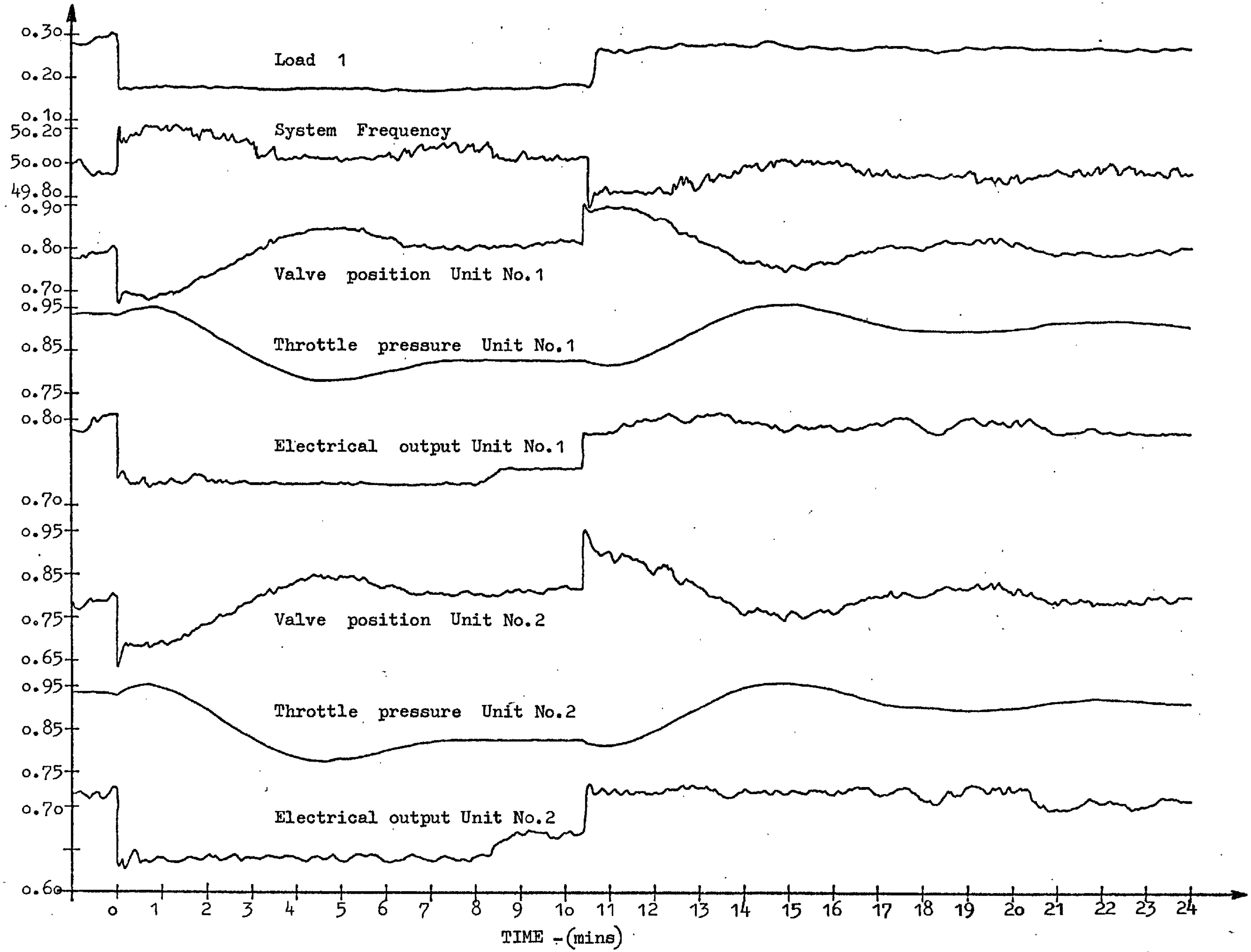

Fig.5.3 Real-time response of the sliding-pressure boiler model to changes in frequency

With this control scheme the response of the electrical power output is superior to that of a plant with CP operation. Such a response was shown in Fig. 2.28 where the mechanical power output of unit no. 1 after the initial step increase drops following the shape of the steam pressure.

The response of the model was tested also in the case where the governor does not act on the valve directly for small frequency changes. It was found that the response was much inferior to that described above. This is because the valve responds at a slower rate through the speeder gear and thus it cannot follow fast changes in frequency. So this approach would give inferior performance, unless the control equipment is designed specifically for such a control scheme.

5.5.2 Response to Large Changes in Demand

In Fig. 5.4 the response of the sliding pressure unit is shown to a step increase in the demand signal PED of 50% (from 30% to 80%). For this test the unit was set to respond only to changes in PED and not to those of frequency (the DF signal shown on Fig. 5.2 was set to zero). The pre-throttling was set to 20%, in other words the valve opening set-point was set to 80%.

As can be seen, the valve departs from its desired position and assists the response of the output while the pressure is still low. After about 2 mins from the introduction of the step input, the pressure has increased sufficiently and the valve begins to return to its set-point. The steam flow at the valve and the electrical output change almost in the same fashion. The rate of change of the output during the first 3 mins is about 11%/min. Then it drops considerably and it reaches the target output after about 7 mins.

From the shape of the response of the firing rate, it can be said that the boiler is over-fired for a considerable amount of time. Over-firing is normal practice at variable-pressure plants[73,75] and it is used to make up for the slow initial response of the boiler.

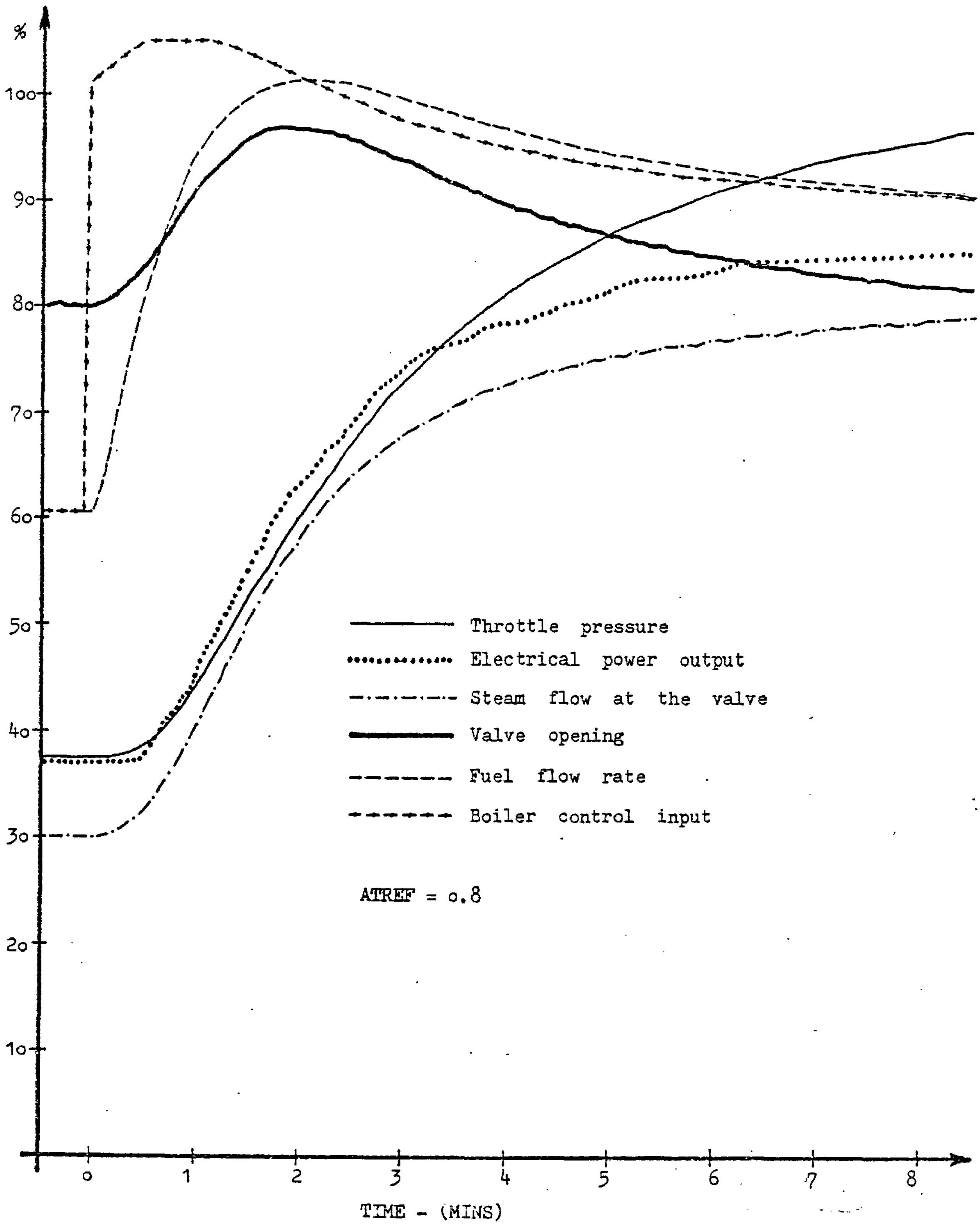

Fig. 5.4 Real-time response of the variable-pressure boiler model. to a 50% step increase in demand.

During the investigation of the response of the model to steps in demand, it was found that the rate of change of the output depended on the magnitude of the step input. The bigger the step input, the faster the rate of response. It is felt that this is mainly a result of the boiler controller (a PID algorithm). A second factor affecting the response is the pressure characteristic on which the unit is operating. In other words, depending on the pre-throttling used, the pressure/output characteristic is different as was shown on Fig. 5.1(a). As this becomes steeper, the pressure range is higher and the response becomes faster.

The first factor affects the response more than the second. To counteract its effect, the time constant TWT of the first order lag forming the desired response of the steam flow WTI (Fig. 5.2) was made a function of the step change in demand (ADPE), as shown in Fig. 5.5(a). The smaller the step change, the smaller becomes the TWT, to make the WTI faster. Fig. 5.5(b) shows the way the TWT is formed for successive step changes in demand.

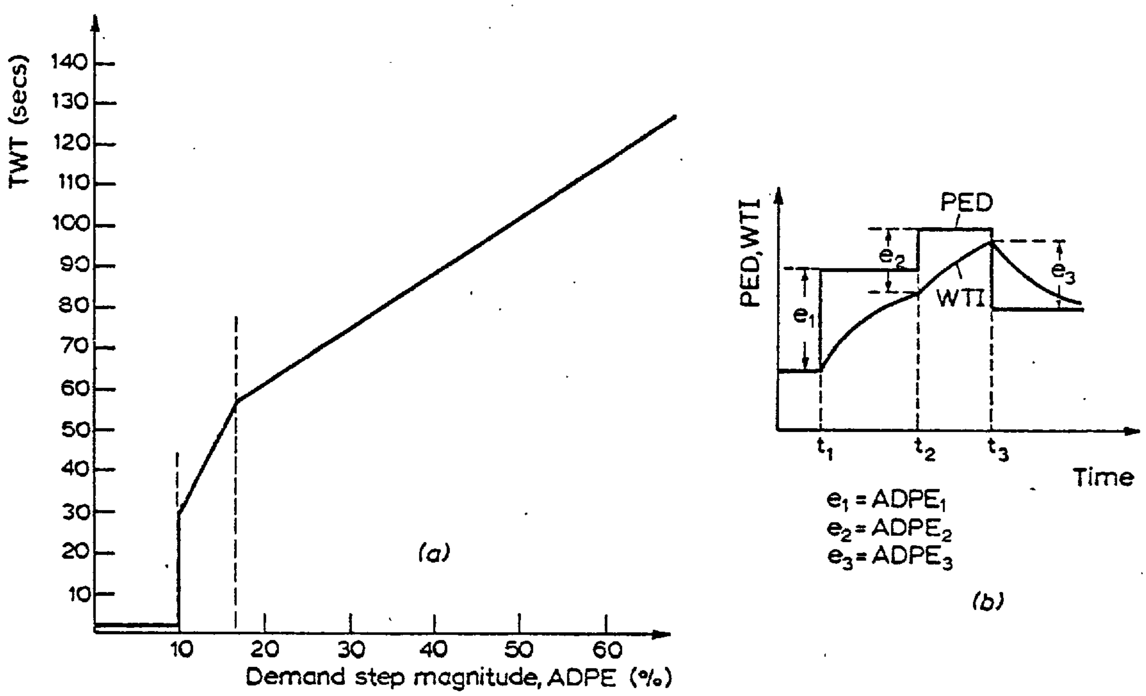

Fig. 5.5

But even with this scheme there is very little improvement in the response to small changes in demand. For bigger changes this scheme becomes more effective. For the test shown in Fig. 5.4, TWT $\approx$ 103 s. Some further improvement of the response to small changes in demand can be achieved by increasing the gain G_A (Fig. 5.2) during them. With a value of $G_A = 2.0$, the response is almost 5%/min. This is obviously accomplished with increased valve opening. The only drawback is that the output overshoots the demand after a while. This is because the boiler pressure has risen to its new level by that time.

Another characteristic which came out of the tests,was that when large changes in output are requested from the unit, the valve opening set-point must be relatively low in the region around 70% or 80%. This is because when it is higher, for example 90%, with an increase in demand the valve opening goes very quickly to its limit and stays there. During this time interval it does not assist the response of the output. So the change in the unit's output depends again mainly on the response of the boiler. A small amount of pre-throttling is, therefore, more useful when the unit operates in frequency regulation mode with small changes in demand.

The simple transfer functions which were used to shape a desired steam flow response (as shown in Fig. 5.2), can be substituted by more elaborate expressions which could produce a better plant response. Such a scheme, however, would be more complicated and perhaps bigger than the boiler simulation itself. This is the main reason why such a scheme was not investigated in this work.

CHAPTER SIX

THE SIMULATION SOFTWARE

6.1 SIMULATION PROGRAMS

A separate program was written for each type of plant. Each contains the set of equations presented on Tables 2.4, 3.2 and 4.2 for the conventional, nuclear and hydro models. Three other programs were also developed, each simulating more than one type of plant. They are all presented on Table 6.1. Every program has to be fixed in core when it runs in real-time, because it is scheduled to run very frequently (every 0.3 s).

Each of the first four programs fits in the core partition P4.1 (Fig. 2.21a). But when more than one type of plant is required in the simulation, it is not possible to run any two of these programs simultaneously. The partition is not big enough for it.

For this reason the first three programs were incorporated into a single one (BOIL1). Every effort was made to reduce the amount of core needed by this combination. The fact that some of sections of the steam generation are the same in both, the conventional and the nuclear models, was used to the best advantage. The hydro model was placed after the combined conventional boiler/nuclear set of equations, as the final part of the program. Therefore, as the execution of the program starts and all three types of plant are needed, the conventional model will run first, followed by the nuclear and the hydro, in that order.

The selection of the proper set of programs in BOIL1 is based on the number of units of each type selected by the Simulator user. So this program can also be used to simulate only one type of plant, if it is desired.

Table 6.1 Simulation Programs

Name	Types of plant simulated
1) BOILC	Conventional constant-pressure
2) BOILN	Nuclear
3) BOILH	Hydro
4) BOILP	Conventional variable-pressure
5) BOIL1	Conventional (CP) + Nuclear + Hydro
6) BOILD	Conventional (CP) + Conventional (VP)

With BOILD, conventional boiler units can be simulated in either constant-pressure or variable-pressure operation. Unlike BOIL1, in this program the order of execution for the two types of plant is not fixed. Either type can be selected to run first.

The common area used by all six programs is the BLSIM (Fig. 2.21a). Provision is made for six units. BOILP and BOILD also make use of the common area SYSCOM, where some additional variables are stored. These are used by the sliding-pressure model and they provide space for two units only, because of lack of space in the two common areas mentioned.

For the conventional boiler model operating in the CP mode and the nuclear model, operating in the regulating mode, the simulation program has:

Inputs: a) Throttle pressure set-point (APS)
b) The "current" value of the valve opening (AT)

Output: Throttle pressure.

For the nuclear model operating in the non-regulating mode:

Inputs: a) Throttle pressure set-point (APS)
b) Frequency

Outputs: a) Throttle pressure
b) Raise/lower pulses to the speeder motor

For the hydro plant model:

Inputs: a) Frequency
b) Desired output
c) Command for fast closing or opening of the gate

Output: Mechanical power

For the boiler model operating in the variable-pressure mode:

Inputs: a) The valve opening set-point (ATREF)
b) The additional power output required (ADPE)
c) The frequency
d) The "current" value of the valve opening (AT)

Outputs: a) The throttle pressure

b) Raise/Lower pulses to the speeder motor

6.2 PLANT SIMULATION SET-UP

The procedure of starting the simulator has two basic steps. First, a power system is selected and patched and the analog part of the simulator with the interface to the computer is switched on. Second, the real-time system is loaded on the computer and the basic I/O programs are started.

To start the digital simulation, the program called PLINT is requested from the teletype. The logic of this program is shown in Fig. 6.1.

When a normal initialization is desired, the number of each type of plant is selected by the user. If a number of conventional plants were requested, the user is asked to specify if some of them are variable-pressure units. If none of them is, the appropriate initialization program is requested and the algorithm proceeds to check if nuclear and hydro units are included in the simulation. When this is so, the corresponding initialization programs are requested. The proper simulation program is then fixed in core and the PLINT is removed from the core to allow the first in-line initialization program to start. This is because all these programs run in the same core partition (P5).

In the case where it is desired to simulate variable-pressure conventional units, the user is asked to specify their number. If all of the conventional units are VP units, the initialization program PINIT is requested and the BOILP simulation program is fixed in core. When there is a mixture of CP and VP units, a selection can be made of which type will run first and the units are initialized in that order.

As can be seen, PLINT permits also the re-initialization of one particular unit, with its number and type specified by the user. This is very useful, because if something goes wrong with one unit, only this need be dealt with while the rest continue their run unaffected.

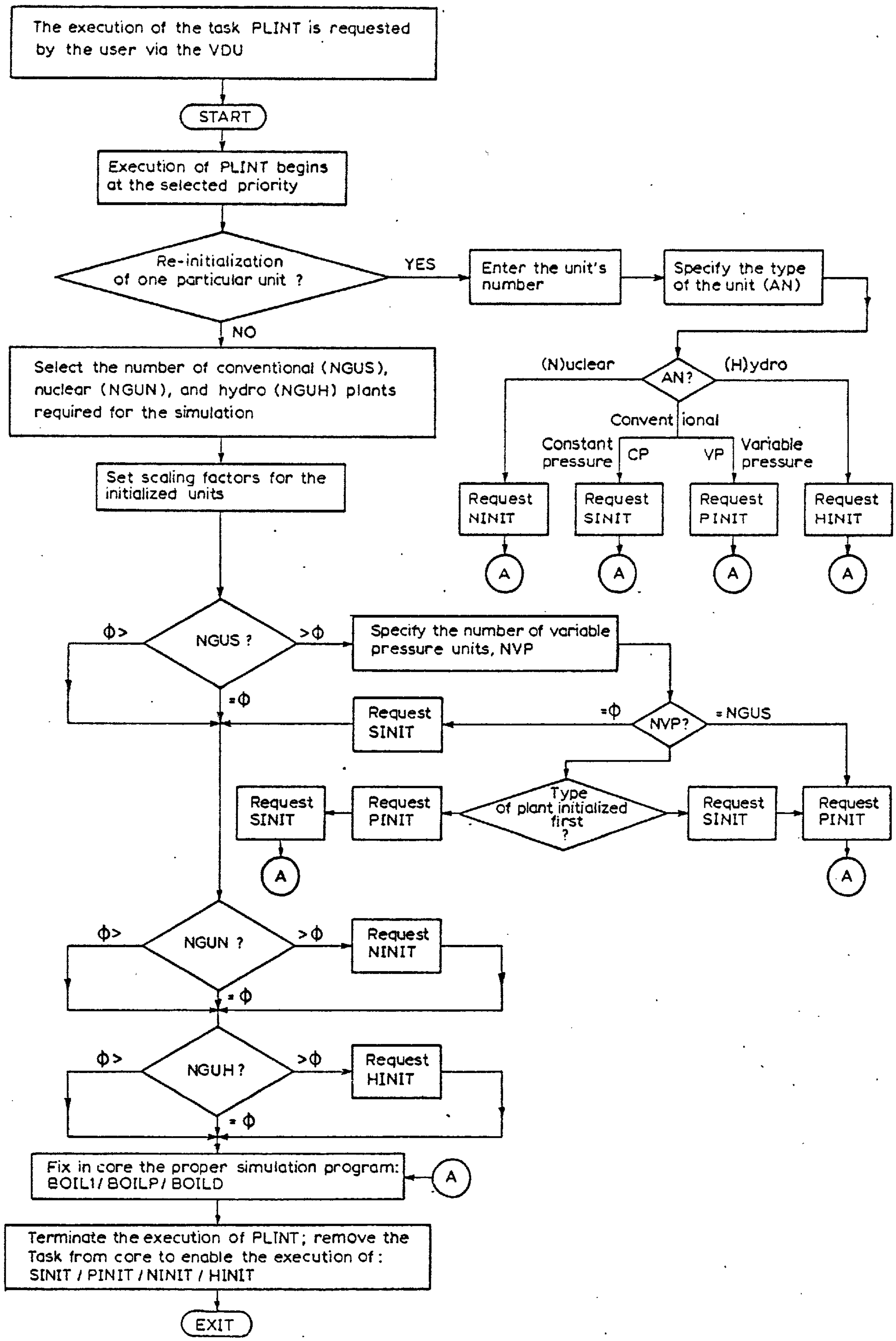

Fig. 6.1 Flow diagram of the Plant Initialization program (PLINT).

PLINT can be easily modified to accommodate any other combination of simulation programs and their initialization routines.

6.3 INITIALIZATION PROGRAMS

There are four such programs, one for each type of plant. Their purpose is to provide the necessary information to the corresponding simulation programs to enable them to start and run successfully. All are scheduled to run in the partition P5 (Fig. 2.21a) at a very low priority. Each of them, as a single program, is much bigger than 4 k of core. For this reason they are all divided in subroutines overlaying each other, thus making possible the execution of the program in P5. They are all disc resident. Their basic structure is presented briefly in the following subsections.

6.3.1 Constant-Pressure Boiler Model

The initialization program is the SINIT and its flow diagram is shown in Fig. 6.2. As it starts, it identifies itself and informs the user about the unit that is to be initialized. Then the pressure set-point and the current valve opening are acquired from the analog part of the model. These are the two variables which determine the operating conditions of the unit. They are scaled so as to have a value of 1.0 for full-load operation.

Next the values of the time constants of the drum and the air-fuel section can be selected, as well as the gains for the pressure controller. This provides the flexibility of having units with different transient characteristics and to change these characteristics any time it is desired. Default values are given by the program for three sets of time constants and gains, representing faster and slower units.

As default values are also given the values of all the model variables corresponding to the M.C.R. If the operating point of the generating unit is different from the M.C.R., the new steady-state is computed and it replaces the default values in the common area. This computation is presented in Appendix C.1.

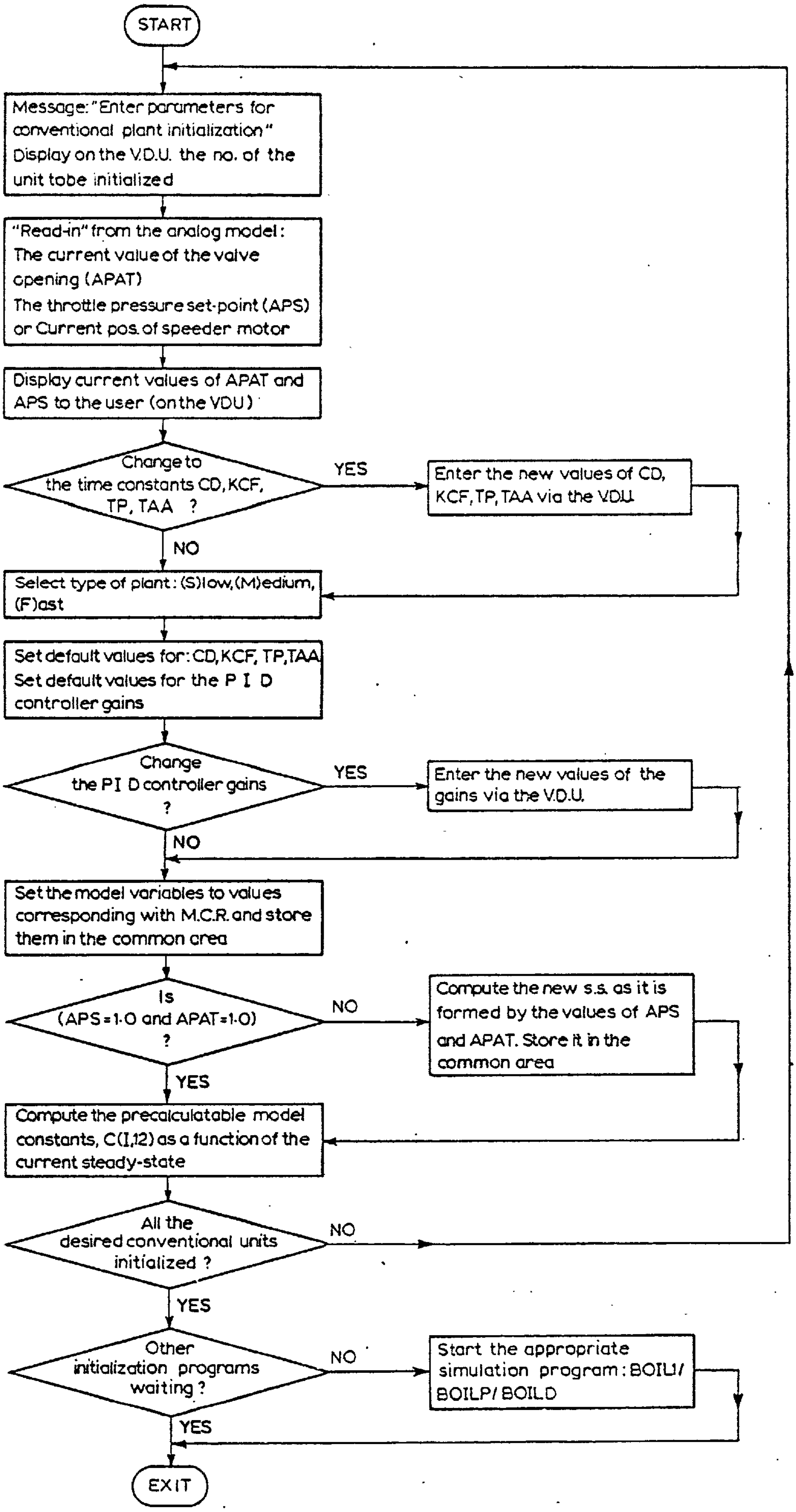

Fig. 6.2 Initialization program for the constant-pressure boiler model (SINIT).

Any constants used by the simulation program, which depend on the initial steady-state, are computed during the initialization and stored in the common area. Thus the simulation program is relieved from additional computation.

The whole procedure is repeated until all the units of this type, selected by the user, have been initialized. At this point, if no other initialization program is waiting to run, the appropriate simulation program is requested to start its scheduled runs. If this is not the case, the SINIT returns to the disc, making the partition P5 available to other programs.

This method of initialization ensures that when the simulation starts, the digital model will not experience a big step change in its inputs and consequently its output will not unduly upset the rest of the power system. So analog and digitally simulated sections integrate smoothly and efficiently.

6.3.2 Nuclear Plant Model

The initialization for both operating modes is done by the same program, NINIT. Its structure is basically the same as that of SINIT and it provides the initialization for the regulating mode of operation. The non-regulating version is treated as a sub-case, as can be seen in the flow diagram of Fig. 6.3. For this case it is assumed that the auxiliaries are operating at full output. Therefore it is enough for the program to provide the values of the model variables corresponding to full-load operation.

For the regulating version, a new steady-state is computed if necessary, based on the information provided. This computation is shown in Appendix E.1

6.3.3 Hydro Plant Model

The initialization program is the HINIT and its flow diagram is shown in Fig. 6.4. In this case, the operating point of the unit is determined by the desired power output (APR). This can be entered either by the user or it can be read-in from the analog part of the model.

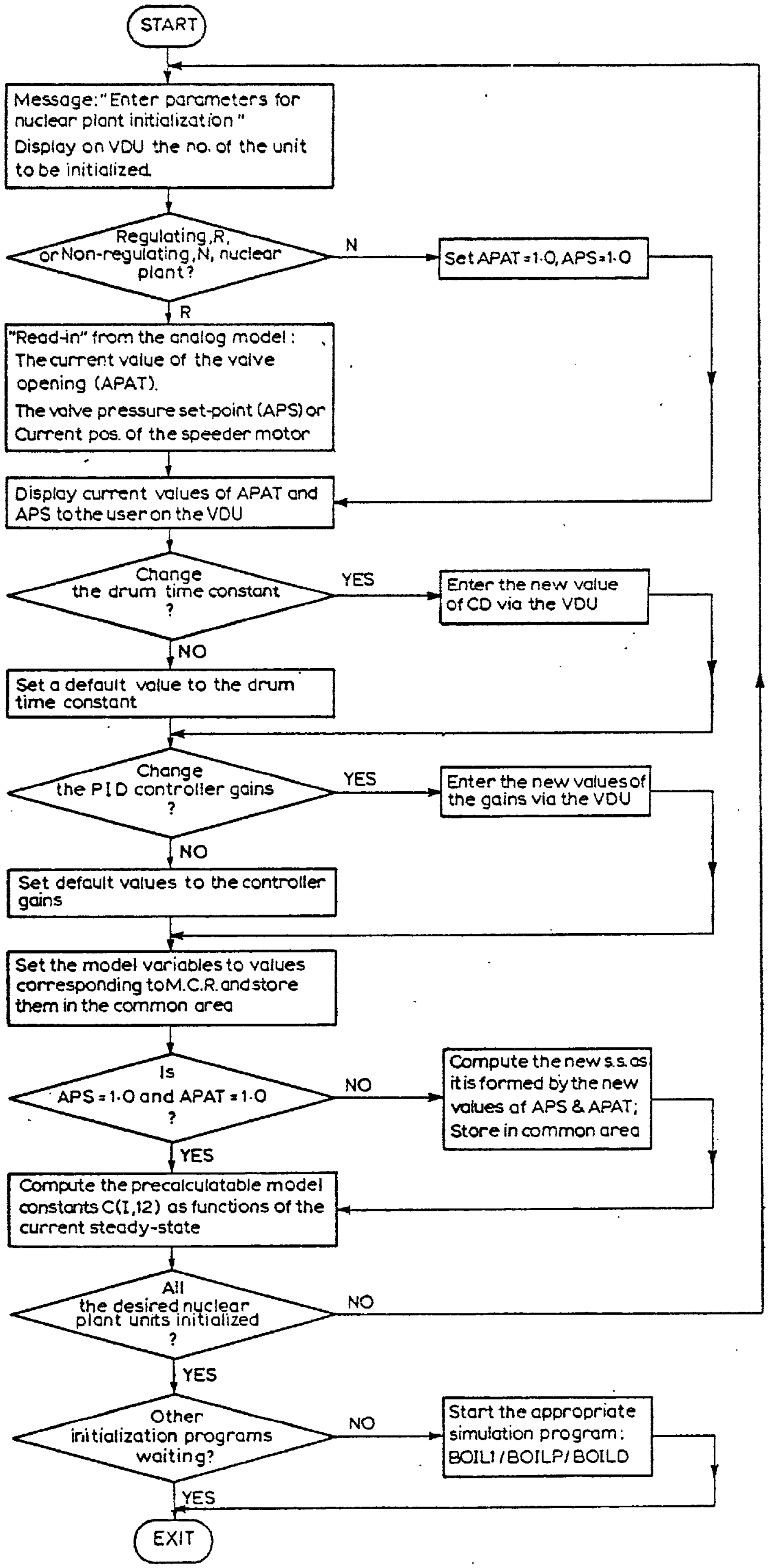

Fig. 6.3 Initialization program for the nuclear plant model (NINIT).

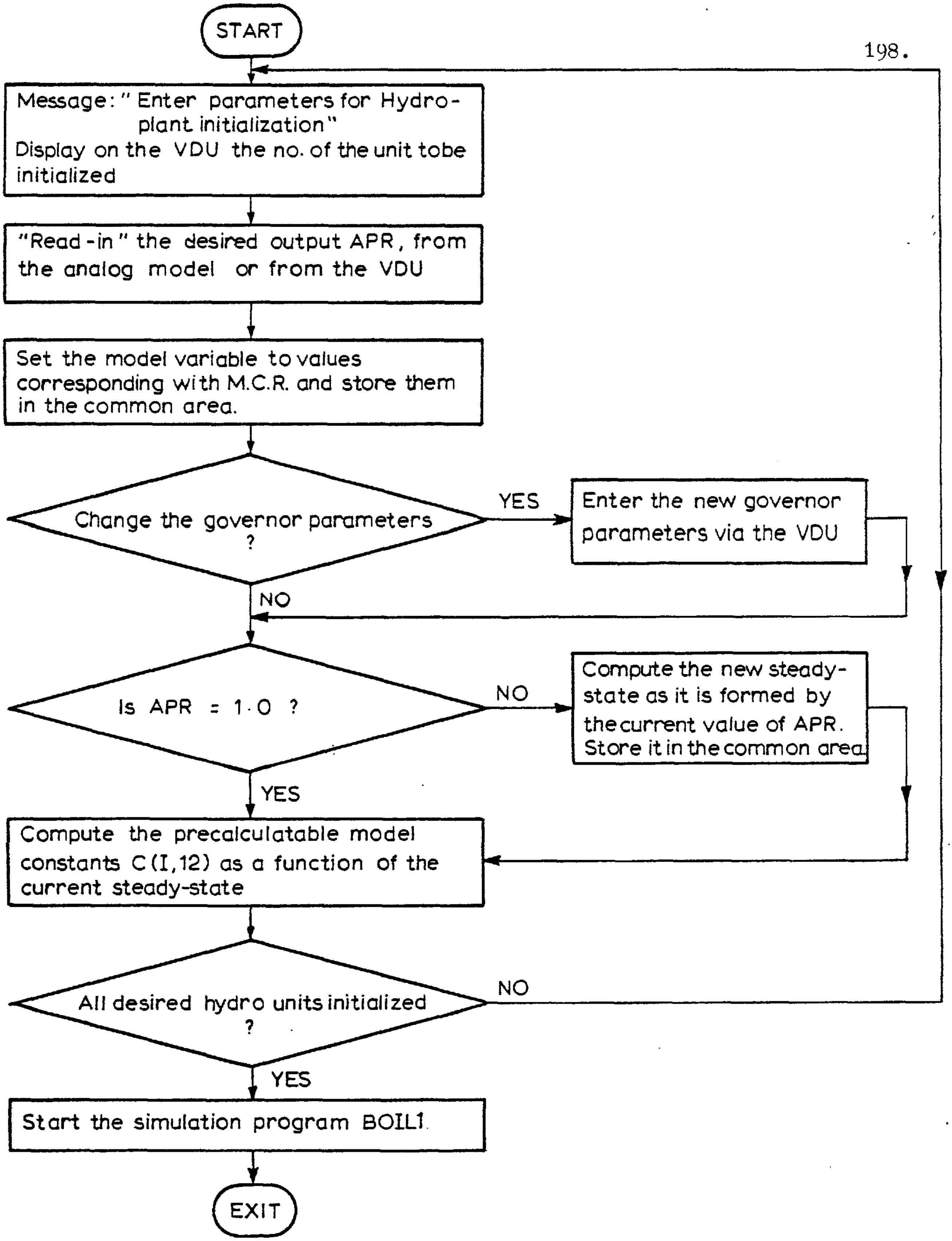

Fig. 6.4 Initialization program for the hydro-plant model (HINIT).

During the initialization, it is assumed that the frequency is 50 Hz. So the only input to the governor equations is the desired output. The governor parameters can be selected different from their default values. It would be possible to select on-line other model parameters, like the length of the penstock, the water flow rate, etc., but this is not included in the program in its present form. Also, at the end of HINIT, the simulation program BOIL1 is started because there are no other initialization programs waiting to run.

6.3.4 Variable-Pressure Boiler Model

The logic of this program (PINIT) is the same as that of SINIT, as can be seen in Fig. 6.5. As mentioned in Section 5.3, the quantities which determine the unit's operating point are: the desired output (PED) and the desired valve opening (ATREF). Both are selected on-line and from them the throttle pressure set-point is computed. From then on, the program proceeds as in the case of the constant-pressure unit.

6.4 PROCESSOR AND CORE USAGE

On Table 6.2, a summary is given of the processor and core usage by the simulator and the initialization programs. As can be seen, the conventional boiler model is the most expensive in computation time. When used in CP operation mode and all six units are simulated, around 44% of the system's time is consumed by them.

The main difference in computation time between this model and the nuclear and hydro models, is the absence of a square root computation for the last two. It was found that it takes around 1% of the system's time. The variable-pressure boiler model requires much more computation time than the constant-pressure one, although it does not include a square root. But the more complex control scheme (Fig. 5.2), introduces a fair number of additional operations.

If only one type of plant is required, then one of the programs that simulate only this type can be used instead of BOIL1. This can save some computation time because in BOIL1 additional computations and checks are required to separate the three models.

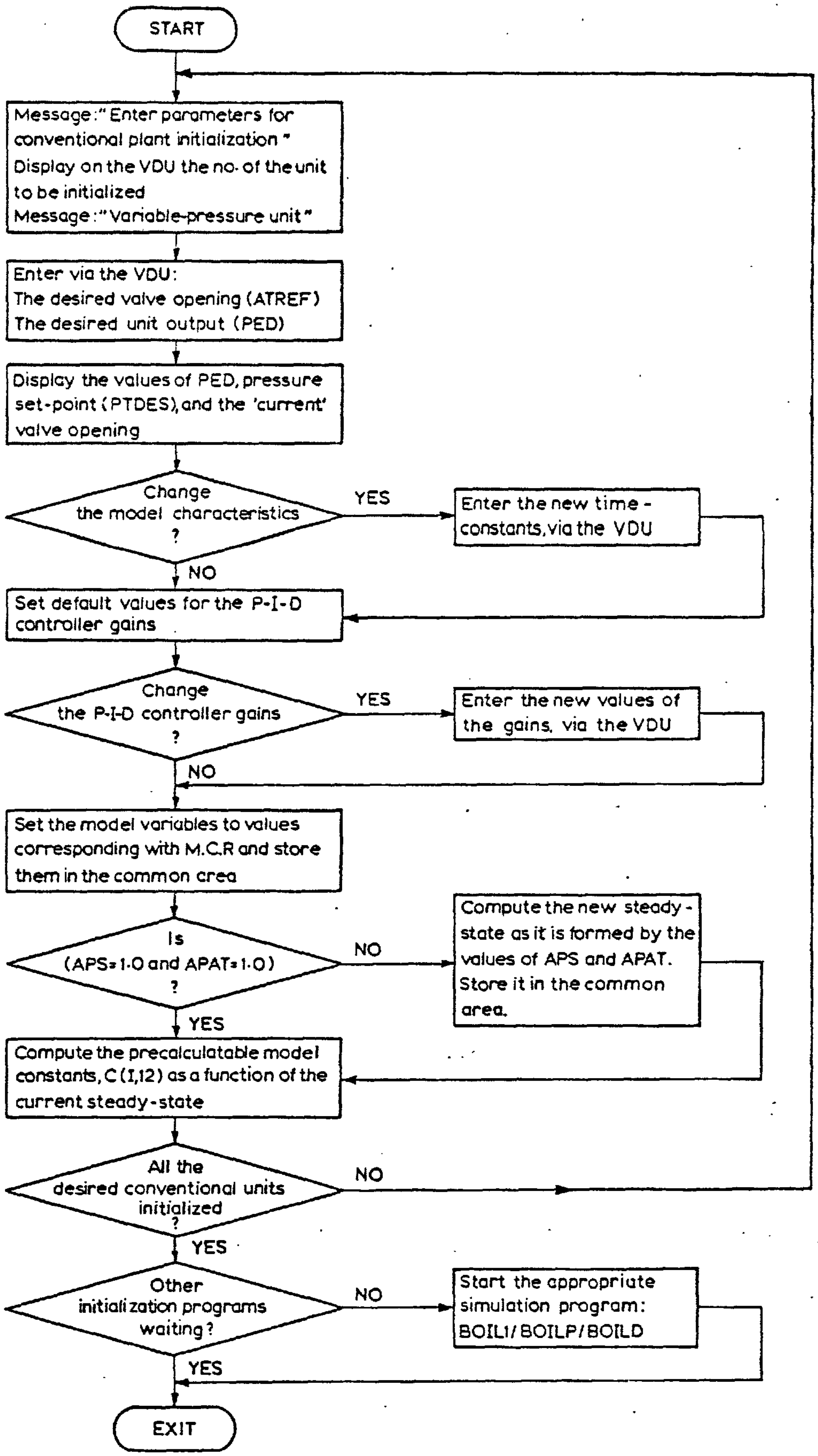

Fig. 6.5: Initialization program for the variable-pressure boiler model (PINIT).

Table 6.2: Core and Processor Usage by the Sumulation and Initialization Programs

Program (Task) Name	Core needed by the program (octal words)	Core needed by the Task (octal words)	Average execution ti-me for a single unit (% of system's time)	Execution time for six units (% of system's time)	Partition	Residency
BOILC	1720	3644	6.4	38	P4.1	Core
BOILN	1612	3554	4.4	26	P4.1	"
BOILH	2101	3636	4.7	28	P4.1	"
BOILP	2721	4442	11.6	——	P4.1	"
BOIL1	4474	6470	Conv. 7.4, Nuc. 5.4, Hyd. 4.7	Conv. 44, Nuc. 32, Hyd. 28	P4.1	"
BOILD	3116	5106	22(1 CP+1 VP units)	——	P4.1	"
SINIT	For the resident code 5711	7632	——	——	P5	Disc
NINIT	5632	7304	——	——	P5	"
HINIT	6531	7732	——	——	P5	"
PINIT	5733	7620	——	——	P5	"
PLINT	6613	7140	——	——	P5	"

BOIL1 is the biggest of the simulation programs, requiring just under the 7000 octal words of core allocated to the partition P4.1.

All the simulation Tasks are installed in the real-time system and the start program PLINT fixes the appropriate Task in core, according to the model selection.

On Table 6.3 the core and processor usage is shown for the basic real-time programs used.

Table 6.3 Core and Processor Usage by the basic real-time programs

Program name	Partition	Size	Residency	Frequency of Execution	Processor Usage %
RSX	-	-	Core	-	3
ANIN2	INAN	250	Core	100 ms.	12
ANOUT	OUTAN	63	Core	400 ms.	1
DIGIN	STATIO	230	Core	200 ms.	v.small
SIMLD - manual loads	P2.4	3450	Core	1 s.	1
- auto loads					3.5
- random fluctuations					9.5

CHAPTER SEVEN

CONCLUSIONS

7.1 CRITICAL REVIEW OF THE WORK

The aim of the work which is presented in this thesis was to provide the Power Systems Simulator with a representation of the prime mover storage times involved in the power generation. The simulator was not designed for the study of the fast transients following a disturbance. It is geared towards the investigation of the phenomena occurring as a result of rather prolonged imbalances between generation and consumption. In other words, the long-term response of the system. For this reason, in developing the models, the emphasis was put on obtaining a credible gross response of each power plant. It is this which affects the operation of the rest of the system. But at the same time it was thought appropriate to include in the models some of the basic process variables. This will give the opportunity to the simulator user to study their behaviour in conjunction with the other main variables of the system.

It was decided to use digital simulation to avoid problems involved in the implementation of long time constants with electronic circuits, such as off-sets and drifts in the operational amplifiers. The analog part of the simulator was designed for real-time operation. Therefore the same requirement was set for the digital part. This meant that the development of the models should be done within the constraints imposed by the existing software and hardware of the operating system. In other words, the models had to be simple and fast.

Constant-pressure boiler model

In Section 2.2 an outline is given of the most common ways found in the literature with which to simulate the various boiler sections. It is well established that the "lumped" parameter representations and the use of ordinary differential equations can describe the process adequately. So a mixture of non-linear algebraic and differential equations was used for the model. Their number and their complexity was limited by the real-time operation requirements. Limited amount of core was allocated to the digital simulation. This meant that several attempts had to be made before a reasonably accurate representation was found, which will fit in the assigned core partition.

At the same time, equally serious consideration had to be given to the constraints on the computation time. The maximum number of units for which the program was designed is six. Therefore the computation time for each unit had to be less than 50 ms (the simulation program runs every 300 ms). It was found that the computation of square roots and exponentials needed long computation time. So the model had to be modified accordingly. Also some space had to be allowed for the instructions which enable the model to communicate with the analog part of the simulator. This was the main reason why the superheater has only one section. A second section involved another square root. Having decided on the number of equations and their kind, then every effort was made to minimise the number of operations needed by them. This is very useful and sometimes can save considerable computation time. Therefore, reasonable knowledge is needed beforehand about the core available and the computational capabilities of the computer. All these give an indication of the kind of problems with which one is faced in a real-time application.

The data used for this model were taken from reference 14. They correspond to a 200 MW coal-fired, drum-type boiler operating at full-load. It is believed that the use of real data is very important. It gives a more immediate insight into the process. It also helps to spot with greater ease that the model response is not right, by just looking, for example, to an unreasonably high value of pressure. Unfortunately the complete data of this kind are not readily available in the literature. Scattered data for different sections can be found in different papers. So it is important to have data of a single system, and not use incompatible data.

The responses of the model in real-time (shown in section 2.6.3) are considered very satisfactory. The model has been used successfully together with the analog part of the simulator for various types of tests.

Discretization of the continuous equations

The numerical methods of integration are unsuitable for real-time applications. They require a very small integration step to give stable responses. Also with the set of equations used for the boiler model, it was not straightforward to have the non-linearities isolated between transfer functions. So the digital simulation methods which require this kind of model representation could not be used. The method of substituting the continuous integrator with an approximate discrete one, is a very attractive method and it was found well suited to the problem in hand. It is easy to apply and there is a variety of approximate integrators to choose from. No problems were encountered when two different approximate integrators were used, for different sections of the same model. This helped a lot in putting the equations in a programmable order. So it can be said that the discretization method to be used, must be selected according to the problem.

The initial development of the model was done off-line. During this stage the sampling interval (or integration step) was chosen. This is desired to be as big as possible, to reduce the loading on the operating system. The 300 ms finally chosen is not very big, but that does not present particular problems. The maximum of 44% loading shown on Table 6.2 for six units is relatively high. But there is no other software so expensive in computation time to be added. So a loading of 60-65% on the system is not so bad for the purposes that the simulator is presently used.

Nuclear model

Here the assumption that the secondary circuit can be represented as in the conventional model is valid. The response of the nuclear model in the regulating mode is reasonable. With a more elaborate feedwater controller, the response of the throttle pressure could be much better. The non-regulating response is also good. As long as the raise/lower mechanism in its present form is used to change the valve position (in response to frequency level), this response cannot be particularly smooth. The filtering of the frequency input signal helps, but not very much.

Hydro model

The overall response of this model proved very successful. The solution of the water-hammer equations with the Laplace Transform method is very suitable for modelling. Despite the fact that only the first order approximation of the hyperbolic terms involved was taken, the response is very good. It would be interesting to see what this model can give with a higher order approximation. The coupling between the digital part and the analog generating unit was successful, despite original misgivings.

Data from the Appalachia plant were used in the model (see Appendix F.1). A differential surge tank is used at the Appalachia plant. In the model, the inclusion of the equations describing this type of tank, made it impossible to get a stable response. A restricted-orifice surge tank representation was used instead. But the water oscillations in the tank after a full-load rejection and a full-load acceptance test, were the same as those reported for the Appalachia plant. This indicates that the design of the parameters of the tank determines the good or bad response.

The use of a linear and a non-linear expression for the computation of the head at the turbine entrance, serves its purpose well. The only undesirable effect of it, is that "jump" which it causes to the model output at around 20% gate opening, during an increase in demand (Fig.4.20).

The governor dead-band and the speed effect of the turbine were not included in the model. But their inclusion is straightforward in the simulation program, for anyone who wishes to study their effect on the response.

It would be very desirable to compare the model's response to that of the real plant. This is true for all the models, but unfortunately this kind of real life response cannot be found easily.

Variable-pressure boiler model

The concept of variable-pressure is not a new one. But the interest in this kind of operation of big conventional plant has grown over the last few years. So it was considered appropriate to include a model of this kind in the simulator. Obviously the fundamental benefit of such a plant lies in the improved efficiency at low loads and the flexibility during start-up and shut-down. These properties cannot be studied from the used model. What can be studied is the control of the plant's output and the impact of its operation on the rest of the power system.

The model can be operated in the passive and active pressure governing mode. The latter provides some interesting control problems. As was shown in Sections 5.3 and 5.4, the critical factor is the control of the valve opening. It must assist the initial response of the output and return to its desired value when the pressure has risen enough to support the increasing output. The control scheme described in Section 5.4 does this job with reasonable success. However, it is clear that a much more sophisticated algorithm is needed to improve the response. This is, of course, the response during a change in the demand signal.

The response of the model to frequency changes is particularly good. The governor acts normally on the valve in response to frequency deviations. The valve opening is kept by the controller around this initial value, giving time to the pressure controller to react and change the pressure accordingly. The creation of an appropriate transient set-point for the valve opening, forms the heart of this response.

Software

The two main blocks of software developed during this work are the simulation programs and the initialization programs. Other programs are developed as well for testing, logging, displaying, etc., but they are not described in Chapter 6. In the simulation programs the main point of attention is the reduction of their computation time, particularly when more than one type of plant model is involved.

The initialization programs are large and for this reason they were split into a number of subroutines. They were chained to the main program. The form of the initialization program is very important, because it determines how easy it is to start the digital simulation. In other words, how flexible is the use of the digital simulation in setting up a complex power system on the simulator.

The method of computing the "current" steady-state of the initialized unit just before the unit is put on-line to the system, proved very successful. In this way the digital simulation integrates into the system smoothly, without upsetting its operation. In addition to that, the initialization programs interact with the user in a conversational mode. So they provide the opportunity to change some of the basic parameters of each model and so to give different characteristics to each unit.

General comments

The models were kept non-linear. As was shown in Sections 2.5.1, 2.7 and 4.5, the non-linearities provide a more realistic model. What is more important is that it can be used over most of its operating range. This was essential in order to keep in line with the analog part of the simulator which has this capability.

Fortran IV was the inevitable choice for the digital simulation, although these programs are executed three times a second. The assembler language is much more efficient, but it would make the writing of mathematical programs very time-consuming. In addition it reduces the flexibility of modifying them easily.

The operator action was not included directly in the models. The reasons for this are the following:

(a) The most likely way of simulating this action is by an integrator which will start acting at a specified time interval after a disturbance. This can be done easily by the simulation program. But only the response after one disturbance could be studied. The simulation runs carried out on the simulator are usually continuous over a long period of time. Under these circumstances it is very difficult to simulate repeated operator actions.

(b) The simulator hardware provides the facilities to the user to intervene manually himself, thus playing the part of the operator. This is a far better way of introducing operator action than to include a rather unrealistic representation in the program.

In conclusion, it can be said that the addition of the digital simulation of the power plants provided the simulator with the capability of realistically representing the operation of a complete power system. The variety of power plant models provides the choice of systems with different generation configurations.

The work reviewed in this section represents the bulk of the author's contribution to the simulator project.

7.2 FREQUENCY CONTROL TESTS

To demonstrate the use of the Simulator to further studies of power system behaviour, some results of Load Frequency Control (LFC) (or Automatic Generation Control - AGC) studies are briefly presented below.

Mogridge in his thesis[43] tested three schemes of AGC. They are:

(i) Simple Tie-Line Bias
(ii) Error Adaptive Control Computation (EACC)
(iii) Non-Linear Tie-Line Bias

The first is the method which is used for many years by most of the power utilities. The Area Control Error (ACE) is formed by the well known expression:

$$ACE = \Delta P_{tie} - B.\Delta f$$

and then it goes through a PI controller to compute the generation change required by the area.

The second method represents an improvement to the basic tie-line bias algorithm. According to this method, the probability is assessed that control action is required and the gains of the PI controller are modified accordingly[79,80,81]. This is aimed at reducing the control action for small rapid load changes, while providing decisive action during large load changes. The third method recognises the fact that the Area Frequency Response Characteristic, β , is not linear. For small frequency deviations the characteristic has a smaller value. This is largely due to the governor deadbands. Therefore the tie-line frequency bias B should itself be non-linear.

As a small step further, some more tests were carried out during the present work to verify the performance of the scheme using:

(iv) Non-Linear Tie-Line Bias <u>and</u> EACC.

For all these tests the power system configuration shown on Fig. 2.23 was used. The two generators were driven by the digital constant-pressure boiler model. The system was isolated from the tie-line. Each test lasted 20 mins and the analysis of the results was based on 1200 samples taken over this interval. The generation allocation program looks at each generator in turn and allocates an appropriate change in generation taking into account the operating limits of the unit.

The EACC scheme does the following tests: the ACE and its integral are summed up to a maximum value. If the sign of the sum remains constant and its magnitude greater than a specified value for more than a specified time interval, the gain of the controller is changed from zero. In other words, the PI controller is allowed to take action. This check is done for two levels of error magnitude and duration. For a third check, only the ACE is considered. If it is very large, a big gain is given to the controller. The parameters and gains used for the EACC algorithm areshown in Appendix G. More details about the implementation of the algorithm can be found in reference 43.

Two sets of tests were done. In the first, only random load fluctuations were imposed on the system. The second involved large trend load changes with the random fluctuations superimposed. The results of these tests are shown on Tables 7.1 and 7.2. The comparison criteria are the standard deviation of the frequency and the total control action by all generators in the area.

For small load variations (Table 7.1): the EACC indeed results in less control action with comparable (to the simple tie-line bias) quality of frequency control. The use of non-linear frequency bias clearly is favoured by the small load variation situation. This method provides with even better frequency control. So the combination of both EACC and non-linear bias methods in algorithms 4 and 4a leads to even better frequency control and generator control action.

The EACC is favoured by the large load fluctuation conditions. As can be seen on Table 7.2, it gives better overall control than the simple and non-linear tie-line bias methods. But again the algorithm no. 4 combines the qualities of methods 2 and 3 and gives better performance in every aspect.

The comparison between algorithms 4 and 4a shows that the latter gives marginally better generator control action. This is what was expected when the specified time interval for the second EACC test was increased (see Appendix G).

The performance of the variable-pressure boiler model was tested with some of the AGC schemes just described. The algorithms were kept the same, but the generation allocation program was changed. This was because these units respond to changes in their demand signal and not to raise/lower pulses to the speeder gear. The additional generation was divided equally between the units, taking into account their operational limits.

With the simple tie-line bias algorithm running every 3 s, it was found that the frequency control was much worse than with the system left alone (for random load fluctuations only). This was because the VP units were introducing oscillations into the system because of the way of changing their outputs. With the same algorithms running every 6 or 9 s, the situation improved slightly. Some improvement was also observed when using the non-linear bias algorithm. Therefore it can be said that the VP units are not suitable for normal LFC algorithms. They need to change their output over a much larger period of time. Thus they would favour a control algorithm which sets an output target for them at some moment in the future. A scheme of this nature was proposed by Keyhani et al[82].

Table 7.1: AGC of Random Load Fluctuations

A G C Algorithms	σ_f	σ_{ACE}	Total Generator Control Action (No. of Pulses)				
			Fast Raise	Slow Raise	No Action	Slow Lower	Fast Lower
None*	0.0970				800		
1*	0.0374	0.0187	282	46	165	58	249
1*	0.0374	0.0187	280	46	158	51	265
2*	0.0387	0.0195	239	6	349	0	206
2*	0.0412	0.0205	234	4	353	1	208
3*	0.0332	0.0167	228	51	251	56	214
3*	0.0332	0.0167	199	72	279	58	192
4	0.0224	0.0110	81	33	600	9	77
4	0.0224	0.0114	100	14	588	8	90
4a	0.0245	0.0118	90	13	618	9	61
4a	0.0200	0.0100	69	17	644	16	64

σ_f Standard deviation of frequency

σ_{ACE} Standard deviation of ACE

* Taken from reference 43

AGC Algorithms
1 – simple tie-line bias
2 – EACC
3 – non-linear frequency bias
4, 4a – EACC + N.L. frequency bias

Table 7.2: AGC of large load changes

A G C Algorithms	σ_f	σ_{ACE}	Total Generator Control Action (No. of Pulses)				
			Fast Raise	Slow Raise	No Action	Slow Lower	Fast Lower
None*	0.1723	—	—	—	800	—	—
1*	0.0557	0.0277	280	56	175	44	245
1*	0.0500	0.0249	285	26	258	21	210
2*	0.0500	0.0251	266	16	294	4	220
2*	0.0458	0.0228	267	26	271	11	225
3*	0.0574	0.0286	288	41	187	47	237
3*	0.0529	0.0228	277	26	272	26	199
4	0.0469	0.0232	207	31	385	12	165
4	0.0480	0.0243	207	22	382	14	175
4a	0.0458	0.0228	198	23	403	15	162
4a	0.0490	0.0245	213	17	376	7	187

σ_f Standard deviation of frequency

σ_{ACE} Standard deviation of ACE

* Taken from reference 43

AGC Algorithm

1 – simple tie-line bias
2 – EACC
3 – non-linear frequency bias
4
4a – EACC + N.L. frequency bias

Such a scheme was not investigated in the present work, but it seems to be the most appropriate method of involving a variable-pressure unit in the frequency control.

The nature of the tests described in this section demonstrates the potential of the simulator for the study of the overall system response under various operating conditions.

7.3 RECOMMENDATIONS FOR FURTHER WORK

The aim in developing the conventional, nuclear and hydro plant models was that each of them could be used with the full capability of the simulator, i.e. six units. From this point of view there is little improvement or modification that can be done to these models, especially to the conventional. They are all very near the limits from the core usage and execution time points of view. However, if each model is used individually and no more than 2 or 3 units are simulated at the same time, there is room for some expansion and improvement.

In this light, the constant pressure boiler model could be extended to include a steam temperature loop or a more detailed representation of the air and fuel inputs. A second superheater section could also be added. For the nuclear plant model the two obvious additions would be a simple representation of the reactor dynamics and a more sophisticated control of the final pressure. The former addition would mean having a control loop for the gas outlet temperature, instead of assuming it constant.

For the hydro plant model there is perhaps more work that can be done, if more detailed studies of its effect on the whole system are desired. The inclusion of a dead-band in the governor is straightforward, as it is the speed effect at the turbine entrance. A better way of making possible the use of the model at its lower operating range could also be investigated. A second or third order approximation of the hyperbolic terms involved in the solution of the water-hammer equations can be taken and the difference in the response of the model compared. Of course, this might be a little expensive in computation time. Finally, other configurations or performance improvements for the governor can be investigated. For example, a separation of the overall generation and the speed channels, so that the speed control is not superseded by the generation control, as was reported in reference 83.

In the variable-pressure model the control configuration of the output can be improved. Here again the limitation would be the computation time, since the unit in its present form needs around 11% of the system's time.

It must, however, be stressed that beyond a certain complexity the study of the behaviour of a plant model does not benefit from the real-time environment. Off-line investigation is more suitable.

From the AGC point of view, certainly more work can be done in testing improvements to the tie-line bias concept. The LFC tests done so far do not include optimal dispatching. When the corresponding programs being developed are ready, the same tests can be repeated and the results compared to those already obtained. Optimal control approach is, of course, the next in line. Fosha and Elgerd[84] published one of the first investigations in this context and others followed. It is the author's opinion that in such an attempt, attention must be focused on the following points: the states of the system that will be used, must represent variables which are already available. Estimators can be used for other states needed. The output of the feedback controller (which is the input to the system) must be a meaningful quantity which can be used directly with the existing hardware in each station. For example, the corresponding output in the algorithms presented in Section 7.2 is the required change in generation. This is implemented by sending raise/lower pulses to each generating unit. With an optimal scheme, some modification to the existing hardware might become necessary.

Some kind of load prediction algorithm can be developed for the interval of 5-10 mins ahead. This can be used to provide the demand for the variable pressure unit. The effects of such a scheme within a system with normal AGC can be investigated. Another interesting problem is what is the percentage of units operating in the variable-pressure mode, that can keep the system stable. This could be investigated on the simulator, although it would require more than two generating units.

On the hardware side, the most immediate requirements are to build some more generating units and external system equivalents. They will be used to represent other areas in the AGC studies.

So there is a wide variety of studies that can be made on the simulator. This highlights its usefulness as a research and as an educational tool, the two main areas for which it is presently used.

7.4 THE SIMULATOR IN THE FUTURE

The drawbacks of the simulator at its present form can be summarised as follows. The analog hardware (with the exception of the interface) is in a state which makes its maintenance difficult for anyone who was not involved inbuilding it. The calibration of the various variables is not easy. Therefore it would be of great benefit if most parts of it are rebuilt on the existing design. A compact modular form of the various sections is needed, with the calibration and other critical points easily accessible. Better quality components could also be used in some sections to improve the accuracy of the simulation.

In the computer side, the 24 k of memory is just enough for the moment. But as new real-time programs are developed, the situation will deteriorate. The floating point arithmetic is done by software. This increases the loading of the operating system. It must also be kept in mind that the computer is not used only for control algorithms, but also for simulation. The addition of hardware for the floating point operations will radically change the situation. The time factor on most of the big programs would not be critical. The performance of the operating system could also be greatly enhanced if the most frequently executed Tasks are core resident. The answer to this is the addition of more memory. This is becoming more and more a cheap solution,with today's prices for non-volatile memory.

The interest in simulators for research, design, training and education purposes keeps rising. More and more sophistication is required from the employed hardware and software. The question that is often asked is: what should be the future of the simulators? Will they all be analog or is it preferable to use the capabilities of today's digital computers and go for all-digital simulation? Clearly the requirements of the specific job in hand must be studied carefully before a decision is made. But it seems that the combination of analog and digital techniques offers many advantages. Also, the real-time simulator has the edge in a great deal of applications. It provides the operator with real life experience, which cannot be acquired cheaply in any other way.

Finally, in keeping up with the state of the art, the feasibility of using microprocessors as plug-in modules each representing a section of the process, is worth investigating.

APPENDIX A

DERIVATION OF THE STATE-EQUATIONS OF THE CONVENTIONAL BOILER MODEL

The relations between the variables describing the condition of the steam at the different points of the Rankine cycle are very complicated[26,28] and unsuitable for use in the simulation. Therefore, the only way to derive useful relations between the variables of interest is to approximate the complicated expressions with simpler ones over their operating range. Obviously the smaller this range, the simpler and more accurate is the approximate expression.

For this purpose, values from the steam tables in references 26 and 28 were used. The basic tool in performing this approximation was the subroutine: EØ2ABF of the N.A.G. Library. This routine requires a certain number of points (x,y) and the maximum degree of the polynomial, which would be the "best fit" to these points. It outputs the coefficients of the polynomial.

This technique was used to derive the state equations for the drum. For the equations of the form: $T = f(h,P)$, the procedure was as follows: first an approximation of the form of $T = f_1(h)$ was sought, with P = constant. This was repeated two or three times for different values of P each time. Finally the f_1 function was augmented by a first order term containing the pressure P.

For the equations of the form: $P = f(T,\rho,h)$, the technique described above was not successful. Instead, a more empirical technique was used. According to this:

(a) The form of the expression needed is firstly defined; the expression $P = a(h) + b(\rho \cdot T) + c(\rho) + d$ was chosen.

(b) For four pairs of (pressure, temperature) values spreading through the chosen operating range, the values of: $P,h,(\rho.T),\rho$ are computed from the steam tables. So a system of four equations with four unknowns (a,b,c,d) is formed and solved.

(c) The values of P are computed for the four points, from the expression found in (b). If they are different from the value of the pressure corresponding to these four points, a correction in the slope of the expression found is performed and finally the constant term is adjusted to give a better approximation. So the state equations of the different sections are presented below:

For the economizer section:

$$T_{EO} = f(h_{EO}, h_{EO}^2, P_{EO})$$

A quadratic approximation was sought here between 2250 psia and 3000 psia:

$$T_{EO} = 0.00142205.h_{EO}^2 - 0.714374.h_{EO} + 492.688 + (P_{EO}-2250.).0.02622 \qquad (A.1)$$

The value of P_{EO} was considered to be constant at 2690 psia. T_{EO} is expressed in (^oF) and h_{EO} in (Btu/lb).

For the drum:

According to Kwatny et al[17], it is possible to express most of the important variables of this section as a first order approximation of the steam density. This was done and the equations considered are shown below:

$$P_{SD} = 182.25.\ \rho_{SD} + 1104.3495 = E4.\ \rho_{SD} + EE4 \qquad (A.2)$$

$$h_{SD} = -18.508189.\ \rho_{SD} + 1232.77 = E1.\ \rho_{SD} + EE1 \qquad (A.3)$$

$$T_{SD} = 12.374294.\ \rho_{SD} + 570.782 \qquad (A.4)$$

$$h_{DW} = 28.9252.\ \rho_{SD} + 502.55365 = E2.\ \rho_{SD} + EE2 \qquad (A.5)$$

$$\rho_{DW} = -1.8452.\ \rho_{SD} + 49.16861 = E3.\ \rho_{SD} + EE3 \qquad (A.6)$$

Radiant superheater:

$$T_{RSHO} = f(h_{RSHO}, h_{RSHO}^2, P_{RSHO}), \quad P_{RSHO} = f(h_{RSHO}, T_{RSHO}, \rho_{RSHO})$$

The range of values in which the approximation was sought is 2700-2500 (psia) and 870-680 (^oF) for the first equation. For the second equation, the pressure range was: 2300-2600 (psia) and the same range of temperatures. So:

$$T_{RSHO} = 0.00202374.h^2_{RSHO}-4.21809.h_{RSHO}+2860.993713+0.111956. .(P_{RSHO}-2500.) \quad (A.7)$$

$$P_{RSHO} = -12.914237.h_{RSHO}+3.29762.(\rho_{RSHO}.h_{RSHO})-2524.341.\rho_{RSHO}+ +4.9682.\ T_{RSHO}+15291.15032 \quad (A.8)$$

Primary Superheater:

$$T_{SO} = f(h_{SO},h^2_{SO},P_{SO}), \quad P_{SO} = f(h_{SO},T_{SO},\rho_{SO})$$

The range of values for approximating the first equation is: 2300-2550 (psia) and 700-1000 (^oF). For the second equation: 2300-2600 (psia) and 700-1000 (^oF), respectively. The two equations are:

$$T_{SO} = 0.00169706.h^2_{SO} - 3.38587.h_{SO} + 2332.715732 + + 0.057608.(P_{SO}-2500.) \quad (A.9)$$

$$P_{SO} = 0.478726.h_{SO} - 1.211622.(\rho_{SO}.T_{SO}) - 1.68442.T_{SO} - - 552.51852.\rho_{SO}+1390.564147 \quad (A.10)$$

Secondary Superheater:

$$T_{SSO} = f(h_{SSO},h^2_{SSO},P_T), \quad T_{SS} = f(h_{SS},h^2_{SS}, \frac{P_T+P_{SO}}{2}), \text{ and}$$

$$P_T = f(h_{SSO},\rho_{SSO},T_{SSO})$$

The range of values for approximating the first two equations was: 2200-2450 (psia) and 1140-740 (^oF), while for the third 2200-2500 (psia) and the same as before for the temperature.

$$T_{SSO} = 0.00136038.h^2_{SSO}-2.47266.h_{SSO}+1710.1725+0.03028.(P_T-2400.) \quad (A.11)$$

$$T_{SS} = 0.00136038.h^2_{SS}-2.47266.h_{SS}+1710.1725 + + 0.03028\ (\frac{P_T+P_{SO}}{2} - 2400.) \quad (A.12)$$

$$P_T = 7.506323.h_{SSO} + 0.791613.(\rho_{SSO}.T_{SSO}) + 56.574279.\rho_{SSO}$$
$$- 4.432895.T_{SSO} - 6783.397 \qquad (A.13)$$

APPENDIX B

B.1 DISCRETIZATION OF THE DRUM AND SH EQUATIONS USING TUSTIN'S OPERATOR

The continuous-time equations are:

$$(Q_W+W_{EO}\cdot h_{EO} - W_{SD}\cdot h_{SD}) = (1/C_D)\cdot\frac{d}{dt}(P_{SD})$$

$$W_{SD} = \sqrt{F_{SDI}\cdot\rho_{SD}\cdot(P_{SD}-P_T)}$$

$$\rho_{SD} = (P_{SD} - EE4)/E4$$

$$T_{SD} = E5.\rho_{SD} + EE5$$

$$h_{SD} = E1.\rho_{SD} + EE1$$

$$\frac{d}{dt}(P_T) = (1/C_{SSH})\cdot(W_{SD}-W_T)$$

$$W_T = K_T.A_T.P_T$$

Substituting the Tustin integrator, they become:

$$P_{SD}(K) = P_{SD}(K-1)+(\frac{C_D.T}{2})\left[(Q_W(K)+Q_W(K-1))+(W_{SD}(K)+W_{SD}(K-1)).\right.$$
$$\left. .(E6.P_{SD}(K)+EE6)\right] \qquad (B.1.1)$$

$$W_{SD}(K) = \sqrt{F_{SDI}\cdot\rho_{SD}(K)\cdot(P_{SD}(K)-P_T(K))} \qquad (B.1.2)$$

$$\rho_{SD}(K) = (P_{SD}(K)-EE4)/E4$$

$$T_{SD}(K) = E5.\rho_{SD}(K)+EE5$$

$$P_T(K) = P_T(K-1)+(\frac{T}{C_{SSH}.2}).\left[W_{SD}(K)+W_{SD}(K-1)-W_T(K)-W_T(K-1)\right] \qquad (B.1.3)$$

$$W_T(K) = K_T.A_T.P_T(K) \qquad (B.1.4)$$

where: $E6 = -(E1/E4)$ and $EE6 = h_{EO}-(EE1-(EE4.E1/E4))$

B.2 P I D Controller - Conversion to its discrete form

The basic form of an analog P I D controller is:

$$D_1(s) = K\left[1 + \frac{1}{T_{RR}s} + T_{DD}s\right] \qquad \text{(B.2.1)}$$

where: K = proportional gain,

T_{RR} = reset time constant,

T_{DD} = rate time constant.

The input of the controller is sampled. Sampling may drastically change the response of the system. Now, if a data reconstructor is placed after the sampler, then the sampled response should be similar to the one of the system with a continuous circuit (at the sampling instants):

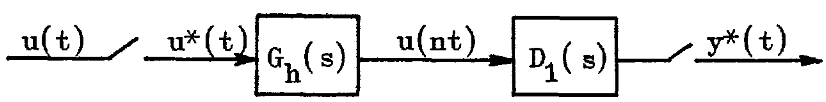

The data reconstructor $G_h(s)$ here, would be the Z.O.H., i.e. $G_h(s) = (1-e^{-Ts})/s$. So, the overall transfer function would be:

$$D(s) = G_h(s).D_1(s) = (1-e^{-Ts}).\left[\frac{K}{s} + \frac{K}{T_{RR}s^2} + K.T_{DD}\right] \qquad \text{(B.2.2)}$$

Taking the Z-transform, this relation becomes:

$$D(z) = \frac{P(z)}{E(z)} = \left[KPP + KIP.\frac{z^{-1}}{(1-z^{-1})} + KDP.(1-z^{-1})\right] \qquad \text{(B.2.3)}$$

where: $KPP = K$, $KIP = (K.T/T_{RR})$ and $KDP = (K.T_{DD})$.

Now, if $C(z) = (\frac{z^{-1}}{1-z^{-1}})E(z)$ the equivalent difference equation is:

$$C(K) = E(K-1)+C(K-1) = E(K-1)+E(K-2)+E(K-3)+\ldots = \sum_{j=1}^{K} E(K-j) \qquad \text{(B.2.4)}$$

Therefore, the difference equation for the P I D controller as a whole, would be:

$$P(K) = KPP.E(K) + KIP.\sum_{j=1}^{K} E(K-j) + KDP.(E(K)-E(K-1)) \qquad (B.2.5)$$

This algorithm is called absolute or Positional Algorithm because P(K) gives the actual value of the controlled variable at this particular instant.

APPENDIX C

C.1 COMPUTATION OF A NEW STEADY-STATE FOR THE CONVENTIONAL BOILER MODEL

The values of the variables corresponding to the full-load (100%) operating conditions are designated as X, while the corresponding values of the new steady-state as X' (e.g. W_{SD} and $W_{SD'}$).

Let us assume that both the valve position and the boiler pressure set-point values (in p.u.) are different from those corresponding to M.C.R. Both APAT and APS and therefore different from 1.0, but known. Then, from the model equations (Table 2.3), the values of the new steady-state are:

$$W_{SD'} = APS.APAT.W_{SD}$$

$$P_{T'} = APS.P_T$$

$$CCC = (P_{T'}.EE4) - ((W_{SD'})^2.(E4/F_{SDI}))$$

$$P_{SD'} = ((P_{T'}+EE4) + \sqrt{((P_{T'}+EE4)^2 - 4.CCC)})/2$$

$$T_{SD'} = (E5/E4).(P_{SD'}-EE4) + EE5$$

$$+W_{SD'} = \sqrt{(F_{SDI}/E4).(P_{SD'}-EE4).(P_{SD'}-P_{T'})}$$

$$W_{T'} = W_{SD'}$$

$$Q_{W'} = W_{SD'}.(E6.P_{SD'} + EE6 - h_{EO})$$

$$T_{RM'} = (Q_{W'}/K_{RS})^{(1/3)} + T_{SD'}$$

$$+Q_{W'} = K_{RS}.((T_{RM'}-T_{SD'})^3)$$

$$Q_{GW'} = Q_{W'}$$

$$R_{SD'} = (P_{SD'}-EE4)/E4$$

$$+T_{SD'} = E5.R_{SD'} + EE5$$

$$Z154 = (Q_{W'}/K_{RW}) + (0.55556.T_{RM'} + 255.372)^4$$

$$T_{G'} = ((Z154)^{0.25} - 255.372)/0.555556$$

$$X5 = (T_{G'}-T_A)/C(I,11)$$

For: $T_{G'} < 2633.037 \Longrightarrow L_{F'} = 218.0/(K_F((1/X5)-0.87)-K_A\cdot 2.342549026)$

For: $T_{G'} > 2633.037 \Longrightarrow L_{F'} = 286.0/(K_F((1/X5)-0.87)-K_A\cdot 1.367520004)$

+ The equations marked with (+) show the cases where some variables had to be computed again from equations, exactly as they are in the model, in order to assume values which will give a "stable" steady-state.

$A' = K_A.L_{F'}$

For: $T_{G'} < 2633.037 \Rightarrow W_{A'} = 218 + A' \cdot 2.342549026$

For: $T_{G'} > 2633.037 \Rightarrow W_{A'} = 286 + A' \cdot 1.36752004$

$MCR' = (K_F/K_{CF}).L_{F'}$

$W_{FI'} = K_F.L_{F'}$

$W_{GF'} = 0.87.W_{FI'} + W_{A'}$

$S_{E'} = L_{F'}/KIP$

C.2 PRECALCULABLE CONSTANTS FOR THE CONVENTIONAL MODEL

From Table 2.3, where both the discrete and the "real-time" representation of the model equations are shown, the constants which can be precalculated can easily be deduced. They are:

$$C(I,1) = (2-(T.K_{CF}))/(2 + (T.K_{CF})) \quad (C.2.1)$$

$$C(I,2) = (T.K_F)/(2 + (T.K_{CF})) \quad (C.2.2)$$

$$C(I,3) = (2.T_P-T)/(2.T_P+T) \quad (C.2.3)$$

$$C(I,4) = (T.K_{CF})/(2.T_P + T) \quad (C.2.4)$$

$$C(I,5) = (2.T_{AA}-T)/(2.T_{AA}+T) \quad (C.2.5)$$

$$C(I,6) = (K_A.T)/(2.T_{AA} + T) \quad (C.2.6)$$

$$C(I,7) = (T.E6)/C_D \quad (C.2.7)$$

$$C(I,8) = T/C_D \quad (C.2.8)$$

$$C(I,9) = EE6 - h_{EO} \quad (C.2.9)$$

$$C(I,10) = T/C_{SSH} \quad (C.2.10)$$

$$C(I,11) = F.n/C_{GF} \quad (C.2.11)$$

$$C(I,12) = T.C_M \quad (C.2.12)$$

From them, C.2.2, C.2.4, C.2.6, C.2.7 are computed in the program SINIT as functions of the "current" steady-state variables and the rest of the constants,and not as they are presented above.

APPENDIX D

LINEARISATION OF THE CONVENTIONAL BOILER MODEL EQUATIONS

The equations are considered in the order in which they appear in Table 2.3. The procedure is to denote the values of the variables corresponding to original steady-state as X_o and assume small excursions from this steady-state, which are denoted as X. So:

- The equations (2.91), (2.92), (2.93), (2.95) are already linear.
- Equation (2.94) becomes:

$$WA_o + W_A = W_R{}^3 . \sqrt{A_o + A} \quad \text{or} \quad (WA_o + W_A)^3 = (W_R)^3 . (A_o + A)$$

or $$(WA_o)^3 + 3(WA_o)^2 . W_A + 3(WA_o) . (W_A)^2 + (W_A)^3 = (W_R)^3 . A_o + (W_R)^3 . A$$

or $$W_A = (WA_o / 3 . A_o) . A \qquad \text{(D.1.1)}$$

- Equation (2.96) becomes:

$$\frac{d}{dt}(P_{SD_o}) + \frac{d}{dt}(P_{SD}) = (1/C_D) . \left[QW_o + Q_W + (W_{SD_o} + W_{SD}) . (E6.P_{SD_o} + E_6 . P_{SD} + EE6)\right]$$

or $$\frac{d}{dt}(P_{SD}) = \left[E6.W_{SD_o}\right] . P_{SD} + \left[E6.P_{SD_o} + EE6\right] . W_{SD} + Q_W$$

or $$\frac{d}{dt}(P_{SD}) = (K11 + K12.K16) . P_{SD} + (K12.K17) . P_T + (K13) . T_{RM} \qquad \text{(D.1.2)}$$

where:

$$K11 = (E6.W_{SD_o} - K26)/C_D$$

$$K12 = (E6.P_{SD_o} + EE6)/C_D$$

$$K13 = K25/C_D$$

- Equations (2.97) and (2.98) become:

$$\rho_{SD} = P_{SD}/E4 \qquad \text{(D.1.3)}$$

$$T_{SD} = (E5/E4) . P_{SD} \qquad \text{(D.1.4)}$$

– Equation (2.99) becomes:

$$(W_{SD_o}+W_{SD})^2 = F_{SDI}.(\rho_{SD_o}+\rho_{SD}).(P_{SD_o}+P_{SD}-P_{T_o}-P_T)$$

or $$W_{SD} = \left[\frac{F_{SDI}}{2.E4.W_{SD_o}}\right].\left[P_{SD}.(2.P_{SD_o}-P_{T_o}-EE4)+P_T.(EE4-P_{SD_o})\right]$$

or $$W_{SD} = K16.P_{SD} + K17.P_T \tag{D.1.5}$$

where: $$K16 = (F_{SDI}/2.E4.W_{SD_o}).(2.P_{SD_o}-P_{T_o}-EE4)$$
$$K17 = (F_{SDI}/2.E4.W_{SD_o}).(EE4-P_{SD_o})$$

– Equation (2.101) becomes:

$$(W_{T_o}+W_T) = K_T.(A_{T_o}+A_T).(P_{T_o}+P_T)$$

or $$W_T = (K_T.A_{T_o}).P_T + (K_T.P_{T_o}).A_T \tag{D.1.6}$$

– Equation (2.100), after substituting equations (D.1.5) and (D.1.6) into it, becomes:

$$\frac{d}{dt}(P_T) = P_{SD}.(K16/C_{SSH})+P_T((K17-K_T.A_{T_o})/C_{SSH})+A_T(-K_T.P_{T_o}/C_{SSH})$$

or $$\frac{d}{dt}(P_T) = P_{SD}.(K16/C_{SSH}) + P_T.K14 + A_T.K15 \tag{D.1.7}$$

where: $$K14 = (K17-K_T.A_{T_o})/C_{SSH}$$
$$K15 = -K_T.P_{T_o}/C_{SSH}$$

– Equation (2.102) becomes:

$$(T_{G_o}+T_G) = T_A+(F.n/C_{GF}).((W_{FI_o}+W_{FI})/(W_{GF_o}+W_{GF}))$$

or $$T_G = ((T_A-T_{G_o})/W_{GF_o}).W_{GF} + (F.n/C_{GF}.W_{GF_o}).W_{FI}$$

or $$T_G = K18.W_{GF}+K_{19}.W_{FI} \tag{D.1.8}$$

where: $$K18 = ((T_A-T_{G_o})/W_{GF_o})$$
$$K19 = (F.n/C_{GF}.W_{GF_o})$$

- Equation (2.104) becomes:

$$(Q_{W_o}+Q_W) = K_{RS}.(T_{RM_o}+T_{RM}-T_{SD_o}-T_{SD})^3, \text{ which ends up as}$$

$$Q_W = K25.T_{RM}-K26.P_{SD} \qquad (D.1.9)$$

where: $K25 = 3.K_{RS}.(K_{24})^2$

$K26 = 3.K_{RS}.K23.(K24)^2$

$K23 = E5/E4$

$K24 = T_{RM_o}+K22-(K23.P_{SD_o})$

$K22 = ((E5.EE4)/E4)-EE5$

- Equation (2.105) becomes:

$$(Q_{GW_o}+Q_{GW}) = K_{RW}.((T_{G_o}+T_G)^4-(T_{RM_o}+T_{RM})^4),$$

where T_G, T_{RM} are in (^oK). Again, after some manipulation one ends up with:

$$Q_{GW} = K29.T_G - K30.T_{RM} \qquad (D.1.10)$$

where: $K29 = 2.22223.K_{RW}.(K27)^3$

$K30 = 2.22223.K_{RW}(K28)^3$

$K27 = 0.555556.T_{G_o} + 255.372$

$K28 = 0.555556.T_{RM_o} + 255.372$

- Equation (2.103):

This is a linear equation, but it requires substitution of the linearised expressions of Q_W and Q_{GW}, i.e. equations (D.1.9) and (D.1.10). So:

$$\frac{d}{dt}(T_{RM}) = (K31).P_{SD}+(K32).T_{RM}+(K33).A+(K34).W_{FI} \qquad (D.1.11)$$

where: $K31 = C_M.K26$

$$K32 = -C_M.(K30 + K25)$$

$$K33 = (C_M.K29 \cdot K18 - W_{A_o})/(3.A_o)$$

$$K34 = (C_M.K29).(0.87 \cdot K18 + K19)$$

The state-space form of the model is shown in Table 2.5.

APPENDIX E

E.1 COMPUTATION OF THE NEW STEADY-STATE FOR THE NUCLEAR PLANT MODEL

The values of the new steady-state are denoted by a dash (i.e. X for the initial steady-state, X' for the new steady-state value). The values of APS and APAT are different from 1.0 for a steady-state other than the initial one. Therefore:

$$P_{T'} = APS.P_T$$

$$W_{SO'} = APS.APAT.W_{SD}$$

$$A_{T'} = APAT.A_T$$

$$B = P_{T'} + EE4$$

$$CCC = (P_{T'}.EE4)-((W_{SD'})^2.(E4/F_{DSI}))$$

$$P_{SD'} = (B+\sqrt{B^2-4.CCC})/2$$

$$T_{SD'} = (E5/E4).(P_{SD'}-EE4)+EE5$$

$$* \; W_{SD'} = \sqrt{(F_{SDI}/E4).(P_{SD'}-EE4).(P_{SD}-P_{T'})}$$

$$W_{T'} = W_{SD'}$$

$$XX' = 11.97777781.A_{T'}+112.222222$$

The computation of the new value for the metal temperature, T_{RM}, comes from the real root of a third order equation. This equation is derived from the relation:

$$\frac{Q_{W'}}{Q_{GW'}} = \frac{K_{RS}.(T_{RM'}-T_{SD'})^3}{XX'.(T_{CG} - T_{RM'})} = 1.0$$

So the new value for T_{RM} is computed as follows:

$$\left.\begin{aligned}
A1 &= -3.T_{SD'} \\
A2 &= 3.(T_{SD'})^2 + (XX'/K_{RS}) \\
A3 &= -(T_{SD})^3 - ((XX'/K_{RS}).T_{CG}) \\
Q &= (3.A_2-A_1{}^2)/9 \\
R &= (9.A1.A2-27.A3-2.A1^3)/54 \\
DD &= Q^3 + R^3
\end{aligned}\right]\text{ Computation of the real root}$$

$$R1 = R + \sqrt{DD}$$

$$R2 = R - \sqrt{DD}$$

$$S = \sqrt[3]{R1}$$

$$TT = \sqrt[3]{|R2|} \quad \begin{cases} \text{For } R2 < 0, & TT = -TT \\ \text{For } R2 > 0, & TT = TT \end{cases}$$

$$T_{RM'} = S + TT - (A1/3)$$

Computation of the real root

$$Q_{GW'} = XX'.(T_{CG} - T_{RM'})$$

$$Q_{W'} = Q_{GW'}$$

$$H = W_{SD'}.(E66.P_{SD'} + EE66 - h_{EO})$$

$$CC' = (H - Q_{W'})/h_{EO}$$

$$S_{E'} = CC'/KIP$$

$$W_{EO'} = W_{SD'} + CC'$$

where: $E66 = (E1/E4)$ and $EE66 = EE1 - ((EE4.E1)/E4)$

The values of E1, EE1, E4 and EE4 can be found in Appendix A.

E.2 PRECALCULABLE CONSTANTS FOR THE NUCLEAR PLANT MODEL

From the discrete and the "real-time" representation of the model equations, the constants which can be precalculated are:

$$C(I,7) = (T.E66)/C_D \tag{E.2.1}$$

$$C(I,8) = T/C_D \tag{E.2.2}$$

$$C(I,10) = T/C_{SSH} \tag{E.2.3}$$

$$C(I,12) = T.C_M = T.1.0670585552E - 05 \tag{E.2.4}$$

From them, C(I,7) is computed (in the program) as a function of the "current" values of the state variables and not as is given above.

APPENDIX F

F.1 NUMERICAL VALUES FOR THE HYDRO MODEL

The numerical values for the main variables and the other parameters of the hydro model, which correspond to full-load operating conditions, are presented below in Table F.1. They belong to the Appalachia hydro plant and they were taken from references 53, 58 and 60. All of the numbers are not exactly the same as the ones in these references, because they were adjusted to fit in the present model and to give a stable steady-state. Clarifications for any simplifications made are given below:

(a) For complex conduits, there is a reflection of pressure waves in points where changes in pipe thickness and diameter occur. In such cases, it is common practice to substitute the complex conduit with a simple one of uniform thickness and diameter. The cross-section area for such a conduit is given by the relation:

$$A_{eq} = \frac{\sum_i L_i}{\sum_i (L_i/A_i)} \qquad \text{(F.1.1)}$$

where: i = the i^{th} section of the complex conduit,

eq = stands for "equivalent".

(b) The height of the water level in the reservoir (H_R) was assumed to be constant.

(c) The friction losses in the tunnel up to the surge tank were taken to be: 100 (ft). For this value, the coefficient of frictional resistance is computed as: $f_2 = 0.016356$. For each penstock the frictional loss was taken to be: 25 (ft).

(d) The Appalachia plant has a differential surge tank. Instead, a restricted orifice tank was adopted in the model.

(e) For the governor, the typical values represented in references 68 and 69 were used for the time constants and the two droops.

TABLE F.1: STEADY-STATE VALUES FOR THE HYDRO MODEL VARIABLES

L_2 = 43200. (ft) — 41200, of 18-ft diam. concrete-lined tunnel; 2000, of 16-ft diam. steel-lined tunnel

A_2 = 251.38 (ft^2) equivalent cross-section

L_1 = 730.00 (ft)

A_1 = 95.0331 (ft^2)

V_2 = 12.769512 (ft/sec) for basic discharge of 3210.00 (ft/sec^2) for both units

V_1 = 16.88884 (ft/sec)

H_R = 419.34 (ft) constant

H_S = 319.34 (ft)

H_{S1} = H_S (ft) at steady-state

C_2 = 0.613270 (sec^2/ft)

f_2 = 0.016356 the coefficient of frictional resistance

H_T = 294.34 (ft)

C_1 = 0.087648 (sec^2/ft)

PTI = 40000.0 (kW) each unit

K_P = 8.046571681 ($kW.sec/ft^2$)

α_1 = 3500.0 (ft/sec) wave speed in tne penstock

α_2 = 4280.0 (ft/sec) wave speed in the tunnel

A_S = 3000.0 (ft^2)

KKA = 2500.

KKB = 146.546

KK1 = $(A_S)^2/T^2 \cdot 80000.\ (sec^2/ft^5) = \left[(A_S)^2/T^2\right].KK$

Governor:

T_G = 0.2 (s)

T_R = 5.0 (s)

T_P = 0.04 (s)

δ = 0.3

σ = 0.04

CC = $(\sigma .G)$

R = 0.0

E = T_G.R

D_N = 0.0

G = 1.0

K_1 = 1.0319285

F.2 COMPUTATION OF THE NEW STEADY-STATE OF THE HYDRO PLANT MODEL

As in Appendices C.1 and E.1, the variables corresponding to the full-load steady-state are designated as X, while those of the new steady-state are designated X' (e.g. V_1 and V_1').

Let us assume that the "current" position of the speeder motor in p.u. representation is APR (for full-load conditions, APR = 1.0), and that the frequency is at 50 Hz, so there is no frequency error. Then, the new steady-state of the model can be computed from the following equations:

$$\text{AAG} = \text{APR}$$

$$\text{AACC} = \text{AAG}$$

If equation (4.32) is used for the computation of the head at the turbine entrance (H_T), then:

$$\text{AAHT} = (\text{RRR})/(1 + (\text{AAG})^2.(\text{RRR}-1))$$

$$\text{AW} = \text{AAG}.\sqrt{\text{AAHT}}$$

$$\text{AAP} = \text{AVV.AAHT}$$

$$\text{AAS1} = (\text{AAHT} - (\text{AVV})^2).\text{XXX} + (\text{AVV})^2$$

If equation (4.31) is used for the computation of the head at the turbine entrance, then:

$$\text{AAA} = (1-\text{XXX})/\text{XXX}$$

$$\text{BBB} = (\text{KKA.GR})-\text{AAA}$$

$$\text{CCC} = -(\text{KKA.GR.AAG})$$

$$\text{AVV} = (-\text{BBB} + \sqrt{(\text{BBB})^2-4.\text{AAA.CCC}})/(2.\text{AAA})$$

$$\text{AAS1} = (\text{AVV})^2 + (H_R/H_{S1}).(1 - (\text{AVV})^2)$$

$$\text{AAHT} = (\text{AAS1}/\text{XXX}) - \text{KKA.AAG.GR} + \text{KKB.AVV.RVH}$$

$$\text{AAP} = \text{AVV.AAHT}$$

where:

$$\text{XXX} = (H_T/H_{S1})$$

$$\text{RVH} = (V_1/H_T)$$

$$\text{RRR} = (H_R/H_T)$$

$$\text{GR} = (G/H_T)$$

Finally, the new steady-state values are:

$$D_{PE'} = 0.0$$
$$R' = 0.0$$
$$G' = AAG.G$$
$$CC' = AACC.CC$$
$$H_{T'} = AAHT.H_T$$
$$V_{1'} = AVV.V_1$$
$$V_{2'} = AVV.V_2$$
$$H_{S1'} = AAS1.H_{S1}$$
$$H_{S'} = H_{S1'}$$
$$PTI' = AAP.PTI$$

F.3 PRECALCULATED CONSTANTS FOR THE REAL-TIME VERSION OF THE HYDRO PLANT MODEL

On Table 4.2, the discrete-time equations for the hydro model are shown together with their real-time version set of equations. From those two sets, the constants which can be precalculated (in the initialization program) are:

$$C(I,1) = C1 = (H_{S1}(I)-H_T(I))/(V_1(I).V_1(I)) \quad (F.3.1)$$

$$C(I,2) = C2 = (H_R-H_{S1}(I))/(V_2(I).V_2(I)) \quad (F.3.2)$$

$$C(I,3) = (T/T_G)/(T+2.T_P) \quad (F.3.3)$$

$$C(I,4) = (T-2.T_P)/(T+2.T_P) \quad (F.3.4)$$

C(I,5) = It can be used as a lower limit for the rate of change in the valve opening (F.3.5)

C(I,6) = It can be used as a higher limit for the rate of change in the valve opening (F.3.6)

$$C(I,7) = PTI(I)/(H_T(I).V_1(I)) \quad (F.3.7)$$

$$C(I,8) = ((\sigma.T)+2(\sigma+\delta).T_R)/(T+2.T_R) \quad (F.3.8)$$

$$C(I,9) = ((\sigma.T)-2(\sigma+\delta).T_R)/(T+2.T_R) \quad (F.3.9)$$

$$C(I,10) = ((C(I,8).G(I)+C(I,9).G_1(I))/CC(I))-1 \quad (F.3.10)$$

$$C(I,11) = (T-2.T_R)/(T+2.T_e) = (A_S/T)^2.(1/80000) \qquad (F.3.11)$$

$$C(I,12) = (H_T(I).(G(I).G(I)))/(V_1(I).V_1(I)) \qquad (F.3.12)$$

As can be seen, some of the constants are computed as functions of other constants and model variables; this was done for the purpose of achieving a "stable" steady-state for the model every time the initialization program is run.

A number of other constants are computed and entered as data in the beginning of the simulation program. Obsiously these constants do not change for every new steady-state that the model assumes. They are:

$$\left.\begin{array}{lll} CE1 & = & (2.A_1.g.L_1)/(\alpha_1^{\,2}.A_S) \qquad (F.3.13) \\ CE2 & = & (T.A_2)/A_S \qquad (F.3.14) \\ CE3 & = & (2.A_1.T)/A_S \end{array}\right] \text{ stored in the COMMON-BLSIM}$$

$$\left.\begin{array}{lll} CT1 & = & (T.g)/L_1 \qquad (F.3.16) \\ CT2 & = & (T.g)/L_2 \qquad (F.3.17) \\ CT3 & = & (T/2) \qquad (F.3.18) \end{array}\right] \text{ Entered as DATA}$$

APPENDIX G

PARAMETERS FOR THE EACC ALGORITHM

The parameters and the gains for each of the three tests done by the EACC are shown on Table G. The gain is applied to the PI controller as:

$$\text{Generation change} = \text{GAIN}.\left[K_P.\text{ACE}+K_I.\text{IACE}\right]$$

The choice of parameters for the AGC algorithms 4 and 4a was based on the following arguments. If the parameters were kept the same as for the algorithm no. 2, then:

- For small load variations the EACC will dominate all the time and because the errors will generally be small, the controller gain will be zero for most of the time. To bring into effect the presence of the non-linear bias, the EACC should be made to react to smaller errors. Hence the values for the maximum IACE and the time interval should be decreased.

- For large load changes, it is desirable that the EACC should dominate the algorithm for large errors. But even here the response to medium size errors must be limited.

TABLE G: EACC-Parameters for 3 s scheduling.

AGC Algorithm	Test No.	Max. IACE (p.u.)	Error magnitude for comparison (p.u.)	Time Interval (s)	Gain
2	a*	0.003	0.0036	24	0.75
	b*	0.006	0.009	12	1.00
	c*	0.0	0.015	1	1.5
4	a	0.0018	0.0021	18	0.85
	b	0.0045	0.0075	9	1.0
	c	0.0	0.015	1	1.5
4a	a	0.0018	0.0021	18	0.85
	b	0.0045	0.0075	→ 12	1.0
	c	0.0	0.0015	1	1.5

* Taken from reference 43.

REFERENCES

1. Bolton, M.J., Giles, C.B., Ramakers, H., Sheldrake, A.L. and Short, M.J., "Real-Time Hybrid Power System Simulator", PICA Conference 1975.

2. Sheldrake, A.L., "A Semiconductor analogue for the study of Dynamic Power Systems", Ph.D. Thesis, University of London, 1976.

3. Giles. C.B., "Development of a Hybrid Simulator for Power System Control Investigations", Ph.D. Thesis, University of London, 1976.

4. Mogridge, L., "Basic Software for the Digital Computer Section of a Hybrid Power System Simulator", M.Sc. Dissertation, University of London, 1975.

5. "Modern Power Station Practice", C.E.G.B., 1964, Vols. II-V.

6. Babcock & Wilcox Ltd., "Steam, its Generation and Use", New York, 1972.

7. Chien, K.L., Ergin, E.I., Ling, C. and Lee, A., "Dynamic Analysis of a boiler", Trans. Amer. Soc. Mech. Engrs., 1958, 80, p.1809

8. Daniels, J.H., Enns, M., Hottenstine, R.D., "Dynamic Representation of a Large Boiler-Turbine Unit", ASME Paper 61-SA-69, 1961.

9. Mark Enns, "Comparison of Dynamic Models of a Superheater", Trans. of the ASME, J. of Heat Transfer, November 1962, pp. 375.

10. Nicholson, H., "Dynamic Optimization of a Boiler", Proc. IEE Vol. 111, No. 8, August 1964.

11. Thomson, F.T., "A Dynamic Model for a Drum-type Boiler System", IEEE Trans., 1967, PAS-86, No. 5, pp. 625-635.

12. Anderson, J.H., "The Simulation and Control of a Power Boiler", Ph.D. Thesis, University of Manchester, May 1967.

13. Qualtrough, G.H., "Digital Computer Simulation and Control of a steam boiler", Ph.D. Thesis, University of Manchester, 1967.

14. Kwan, H.W., "Studies related to the simulation and control of a 200 MW Generating Plant", Ph.D. Thesis, University of Manchester, 1968.

15. Anderson, J.H., "Dynamic Control of a Power Boiler", Proc. IEE, Vol. 116, No. 7, July 1969.

16. Kwan, H.W. and Anderson, J.H., "A mathematical model of a 200 MW boiler", Int. J. Control, 1970, Vol. 12, No. 6, pp. 977-998.

17. McDonald, J.P., Kwatny, H.G. and Spare, J.H., "A non-linear model for Reheat Boiler-Turbine-Generator Systems",Part I -"General Description and Evaluation", and Part II -"Development", Proc. 12th Joint Automatic Control Conference, 1971, pp. 219-226 and pp. 227-236.

18. Laübli, F. and Fenton, F.H., "The flexibility of the supercritical boiler as a partner in power system design and operation", Parts I and II, IEEE Trans., 1971, PAS-90, pp. 1719-1733.

19. Aström, K.J. and Eklund, K., "A simplified non-linear model of a drum boiler-turbine unit", Int. J. Control, 1972, Vol. 16, No. 1, pp. 145-169

20. Hernandez, R. and Freris, L.L., "Micromachine Simulation of Steam Power Plant", Proc. IEE, Vol. 121, No. 6, June 1974.

21. Ashmole, P.H., Battlebury, D.R. and Bowdler, R.K., "Power System Model for large frequency disturbances", Proc. IEE, Vol. 121, No. 7, July 1974.

22. Anderson, P.M. and Nanakorn, S., "An Analysis and Comparison of certain Low-order Boiler Models", ISA Trans., Vol. 14, No. 1, pp. 17-23.

23. De Melo, F.P., Mills, R.J. and B'Rells, W.F., "Automatic Generation Control - Part I: Process Modelling", Trans. IEEE, PAS-92. 1973, pp. 710.

24. Sekoguchi, K. and Yang, W.J., "Dynamic analysis of drum-type boiler system through digital simulation", 2nd IFAC Symp. on Multi-variable Technical Control Systems, Düsseldorf, Germany, 11-13 October 1971.

25. Jacob Hawkins, "Elements of heat transfer", John Wiley & Sons, New York, 1957, 3rd Edition.

26. Keenan, J.H. Keyes, F.G., Hill, P.G. and Moore, J.G., "Steam Tables", John Wiley, New York, 1969.

27. U.K. Committee on the Properties of Steam, "U.K. Steam Tables in S.I. Units, 1970", Edward Arnold Ltd.

28. Hütte I , "Theoretische Grundlagen", W. Ernst & Son, Berlin.

29. Rosko, J.S., "Digital Simulation of Physical Systems", Addison-Wesley, 1972.

30. Sage, A.P. and Smith, S.L., "Real-Time Digital Simulation for Systems Control", Proc. IEEE, Vol. 54, No. 12, December 1966.

31. Sage, A.P. and Burt, R.W., "Optimum Design and Error Analysis of Digital Integrators for Discrete System Simulation", Fall Joint Computer Conference, 1965.

32. Durran, O.W., "Operation and Control of Once-Through Boilers during Electric Power System Emergencies", ISA Trans., Vol. 9, No. 4, pp. 284-297, 1970.

33. Taylor, E., "Modelling of once-through boiler dynamics", Proc. Int. Conf. on Boiler Dynamics and Control in Nuclear Power Stations, London 22-23 March 1973.

34. Adams, J. Clark, D.R., Louis, J.R. and Spanbauer, J.P., "Mathematical Modelling of once-through boiler dynamics", Paper 31 TP65-177, IEEE Winter Power Meeting, New York, Jan. 31-Feb. 5, 1965.

35. Hammons, T.J., "Simulation for once-through boilers employed for steam supply to large thermoelectric power units", 7th Univ. Conf., Bradford, June 1972.

36. Ruchinski, V.M. "Dynamics of the Automatic Control of a Boiler-Turbine Unit", Proc. 1st Int. Cong. of IFAC, Moscow, 1960, Vol. 4, pp. 365.

37. Davidenko, K. Ya. and Ruschinski, V.M., "Constructing a high-speed Non-linear model of a once-through steam generator", Thermal Engineering, Vol. 19, No. 3, pp. 115-120, 1972.

38. D.E.C., "RSX Real-Time Executive Reference Manual".

39. D.E.C., "Advanced Monitor Software System".

40. D.E.C.,"Chain and Execute, utility programs".

41. D.E.C.,"MACRO-15 Assembler, Programmers Reference Manual".

42. D.E.C., "PDP-15 FORTRAN IV, Programmers Reference Manual".

43. Mogridge, L. "Power System Load Variations and Frequency Control", Ph.D. Thesis, University of London, 1977.

44. Collier, J.G., Cox, R.F., Evans, L.S. and Bainbridge, G.R., "Potassium/Steam Cycle of high efficiency gas-cooled reactor power station", Electrical Review, 1 November 1974.

45. Landis, J.W. and Glendinning, F.S., "Commercial Development of the H.T.R. forges ahead", Electrical Review, 16 August 1974.

46. Röhler, E., Schlösser, J., Tegen, W. and Thurnher, K., "1160 MWe Nuclear Power Station Project with High-Temperature Reactor", Brown Boveri,Rev. 9-73.

47. Bogorinski, P., Friedrich, K., Schutz, J. and Vollmer, H., "Dynamics and Control of the Thorium High-Temperature Reactor (T.H.T.R.) power station", Proc. Int. Conf. on Boiler Dynamics and Control in Nuclear Power Stations, London, March 1973.

48. Schultz, M.A., "Reactors and Power Plants", McGraw-Hill, New York, 1961, 2nd Edition.

49. Schulten, R. and Jantsch, E., "The Brown Boveri-Krupp High-Temperature Gas-Cooled Reactor", The Brown Boveri Review, Vol. 47, No. 1/2.

50. Wunderlich, R.G., Darly, R.H. and Burn, R.R., "Fulton Station H.T.G.R. - Instrumentation and Control", Nuclear Engineering International, Auguat 1974.

51. Rippon, S., "The Commercial Steam Generating Heavy-Water Reactor", Nuclear Eng. International, August 1974.

52. C.E.G.B. Report MS/C/P129, STB/12/71, "SYRESØ1 - System Response Program", July 1971.

53. Davis & Sorensen, "Handbook of Applied Hydraulics", McGraw-Hill, 1969, 3nd Edition.

54. Creager and Justin, "Hydroelectric Handbook", John Wiley, 1950, 2nd Edition.

55. IEEE Committee Report, "Survey of Pumped Storage Project in the United States and Canada", IEEE Trans., Vol. PAS-95, No. 3, May/June 1976.

56. Jenkin, F.P., "Pumped-storage is cheapest way of meeting peak demands", Electrical Review, 16 August 1974.

57. "Pumped-storage reshapes the supply in Ireland", Electrical Review, 20 September 1974.

58. Oldenburger, R. and Donelson, Jr., J., "Dynamic Response of a Hydroelectric Plant", IEEE Trans., PAS-81, October 1962, pp. 403.

59. C. Samuel Martin and Henry C. Jackson, "Combined Surge Tank and Water-Hammer Analysis by Digital Computer", Water Power, April 1972, pp. 123.

60. Streeter, V.L. and Wylie, E.B., "Hydraulic Transients", McGraw-Hill, 1967.

61. Concordia, C. and Kirchmayer, L.K., "Tie-Line Power and Frequency Control of Electric Power Systems - Part II", IEEE Trans., PAS-73, April 1954, pp. 133.

62. Horn, Hans Eric, "Dynamic Description of a Hydraulic Turbine and Penstock for Simulation and Control Design Purposes", Internal Report, Elec. Eng. Dept., University of Trondheim, September 1976.

63. Atkinson, C.H. and Cronin, D.L.R., "Single tank analysis by computer", Water Power, February 1971, pp. 56.

64. Yu Tek Li, "Orifice head loss in a T-section of a throttled surge tank", Water Power, September 1972, pp. 326.

65. Mojonyi, E. and Seth, H.B.S., "The surge tank - a device for controlling water hammer", Water Power, February 1975 (Part I), March 1975 (Part II).

66. Young, C.C., "Equipment and System Modelling, for large-scale stability studies", Stability of Large Electric Power Systems, IEEE Press, 1974.

67. Leum, M., "The Development and Field Experience of a Transistor Electric Governor for Hydro-Turbines", IEEE Trans., Vol. PAS-85, No. 4, April 1966.

68. Ramey, D.G. and Skooglund, J.W., "Detailed Hydrogovernor Representation for system stability studies", IEEE Trans. on P.A.S., January 1970.

69. IEEE Committee Report, "Dynamic Models for Steam and Hydro Turbines in Power System Studies", IEEE Trans. Power App. Syst., November/December 1973.

70. K. Buchwald, L. von Enzenberg, H. Müller, W. Riess, and H. Waldmann, "Design, Behaviour and Operational Experience of Sliding-Pressure Power Station Units", Inst. of Mech. Engrs., "Convention on Steam Plant Operation", London, May 1973, Conference Publication 12, pp. 37-54.

71. Lovejoy, S.W. and Riess, W.G., "Variable-pressure operation and start-up of large turbines in utility power plants", American Power Conference, 20-22 April, 1971, Chicago, Illinois.

72. Daniels, J.H. and Sandt, F.T., "DDC comes of age at Martins Creek", ISA IPI, Vol. 17, pp. 1-11, May 1974.

73. Lansing, E.G., "Variable pressure peaking boiler, operation, testing and control", Trans. of ASME, Journal of Engineering for Power, July 1975, pp. 435.

74. Silvestri, G.J., Aanstad, O.J. and Ballantyne, J.T., "A Review of sliding throttle pressure for fossil-fuelled steam turbine generators", American Power Conference, Chicago, Illinois, 18-20 April, 1972.

75. Rudd, A.H. and Durrant, D.W., "Designs and systems for large fossil-fuel units intended for cycling service", American Power Conference, Chicago, Illinois, 29 April-1 May 1974.

76. Buchner, H., Biermann, F. and Zellmer, W., "Measures designed to improve the availability and economy of large steam power stations", Combustion, August 1970, pp. 26.

77. Bender, R.J., "U.S. welcomes variable-pressure concept", Power, August 197[illegible], pp. 56.

78. Lovejoy, S.W., Brandon, R.E. and Blakeslee, C.E., "Improved station heat rate with variable pressure operation", ASME Paper 62-WA-180, November 1962.

79. Ross, C.W. and Green, T.T., "Dynamic performance evaluation of a computer-controlled electric power system", IEEE Trans., PAS-91, May/June 1972, pp. 1158-1165.

80. Ross, C.W., "Error-adaptive control computer for interconnected power systems", IEEE Trans., PAS-85, No. 7, 1966, pp. 742-749.

81. Ross, C.W., "A comprehensive direct digital load frequency controller", PICA 1967, Pittsburgh, Pennsylvania, 1967.

82. Keyhani, A., El-Abiad, A. and Lansing, E.G., "Dynamic system load generation control using variable-pressure steam generators", IEEE PES Summer Meeting, 1975, Paper A 75 590-0.

83. Eilts, L.E. and Schleif, F.R., "Governing features and performance of the first 600 MW Hydrogenerating Unit at Grand Coulee", IEEE Trans., PAS-96, No. 2, March/April 1977, pp. 457-466.

84. Fosha, C.E. Jr. and Elgerd, O.I., "The Megawatt-frequcncy control problem - A new approach via optimal control theory", PICA, May 1969.